The Pathogenesis of 263K Scrapie in Syrian Hamsters Following Oral Infection

Patricia McBride

A thesis submitted in partial fulfilment of the requirements of the University of Edinburgh for the degree of Doctor of Philosophy

The programme of research was carried out at the Institute for Animal Health's Neuropathogenesis Unit in Edinburgh

March 2004

Declaration

I declare that the work presented in this thesis is my own, except where otherwise stated. All experiments were designed by myself or in collaboration with Dr. Michael Beekes. No part of this work has been, or will be, submitted for any other degree or professional qualification.

Patricia McBride

March 2004

Acknowledgements

I would like to thank my supervisors Jean Manson and David Price for reading the text, providing advice and useful comments and bearing with me over the past few years.

I would also like to acknowledge the work of a number of scientists at the Neuropathogenesis Unit (and formerly at the Animal Breeding Research Organisation) in Edinburgh. These include Moira Bruce, Alan Dickinson, Hugh Fraser and Richard Kimberlin whose fundamental research contributed so much to our knowledge about the pathogenesis of scrapie in rodents. I'd like to single out Moira and Hugh for thanks as they have inspired my respect and admiration for many years. Richard Kimberlin deserves a special mention because it was his initial insightful experiments that laid the foundation for this project.

Also included are Karen Brown, Christine Farquhar, Neil Mabbott and the other members of the NPU Peripheral Pathogenesis Group who were very supportive throughout the project and beyond. Many NPU colleagues gave me encouragement; none more than Christine, and Robert Somerville. Thankyou.

I would like to take this opportunity to express my gratitude to Maura Donaldson and Jill Oxley who have helped me so many times and in so many ways. Maura assisted me with the intricate dissections and time consuming embedding of tissue - even on Saturdays. She and Jill cut lots of sections and carried out PrP immunostaining. The quality of this work allowed easier interpretation of the data and enabled me to take the photographs of PrP pathology depicted in the results. For this I am extremely grateful.

I thank the Histology Group (Anne Suttie and the two Sandras; Coupar and Mack) for enduring the disruption I caused to their 'routine' during the dissections and embedding.

Thanks are due to my collaborators Michael Beekes and Walter Schultz-Schaeffer. As well as encouragement and stimulating discussion, both provided practical help. Michael and his wife Elizabeth's Western blotting preliminary research was the starting point for my work. Walter showed me how to locate and dissect out parts of the peripheral nervous system and perform PET blots. Michael carried out dissections and infectivity assays.

Lastly I reserve a very big thankyou to my husband Derek and daughter Julie whose continuing support means everything.

Table of Contents

List of Figures

List of Figures (continued)

List of Tables

Abbreviations

ABC	Avidin Biotin Complex
BSE	bovine spongiform encephalopathy
C	cervical (spinal cord)
CJD	Creutzfeldt-Jakob disease
CMGC	coeliac and mesenteric ganglion complex
CNS	central nervous system
CV/LFB	cresyl violet/luxol fast blue
CWD	chronic wasting disease
DAB	diaminobenzidine
DC	dendritic cells
DMNV	dorsal motor nucleus of the vagus nerve
Dpi/e	days post inoculation/exposure
DRG	dorsal root ganglion
ENS	enteric nervous system
FAE	follicle-associated epithelium
FDC	follicular dendritic cell
GALT	gut-associated lymphoid tissue
GI tract	gastrointestinal tract
GSS	Gerstmann-Straussler syndrome
H&E	haematoxylin and eosin
i/c	intracerebral
ICC	immunocytochemistry
IML	intermediolateral cell column
i/p	intraperitoneal
L	lumbar (spinal cord)
LRS	lymphoreticular system
M cells	microfold cells
MLN	mesenteric lymph node
NG	nodose ganglion
NS	nervous system
PAP	peroxidase anti-peroxidase
PET blot	paraffin embedded tissue blot
PK	proteinase K
PLP	periodate lysine paraformaldehyde fixative
PNS	peripheral nervous system
PP	Peyer's patch(es)
PrP	protease-resistant protein/prion protein
PrP^{C}	cellular (host) PrP
PrP^{d}	disease-associated PrP
PrP^{res}	protease resistant PrP
PrP^{sc}	protease resistant PrP/scrapie-specific PrP
PrP^{sen}	protease sensitive PrP
SAF	scrapie-associated fibrils
SCID	severe combined immunodeficient mice
sCJD	sporadic Creutzfeldt-Jakob disease
SN	solitary tract nucleus
T	thoracic (spinal cord)
TME	transmissible mink encephalopathy
TNF	tumour necrosis factor
TSE	transmissible spongiform encephalopathy
vCJD	variant Creutzfeldt-Jakob disease

Abstract

Epidemiologically, the oral route of infection is the most relevant for natural transmission of Transmissible Spongiform Encephalopathies (TSEs) within and between different species but relatively little is known about how the infectious agent reaches the CNS once it has gained access to the gastrointestinal (GI) tract. Although the ultimate target of infection is the CNS there is evidence that the peripheral nervous system (PNS) and lymphoreticular system (LRS) are involved in the peripheral pathogenesis of TSEs. Early experiments that traced the spread of scrapie infectivity after parenteral or intragastic challenge of rodents suggested that the infectious agent entered the CNS at the thoracic spinal cord and spread towards the brain. Western blot analyses of protease-resistant PrP, the protein marker of TSE disease, narrowed the entry site to thoracic spinal segments 4–9 and provided evidence of a further pathway that permitted the infectious agent direct entry into the brain. The main aim of this project was to define the neuroanatomical pathways by which the infectious agent gained access to the brain and spinal cord after oral challenge of hamsters with 263K scrapie. Immunocytochemistry, paraffin-embedded tissue blotting and selective bioassays of agent were used to identify the location and temporal sequence of disease-associated PrP (PrP^d) accumulation in the CNS, PNS and enteric nervous system (ENS) of hamsters. To elucidate the temporal relationship between the ENS and LRS in this model system, spleen and gut-associated lymphoid tissue (GALT) were included. Results showed that invasion of the brain occurred directly via the vagus nerve rather than by spreading along the spinal cord. The infectious agent reached the CNS simultaneously by two pathways. One route accessed the thoracic spinal cord via the intermediolateral cell column and another entered the dorsal motor nucleus of the vagus of the brain. Thereafter spread occurred between interconnected neurones. By identifying and quantifying the presence of PrP^d in the CNS, vagal and splanchnic nerve circuitry and the GI tract, it was possible to precisely identify routes and timing of neuroanatomical spread. PrP^d accumulated, in sequence, in target sites that accurately reflected known autonomic and sensory relays. PrP^d was observed in enteric and autonomic neurones prior to sensory neurones suggesting that the infectious agent primarily utilised synaptically-linked autonomic ganglia and efferent fibres to invade the CNS. Infectivity was present in the PNS at low to moderate levels. Therefore, after ingestion of 263K scrapie, the PNS and specifically, autonomic components of the vagus and splanchnic nerves are important in conveying the infectious agent to target sites in the CNS. The temporal interaction between lymphoid cells (follicular dendritic cells, macrophages, dendritic cells and Peyer's patch epithelium) and enteric neurones suggested that lymphoid elements are sequentially involved in PrP^d processing. Existing evidence is compatible with the LRS being an optional mediator rather than a key player in neuroinvasion in this experimental model but the early involvement of GALT in oral pathogenesis requires further investigation.

Chapter 1: Introduction

1.0 Transmissible Spongiform Encephalopathies

Scrapie affects sheep and, less commonly, goats and is the most extensively studied member of a group of transmissible diseases that affect a range of animal species and man (Table 1.1). These include Creutzfeldt-Jakob disease (CJD), Gerstmann-Straussler syndrome (GSS) and kuru of humans, bovine spongiform encephalopathy (BSE) of cattle, chronic wasting disease (CWD) of captive or free-ranging deer and transmissible mink encephalopathy (TME) of captively-reared mink. All these diseases, collectively called the transmissible spongiform encephalopathies (TSEs), cause a progressive degeneration of the central nervous system (CNS) that is eventually fatal. Transmissibility is a prerequisite for inclusion in the group. Scrapie, CWD, and TME occur naturally and can be transmitted between and within flocks, herds or colonies. Sporadic CJD (sCJD) is also naturally-occurring but there is no evidence of interspecies transmission. CJD can also be contracted genetically (see Table 1.1) and while there are no equivalent inherited TSEs recognised in animals, studies with natural and experimental scrapie of sheep have shown the PrP gene is an important factor in disease susceptibility (Hunter *et al.,* 1997a,b). Furthermore, the susceptibility (or resistance) to scrapie displayed by animals that inherit particular PrP genotypes have formed the basis for the National Scrapie Plan in which sheep are bred specifically to prevent scrapie developing (Dawson *et al.,* 2003).

The most recent additions to the TSE group have come about through accidental transmission. A number of cases of CJD have occurred iatrogenically via treatment with human growth hormone or dura mater grafts. Both these materials were derived from cadaveric tissues that were later found to be contaminated with the CJD agent (Brown *et al.,* 1992). However, it was the emergence and transmission of a new TSE strain (Wells *et al.,* 1987), subsequently shown to be BSE, which has accounted for the majority of TSE cases. The United Kingdom BSE epidemic has had devastating and far-reaching consequences for agriculture and man. BSE appears to have been transmitted by ingestion of TSE-contaminated protein supplements derived from rendered carcasses of sheep and cows. The original source of the strain or the conditions that permitted the emergence of BSE remain unclear (reviewed by Collee and Bradley 1997a,b) but a link has been found between the practise of feeding meat and bone meal (MBM- a protein supplement) to cattle during the 1970s and 80s and the appearance of BSE (Wilesmith *et al.*, 1991,92). The BSE agent was also transmitted to domestic cats, wild felines and a variety of zoo animals including ungulates such as Kudu and Oryx (Kirkwood *et al.*,1990). Dogs that are fed a similar commercially available diet to cats, and pigs which would have been exposed to contaminated

Table 1.1 **Transmissible Spongiform Encephalopathies of Animals and Man**

Type of TSE	Name	Species	Cause
Naturally occurring	Sporadic CJD	Man	Unknown
	Scrapie	Sheep/goats	Transmission of infection
	Chronic Wasting Disease	Deer/elk	"
	TME	Mink	"
Genetic	FFI	Man	PrP gene mutation
	GSS	"	"
	Familial CJD	"	"
Infectious	Iatrogenic CJD	"	Surgical/medical contamination
	Kuru	"	Ritual cannibalism (obsolete)
	Variant CJD	"	Accidental transmission
	BSE	Cows	"
	FSE	Cats	"
	TSE (not specifically named)	Zoo animals (includes ungulates and wild cats)	"
Experimental	Mainly scrapie & BSE	Rodents, inc. trangenics	Deliberate transmission
		Sheep, goats	"
		Cows	"
		Deer	"
		Non-human primates	"

Abbreviations: TME; Transmissible Mink Encephalopathy, FFI; Fatal Familial Insomnia, CWD; Chronic Wasting Disease, FSE; Feline Spongiform Encephalopathy, GSS;Gerstmann-Strausler Syndrome

MBM feed do not seem to be naturally susceptible to the BSE agent (Bradley 1996, Wells *et al.,* 2003). A current fear is the possibility that sheep that were also exposed to contaminated MBM are at risk of contracting BSE. Scrapie and BSE of sheep exhibit a similar clinical appearance that is not readily distinguishable and while scrapie does not appear to have crossed the species barrier from sheep to man, there is no certainty that this will be the case with ovine BSE.

Equally concerning as BSE was the discovery in 1996 (Will *et al.,* 1996) of a new variant of CJD (vCJD) that affected young rather than ageing individuals. Strain typing experiments showed convincingly that the strain of TSE that causes vCJD is BSE (Collinge *et al.,* 1996, Bruce *et al.,* 1997, Hill *et al.,* 1997) and that the most likely scenario for transmission of BSE to man was through dietary exposure. The human TSEs do not appear to transmit easily from one individual to another; the incidence of sCJD is low (approximately one case per million). Higher incidences have been due to iatrogenic transmission (Brown *et al.,* 1992) or to the cannibalistic transmission of kuru, a TSE that was prevalent several decades ago in the Fore tribe of New Guinea (Gajdusek, 1977). The eventual incidence of vCJD is still unknown. To date there have been many cases of vCJD (143 to October 2003) but far fewer than at first envisaged and the epidemic predicted by some seems less likely. Even so, given that all those affected were of the same PrP genotype i.e. homozygous for methionine at codon 129 (Colm & Knight, 2002), and that the percentage exposure may be very high, there are still concerns many of the population may yet succumb.

The public alarm surrounding the appearance and persistence of BSE and vCJD has renewed scientific interest in oral transmission of TSE. In the past, this route has been inadequately documented. Consequently, the mechanisms of oral transmission and the routes by which the agent accesses the CNS after it has gained entry to the gastrointestinal (GI) tract are poorly understood. The object of the work undertaken in this thesis is to partly address this deficiency.

1.1 PrP and its involvement in TSEs

One of the most significant scientific advances in TSE research in the last 20 years was the discovery of PrP (protease-resistant protein, prion protein).

PrP, a protease-resistant protein with a molecular weight of 27,000-30,000 (PrP27-30) was discovered, purified and characterised by Stanley Prusiner and colleagues in the early 1980s during experiments to identify the nature of the scrapie agent (Bolton *et al.,*1982, Prusiner *et al.,*

1982a,1983a,84, McKinley *et al.*, 1983). A larger PrP protein of molecular weight 33,000-35,000 (PrP33-35) was seen in Western blots of tissue extracts from both normal and infected brain that had not been treated with proteinase K (PK). On PK treatment, it was found that while PrP PrP33-35 from an uninfected animal was completely hydrolysed, the PrP33-35 derived from infected animals was partially degraded to PrP27-30 (Oesch *et al.*,1985). Soon after purification, the PrP gene was cloned and found to be encoded by the host genome (Oesch *et al.*,1985, Chesebro *et al.*,1985). The gene was transcribed in equal quantities in both unaffected and scrapie infected brain and apparently existed as two isoforms; the normal cellular form (PrP^{C} [cellular] or PrP-sen [sensitive to PK], that corresponded to PrP33-35) and a disease specific form seen only in infected animals (PrP^{Sc} [scrapie] or PrP-res [resistant to PK], that corresponded to PrP27-30)[Caughey *et al* 1991]. The primary amino acid structure of PrP was shown to be the same in both infected and unaffected animals (Basler *et al.*,1986). Differences between the isoforms occur in the protein's secondary and tertiary structure that determine conformation. Fourier transform infrared and circular dichroism experiments have shown that the structure of PrP^{C} comprises around 43% α-helix and only 3% β-sheet while PrP^{Sc} retains 34% α-helix but incorporates a greatly increased (43%) amount of β-sheet (Pan *et al.*,1993). During pathogenesis, PrP^{C} is post-translationally converted to PrP^{Sc} (Borchelt *et al.*,1990). The mechanism by which these changes in structure occur is unknown but has lead to the prion hypothesis which asserts that scrapie and related diseases result from aberrations of PrP protein conformation and that the altered protein alone comprises the infectious agent (see 1.2 Nature of the Agent).

PrP27-30 was originally identified as being the major component of fibrillar structures, initially termed scrapie-associated fibrils [SAF] (Mertz *et al.*,1981) or prion rods (Prusiner *et al.*,1983b, Diringer *et al.*,1983b) that were isolated from detergent-treated tissue extracts of scrapie-infected brains. SAFs (now usually referred to as PrP^{Sc} fibrils) have been detected in all TSE-infected tissues tested. The fibrils are products of *in vitro* purification but ultrastructurally they resemble the fibrillar arrays seen in amyloid plaques of scrapie-infected rodents (Bendheim *et al.*,1984, Jeffrey *et al.*,1994). Presence of PrP^{Sc} fibrils, amyloid plaques and other forms of PrP-related pathology in tissue preparations are often used to provide confirmation of infection.

During the course of the disease the modified or disease associated forms of proteinase K resistant PrP (variously termed abnormal or pathological PrP, PrP^{res}, PrP^{Sc}, PrP^{d}, PrP*) accumulate in the CNS and a variety of extraneural tissues of experimental and naturally occurring TSEs (Bruce *et al.*,1989,94a; McBride *et al.*,1992,98,99, Farquhar *et al.*,1994, Foster

et al.,1996, Lasmézas *et al.*,1996, van Keulen *et al.*,1996, Beekes & McBride, 2000 and several others).

The diverse nomenclature used to denote PrP isoforms can be confusing. PrP may be identified by a variety of techniques such as Western blotting, electron microscopy or immunocytochemistry (ICC). The term PrP^{Sc} is commonly used as a pseudonym for both immuno-positive PrP deposits detected by these techniques and the infectious agent itself. However, this term identifies the protease treated product (partially PK-resistant PrP) of a biochemical procedure. The antibodies that are available recognise both cellular and disease specific PrP and although several different forms of PrP can be distinguished in fixed immunostained tissue sections these cannot be definitively identified as being protease resistant. Therefore, in this thesis the term PrP^{d} will be used to describe the disease-associated forms that are observed in PrP-immunolabelled tissue sections, i.e. those forms that are exclusively found in tissues from infected animals.

When disease-associated forms have been shown to be associated with infectivity, as is the case with the hamster model used in this project, (Beekes *et al.*,1996, Baldauf *et al.*,1997) they may also be considered surrogate markers for an infectious agent. In order to show such correlation, infectivity and the accumulation of PrP^{Sc} were quantified in samples of brain and spinal cord taken from hamsters culled at various times after oral administration of 263K scrapie. PrP^{Sc} was quantified by computerised densitrometric analysis of PK-treated dot blots and compared against a calibration curve constructed from samples of known protein values. The agent titre was determined by bioassay of tissue homogenates from the same samples used for assessment of protein and measured by dose-response curves according to recognised methods (Kimberlin & Walker 1977, Prusiner *et al.*,1980). Mathematical comparison of PrP^{Sc} and infectivity showed that 10^{6} molecules of PrP^{Sc} approximated to one infectious unit.

1.1.2 Function of PrP

1.1.2i The role of PrP in unaffected animals

Despite the attention given to the study of PrP during TSE pathogenesis, relatively little is known about the normal function(s) of cellular PrP. PrPmRNA and protein are widely expressed in the CNS (Kretzschmar *et al.*,1986, Manson *et al.*,1992) and to a lesser degree in a number of adult and embryonic peripheral tissues (Oesch *et al.*,1985, Caughey *et al.*,1988, Bendheim *et al.*, 1992, Manson *et al.*,1992). In addition to the brain (DeArmond *et al.*,1987, Bruce *et al.*,1989,

94a, Nakamura *et al.*, 2002, Ford *et al.*, 2001), PrP^C has been identified in several types of cells in a variety of visceral organs including the GI tract (Shmakov *et al.*,2000, Lemaine-Vieille *et al.*, 2000, Pammer *et al.*, 2000), kidney (Manson *et al.*,1992, Fournier *et al.*,1998), lymphoreticular system (McBride *et al.*,1992, Fournier *et al.*,1998, Ritchie *et al.*,1999, Brown *et al.*,2000), lung (Bendheim *et al.*,1992), muscle (Brenner *et al.*,1992, Brown *et al.*,1998, Gohel *et al.*,1999), adrenal, liver, pancreas, testes, thymus and salivary glands (McBride *et al.*,1992,93, Farquhar *et al.*,1994; Brown *et al.*,2000). Expression of PrP^C has also been detected on blood cells, platelets and endothelial cells of a number of mammalian species, albeit at variable levels (Hill *et al.*, 2000, Cashman *et al.*,1990, Šimák *et al.*,2002). The association with a broad range of cell types exhibiting different physiological functions suggests that the role of PrP may be diverse.

The structure of the gene is known and can provide clues to its function. PrP has been highly conserved throughout evolution and is present in a number of species (Westaway & Prusiner 1986, Wopfner *et al.*,1999). To aid the search for possible functions, gene targeting was used to produce mice in which PrP was ablated. In two lines, NPU *Prnp*$^{-/-}$ (Manson *et al.*,1994a) and Zurich *Prnp*$^{-/-}$ (Büeler *et al.*,1992) ablation of the gene does not adversely affect development of PrP null mice nor appear to result in any obvious phenotypic deficits (Büeler *et al.*,1992, Manson *et al.*,1994a). The reason for this may be that *Prnp* is so crucial that the lethal consequences of its loss are alleviated by gene compensation. Although these mice breed and behave normally, lack of PrP does elicit a number of subtle abnormalities including perturbation of sleep and circadian rhythms (Tobler *et al.*,1996, Sanchez-Alavez *et al.*,2000) and a reduced T lymphocyte response (Mabbott *et al.*,1997). In another two lines, ICM *Prnp*$^{-/-}$ (Moore *et al.*, 1995) and Japan *Prnp*$^{-/-}$ (Sakaguchi *et al.*,1996) the mice showed signs of progressive cerebellar ataxia in maturity. This phenotype appears to be due to overexpression of a related gene, *Prnd*, whose product is a protein called doppel (Moore *et al.*,1999) rather than a lack of PrP expression.

Given the high levels of PrP found in the CNS it is unsurprising that many of the observed deficiencies have been ascribed to the functionality of neuronal transmission (Collinge *et al.*, 1994, Manson *et al.*,1995, Colling *et al.*,1996, Carleton *et al.*,2001), survival, differentiation and memory formation (Graner *et al.*,2000) and axon growth (Salès *et al.*,2002). There is accumulating evidence showing that PrP^C is expressed at the synapse. Initial reports using electrophysiology claimed differences in long term potentiation between PrP knockout mice and controls (Collinge *et al.*,1994, Manson *et al.*, 1995). However, other studies either show some

disparity with these findings (Brenner *et al.*,1992, Herms *et al.*,1995, Curtis *et al.*,2003) or suggest that this function is not the most significant or only role for PrP at this location. Due to it having been found both pre- and post synaptically (Herms *et al.*,1999, Salès *et al.*,1998, Fournier *et al.*,2000) other possible functions include an involvement in intracytoplasmic membrane recycling and trafficking (Gohel *et al.*,1999) or as a physiological post-synaptic receptor (Askanas *et al.*,1993).

A major role for PrP^C may be in promoting neuronal survival by suppressing programmed cell death. The presence of PrP^C, *in vitro*, seems to protect against apoptosis (Kuwahara *et al.*,1999, Bounhar *et al.*,2001). Recent attention has focused on the copper-binding capability of PrP^C and its association with the protective effects of antioxidants (Brown *et al.*,1997a,b; Pauly & Harris, 1998). There is evidence to show that PrP^C is sensitive to various forms of physiological stress including the damage caused by exogenous copper, hydrogen peroxide, reactive oxygen species and oxidative stress (Brown *et al.*,1997a,b, 1998, 2002, Herms *et al.*,1999, Guentchev *et al.*, 2000, Milhavet *et al.*,2000, Klamt *et al.*, 2001, Wong *et al.*,2001). Collectively, these observations suggest a neuroprotective role for PrP^C.

1.1.2ii The role of PrP during TSE infection

The role of PrP^C is interesting but with no obvious vital function its significance lies in providing insights into TSE disease. PrP is fundamental to the development (Büeler *et al.*, 1993, Manson *et al.*, 1994a) and our understanding of scrapie and related diseases. PrP knockout ($PrP^{-/-}$) and transgenic mouse models have been greatly used to study TSE pathogenesis. PrP nulls do not develop scrapie nor replicate the infectious agent (Büeler *et al.*, 1993, Prusiner *et al.*, 1993 Manson *et al.*, 1994a). Consequently, the presence of PrP is crucial to TSE pathogenesis. Experiments grafting wild-type brain grafts into PrP null mice have shown that PrP^C must be present for the disease to develop and spread (Brandner *et al.*, 1996). Engrafted mice did not succumb to infection even though the transplanted tissue developed lesions typical of scrapie neuropathology. Scrapie survival is also influenced by PrP gene dosage (Manson *et al.*, 1994b). Studies comparing wild-type (WT) $PrP^{+/+}$ mice with PrP heterozygotes ($PrP^{+/-}$) showed that while the incubation period was shorter in WT, both the amount and pattern of PrP^{Sc} deposition appeared equivalent in both groups. Hence, the level of PrP^C in the brain does not determine the extent of PrP^{Sc} deposition achieved at the end-stage of disease.

Many studies have used a synthetic fragment of PrP^{Sc}, $PrP^{106\text{-}126}$, or PrP^{Sc} extracts (Brown 2000, Häik *et al.*, 2000) to demonstrate the neurotoxicity of PrP^{Sc} and there is also mounting evidence

to show that neuronal death is indirectly linked to the upregulation of microglia during TSE infection (Bate *et al.*, 2001; Brown 2001). Conversion of PrP^{C} to PrP^{Sc} activates microglial cells. These release damaging free radicals that in turn may increase the sensitivity of neuronal cells to oxidative stress. It may be that the innate neuroprotection afforded by PrP^{C} is insufficient for infection-weakened neurones to withstand the free radical challenge.

1.2 The nature of the scrapie agent

The nature of the agent that causes scrapie and related diseases has been the focus of much debate and speculation for many years. Once scrapie had been established as an experimental model in rodents it became clear that the properties of the agent did not fit with established criteria for how infectious diseases were known to behave. For example, the TSE pathogen is transmissible, replicates and exists as many strains with genetically stable phenotypes (Dickinson & Outram 1979). One strain, 87A has also been shown to mutate to form a separate strain (ME7) over serial passage (Bruce & Dickinson 1987). These properties are consistent with the activity of viruses yet the pathogen causing TSEs displays extreme physicochemical stability and cannot be as effectively inactivated. Scrapie is resistant to inactivation by dry heat, ultra-violet light, ionising radiation and chemical treatment by proteases and viricides (Kimberlin *et al.*, 1983a, Brown *et al.*, 1986, Taylor *et al.*,1996a, Somerville *et al.*, 2002). The agent also appeared to spread through the body in a virus-like fashion but at very much slower rates than convential neurotropic viruses such as Herpes Simplex or Reovirus, taking weeks or months rather than days to reach its target (Kimberlin & Walker 1980,82,86, Kimberlin *et al.*, 1983b, Fraser & Dickinson 1985).

PrP^{Sc} extracted from infected brains copurifies to varying extents with infectivity (Diringer *et al.*, 1983a, Somerville *et al.*,1986, Beekes *et al.*,1996). While infectivity and PrP^{Sc} ratios correlate well in some cases (Bolton *et al.*,1982, Beekes *et al.*,1996), in others the level of infectivity is inconsistent with the amount of detectable PrP^{Sc} (Somerville & Dunn 1996, Lasmézas *et al.*, 1997, Manson *et al.*,1999, Barron *et al.*,2001). Despite extensive biochemical analyses and electron microscopy, no scrapie-specific virus has been seen (or recognised) in tissue preparations - while the disease-associated protein is usually very evident.

Over the years, several theories were proposed that sought to resolve biological inconsistencies and explain the structure of the agent. An early theory advanced was that the infectious agent could be encoded by a viroid and, as in plants, could be a simple nucleic acid of very small size (Deiner 1973). Another idea suggested that the infecting agent was a conventional virus that

replicates, initially in the lymphoid system, and spreads to the CNS where it induces amyloidosis (Diringer *et al.*,1984,1991). For some researchers the parallels with virus-causing diseases remain compelling (Rowher 1991, Manuelidis 1994). The two fields of thought that gain most scientific support are the virino hypothesis (Dickinson & Outram 1979, 88; Bruce & Dickinson 1987) and the prion or 'protein only' hypothesis (Prusiner *et al.*,1982b, 91, 97). Evidence for both is strong and robustly defended.

The virino hypothesis proposes that the infectious agent is an informational hybrid with contributions from both the scrapie strain and the host it infects. Many strains of TSE exist and, as stated previously, these specify or encode a range of characteristics (clinical signs, incubation period, targeting of pathology) in the host (Bruce & Fraser 1991, Bruce *et al.*,1991). Supporters of the virino hypothesis believe that that the infectious agent must be able to encode the information for strain variation and must also include properties that enable it to evade destruction by the host's own immune system. Although PrP is clearly important in TSE pathogenesis, it is disputed whether the protein alone can carry the information required to specify the observed strain diversity. Before the discovery of PrP, Dickinson who originally proposed the virino hypothesis, had suggested the existence of replication sites that were formed from *Sinc* encoded protein - which has now been shown to be PrP (Moore *et al.*,1999). The current hypothesis proposes that the infectious particle or virino be comprised of nucleic acid that is bound to and protected by PrP host protein. Such a molecule would have the ability to differ structurally between strains and contain a strain specific genome whose capability to replicate was independent of its host. To explain the current lack of detection, the nucleic acid must be small. This is physically possible (Rowher 1984) and if enveloped by PrP^{C} there would be no requirement to encode viral coat proteins. The presence of nucleic acid is key to the virino hypothesis as this is the only molecule known to biology that is capable of replication and transfer of genetic information. The opposing viewpoint argues that strain specificity can be accounted for by differences in conformation and glycosylation of PrP^{Sc}.

The suggestion that the unconventional properties of scrapie might be caused by an unconventional biological agent was first advanced as early as 1967 by JS Griffith (Griffith 1967) who proposed that the scrapie agent was a self-replicating protein derived from a normal cellular protein. It was known that protein was an important part of the pathogen; scrapie infectivity is reduced by treatments that denature, disaggregate or destroy proteins (Hunter GD 1979, Millson GC & Manning EJ 1979, Rohwer RG *et al.*, 1979, Latarjet R 1979). UV irradiation had identified the target molecule as being extremely small and this had cast doubts

on the existence of a scrapie-specific nucleic acid (Alper *et al.*, 1967) which by the early 1980s was still eluding isolation. On his identification of a unique 27-30Kd protein that co-purified with the scrapie agent (Bolton *et al.*,1982, Prusiner *et al.*,1982a), Prusiner challenged existing scientific dogma by claiming that scrapie was caused by prions - 'novel proteinaceous infectious particles' that lacked nucleic acid (Prusiner 1982b). According to the original prion hypothesis, prion protein (PrP), was the sole component of the infectious agent. Prusiner suggested that scrapie and related diseases result from aberrations of PrP protein conformation, i.e. some insult (genetic or biochemical) triggers host neuronal PrP to refold from the normal largely α-helical form to the predominantly β-pleated sheet disease-causing form. PrP^{Sc} then catalyses ongoing conformational change by recruitment of susceptible PrP^{C}. With time, the existence of scrapie strains was universally accepted and the theory was adapted to fit the evolving research. If the agent were to consist purely of PrP, the phenotype of each strain must be inherent within this. Accordingly, prion strains were suggested to be encrypted through differing PrP^{Sc} conformers (Prusiner 1991). The incubation-prolonging effect of the species barrier was argued as being due to mismatches between host PrP^{C} and the PrP^{Sc} of the inoculum (Prusiner *et al.*, 1990). Transgenic mice expressing chimeric PrP were used to test this theory. An initial experiment in which the species barrier to hamster scrapie was reduced in mice expressing hamster PrP^{C} appeared to bear this out (Scott *et al.*,1989, Race *et al.*,1995). The anomalies that arose from extending this theory to humans (Telling *et al.*,1994,95) were suggested to be explained by the existence of protein X (Telling *et al.*,1995, Prusiner & Scott, 1997) a host ligand that could interact with PrP^{C} in a species dependent manner. That is, mouse protein X would compete more favourably and bind more efficiently with mouse PrP^{C} than it would with human PrP^{C}. Despite this, inconsistencies remain and the mechanism by which the disease-specific form(s) are created from and interact(s) with host PrP to cause disease remains to be established.

When it was first proposed, the idea that scrapie could be caused solely by an infectious protein was radical. Many scientists remain unconvinced and the nature of the causative infectious agent remains unproven even though extensive work has been carried out or is in progress to test individual hypotheses experimentally. The ability to separate infectivity from PrP^{Sc} is seen as an argument against the prion hypothesis. The extent to which PrP^{Sc} can be separated from infectivity has been shown to be dependent on the chemical treatment or temperature to which a strain is subjected (Manuelidis *et al.*,1987, Shaked *et al.*,1999, Wille *et al.*,2000, Somerville *et al.*, 2002). This has lead to the suggestion (and counter argument) that only a proportion of PrP^{Sc} (designated PrP*) is infectious (Weissmann 1991, Aguzzi & Weissmann 1997). The requirement of PrP for disease development (Büeler *et al.*, 1993, Manson *et al.*, 1994a) appears to support the

protein-only theory. The prion hypothesis was partially upheld with the *in vitro* conversion of PrP^{C} to the protease-resistant form (Kocisko *et al.,* 1994) but, crucially, to date, synthesised PrP^{Sc} has not been able to transmit infectivity.

1.3 Scrapie: Disease characteristics

Natural scrapie has a long incubation period ranging from several months to years. Onset is slow and there are no visible indicators of early infection. During this time the infectious agent replicates in the CNS and extraneurally, and through time the affected individual displays obvious neurological dysfunction and, eventually, dies. The clinical phase is short in comparison to the protracted asymptomatic period and is characterised by ataxia (abnormal gait), pruritis (itching) and recumbency (inability to stand). There is no cure and no therapeutic intervention that significantly affects the lethal outcome.

The name 'scrapie' is an old Scottish word and describes the infected animal's tendency to scrape or scratch itself against fence posts and similar objects, resulting in bald patches on the fleece. Scrapie has been a farming problem for at least 250 years and has been the subject of scientific interest for around fifty. As such it is the most understood of the TSEs or prion diseases. In the past these diseases were called the transmissible degenerative encephalopathies and unconventional or slow viral encephalopathies. These names describe the hallmarks of the diseases, that is; their transmissibility, neurodegenerative pathology, slow progression and the unusual nature of the pathogen that infects the host.

Although these diseases are infectious, there is no classical immune response, no inflammatory pathology and no antibodies are produced. However, as is discussed later in section 1.5.1 a functioning immune system is necessary for peripheral infection in some models and it now appears that although the agent does not elicit an overt immune reaction, the lymphoreticular system (LRS) may influence peripheral pathogenesis in a more subtle fashion. The host cellular protein PrP has been implicated in lymphocyte activation (Cashman *et al.*, 1990, Mabbott *et al.*, 1997). There is also evidence that complement cascade components facilitate peripheral pathogenesis (possibly by mediating the retention of PrP in FDC networks) because complement depletion significantly delays onset of scrapie (Klein *et al.*, 2001, Mabbott *et al.*, 2001). In addition, disease-induced cytokines such as prostaglandin E-2, interleukin-1 beta and tumour necroisis factor-alpha are present in the brains of mice with experimental scrapie and co-localise with areas of PrP^{d} deposition and astrogliosis. The extent of cytokine gene expression or

production appears to relate to the degree of reactive gliosis which, in turn, may contribute to the development of scrapie pathology (Williams *et al.*, 1997a, Brown *et al.*, 2003).

Intra-species transmissibility was first demonstrated in 1939 by intra-ocular challenge of sheep with a spinal cord homogenate derived from natural scrapie (Cuillé & Chelle 1939). Another early, but accidental transmission of natural scrapie provided clues to the resistance of the agent to chemical decontamination. Sheep that had been treated against louping ill subsequently developed scrapie through contamination of the formalin-inactivated lymphoid tissue that was used as a vaccine (Gordon 1946). Scrapie is transmissible both horizontally among the flock and vertically from ewe to lamb, and from the early 1960s has been transmitted experimentally to a number of laboratory rodents including inbred mice and hamsters (Chandler 1961,63, Marsh & Hanson 1977) in which the disease can be studied more easily, quickly and in controlled conditions (Dickinson & Fraser 1979).

1.4 Experimental rodent models of scrapie and strain identification

Several experimental rodent scrapie strains have been selected from the mixture of isolates that occur in the natural disease. Serial passage of natural scrapie over many generations, mainly through inbred mice, have produced single strains that can be differentiated from each other by their differing disease characteristics (Dickinson & Meikle 1971, Dickinson & Fraser 1977, Dickinson & Outram 1988, Fraser 1976, 79; Bruce & Fraser 1976, Bruce & Dickinson 1987). Around 20 different scrapie strains have been isolated. The main criteria by which individual strains can be identified are by the highly reproducible incubation periods and the defined patterns of vacuolar pathology. The particular clinical signs displayed during the course of the disease (Bruce & Fraser 1976, Bruce *et al.*, 91, Carp *et al.*, 1984) and physicochemical properties (Kimberlin *et al.,* 1983a, Somerville *et al.*, 2002, Taylor *et al.*, 2002) are additional useful indicators. More recently, and controversially, a technique called glycoform analysis has been used to distinguish TSE strains (Parchi *et al.*, 1995, Collinge *et al.*, 1996, Hill *et al.*, 1997, Somerville *et al.*, 1997, Somerville 1999) although the relationship between PrP glycoform and TSE strain remains to be identified.

1.4.1 Incubation period

Scrapie survival depends on the scrapie strain and the genotype of the host it infects. The major influence on the length of the incubation period is the exerted by the *Sinc* (*S*crapie *inc*ubation) gene. This discovery in the 1960s (Dickinson *et al.*, 1968) was due to the recognition that in any experimental rodent model, the period of time from infection to death was extremely predictable.

Sinc has two alleles, s7 and p7, and exerts precise control over the timing of scrapie incubation in rodents. Each scrapie strain has a highly repeatable, tightly controlled incubation period in each of the three *Sinc* genotypes. Mice homozygous for the *Sinc* genotype s7s7 have short incubation periods when infected by, for example, the ME7 strain. Mice carrying p7p7 alleles have much longer incubations with this strain of scrapie and those of s7p7 heterzygotes lie in between (Dickinson *et al.*, 1968, Dickinson & Meikle 1971, Dickinson & Fraser 1979). *Sip,* the ovine homologue of *Sinc,* fulfils the same function in sheep (Dickinson & Outram 1988).

Since these early studies, evidence has amassed showing that the host encoded protein PrP is involved in the genetic control of pathogenesis. Experiments were initially undertaken in an attempt to reveal the molecular basis for *Sinc* control of incubation period. DNA sequencing and restriction fragment length polymorphism (RFLP) analyses showed close genetic linkage between the *Sinc* and PrP genes (Carlson *et al.*, 1986, Westaway *et al.*, 1987). Mice with *Sinc* s7 and p7 genotypes encoded PrP proteins that differed at residues 108 and 189 of the PrP gene, *Prnp* (Westaway *et al.*, 1987*)*. This close linkage was shown to be maintained using RFLP analysis of congenic mice that differ only at the *Sinc* locus providing strong evidence that *Sinc* and *Prnp* were very probably same gene (Hunter *et al.*, 1992). Recent gene targeting experiments have now proved that *Sinc* and *Prnp* are the same (Moore *et al.*, 1998) and that PrP is the product of *Sinc* but the way in which this gene controls the phenotypic properties produced has yet to be proven. This discovery and the prominence of PrP (gene and protein) in TSE pathogenesis have overshadowed Dickinson's early work and usage of the *Sinc* terminology is now obsolescent. In current literature, $Sinc^{s7}$ and ^{p7} alleles are commonly referred to as $Prnp^{a}$ and $Prnp^{b}$, respectively.

1.4.2 Vacuolar Pathology

In tissue sections, vacuolar degeneration (commonly referred to as vacuolation) appears as tiny holes in the neuropil of both grey and white matter. This resemblance gives rise to the alternative terms of spongiform degeneration, spongiosis, or the media-coined, 'spongebrain', that describes the microscopic appearance but not the texture of the brain. Vacuolation differs in severity and distribution according to the experimental scrapie rodent model. The variation is dependent mainly on the strain of scrapie but genotype of recipient and routes of challenge also play a part (Fraser & Dickinson 1973, Fraser 1979). If these variables are kept constant, the pattern of vacuolation is predictable and reproducible and can act as a 'fingerprint' for that model. The distribution and severity of vacuolar pathology can be represented in graphic form as a lesion profile that is individual to each scrapie strain. Vacuolation is assessed using light microscopy

by scanning haematoxylin and eosin (H&E)-stained sections of brain from mice culled at the terminal stage of scrapie. The vacuolar lesions in 9 grey and 3 white matter areas are assigned a 'score' on a scale of 0-5 where 0 represents no lesion and 5 the most severe spongiosis. The resulting profile is formed by the line that joins the points of the average of the scores from the individual areas. Lesion profiles are produced by combining the scores from six or more brains, as groups of this size are required to give reproducible and statistically significant results.

Within the invariable parameters described above both incubation period and vacuolar pathology remain constant from passage to passage and when taken together can serve to identify a scrapie model. This method of strain typing has been used at NPU for more than 30 years resulting in a 'tried and tested' reliable system. Such is the accuracy and reproducibility of NPU strain typing that, given the experimental scrapie model, the length of scrapie incubation can be calculated with confidence. Conversely, if the incubation period and pattern of pathology (lesion profile) are known, it is possible to correctly predict the strain of scrapie that caused the death of the animal. The use of this methodology enabled Fraser, Bruce and colleagues to show that BSE was a previously unrecognised strain of TSE (Fraser *et al.*, 1992a) and that this same strain was also responsible for the accidental spread to domestic cats and exotic ruminants (Bruce *et al.*, 1994b, Fraser *et al.*, 1994). Bruce was also able to show that vCJD victims died from an agent that was indistinguishable from BSE and conclude that the most likely scenario for developing the disease was from dietary exposure to BSE (Bruce *et al.*, 1997). As well as showing similarities between BSE and vCJD, strain typing showed that vCJD was distinguishable from sporadic CJD. Lesion profiles from the brains of dairy farmers who died of CJD were consistent with sporadic and not vCJD thereby showing that these individuals did not contract the disease (vCJD) through an occupational link with BSE-infected cows (Bruce *et al.*, 1997).

1.4.3 Glycoform analysis

This method uses the differing degrees to which PrP is glycosylated and the resulting PrP glycoform banding patterns that are obtained by gel electrophoresis to distinguish between TSE strains. Glycoform analysis was used as a diagnostic tool to differentiate sporadic from vCJD (Collinge *et al.*, 1996) and to confirm that BSE and vCJD were the same strain (Hill *et al.*, 1997). PrP has two N-glycosylation sites and can exist as mono, di or unglycosylated forms. Normal cellular PrP (PrP^{C}) is glycosylated at both sites while PrP^{Sc} varies in the degree of glycosylation (Parchi *et al.*, 1995, Somerville *et al.*, 1997). While the diversity of glycosylation patterning that is seen between scrapie strains indicates that glycosylation is controlled by the TSE strain, the heterogeneity of glycosylation found in different brain regions of the same infected animal shows that control is also exerted by

host factors (Kascsak *et al.*, 1985, Somerville *et al.*, 1997,99). In addition, as was shown with sporadic CJD, the degree of PrP^{Sc} glycosylation can also depend on PrP genotype and clinico-pathological presentation (Parchi *et al.*, 1995). Differences in glycoform patterning have also been found between CNS and lymphoid tissues from infected individuals, between brain and spleen of 139A scrapie-challenged mice (Rubenstein *et al.*, 1991) and within brain and tonsil of vCJD patients (Hill *et al.*, 1999). For these reasons glycoform analysis has not been universally accepted as an alternative way to distinguish strains. However, as strain-typing methods are dependent on lengthy transmission experiments, glycoform analysis provides useful supporting data.

1.5 Neuropathology of rodent scrapie.

Macroscopically, the brains of clinically affected rodents, animals and humans appear normal. Microscopically, there are four pathological features that characterise the neuropathology of scrapie and related diseases. These include glial activation that mainly involves a lesion-related increase in size and number of astrocytes (Deidrich *et al.*, 1991, Bruce *et al.*, 1994a, DeArmond *et al.*, 1992, van Keulen *et al.*, 1995) and microglia (Williams *et al.*, 1997b, Peyrin *et al.*, 1999), and neurone loss (Fraser 2002). In one model in which the sequence of neurodegeneration has been characterised, neuronal loss is preceded firstly by PrP^{d} deposition then by loss of synapses, axon terminals and dendritic spines and then gliosis (Fraser 2002). Apart from PrP^{d}, none of these are specific indicators of TSE disease and occur generally in response to neurological disease or trauma. However, astrogliosis is closely associated with disease-associated PrP (PrP^{d}) deposition (Bruce *et al.*, 1994a) and as such can be a useful indicator of early specific scrapie pathology when PrP^{d} is difficult to detect (McBride PA, unpublished observation). The remaining two features, vacuolar degeneration and cerebral amyloidosis, are key to the diagnostic identification of TSEs.

The appearance and distribution of vacuolar pathology has been described previously in conjunction with its role in strain identification (see section 1.4.2)

The other classical lesion associated with scrapie pathology is the presence of cerebral amyloid, notably, in the form of plaques. The term 'amyloid' meaning 'starch-like' is a general classification of fibrillar proteins of 6-10nm that form insoluble aggregates in normal physiological conditions and contain a beta-pleated sheet secondary protein structure. This protein conformation binds the dye Congo red and produces a green birefringence when stained histological sections are viewed with polarised light (Puchtler *et al.*, 1962). The typical plaque is round and composed of a central core of radiating amyloid fibrils and an outer corona. Scrapie

plaques are very similar to senile plaques found in brains of Alzheimer's disease (AD) patients but the major amyloid proteins derive from biochemically distinct classes that can be distinguished from each other immunocytochemically. In AD the core protein is Aβ, while scrapie plaques are principally composed of PrP^d. As with vacuolation, when mapped in H&E-stained tissue sections, the distribution of amyloid plaques in the brains of intracerebrally challenged mice, depends on the scrapie model. Some models produce large numbers while in others there are few or no discernible plaques (Bruce 1976). The fact that plaques are not always present in naturally occurring or experimental TSEs shows that this feature alone is not reliable as a diagnostic indicator.

1.5.1 PrP-related pathology

Historically, scrapie diagnosis was carried out by examination of formalin-fixed, H&E-stained sections. However, the isolation of PrP allowed the production of antibodies and by the late 1980s there were an increasing number of publications in which the developing technique of immunocytochemistry (ICC) was used as a diagnostic tool. Early studies identified PrP-containing amyloid plaques in several TSEs including experimental scrapie of rodents, human TSEs and natural and experimental scrapie of sheep (Bendheim *et al.*, 1984, DeArmond *et al.*, 1985, Roberts *et al.*, 1986, Kitamoto *et al.*, 1987, Wiley *et al.*, 1987, McBride *et al.*, 1988, Millar *et al.*, 1993). Nevertheless, it became apparent that only a proportion of the PrP present was being visualised. PrP^d or PrP^{Sc} could be identified by EM or Western blotting in extracts of affected brains from all scrapie strains including those where no plaques had been observed by H&E or ICC staining. This suggested that in addition to plaques, other forms of PrP pathology existed. The extent, distribution and heterogeneity of PrP^d pathology was revealed by the use of PLP (periodate-lysine-paraformaldehyde) fixation (McLean & Nakane 1974) coupled with a short processing cycle. After this fixative was adapted for use by incorporating very low concentrations of paraformaldehyde (2% instead of the prescribed 10% volumes), a far greater range and quantity of PrP^d was revealed compared to standard formalin fixation (Bruce *et al.*, 1989, McBride *et al.*, 1992,93,98). The carbohydrate preserving property of PLP was well suited for PrP glycoprotein.

The sensitive ICC methods developed at NPU have been used to identify, map and compare distributions of host (PrP^C) and PrP^d in tissues from a variety of rodent scrapie models (Bruce *et al.*, 1989,94a, McBride *et al.*, 1992,93,98,99, Manson *et al.*, 1992,94b, Ritchie *et al.*, 1999; Brown *et al.*, 1999, Beekes & McBride 1998), natural scrapie and BSE (Foster *et al.*, 1996,2001). In immunolabelled sections of terminally-affected mouse brain, a variety of

different forms of PrP pathology can be identified (Figure 1.1). As well as in amyloid plaques, PrP^d can be seen as randomly-distributed irregular aggregates of varying size, within or surrounding astrocytes, as dense inclusions within microglia, encircling cell bodies in specific neuronal groups or tracking along neuronal processes and blood vessels. The most predominant and pathogenically significant form of PrP^d is the diffuse granular deposition that is widespread within particular areas of the CNS (DeArmond *et al.*, 1987,97, Bruce *et al.*, 1989,94a, Beekes & McBride 98). PrP^d is targeted to and associated with neurones in precise anatomical locations. This type of cerebral amyloid-related pathology is not found in AD or other amyloidogenic neurodegenerative diseases and is therefore a unique distinguishing feature of TSE pathology.

The importance of diffuse PrP^d was revealed in time course studies showing that this type of PrP pathology is seen very soon after inoculation or challenge – between ¼ and ⅕ of the way through the incubation time in the models studied. Even at this early stage the protein is accurately and consistently observed in small groups of neurones in specific CNS sites (Bruce *et al.*, 1994a, Beekes & McBride 1998, McBride *et al.*, 1998) suggesting that scrapie strains recognise and selectively target certain groups of neurones for replication but the underlying mechanism for such selectivity is unknown at present.

In the mouse models tested, the manifestation of PrP^d, vacuolation and the onset of clinical disease occur sequentially (Bruce *et al.*, 1989,94b)[Table 1.2]. Amyloid plaques do not appear before diffuse PrP^d but can be found at a relatively early stage in infection confined to the corpus callosum and other ventricle associated sites (Bruce 1976, Bruce 1981). In contrast to plaques, diffuse PrP^d co-localises with areas of intense vacuolation (Bruce *et al.*, 1994a), neuropil damage (Jeffrey *et al.*, 1997) and by association, almost certainly with replication of the scrapie agent. The ubiquitous association of PrP^d with infectivity has more recently been called into question with the finding that significant levels of infectivity can be present in brains without detectable PrP^d or PrP^{Sc} (Lasmézas *et al.*, 1997, Manson *et al.*, 1999).

PrP^d can be seen consistently and reproducibly within particular rodent models of TSE but differs in distribution pattern between models (Bruce *et al.*, 1989,94a &b; Brown *et al.*, 2003). Diffuse PrP^d is located in specific neuroanatomical areas and the patterns of distribution observed at the terminal stage of disease can be used to identify strains (Figure 1.1). The patterns exhibited by mouse strains such as ME7, 87V, 79A, 22A, 22L (Bruce *et al.*, 1989,94a &b), mouse-adapted BSE and vCJD (Brown *et al.*, 2003) and hamster 263K (Beekes & McBride 1998) show differences in area targeted extent of relative deposition and glial involvement.

1.5.2 Visualisation of PrP^C in tissue sections.

Several PrP antisera are available from a number of donor species (mice, hamsters, sheep and cows) that recognise the full-length protein or fragments of it. The structural similarities of PrP allow many of the antibodies to recognise PrP in a variety of species as well as the one that supplied the antigen. There are no antibodies that can specifically identify PrP^C and PrP^d in tissue sections and this can be a problem when ICC is used as a diagnostic tool. PrP^C can be removed by a variety of pretreatments that include autoclaving at 121^0C and immersion in both undiluted formic acid and concentrated guanidine thiocyanate (Bell *et al.*, 1997). These procedures are harsh but appear to be largely effective on human and ruminant tissues. On less robust rodent tissue such treatments can produce artefacts that lead to false positives or uninterpretable results (P. McBride, unpublished observation). However, experimental protocols have been developed that allow PrP^C and PrP^d in the CNS of rodents to be distinguished by their differing physical appearance. Whereas PrP^d is seen in the variety of (largely) extracellular forms described above, in immunolabelled tissue sections PrP^C is intracellularly located and appears as a homogenous, finely granular form in unaffected neurones (Bruce *et al.*,1989, Beekes & McBride 1998). In the CNS of uninfected mice and hamsters, PrP^C immunolabelling can be seen only within a proportion of neuronal cell bodies. The greatest number of PrP^C-containing neurones are found in the brainstem and grey matter of spinal cord but some are also commonly found in the thalamus, hippocampus and dentate gyrus (DeArmond *et al.*,1987, Bruce *et al.*, 1989, Beekes & McBride 1998).

Outwith the CNS differentiation between different forms of PrP remains problematical. Identification of the diseased-state is particularly important in, for example, lymphoid or gastrointestinal tissues because these feature prominently in peripheral pathogenesis. The difficulty can be overcome by use of the recently introduced Paraffin Embedded Tissue (PET) blotting technique. PET blot pretreatments involve incubating sections for several hours in proteinase K to destroy PrP^C and leave only the proteinase K-resistant PrP (Schultz-Schaeffer *et al.*, 2000a).

Figure 1.1 Disease-specific forms of PrP

Amyloid plaques - cored or diffuse

Irregular aggregates

Punctate deposits - synapses, neuronal processes

Perineural accumulations

Neuronal inclusions

Glia - astrocytes, microglia

Diffuse - neuroanatomically targeted

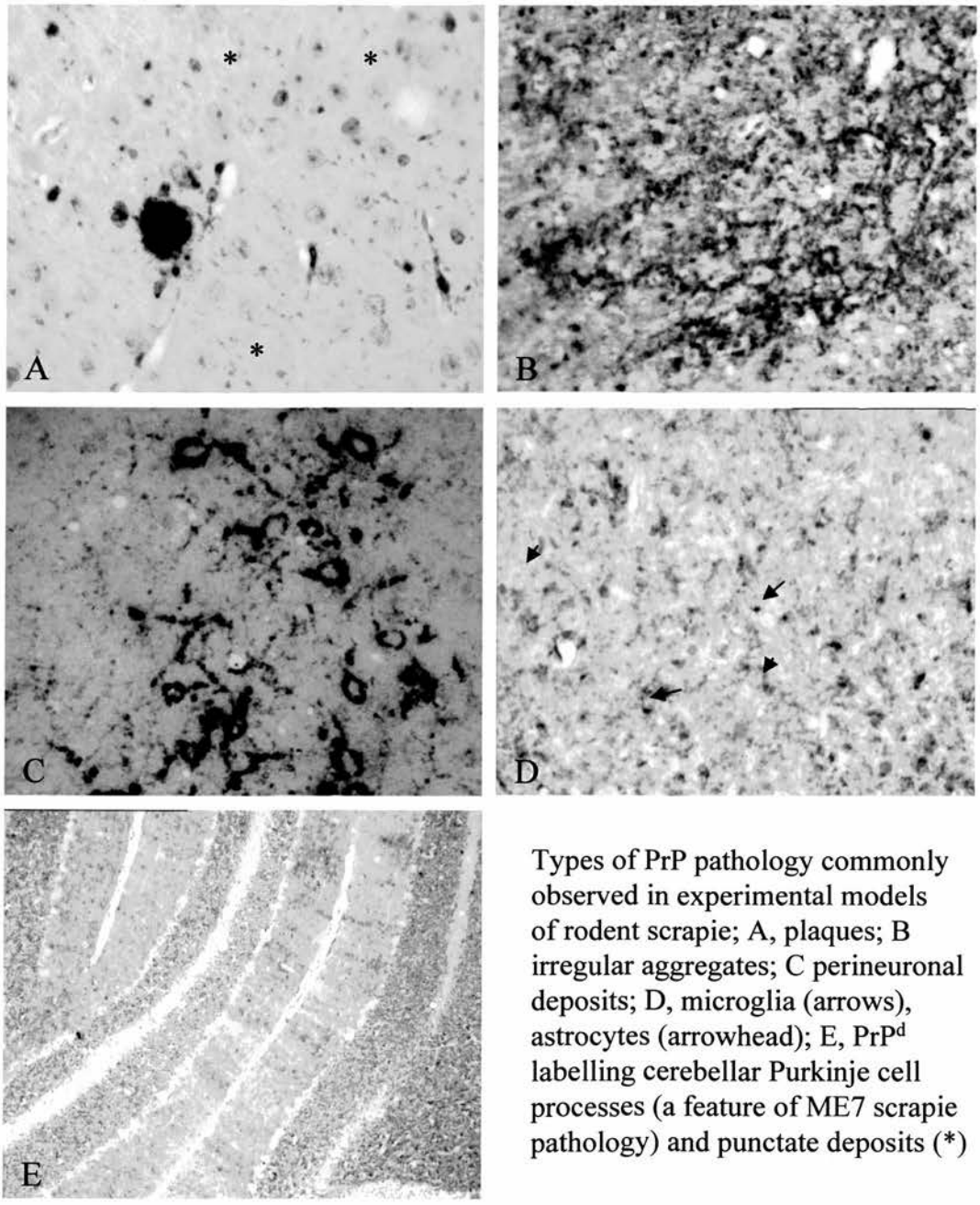

Types of PrP pathology commonly observed in experimental models of rodent scrapie; A, plaques; B irregular aggregates; C perineuronal deposits; D, microglia (arrows), astrocytes (arrowhead); E, PrP^{d} labelling cerebellar Purkinje cell processes (a feature of ME7 scrapie pathology) and punctate deposits (*)

Figure 1.2 Pattern of PrP immunolabelling in ME7 (A) and 87V (B) terminally-affected brain. Diffuse accumulations are prominent and neuroanatomically located in brains from both scrapie strains but areas of targeting differ. With ME7, PrP^d is widely distributed but some regions are more heavily labelled than others, e.g. CA3 region of hippocampus and dentate gyrus (dg). 87V scrapie is very precisely located in the CA2 region of the hippocampus and thalamic nuclei (T). Plaques (in box) are also typically numerous with this strain. The ovals show regions of aggregated PrP and circles, PrP-encircled neurones.

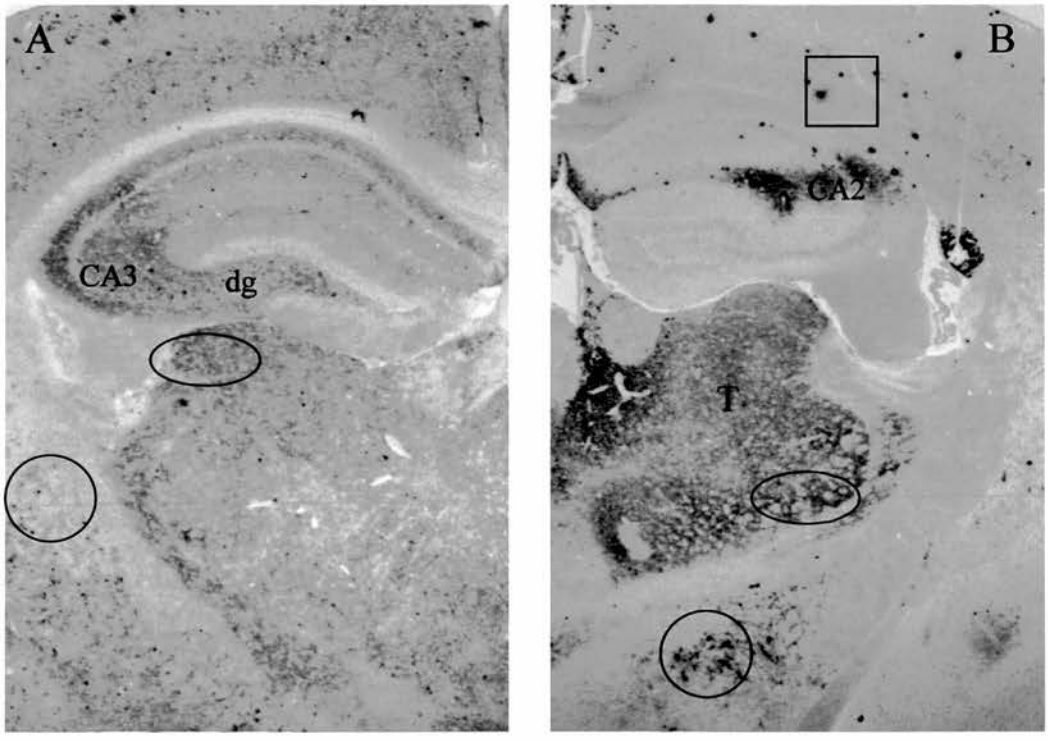

Table 1.2 Relationship of scrapie-related pathology to incubation period. Sequence of events occurring in *Prnp*^{b} *(Sinc p7)* mice after intra-cerebral injection of 87V scrapie brain homogenate. The onset of pathology and clinical signs are reproducible and consistent. Disease-associated PrP (PrP^{d}) appears some weeks before vacuolation and both occur long before the animal becomes ill.

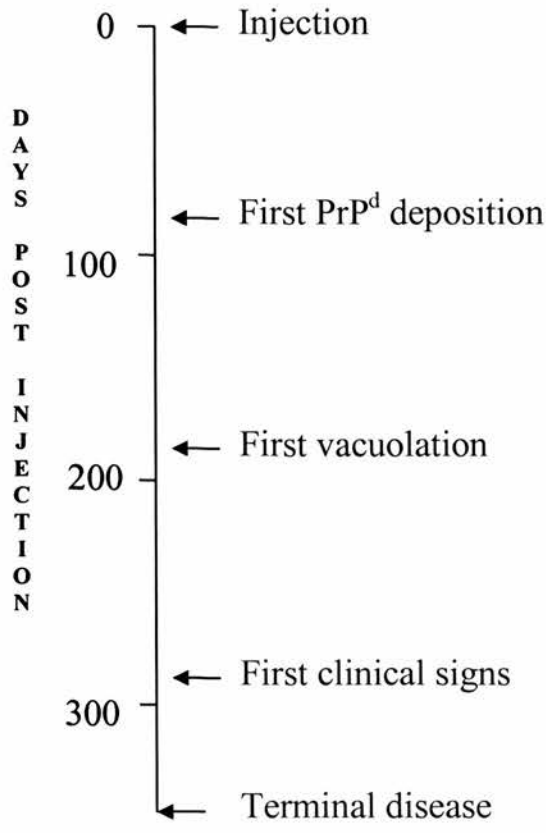

1.6 Peripheral pathogenesis

Until recently, the majority of studies examining the pathogenesis of the TSEs used genetically unaltered rodent models of experimental scrapie. Initially, experiments employed the intracerebral (i/c) route of infection. Although far from mimicking 'natural' infection, this route answered some scientific questions but it was soon recognised that more biologically relevant routes should be examined.

Although the ultimate target of TSE infection is the CNS there is evidence that both the LRS and the peripheral nervous systems (PNS) are involved in pathogenesis prior to CNS invasion. After oral or peripheral infection, neuroinvasion may occur directly via the peripheral nerves that innervate the GI tract or other visceral organs. Indirect neural spread is also likely following initial replication in lymphoid organs such as spleen or gut-associated lymphoid tissue. Haematogenous spread is possible but existing evidence suggests that this route does not contribute significantly to CNS infection in rodent (Dickinson *et al.*,1969, Casaccia *et al.*, 1989), or goat scrapie (Hadlow *et al.*, 1974, Pattison *et al.*, 1961), TME of mink (Marsh *et al.*, 1973) and in kuru, sCJD (Gibbs & Gajdusek 1972, Gajdusek 1977) or vCJD patients (Armstrong *et al.*, 2003). The role of viraemia in BSE remains unclear (Houston *et al.*, 2000). 'Selection' of the route that ultimately leads to neuroinvasion may be dependent of several factors including TSE strain and dose. Nevertheless, it has become convenient to refer to strains that show a propensity to direct neuroinvasion as 'neurotropic' and those that replicate in the LRS prior to CNS invasion as 'lymphotropic'. Possible pathways of neuroinvasion are outlined in Figure 1.3.

Figure 1.3 Possible pathways of neuroinvasion

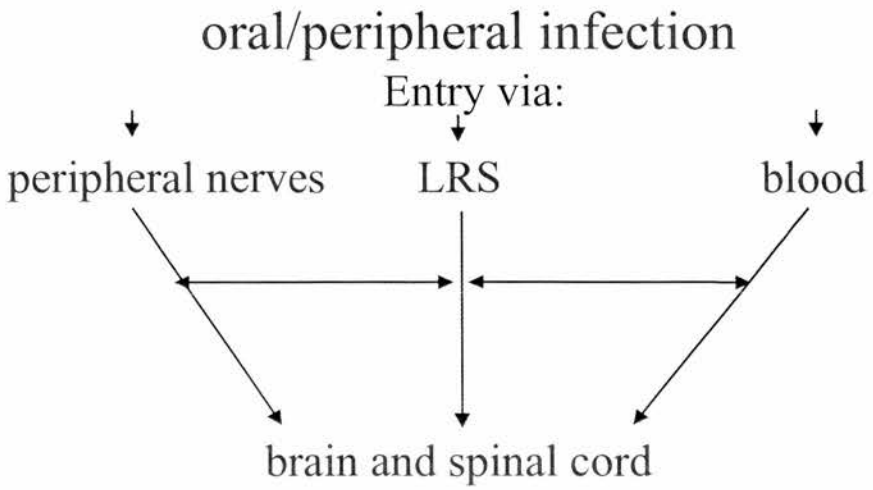

1.6.1 The lymphoreticular system in TSE pathogenesis.

Early studies measuring infectivity levels after intraperitoneal challenge (i/p) of mice with the Chandler strain (Eklund *et al.*, 1967) or in natural scrapie (Hadlow *et al.*, 1982) showed that, outside the CNS, the highest titres of infectivity are found in spleen and lymph nodes. After oral or peripheral routes of infection, several TSE agents replicate in lymphoreticular system (LRS) prior to CNS invasion (Fraser *et al.*, 1992b, Kimberlin & Walker 1979,88,89a, Ehlers *et al.*, 1984, Farquhar *et al.*, 1994, Mabbott *et al.*, 1998).

A functioning immune system has been shown to be necessary for TSE infection after peripheral challenge. Severe combined immunodeficient (SCID) mice which lack mature T and B lymphocytes (and, by association, follicular dendritic cells) resist peripheral infection with a mouse adapted strain of CJD (Kitamoto *et al.*, 1991), nor do they develop scrapie when infected with ME7 (or ME7-equivalent) and fail to replicate infectivity in their spleens (O'Rourke *et al.*, 1994, Fraser *et al.*, 1996, Lasmézas *et al.*, 1996). Engraftment of syngeneic bone marrow from immunocompetent donors restores susceptibility to ME7 infection and replication in spleen (Fraser *et al.*, 1996).

Splenectomy and genetic asplenia extend the incubation period in many rodent models if the spleen is removed before or shortly after i/p infection (Fraser & Dickinson 1970,78, Dickinson & Fraser 1977). Infectivity measurements of spleen fractions suggested that non-lymphoid cells could possibly support scrapie replication (Clarke & Kimberlin 1984). Also, as ionising radiation has no effect on the incubation period of peripherally infected mice, it was concluded that cells involved in scrapie pathogenesis were post-mitotic, long-lived cells which do not depend on stem cell replacement (Fraser & Farquhar 1987, Fraser *et al.*, 1989). Recent studies have demonstrated the importance of follicular dendritic cells (FDCs) in peripheral pathogenesis. These cells are radiation resistant and support scrapie replication in the spleen of mice (Brown *et al.*, 1999, Montrasio *et al.*, 2000). Studies infecting tumour necrosis factor (TNF)-α or interleukin (IL)-6 deficient mice and lymphotoxin beta receptor (LTβR) treated mice also sustain FDC involvement (Mabbott *et al.*, 2000a,b, Manuelidis *et al.*, 2000) in TSE pathogenesis. These mice either lack FDCs or germinal centre support for FDCs. The presence of both T and B lymphoctyes in the lymphoid tissues of these transgenic mice support the evidence that lymphocytes are probably not central to their extended survival after peripheral challenge.

Both cellular and disease specific forms of PrP are associated with FDC in spleen, mesenteric and gut associated lymph nodes (Kitamoto *et al.*, 1991, McBride *et al.*, 1992, Ritchie *et al.*,

1999, Beekes & McBride 2000, Jeffrey *et al.*, 2000). Though these studies suggest that PrP-expressing FDCs are key players, the mechanisms for peripheral replication, uptake and transfer of agent are likely to be complex and strain dependent. For instance, as FDCs rely on B cells for survival and maturity, the studies carried out so far cannot exclude the involvement of radiation-resistant, terminally-differentiated B lymphocytes (Blättler *et al.*, 1997, Klein *et al.*, 1997). Other cells such as macrophages (Beringue *et al.*, 2000) and migratory dendritic cells (Huang *et al.*, 2002) are also putative participants.

While many of the studies examining LRS participation in peripherally-aquired TSEs have been conducted using rodent models, the lymphoid system appears to have an equally important role in natural and experimental scrapie (van Keulen *et al.*, 1996,99, Andréoletti *et al.*, 1999,2000, Heggebo *et al.*, 2000, Schreuder *et al.*, 1998), CWD (Sigurdson *et al.*, 1999, Williams & Millar 2002), BSE in sheep (Foster *et al.*, 2001, Jeffrey *et al.*, 2001a) and possibly also vCJD (Hilton *et al.*, 1998, Collinge *et al.*, 1999, Hill *et al.*, 1999).

Despite this, there are examples where an intact immune system does not appear to be crucial for neuroinvasion. After intragastric or oral infection of mice with 139A or hamsters with 263K scrapie, replication in the spleen is not necessary for CNS infection or disease progression. In these studies, elevated brain infectivity titres preceded those of the spleen (Casaccia *et al.*, 1989, Beekes *et al.*, 1996) and splenectomy did not extend the incubation period (Kimberlin & Walker 1977,86,89a,b, Beekes *et al.*, 1996). Transgenic mice that expressed hamster PrP^{C} in neuronal but not lymphoid cells were susceptible to i/p or orally administered hamster scrapie (263K) even though infection was not established in the spleen (Race *et al.*, 2000). Also, in hamsters intraneurally infected with HY, a hamster-adapted strain of TME, PrP^{Sc} was detected in spleens only after being observed in brain suggesting that in this rodent model too, CNS infection is LRS independent (Bartz *et al.*, 2002). In addition, there is a striking lack of LRS involvement in BSE pathogenesis (Wells *et al.*, 1998) and although PrP has been found in association with lymphoid tissues from vCJD patients (Hilton *et al.*, 1998, Collinge *et al.*, 1999, Hill *et al.*, 1999), transmission studies have indicated that the LRS may not have a primary involvement (Manuelidis *et al.*, 2000). Furthermore, even with the lymphotropic strain ME7, SCID mice do sometimes succumb to peripheral challenge particularly if high doses are given (Fraser *et al.*,1996, Lasmézas *et al.*,1996, Mabbott *et al.*, 2000a). In these experiments using SCID mice, incubation periods were shorter than expected and either no infectivity or no PrP^{Sc} was detected in spleen. Taken together these findings show that after peripheral exposure, including oral

challenge, CNS invasion and disease progression can occur in the absence of LRS infection. An alternative way for this to occur is by way of peripheral nerves.

1.6.2 The peripheral nervous system in TSE pathogenesis

The idea that peripheral nerves could serve as conduits for infectious spread was first suggested by sciatic nerve transection studies and by experiments showing that, after peripheral challenge, extraneural replication could be bypassed if the infectious agent was injected directly into nerves (Kimberlin & Walker 1980, Kimberlin *et al.*, 83b,c,87). Infectivity can spread along linked neuroanatomical relays from outwith (Bartz *et al.*, 2002,03) or within the CNS (Fraser & Dickinson 1985, Scott *et al.*, 1989,1992, Muramoto *et al.*, 1993, Ingrosso *et al.*, 1999) and it has also been reported that PrP^{C} (Borchelt *et al.*, 1994) or PrP^{Sc} (Bartz *et al.*, 2002) can be transported along peripheral nerve axons. Substantial amounts of infectivity have been found in a number of fore and hind limb peripheral nerves of scrapie sheep (Groschup *et al.*, 1996), and in many peripherally-challenged rodent models, neural targeting of infectivity shows a pattern that is consistent with spread along peripheral nerves supplying the viscera (Kimberlin *et al.*, 1983b, Kimberlin & Walker 86).

In his experiments measuring the onset and spread of infectivity in rodent CNS, Kimberlin *et al* proposed that after oral or peripheral challenge, the scrapie agent spread to the spinal cord from abdominal viscera along sympathetic nerves (Kimberlin & Walker 80, 82, 86, 89b). This theory has been supported by studies showing that the incubation period of intraperitoneally infected mice can be extended by chemical or immunological sympathectomy (Glatzel *et al.*, 2001) and by findings presented in this thesis demonstrating the presence of PrP^{d} in spinal cord sympathetic neurones (McBride *et al.*, 2001).

Regardless of whether replication in lymphoid organs is a prerequisite, for disease to develop the infectious agent needs to be transported from peripheral sites to its ultimate target, the CNS. There is persuasive evidence for the involvement of the PNS in peripherally acquired TSEs affecting a variety of species including natural and experimental scrapie (Hadlow *et al.*, 82, Kimberlin *et al.*, 1983b, Lasmézas *et al.*, 1996, Groschup *et al.*, 1996,99, Baldauf *et al.*, 1997, Beekes & McBride 1998, McBride & Beekes 1999, van Keulen *et al.*, 1999,2000, Glatzel & Aguzzi 2000), BSE (Wells *et al.*, 1998), experimental CJD (Muramoto *et al.*, 1993) and vCJD (Niewiadomska *et al.*, 2002; Häik *et al.*, 2003).

From the accumulated data, the relative importance of either system in establishing infection appears to differ according to TSE model. The contribution of the LRS has largely been addressed using SCID and other types of immune-deficient mice. Separating the two interacting systems is not easy but this is now being addressed using transgenic mouse models. Experiments using transplantation and adoptive transfer of PrP-expressing tissue into PrP null mice were undertaken to provide better evidence of PNS involvement in peripheral infection (Blättler *et al.*, 1997, Glatzel & Aguzzi 2000). Engraftment of PrP^{C}-expressing cells into $PrP^{-/-}$ mice restored infectivity and PrP^{Sc} accumulation in lymphoid tissue but did not promote neuroinvasion. This suggested that another non blood-borne component; i.e. peripheral nervous tissue was also required for agent transportation (Blättler *et al.*, 1997). Studies using transgenic (Tg) mice have supplied more formal proof that neuroinvasion can occur independently of LRS involvement. Oral or peripheral 263K infection of Tg mice generated to express hamster PrP in PNS but not LRS compartments developed clinical scrapie. Therefore PrP expression in peripheral nerves (under control of the Neurone-Specific Enolase promoter) was sufficient for the transferral of infectivity from peripheral sites such as the gut to the CNS (Race *et al.*, 2000). The LRS was neither required as a site of replication nor for transferral of agent to the CNS.

1.6.3 Oral infection

It has long been recognised that the most likely way for lambs and sheep to become infected with scrapie is via the GI tract (Pattison *et al.*, 1974, Hadlow *et al.*, 1982) and this route is now generally accepted as the cause of BSE in cows (Wells *et al.*, 1998). TSEs are also recognised in wild species, e.g. TME of mink and CWD of mule deer and elk and although the mode of natural spread has not been formally proven in these animals, oral or alimentary transmission is suspected (Hartsough & Burger 1965, Hadlow & Karstad 1986, Williams & Young 1980, Marsh & Bessen 1993). Nevertheless, transmission of natural scrapie to sheep or goats could occur via scarification of gums or skin as this has been shown to be an efficient route of establishing infection (Carp 1982, Taylor *et al.*, 1996b). There are reports of scrapie outbreaks occurring in 'scrapie-free' flocks kept on pastures that previously housed scrapie infected animals (Pálsson 1979) possibly reflecting the continuing participation of a long-departed contaminant such as infected placenta or rotting flesh (Brown & Gajdusek 1991). In man, kuru was reportedly spread by ritualistic cannibalism (Gajdusek 1977, Cervenakova *et al.*, 1998) but the extent of this practise has been challenged (Taylor 1989). Skin scarification was subsequently suggested as a probable cause with route of entry via cut or abraded skin (Liberski & Gajdusek 1997, Goodfield 1997). The oral route of infection assumed a greater significance when BSE, and then vCJD, were reported. The overwhelming data linking the two diseases (Bruce *et al.*, 1997; Hill *et al.*,

1997) strongly suggests that both cows and human sufferers contracted their illness through eating material infected with TSE agent. However, relatively little is known about how the infectious agent reaches the CNS once it has gained access to the gut. Apart from the alimentary tract being a potential site of early infection and diagnosis, this information is vital for therapeutic intervention in these diseases.

As is the case for PNS involvement, the number of publications addressing the extraneural distribution of infectivity or PrP^d after oral infection has grown rapidly since the arrival of BSE and vCJD. Studies including those generated from this body of work show that the ENS and gut associated lymphoid tissues are early players in oral pathogenesis of these diseases (Wells *et al.*, 1994, 98, Andréoletti *et al.*, 2000, Beekes & McBride 2000, Heggebo *et al.*, 2000, 02, 03, van Keulen *et al.*, 2000, Jeffrey *et al.*, 2001a, McBride *et al.*, 2001, Bons *et al.*, 2002, Terry *et al.*, 2003). Nevertheless, many questions remain unanswered not least the mechanism(s) of uptake and the associated cellular interactions. Thus, though the PNS, LRS and ENS are implicated in TSE peripheral pathogenesis, the relative contribution and interaction between these systems is likely to be multifactorial and strain dependent.

1.7 Aims

Previous approaches addressing the dynamics of spread showed that in a number of peripherally-challenged rodent models of scrapie, infectivity (Kimberlin & Walker 1982,86,89b), and PrP^d (Beekes *et al.*, 1996, Baldauf *et al.*, 1997) was first detected in central portions of the thoracic cord. The infectious agent subsequently spread to the brain and other parts of the spinal cord in a pattern that was consistent with propagation along the autonomic nerves that innervate the visceral organs. However, there was limited information about the neural pathways involved in spread of TSE agents after natural routes of infection. In addition, little attention had been paid to the GI tract and information about possible sites and mechanism of agent uptake agent was lacking even though the most probable portal of entry of the TSE agent is through the alimentary tract.

This study aims to investigate PNS involvement in oral infection and define any neuronal pathways employed by the infectious agent during routing from the GI tract to the CNS. PrP immunocytochemistry was used in conjunction with paraffin-embedded tissue (PET) blotting and selective infectivity bioassays to determine the temporal and spatial location of PrP in the CNS, PNS and ENS of hamsters orally-challenged with 263K scrapie. PrP^d is used as a marker for infection as previous experiments have shown that there is a close correlation between PrP^d

and the infectious agent in the rodent model of scrapie used in this study (Beekes *et al.*, 1996, Baldauf *et al.*,1997).

The first experiment focuses on the sites of PrP deposition in brain to elucidate and locate neuroanatomical region to which PrP^d is targeted at the early stages of infection (Chapter 2). This chapter also reports the sequential development and cellular association of PrP pathology. Subsequent to this, a detailed study examines the temporal appearance and ensuing accumulation of PrP in the circuitry of the vagus and splanchnic nerves (Chapter 4). These nerves innervate a number of visceral organs including spleen and lymph nodes. Gut-associated lymphoid tissue (GALT) and the enteric nervous system (ENS) of the small intestine is also included (Chapter 5) as these are possible sites of uptake of TSE agent and can link directly or indirectly with the CNS. The difficulties associated with excision and microscopic presentation of peripheral components from hamsters necessitated a pilot study to ensure the feasibility of the proposed techniques (Chapter 3).

Chapter 2: Temporal and spatial targeting of PrP^d in the CNS of 263K-fed hamsters

2.0 Introduction

Although the oral route of infection has long been established in experimentally dosed sheep and goats (Pattison & Millson 1961, Pattison *et al.*, 1972,74) prior to the renewed interest through BSE, there had been relatively few publications reporting oral challenge of rodents with scrapie. Also, due largely to the inefficiency of the route or inadequacy of dose, even fewer of those has provided meaningful results (Zlotnik & Rennie 1962, Kimberlin & Walker 1979,86 Carp 1982, Prusiner *et al.*, 1985). However, in the 1970s and 80s Richard Kimberlin and co-workers carried out a series of experiments measuring the onset and spread of infectivity in the brain and spinal cord of rodents after various peripheral routes of infection including intragastric challenge (Kimberlin & Walker 1979,80,82,86,89b, Cole & Kimberlin 1985). These findings suggested that the infectious agent firstly accessed the CNS at the mid-thoracic cord and then spread upwards towards the brain. Later studies focusing on the oral route and using Western blot analysis and protease-resistant PrP (PrP^{Sc}) as a marker for infectivity (Beekes *et al.*, 1996, Baldauf *et al.*, 1997) supported these early findings and localised the entry to thoracic segments T4-T9. In addition, other observations (Kimberlin & Walker 1982, Muramoto *et al.*,1993, van Keulen *et al.*,1995) suggested the existence of a further pathway that, after peripheral challenge, permitted the infectious agent direct entry into the brain. Support for this was provided by Western blot analysis of brain homogenates taken from intraperitoneally infected hamsters that had been culled at successive points through the scrapie incubation period. Results from this study indicated an alternative independent route that by-passed the spinal cord and entered the brain via the medulla (Baldauf *et al.*, 1997) but there were no previous reports describing the specific location of the entry site. The medulla is a large area and while PrP^{Sc} can be demonstrated very satisfactorily using Western blotting the method is limited in that it can detect only the presence or absence of the protein within a sample of homogenised tissue. Therefore, in order to localise disease-specific PrP (PrP^d) precisely, in this study, immunocytochemistry (ICC) was used. This technique allows the specific identification of a protein in tissue sections prepared to retain their original appearance and cellular morphology. As with Western blotting, the desired protein is detected using an antibody-antigen reaction that has been tagged by a chromagen but unlike Western blotting, the protein can be visualised *in situ* so individual cells and their associated components can be identified along with their precise location.

The aim of this first experiment was to identify the presence and anatomical location of PrP^d within the brain and spinal cord of hamsters orally-infected with 263K scrapie. To achieve this, a time-course study was employed with brain and spinal cord being collected at points throughout the incubation period. While bioassays are the method of choice for detection of scrapie agent they require large numbers of laboratory animals and are very time consuming. ICC can be used to elucidate sites of infection by using disease-associated forms of PrP as surrogate markers for infectivity. As was explained in Chapter 1, a close correlation between infectivity and PrP^{Sc} has been previously established in this animal model (Beekes *et al.*, 1996, Baldauf *et al.*, 1997).

After ICC, the presence, physical appearance and temporal deposition of PrP were assessed using light microscopy. Kimberlin had proposed that spread to the spinal cord from peripheral sites occurred along sympathetic nerves (Kimberlin and Walker 1988). Although it was known that neurones were key targets for scrapie pathology, there was little or no information about the specificity of targeting after oral infection, i.e. the actual groups of neurones that were involved. It was hoped that this approach would provide information to aid identification of the neuronal pathways that had been used to reach and invade the CNS after oral challenge possibly by helping to confirm this hypothesis or at least by clarifying the involvement of the medulla in oral pathogenesis.

2.1 Materials and methods

Outbred Syrian Golden hamsters were infected with 263K scrapie by feeding 100µl of a 10% brain homogenate prepared from a pool of hamster brains terminally-infected with 263K agent. Each measured dose of inoculum was placed on a food pellet of standard laboratory diet and left for a few minutes to be absorbed. To ensure each hamster received the correct dosage, cagemates were separated and given their prepared food pellet in individual cages. Prior to this, the hamsters had been deprived of food overnight and the pellets were either eaten readily or within the next one to two hours. On being reunited, the hamsters quickly integrated and the temporary separation had no effect on their subsequent social behaviour. Groups of four hamsters were culled by CO_2 euthanasia at 84, 91, 98, 105, 113, 119, 126, 133 days post infection (dpi) and at 156 dpi, when they had reached the terminal stage of disease. Four uninfected controls were culled when they were between 180 and 210 days of age.

The brain and spinal column (excluding the most caudal lumbar and sacral regions) were removed and immersion fixed in paraformaldehyde-lysine-periodate (PLP) overnight. After fixation, two of the brains were bisected mid-sagitally along the longitudinal fissure. The other

two brains were trimmed coronally into five pieces according to the standard levels used in our laboratory for vacuolar lesion profiling (Figure 2.1A). The spinal column was cut transversely into seven pieces, each containing multiple segments of cervical (C) or thoracic (T) cord. The pieces corresponded to vertebrae segments C1-3, C4-7, T1-3, T4-6, T7-9, T10-11, T12-13 (Figure 2.1B&C). The cord pieces were then marked at their cranial ends with Indian ink and, along with the brain pieces, dehydrated in alcohol over another six hours and embedded in paraffin wax. The seven segments were processed separately and embedded together in one block. To ensure that each piece could be individually identified they were positioned in wax according to a pre-arranged design. When viewed under the microscope each piece was identifiable by its location within the block (Figure 2.1D). The sagittally and coronally sliced pieces of brain were similarly embedded in individual blocks (Figure 2.1E & F).

•Sets of adjacent sections were cut at six microns thick, floated onto a warm water bath and dried in an oven at 37^{0}C. One section was stained with haematoxlyin and eosin to enable the cellular morphology to be assessed. Another was stained with cresyl violet and Luxol Fast Blue (CV/LFB) to aid the neuroanatomical identification of cell types. Two others were used for PrP immunolabelling (one to which PrP antibody was applied and one that was used as a serum control) and two were kept as spares in case the immunolabelling had to be repeated.

Immunolabelling was carried out according to the 'Indirect' method using the mouse anti-hamster monoclonal antibody, 3F4 (Kascsak *et al.*, 1987) to label PrP and diaminobenzidine (DAB) to visualise the reaction product. Prior to immunostaining sections were treated with formic acid for 10 minutes to enhance staining (see Appendix 2 for full description of method). PrP^d was mapped according to its location using an atlas (Stereotaxic Atlas of the Golden Hamster Brain: Morin and Wood: Eds, Academic Press)

Due to the lack of contrast and paucity of early deposition, computerised image analysis could not be employed as an aid to quantification therefore the accumulation of PrP^d observed in immunolabelled sections was scored using light microscopy according to the following criteria:

\+ Punctate deposition on surface of, within and/or in the adjacent neuropil of individual or small groups of neurones. Deposition very focal. Visible only at high magnification.

• Up to this point, the procedures were carried out in Berlin by my collaborator, Michael Beekes, after appropriate histopathology training by the author. All subsequent procedures were carried out at the Neuropathogenesis Unit.

++ Similar cellular appearance and location but greater numbers of individual neurones involved within single groups. More groups included. Extracellular distribution is more extensive but remains localised to associated neurones.

+++ Deposition diffusely granular in appearance and associated with large numbers of neurones and many groups. Substantial extracellular accumulations deposited widely within neuroanatomical areas.

++++ Very heavy deposition characterised by many protein aggregates. Extensive granular deposition throughout most regions. Easily observed at low magnification.

Immunolabelled sections were examined without prior knowledge of the experimental status of the animal.

Figure 2.1 Brain and spinal cord slicing levels

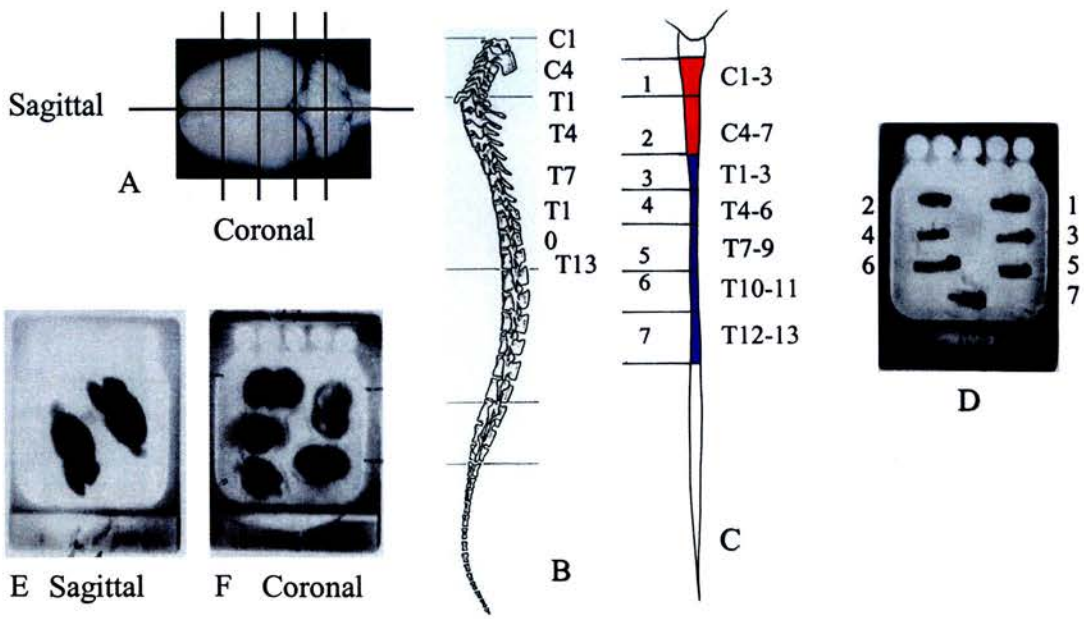

2.2 Results

2.2.1 Temporal appearance and topography of PrP in the CNS of 263K-challenged and uninfected hamsters

Results are summarised in Tables 2.1 and 2.2 and Figures 2.2A and B. The onset of PrP^d deposition varied between individual animals as did the extent of deposition within a group of animals from a given time point, i.e. tissues from the earliest time points did not necessarily contain the least labelling nor later time points the most. This occurrence reflects the biological variation between animals observed previously in similar experiments. The temporal progression of deposition was, therefore, only apparent when results from all cases were viewed overall. For this reason, 'snapshots' of individuals were not representative of the timing of events so results from Figures 2.2A and B and Table 2.1 are pooled to show the trend of spread and accumulation over time. Though the timing of PrP^d deposition was variable, the location of initial deposition and sequence of subsequent target sites was very consistent (Tables 2.1 and 2.2). The results correspond to the sequential appearance and distribution of PrP^{Sc} in the brain and spinal cord that was determined previously by Western blotting (Beekes *et al.*, 1996).

2.2.1i Brain

Figures 2.2A and B show pictorial representations of PrP in sagittal (A) and coronal (B) brain slices. Coronal and sagittally sliced brains were employed to maximise the visualisation of PrP and demonstrate its 3-dimensional distribution more effectively. (A) shows the initial target sites in the medulla and the subsequent caudal to rostral direction of spread and (B) compares the distribution of PrP^d at early and terminal stage of disease. Table 2.1 shows the sequence of the brain areas in which PrP^d appeared against time.

PrP^d was first detected at 91dpi in the medulla of all four hamsters. The first target site for PrP^d deposition was in the dorsal nucleus of the vagus nerve (DMNV) followed immediately afterward by the adjacent commissural portion of the solitary tract nucleus (SN) [Figures 2.3A&B]. Very often both these sites were labelled but when compared, the DMNV was consistently more heavily labelled and contained a wider distribution of PrP^d within the nucleus than the SN (see figure 2.3C). Also, in one brain from the earliest group of 91dpi, PrP^d was present in small amounts in the DMNV but lacking in the SN suggesting that PrP^d was deposited in the DMNV before the SN. Shortly after this, PrP^d was located in the superior vestibular nucleus and in the gigantocellular nucleus of the reticular formation. Labelling extended through the SN towards the area postrema although this was itself negative. Subsequently, PrP^d was observed in several other nuclei of the medulla, predominantly those of the vestibular network or

Table 2.1 Topographical sequence of PrP^d targeting in brain.

Temporal order of appearance ▼

DPI	Medulla	Cerebellum	Midbrain	Thalamus	Cortex
91	DMNV/SN Spinal Vestibular nuc. Superior Vestibular nuc. Gi				
98	ParaGi Raphe obscurus Raphe magna Inferior Olive Accessory Olive	Medial Cerebellar nuc. Interposed nuclei	Red nucleus		
105	Medial Vestibular nuc. PCRt Medullary Retic. nuc.		Substantia nigra (reticular field)		
113	Intermediate Retic. nuc SN medial	Lateral Cerebellar nuc.	Pontine Retic. nuc. Oral Medial Geniculate nuc. Periaqueductal grey matter	Ventrolateral thal. nuc. Ventromedial thal. nuc.	
119	Widespread	Granular layer	Lat. Dors. Tegmental nuc. Retrorubral field	Mediodorsal thal. nuc. Centromedial thal. nuc.	Frontal
126		Widespread	Superior colliculus	Parafascicular thal. nuc.	Parietal
133			Widespread	Dorsolateral Geniculate nuc. Lateral Posterior thalamic nuc. Dorsal hypothalamic nuc. Dorsomedial hypothal. nuc.	Cingulate
156(EP)				Widespread	Occipital Temporal

Abbreviations:DMNV/SN:Dorsal motor nuc. of vagus nerve/Solitary tract nuc.,Gi;Gigantocellular reticular nuc.,PCRt; Parvocellular reticular nuc., EP; Endpoint of disease

Table 2.2 Distribution and accumulation of PrP^d in spinal cord segments of individual hamsters culled in groups throughout the incubation period

Dpi	C1-3	C4-7	T1-3	T4-6	T7-9	T10-11	T12-13
84	-	-	-	-	-	-	-
84	-	-	-	-	-	-	-
84	-	-	-	-	-	-	-
84	-	-	-	-	-	-	-
91	-	-	-	+	+	-	-
91	-	+	++	+	++	+	-
91	-	+	+	+	++	+	-
91	-	+	+	+	-	-	-
98	-	-	$-^P$	-	-	-	-
98	-	-	-	-	+	-	-
98	-	-	-	+	-	-	-
98	-	-	-	-	-	-	-
105	-	-	$-^P$	-	-	-	-
105	+	$-^P$	+	+	++	-	-
105	-	-	-	+	++	-	-
105	-	-	-	+	+	+	-
113	-	$-^P$	+	+	+	+	-
113	-	-	-	-	-	-	-
113	+	+	$+^P$	++	++	+	+
113	-	-	$-^P$	+	-	-	-
119	-	$+^P$	-	+	++	+	-
119	++	++	++	+++	+++	+++	+
119	++	++	$+++^P$	+++	++++	+++	++
119	-	-	-	-	-	-	-
126	-	-	-	-	-	-	-
126	-	$-^P$	$-^P$	$++^P$	+	-	-
126	+	$+^P$	+	++	+++	++	+
126	-	-	-	-	-	-	-
133	++	++	$++^P$	$++^P$	++	+	+
133	++	++	++	+++	+++	+++	++
133	++	+	++	+++	+++	++	++
133	+++	+++	+++	++++	++++	+++	+++
156 EP	+++	$+++^P$	++++	++++	++++	+++	+++
156 EP	++++	+++	++++	++++	++++	++++	+++
156 EP	++++	++++	$++++^P$	++++	++++	++++	++++
156 EP	+++	$+++^P$	+++	++++	++++	+++	+++

P, p: DRG present adjacent to cord segment; P: +ve, p: -ve; EP: endpoint of disease

Figure 2.2A Sequence of PrP^d targeting in the CNS. Selected mid-sagittal slices cover the range between the first appearance at 91dpi and terminal disease. Distribution (shaded areas) represents the trend of accumulation rather than the absolute pattern at a given timepoint. Greater intensity of colour denotes greater deposition. Note: Labelling is present simultaneously and independently in medulla (DMNV) and thoracic cord; Spread occurs in a caudal to cranial direction. Cx, cortex; Cb, cerebellum; Med, medulla; Mb, midbrain; T, thalamus

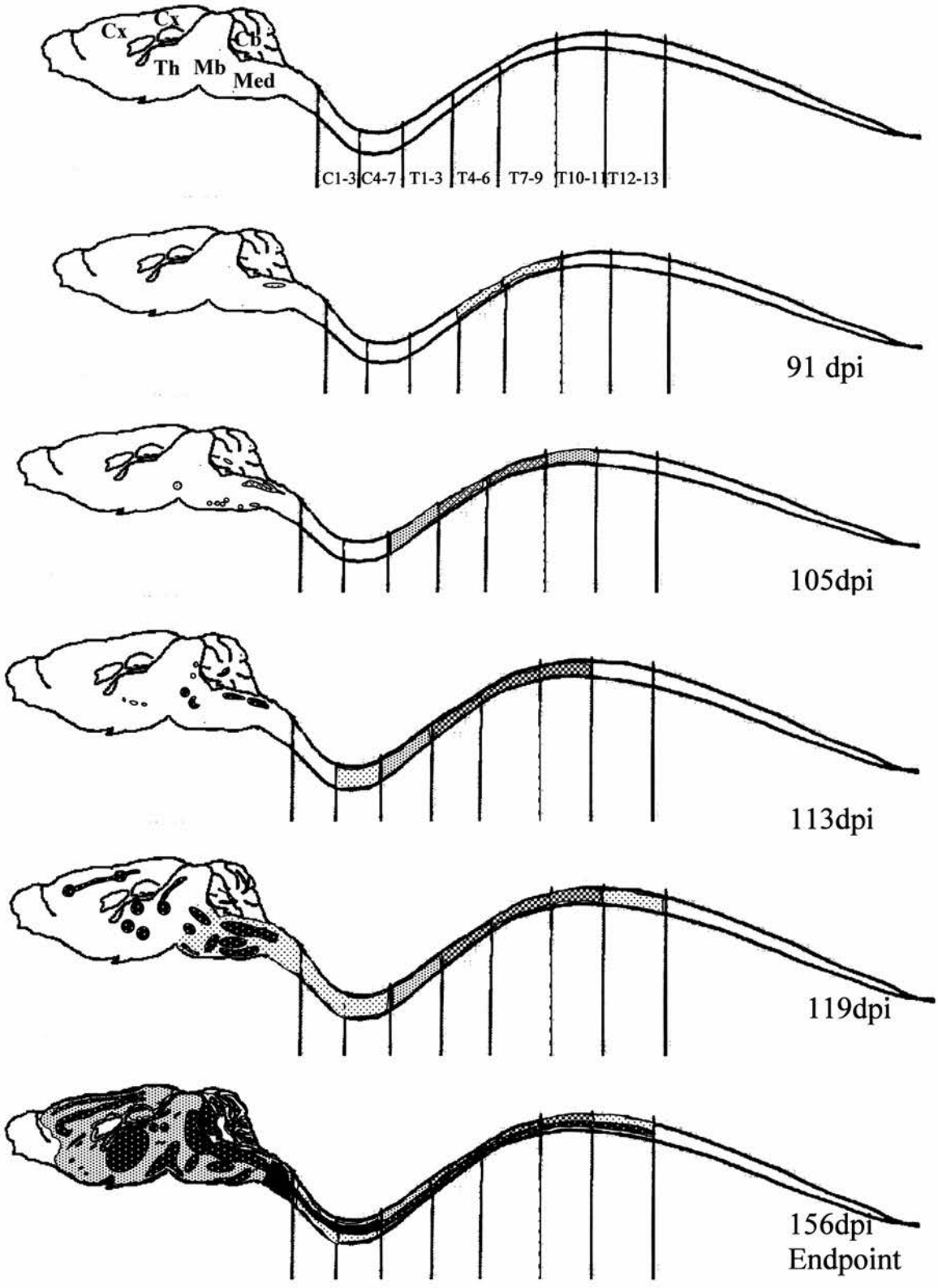

Figure 2.2B Scheme of PrP^d deposition in coronal brain slices. At endpoint, (right column) the heaviest deposition (darker red shading) is frequently found in sites where deposition occurred first (left column). Abbreviations: caudal to rostral; SN; solitary tract nucleus, DMNV; dorsal nucleus of vagus nerve, SpVe; spinal vestibular nucleus; CeN; Cerebellar nucleus, SuVe; superior vestibular nucleus, Gi; gigantocellular nucleus, RMg; Raphe magna, Med GN; Medial geniculate nucleus, RN; red nucleus, SN; substantia nigra, VM; ventromedial thalamic nucleus, FrCx; frontal cortex

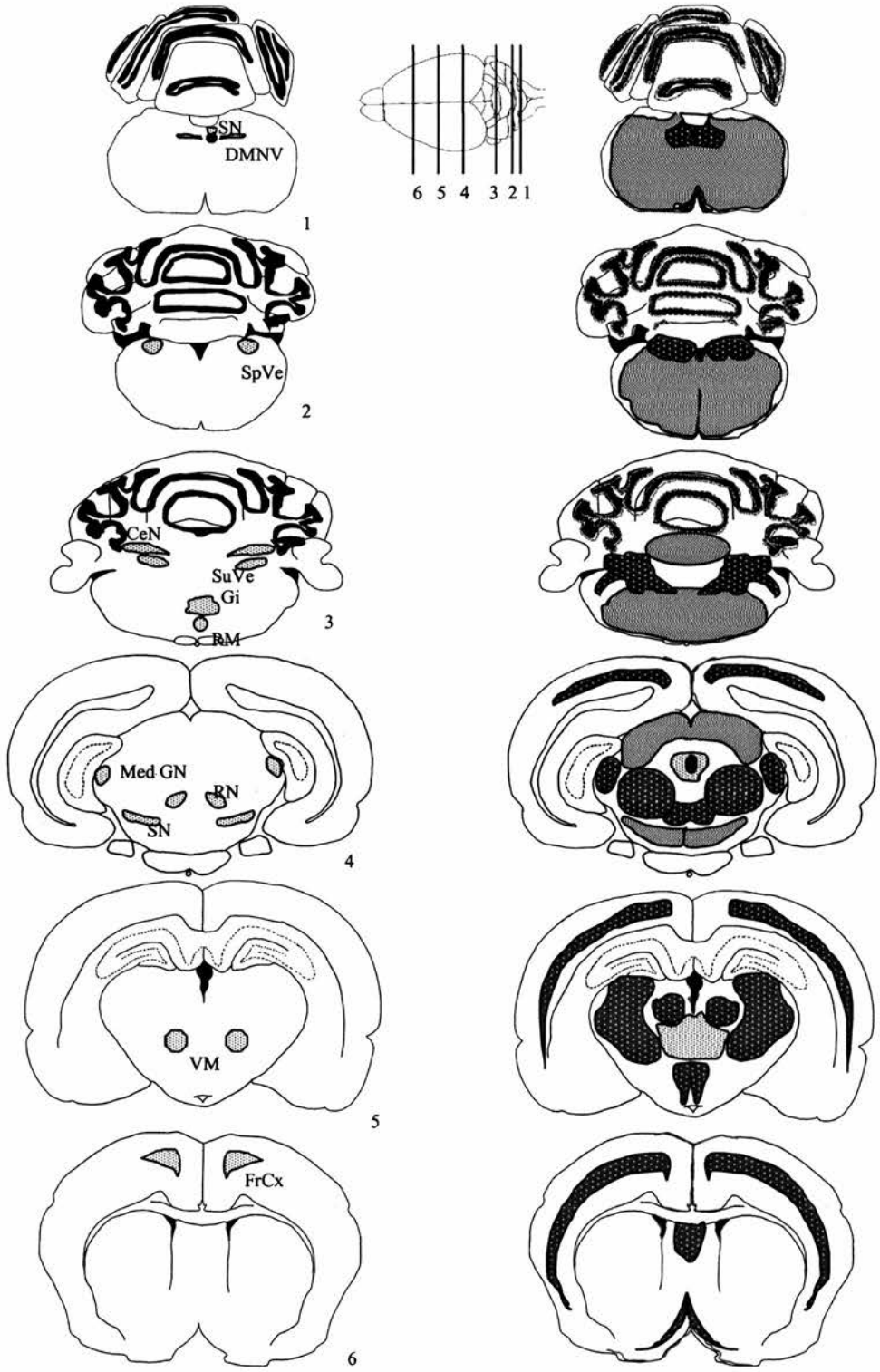

the reticular formation; the spinal and medial vestibular nuclei, the parvocellular reticular nucleus, the inferior and dorsal accessory olives and the lateral paragigantocellular nucleus. Deposition then extended into the medial and interposed nuclei of the cerebellum (Figure 2.3D), pons and midbrain (raphe and pontine nuclei of the reticular formation and red nucleus) [Figure 2.3E]. By comparing the brain maps from individual hamsters, spread from the initial site of entry (DMNV) to the midbrain occurred very quickly – between approximately 91 dpi and 113 dpi. The spread of infection to subsequent target nuclei was so rapid that a clear temporal separation was not possible. Nevertheless, the trend of further spread was in a caudal to cranial direction Figure 2.2A). At 113 dpi, PrP^d could be detected for the first time in the thalamus (ventromedial thalamic nucleus) and by 119 dpi it was throughout the thalamus and in the hypothalamus, medial geniculate nucleus, and in the parietal, cingulate and frontal cortex. At 133 dpi deposition was still located in defined anatomical areas but was considerably more widespread within them. By 156 dpi, when the disease had reached its clinical stage, PrP^d was distributed throughout almost all brain areas (Figure 2.3F).

2.2.1ii Spinal cord

The temporal appearance, segmental distribution and accumulation of PrP^d in spinal cord of individual animals are shown in Table 2.2. Figure 2.2A shows a pictorial representation of the relationship between accumulation in the spinal cord and brain.

As with brain, the first deposits of PrP^d were seen at 91dpi in grey matter of vertebral segments T4-T9. Early labelling was observed in segments T4-6 and T7-9 but the comparatively heavier deposition seen on a number of occasions in segment T7-9, suggests that PrP^d appeared here first. Thereafter, PrP^d was deposited in both cranial and caudal directions being observed next in segments T1-3 and T10-11 and then in C4-7. The temporal appearance of protein in these segments occurred almost concurrently or within days of each other and was observed in all or most of these segments between 91dpi and 113dpi. The rapid pace of events made a precise temporal separation difficult and it was not clear whether PrP^d deposition at the later sites was a consequence of spread from adjacent segments or separate points of entry. PrP^d appeared last in C1-C3 and T12-13, the most cranial and most caudal segments, but in one case all cord segments were positively labelled by 113dpi, albeit at low levels of accumulation (Table 2.2, Figure 2.6 and text of section 2.2.2).

As the spinal cord was cut longitudinally rather than transversely, it was difficult to accurately identify specific nuclei in which deposition occurred. This was especially so with early cases but

in later stages of infection, deposition was very widespread with both dorsal and ventral horns being affected. In the main, PrP^d accumulated around grey matter neurones (Figure 2.4A). White matter remained largely unlabelled (Figure 2.4B). Nerve roots abutting brain or attached to dorsal root ganglia (DRG) were unlabelled and even at end-stage disease the lack of white matter staining visibly contrasted with the heavily stained neurones (Figure 2.4B,C).

2.2.1iii DRG

Dorsal root ganglia had not been included specifically but some had remained attached to segments of the spinal cord. When these were present, the location and extent of PrP labelling was recorded. DRG were present, albeit few in number, in time-points ranging from 98 dpi to 156dpi. PrP^d was first detected within the large sensory DRG neurones at 113dpi (Table 2.2). Deposition was very scant at this and all other time-points except end-point (Figure 2.4C). In all cases, PrP^d was seen in DRG only when the corresponding section of spinal cord also contained PrP^d. Furthermore, accumulations were always more plentiful in cord than in the DRG. In several cases DRG were negative for PrP^d but the associated section of cord was positive but there were no instances where the reverse was seen. This suggests that PrP^d first appeared in spinal cord and then in adjacent DRG. As the two are linked together it seems plausible that 263K scrapie initially entered the spinal cord and spread via adjoining nerve roots to DRG.

2.2.2 Dynamics of PrP accumulation in CNS during the incubation period

Deposition was scored according to the described criteria to indicate the relative amounts of protein in the different areas at various time-points. The score took into account the cellular and regional distribution of PrP^d accumulation. This was important because PrP^d was often present in several different areas of the same brain or cord. Figure 2.5 gives examples of PrP^d deposition and the accumulation that is typically observed over time. Each has been chosen to illustrate how the microscopic assessment relates to the assignation of scores.

At the first time-point at which PrP^d could be detected (91dpi), deposition was in or around only a very few neurones (scored one '+'), [Figure 2.5A]. Scores, reflecting the level of accumulation, rose slowly over time but remained low (mostly around '++') even when PrP^d was present in multiple sites (Figure 2.5B). Even at the relatively late stage of 126dpi (endpoint of incubation was 156dpi), the brains and spinal cords of two of the four hamsters culled at this time had little or no detectable PrP^d. Apart from two hamsters culled at 119dpi, levels of PrP^d did not rise significantly until 133dpi. In the last 4 weeks of the incubation period, there was a sharp rise in the amount of PrP^d present (Table 2.2). Accumulation was rapid, and at the end-stage of

disease very heavy deposits were easily evident at low magnification in all brains and cords (figure 2.5D). However, in the most rostral brain regions, e.g. the frontal and olfactory lobes of brain and the most cranial cervical (C1-4) and caudal thoracic (T12-13) segments of spinal cord remained less heavily stained than the rest of the CNS.

The dynamics of accumulation mirrored the clinical course of the disease. For most of the incubation period animals were asymptomatic of disease. This was followed by a short clinical phase of only a few weeks in which animals exhibited neurological signs and physical deficits. This could be interpreted that the clinical symptoms arise from PrP^d-induced neuronal dysfunction.

As PrP^d deposition correlates with infectivity these results suggest that in the CNS, levels of infectivity are slow to rise and reach significant levels only in the latter stages of the disease. These findings compare favourably with the previous correlative studies (Beekes *et al.,* 1996). The sharpest rise in infectivity occurred in the latter stages of disease but infectivity rose steadily from around 90 days. Infectivity assays are very sensitive indicators of infection and ICC is likely to be comparatively less so. Nevertheless, even allowing for reduced sensitivity, the scoring method applied here provides a useful indicator of the trend of infection. Although scores from individual areas were initially low the number of sites containing PrP^d was slowly increasing thereby adding to the cumulative amount of protein and, by association, replicative capacity.

The estimated amount of PrP^d present in a specific area served as an indicator of the timing of deposition. Areas with substantial accumulations scored higher and were presumed to be at a more advanced stage of pathogenesis than areas where diffuse or less aggregated forms of PrP^d existed. This was borne out by the results. Progressive accumulation was a consistent feature of advancing incubation period. The first sites in which PrP^d was observed (initially the DMNV, SN and medullary nuclei) always received low scores. As time progressed these 'early' sites contained more PrP^d and consequently received higher scores than more rostrally located brain areas e.g. nuclei of midbrain or thalamus in which PrP^d was present for the first time. At terminal stages of disease the greatest levels of accumulation were seen in those sites in which PrP^d had been detected first. Similarly, scores of '+' and '++' predominated in early timepoints while the preponderance of high scores (+++ and ++++) occurred late in the incubation period. In the CNS of one hamster culled at an early time-point the pattern of deposition was temporally more advanced than was usual i.e. deposition was already present in several regions. Nevertheless,

PrP^d was still more abundant in the DMNV and SN and accordingly obtained higher scores than other regions.

When the amount of PrP^d found in the brain of individual hamsters was compared with that seen in the spinal cord of the same animal, the levels corresponded very well. For example if a brain contained either scant or abundant PrP^d accumulations, deposition in the corresponding spinal cord was equally restricted or widespread. The trend of accumulation was also comparable both within and between groups of animals. This consistency of results gives credibility to the method used to estimate PrP^d deposition and showed that it was a useful indicator of progression of PrP pathology.

2.2.3 Summary of Results from 2.2.1 and 2.2.2

Results from temporal appearance and topography show consistently that PrP^d is first located in the DMNV. The reproducibility of this finding together with the progressive accumulation in this site suggests that after oral challenge the 263K agent accesses the brain at this location and subsequently replicates here. In short, the DMNV is an early 'target site' for the scrapie agent in this rodent model.

2.2.4 Cellular and physical appearance of PrP in CNS of unaffected and infected hamsters

2.2.4i PrP in unaffected hamsters

In common with previous findings in mice (Bruce *et al.*, 1989, McBride *et al.*, 1998) in mock-infected control hamsters host PrP (PrP^C) was seen distributed throughout the CNS but only within a proportion of neuronal cell bodies. The greatest number of positively stained neurones was in the brainstem and grey matter of spinal cord but a few were also commonly found scattered in the thalamus and the hippocampus, in particular in the dentate gyrus. The cytoplasm of these cells stained mainly light brown (conferred by the DAB chromagen) but the intensity of the brown labelling varied, perhaps reflecting PrP^C 'turnover' or physical state. PrP^C was of uniform appearance as opposed to granular (Figure 2.6A) but staining was always less intense and differed markedly from any of the (largely extracellular) disease-associated forms found in orally challenged animals. PrP^C positive neurones were occasionally seen in infected hamsters.

Figure 2.3 PrP^d immunolabelling (brown) in the brain. A,B & C. Early (91dpi) target sites (coronal sections); A) DMNV, B) central portion of SN, C) DMNV and medial SN at 105dpi. When compared, deposition is more abundant in DMNV than SN. The underlying hypoglossal nucleus (HN) is unlabelled. D.Cerebellum. Medial vestibular nucleus (arrow) is an early target site. Here at 156dpi neurons of the granular layer (g) are also heavily labelled. E. Pattern of spread in caudal brainstem (119dpi). Labelling is fairly extensive but targeted to particular nuclei of reticular formation including the gigantocellular nucleus (Gi), pontine reticular nucleus (Po) and red nucleus (RN) showing. Labelling in DMNV and SN is extensive compared to the unstained adjacent area postrema (arrow). The medial and interposed cerebellar nuclei are also visible (arrowhead). F. Low-power sagittal view showing distribution at endpoint of disease. Preferential targeting is clearly visible. Bar; A = 20μm, B,C, = 60μm, D = 300μm, E =600μm, F =1mm.

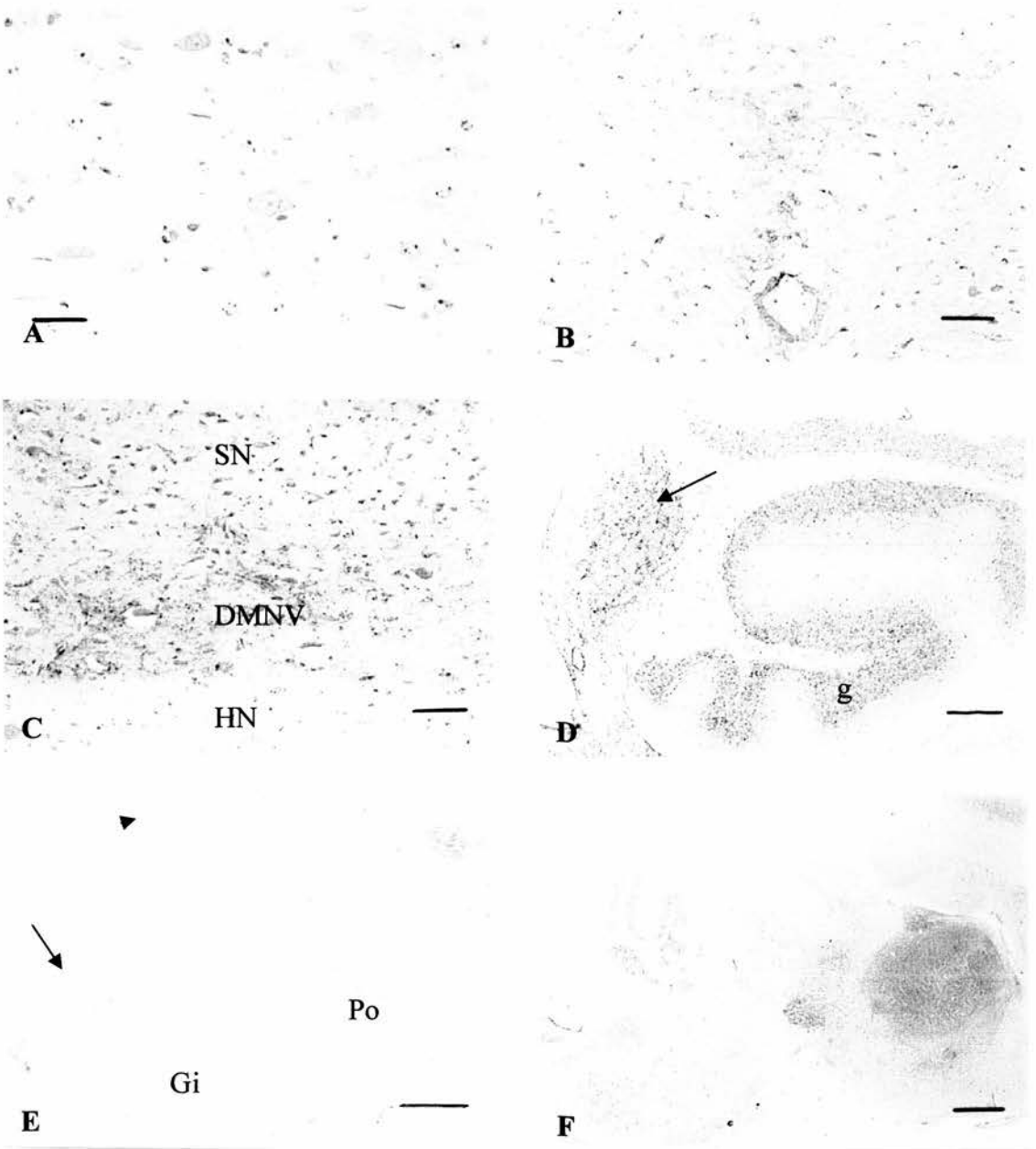

Figure 2.4. PrP^d immunolabelling in the spinal cord. A. Low power view showing distribution in thoracic segment (T) 7-9 at endpoint of disease. Grey matter (centre) is extensively and abundantly labelled. In comparison, white matter (on either side) is relatively spared. A nerve root (arrow) is unlabelled. B. Splanchnic nerve root entering T1-3 segment (156dpi). Grey matter (GM) is positive, white matter (WM) barely positive but the root (NR) is negative. C. DRG from segment T4-6. Even at 133dpi, PrP^d is seen within only a proportion of sensory ganglion cells. Bar; A = 300, B = 200, C = 100μm

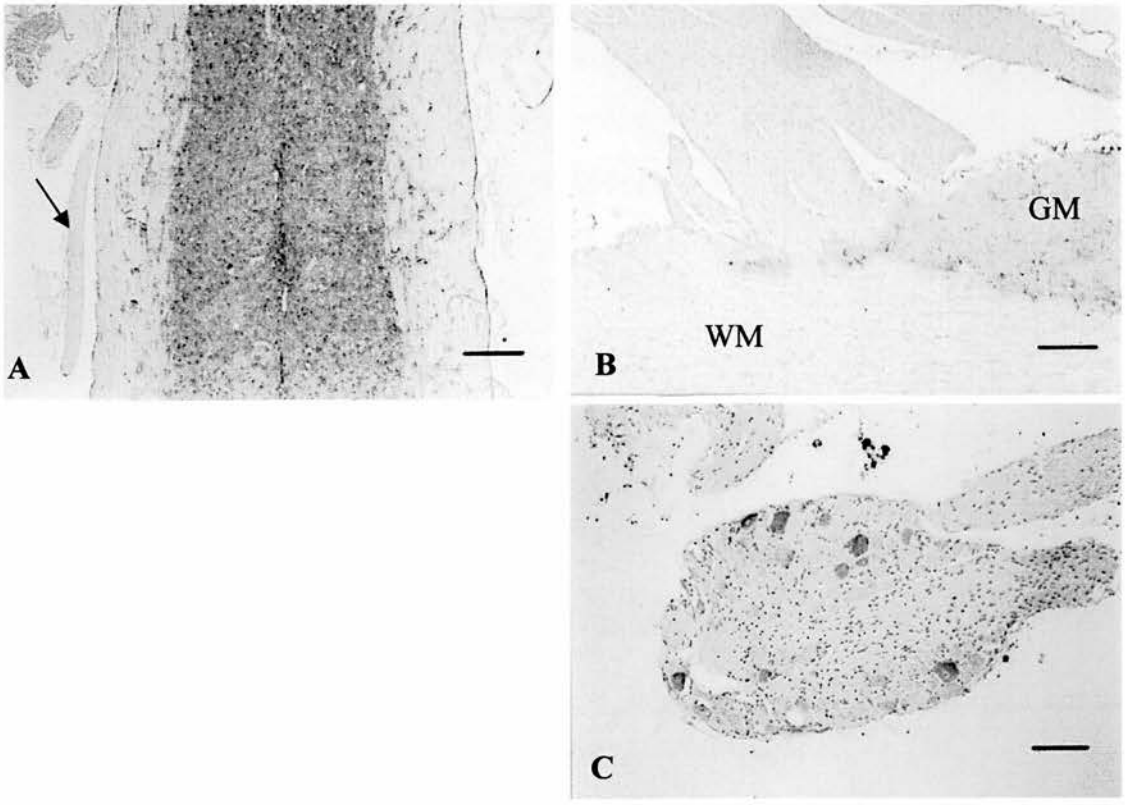

Figure 2.5. Dynamics of PrP^d accumulation. Relative amount of PrP^d accorded by the scoring criteria. A. '+' (98dpi), B. '++' (113dpi), C. '+++' (113dpi), D. '++++' (endpoint). All examples are from spinal cord segment T7-9. Bar = 30 μm

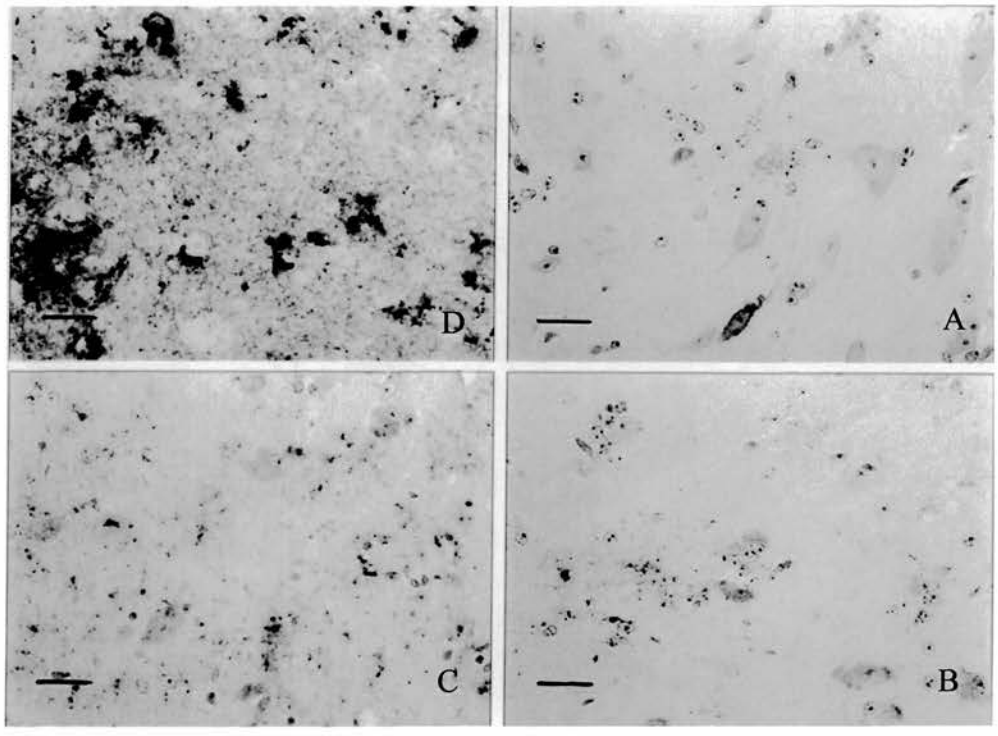

Figure 2.6. PrP immunolabelling of neurons in spinal cord from A; an unaffected hamster, B, C, scrapie-challenged hamsters – early stages of infection. A. Cells display the range of 'homogenous', ungranulated labelling characteristic of PrP^C, B. The intense cytoplasmic labelling of 'reactive' neurons (arrows), C. A mixture of PrP-labelled neurons typically observed at early stages of 263K infection including those showing early granulated PrP^d (long arrow) and a PrP^C-containing cell (short arrow). Bar; A = 30μm, B,C = 22.5μm

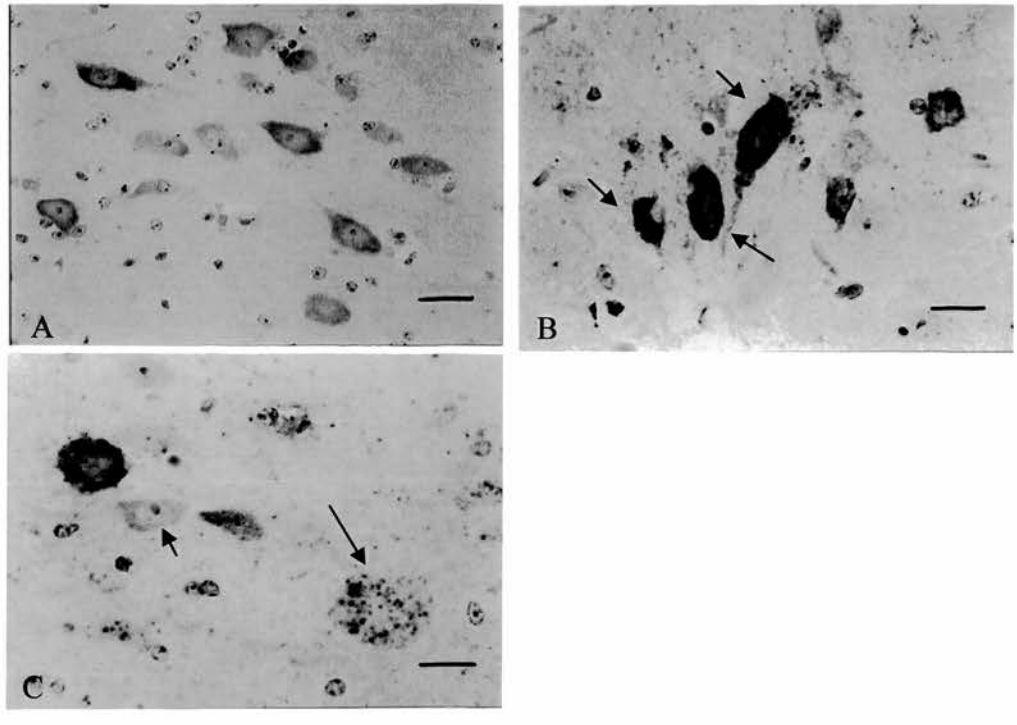

2.2.4ii Cellular localisation of PrP in early stages of infection

Deeply stained neurones exhibiting a similar intracellular distribution of PrP were regularly seen in sections of brain or spinal cord from early time-points. The cytoplasm of these cells, termed 'reactive' neurones to distinguish them from 'normal' neurones found in CNS of uninfected controls, stained more intensely than those of unaffected hamsters and also lacked the overt granularity associated with PrP^d-labelled neurones (Figure 2.6B). Reactive neurones were located in close proximity to normal neurones but were also seen in mixed populations with early PrP^d-positive cells (Figure 2.6C and see below). Such neurones were present during only a short phase concurrent with the appearance of early forms of PrP cellular pathology and possibly represent an *in-vivo* reflection of neurones in a transitional stage of PrP^C conversion to PrP^{Sc}.

In scrapie-challenged hamsters several of the previously described types of PrP^d were present including plaque-like aggregates, glia-associated forms and neuroanatomically-targeted granular diffuse accumulations. However, the physical appearance and cellular location of PrP^d followed a distinct (and previously unreported) temporal sequence of events (Figure 2.7A-F). Apart from the frequent but variable presence of reactive neurones, PrP^d was first seen as punctate deposits localised within and at the cell surface of only one or two individual neurones. The inclusions had the particulate appearance consistent with compartmentalisation in endosomes or lysosomes. Sometimes, several tiny deposits were aggregated on the neuronal membrane producing discretely labelled arcs or rings of protein (Figure 2.7B). The number of inclusions seen within individual cells increased progressively over a short period of time, as did the overall numbers of such neurones (Figure 2.7C). Soon afterwards, PrP^d deposits were observed outside the neurone in the neuropil (Figure 2.7D). Initially the extracellular deposits were immediately adjacent to a particular neurone. Next, punctate labelling was seen in the near proximity and later it was arrayed more widely around the cell body (Figure 2.7E). Concurrent with this the accumulations also appeared to increase slightly in staining intensity. This is probably because small deposits were beginning to aggregate and were more obvious.

PrP^d was detected firstly associated with only a few precisely localised neurones. As incubation time progressed more cells in the same area were labelled until several cells exhibited the types of cellular PrP pathology described above. Although there was variation in the onset of disease in individual animals, this pattern of pathology was a consistent early observation that was repeated at a later time in other CNS nuclei. The temporal reproducibility indicates that both the physical changes associated with individual cells and the subsequent involvement of other cells were part of an ongoing train of events that reflected the developing disease process.

Figure 2.7. Progression of PrP cellular pathology. High power of individual neurons to show appearance of PrP in an unaffected hamster (A); the early pattern of PrP^d development (B,C,D,E); and at a late stage (F) in incubation period. Bar = 10μm

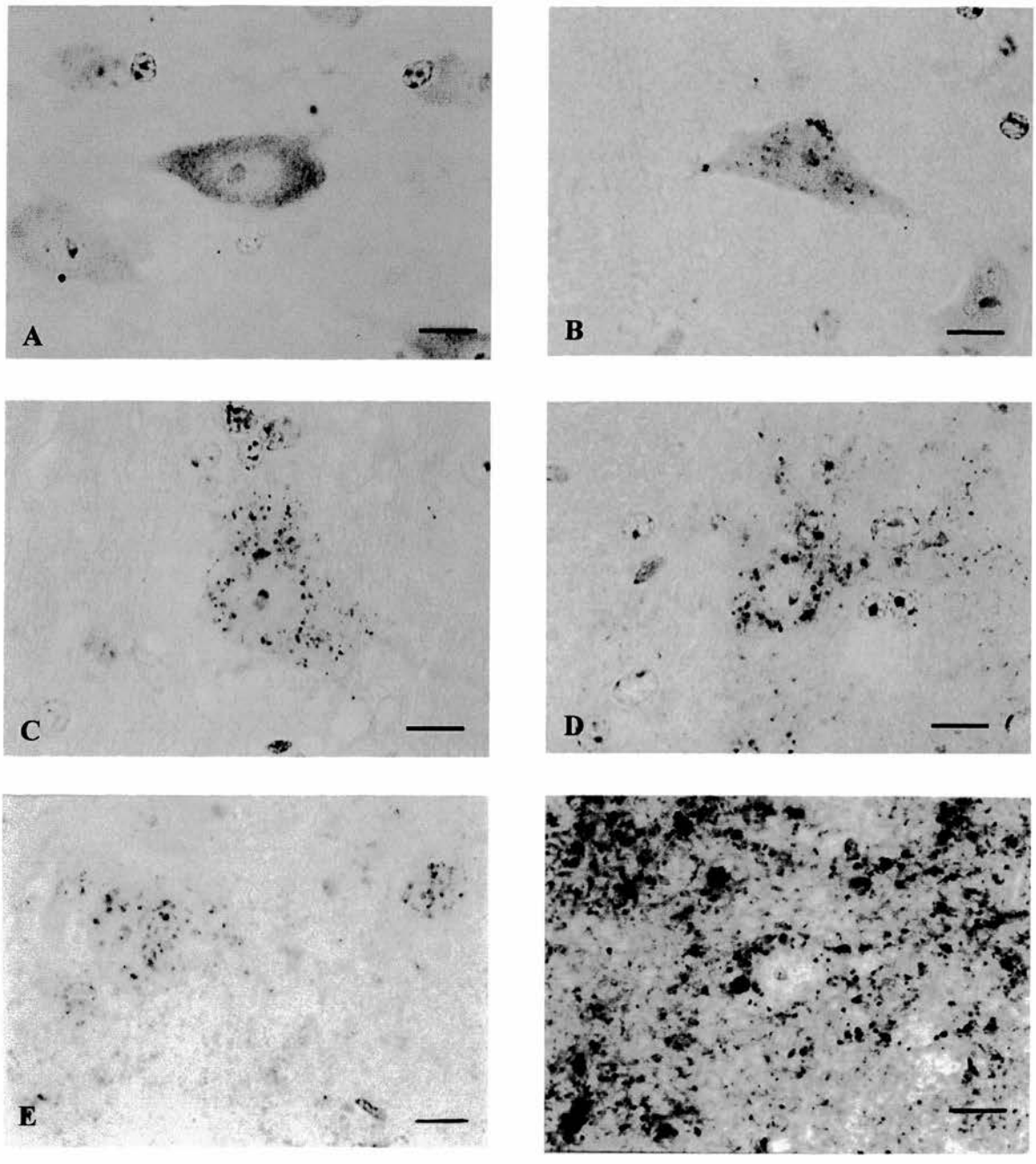

Table 2.3 PrP^d-pathology of neurones: Sequence of cellular changes and relationship with incubation period

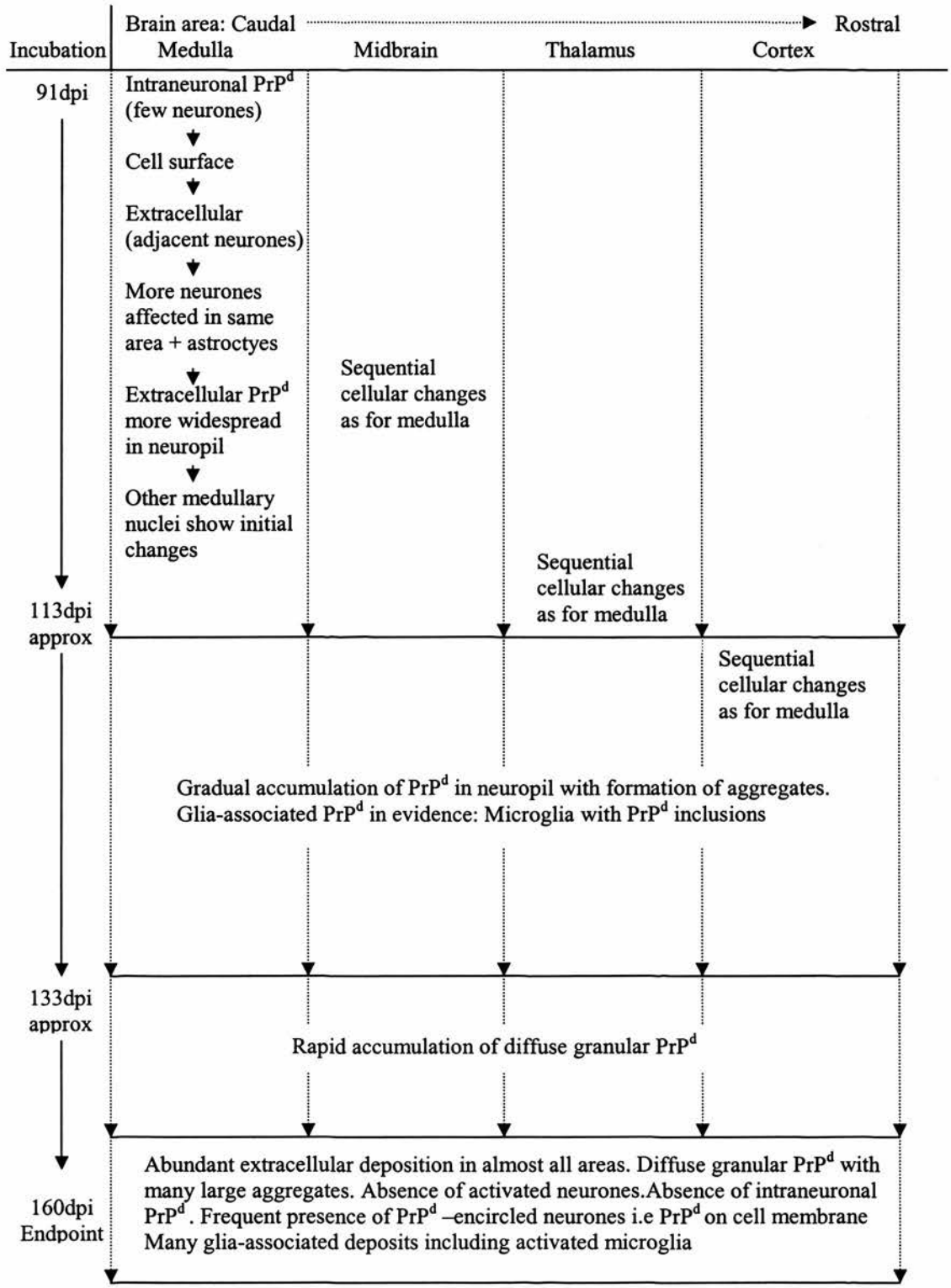

2.2.4iii Localisation of PrP^d with disease progression

With increasing incubation, a greater number of positively labelled foci were present, located as described, in confined neuroanatomical sites. PrP^d accumulations became more obvious and widespread within the early target areas and then more generally throughout the CNS. Within established foci, the PrP^d appeared progressively more 'grainy' and consolidated. Intensely stained punctate deposits, probably representing the expression of PrP^d at synapses were numerous but became less common with time. This may have been due to the degeneration of neuronal circuitry or because they were obscured among the larger granular deposits and aggregates. These latter forms eventually predominated and formed the characteristic pattern that was a feature of end-stage disease (Figure 2.7F). Neurones with intracellular inclusions became rarer and at the terminal stage of disease these were rarely, if ever, encountered. None of the types of PrP^d described above were seen in uninfected controls. The sequence of the PrP-associated cellular pathology and progression of accumulation are summarised in Table 2.3.

2.2.5 Neuroglial cell involvement in PrP pathology

The majority of PrP labelling was associated with neurones but a variety of glial cells were involved with PrP pathology (Figure 2.8). PrP^d was within and/or accumulated around astrocytes, microglia, ependymal cells lining ventricles and choroid plexus (ependymocytes and choroidal epithelial cells). PrP^d was also found along the glial limiting membranes of ventricles and pia mater, and was associated with CNS radial oligodendroglia and satellite cells of the DRG. Blood vessel walls were also labelled via PrP-positive astrocytic end feet that bridge both capillaries and neurones.

The temporal involvement of glia in 263K pathogenesis began very early in the incubation period. Progression of glial involvement was similar to that described previously for neurones; initial deposits and cell numbers were small but both deposition and types and numbers of affected glia increased with time. Glia-associated PrP^d was observed in sections of both brain and spinal cord at the first time-point of 91dpi and corresponded to areas of early neuronal targeting. PrP^d labelling was initially confined to individual astrocytes (Figure 2.8A) that were closely proximal to brainstem or thoracic spinal neurones. PrP^d was first seen in the gigantocellular nucleus of the medulla but also around central canal ependymal cells of mid-thoracic spinal cord segments (Figure 2.8B) and soon afterwards in ependymocytes lining the 4^{th} ventricle. As well as these elements, from around 113dpi, the external walls of blood vessels (Figure 2.8C) and pia mater were also labelled (Figure 2.8C, D). With time, ventricles, BVs and pia mater became progressively more heavily stained due to PrP^d accumulating around

astrocytes of the closely attached glial limitans. Microglia containing PrP^d inclusions were apparent, after extracellular deposition was evident (Figure 2.8D) indicating that these cells had probably phagocytosed PrP^d from the neuropil. PrP^d was seen surrounding the cell bodies and long processes of radial oligodendroglia in white matter and at late stages of the disease the appearance of the protein 'tracking' along white matter fibres was a common pathological feature in the spinal cord (Figure 2.8E). However, compared to grey matter, PrP^d was seen to a much lesser extent in oligodendrocytes or Schwann cells of white matter tracts and there was no evidence of PrP^d accumulation in nerves (Figure 2.8C and see Figure 2.4A&B). Glia outnumber neurones tenfold, therefore it is reasonable to presume that PrP^d was predominantly expressed by neurones and that while glia may have a role in transportation, neurones rather than glia were preferentially responsible for agent replication.

Although glial (but more specifically astrocytic) staining was observed from the earliest time-points it was never present prior to neuronal PrP^d deposition. Similarly, in DRG, PrP^d was present first at 113dpi in both the large sensory neurones and associated satellite glia. Mostly both neurones and satellite cells were labelled but sometimes DRG neurones containing granular PrP^d were seen directly adjacent to unlabelled satellite cells (Figure 2.8F) indicating that PrP^d association with satellite cells occurs very shortly after neuronal involvement. As glial activation occurred after PrP^d deposition it is likely that astrocytes, microglia and satellite cells were responding to rather than initiating the related pathology.

Figure 2.8. Glial involvement in PrP pathology. A: PrP^d-labelled astrocyte-like cell (arrow) adjacent to neurone in parvocellular reticular nucleus (105dpi). B: Accumulation along the central canal at segment T7-9 (133dpi). C: Deposition around blood vessel (bv) walls at T10-11. D: Pia mater of the frontal cortex. PrP^d is deposited along the glial limitans (gl) and appears to be internalised by microglia (arrow). E: PrP^d 'tracking in' white matter of T4-6 segment at 133dpi. PrP^d extends from the gray matter (RHS) across WM tracts to pia mater (arrow) on LHS. F: Thoracic DRG (133dpi) with several PrP^d-laden sensory neurones. Adjacent satellite cells (arrows) are also strongly labelled. Bar: A,D = 10μm; B,C,E = 60μm; F = 30μm

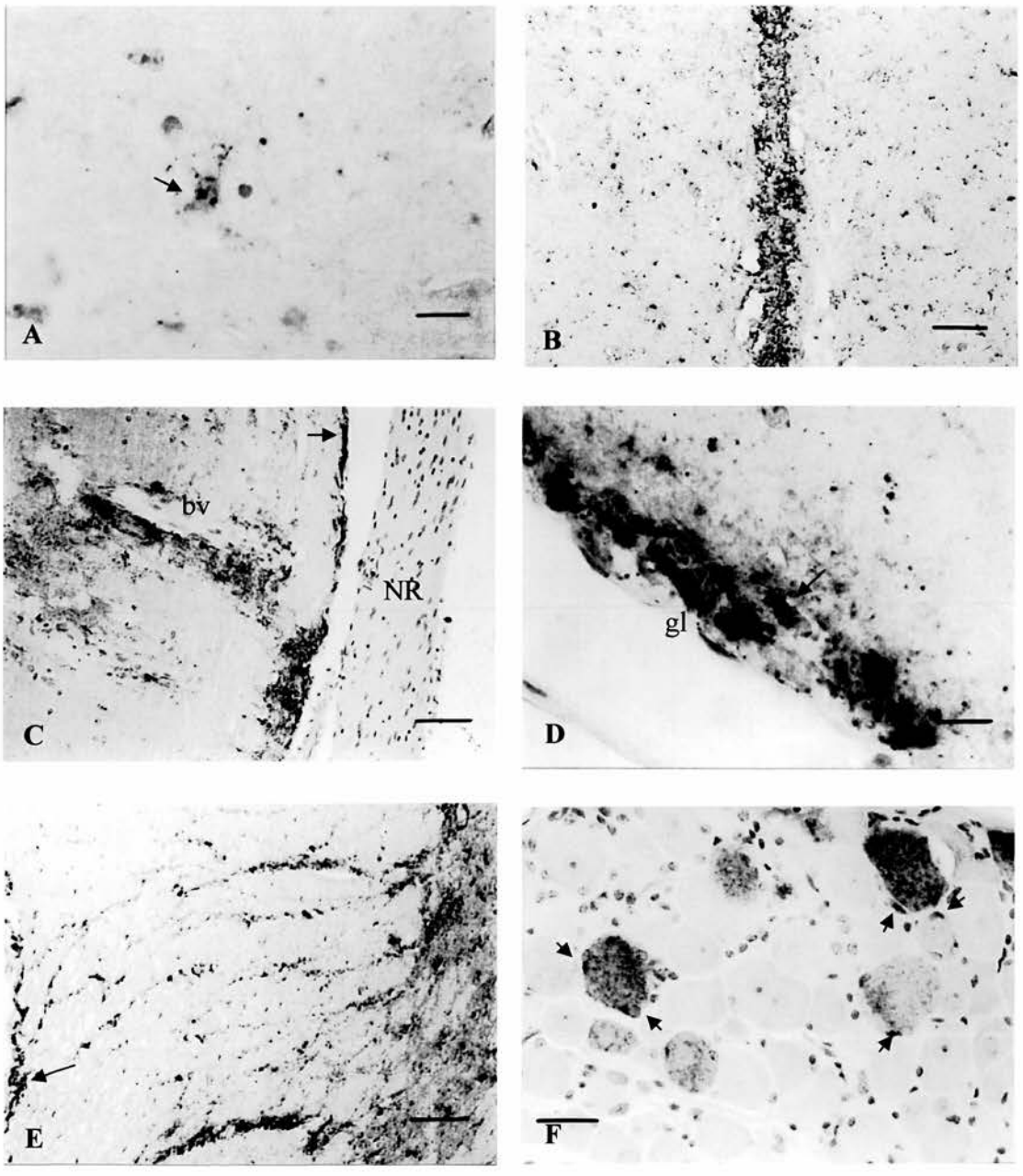

2.3 Discussion

Previous studies investigating spread of the scrapie agent from the periphery to the brain and spinal cord have used either infectivity assays or Western blotting. This study employed ICC to identify specific sites of PrP^d accumulation and trace the temporal deposition of PrP^d. The advantage of this methodology over these others is that, in contrast to results obtained from homogenised small samples, whole slices of brain are available for viewing under a microscope and individual or groups of cells can be identified by morphology and location. In TSE studies disease-related pathology can be visualised and assessed in the differing areas and cell types. This approach revealed several important findings.

1. After ingestion of 263K scrapie, PrP^d, the surrogate marker of the infectious agent, reached the CNS by two independent pathways. Targeting to brain and cord occurred simultaneously showing that the brain could not have been affected by spreading along the cord.
2. The precise locations of the initial cerebral target sites were identified providing strong evidence that the vagus nerve is a primary pathway to the brain in this model. In addition, the temporal and neuroanatomical targeting suggested that the infectious agent initially spreads along motor rather than sensory pathways of the vagus.
3. The rapid temporal sequence of targeting to spinal cord suggests multiple points of entry via splanchnic nerve branches.
4. The pattern of targeting within the brain is indicative that spread is not random but occurs along defined synaptically linked neuronal circuitry.
5. The physical appearance and cellular location of the earliest PrP^d deposition in neurones followed a distinct sequence of events. This is the first report showing the evolution and progression of PrP pathology at the cellular level.

2.3.1 Evidence that 263K scrapie reaches the CNS by two independent pathways

The data showed that the 263K agent reached the CNS by two main routes; one that entered at the mid-thoracic level of spinal cord and the other entering the medulla at the DMNV. This is in contrast to previous work reporting that, after peripheral or intragastric challenge of rodents with 139A or 263K scrapie strains, the infectious agent entered the CNS at the thoracic cord and reached the medulla by upward spread (Kimberlin and Walker 1988). In this study, PrP^d was initially observed simultaneously in both DMNV and mid thoracic cord and the amount of PrP^d deposition in the two sites was comparable. This indicates two independent points of entry. The idea that PrP^d/infectivity spreads towards the cranium via cell to cell transfer within the grey matter also appears to be ruled out by the observed temporal pattern of deposition: PrP^d is well

established in the medulla before it is observed in the cranial portion of spinal cord. It is also unlikely that early infection of the DMNV and SN occurs via ascending (or descending) white matter tracts of the thoracic cord as these are not directly linked. These data strongly indicate that infection enters the brain via anatomical projections outside the CNS and the most likely conduit is the vagus nerve.

Haematogenous spread is also a possibility but this is not suggested by the systematic nature of the targeting or the lack of labelling in brain sites such as the area postrema in which the blood brain barrier is compromised. Although the DMNV/SN complex lies adjacent to the area postrema, this was not an early target site and was not even greatly labelled at late stages of the disease.

Kimberlin and co-workers reported that after a variety of peripheral routes of infection (intraperitoneal, intravenous, subcutaneous and intragastric) scrapie infectivity was detected in the spinal cord before being found in the brain (Kimberlin & Walker 1979,80,82). Much of Kimberlin's peripheral pathogenesis work used the Chandler (139A) strain of scrapie but he reported similar findings with intraperitoneal 263K infection in hamsters (Kimberlin & Walker 1986). In contrast, the findings presented here do not point to a single route of entry but clearly indicate that, at least after oral challenge, the infectious agent reaches the CNS by two routes. The data concurs with the early studies that entry is via the thoracic cord but does not support Kimberlin's assertion that the agent reached the brain by upward spread.

There are a number of possible explanations for the discrepancies between the findings in this study and the early work. Kimberlin and co-workers tested the dynamics of agent replication during the early stages of disease. The studies consisted of infectivity assays - measuring incubation periods of groups of serially culled mice that had been injected with pooled spinal cord or brain. In his early experiments (Kimberlin & Walker 1979), the assay tissues were derived from homogenised whole brain and much of the cord. In the study presented here, PrP^d was found earliest in discreet areas of the CNS; the most caudal portion of the brain in the DMNV and SN and in T4 and T9 of spinal cord. Although Kimberlin's findings apply to a different scrapie strain, the dynamics of oral 263K pathogenesis have remarkably similar parallels and given the existing comparability between the sets of data, it is reasonable to presume that the early PrP^d deposition found in oral 263K may mirror that of 139A infectivity. If this were assumed to be the case, the portion of assay material derived from a whole brain would contain little or no PrP^d/infectious agent. It is therefore probable that any infectivity present

would have been undetectable. It is also possible that infectivity was not detected in the brain assays because the DMNV/SN complex was not included in the assay sample. This region is located in the most caudal position in the brain (see Figure 2.2a) and being less accessible is often missing or damaged at removal. In later more comprehensive studies (Kimberlin & Walker 1980,82), where multiple samples of brain and cord were assayed, the indicators of independent entry to the medulla were present, i.e. infectivity was present simultaneously in thoracic cord and in medulla and appeared in cervical cord *after* the medulla.

Apart from the discussed disparity, all other findings from Kimberlin's experiments agree with those seen with 263K oral challenge. Though the data was generated using different scrapie strains, infectivity and PrP^d were both seen first in thoracic spinal cord and medulla and temporal, geographical and pathological dynamics of both are also in accord. Combined these provide strong evidence that after peripheral routes of infection a) the agent initially accesses the spinal cord at the thoracic level, b) subsequent spread occurs along neural pathways in a caudal to rostral direction within both cord and brain. The fact that the pattern of infection is so similar in both scrapie strains also raises the possibility that there may be a common mechanism of peripheral neural routing but this must be formally tested using a wider range of TSE strains.

2.3.2 Evidence that the vagus nerve is a primary pathway to the brain and that early spread occurs along motor pathways

Two pieces of data that provide significant indicators that spread to the medulla and thoracic cord initially occurred along motor rather than sensory fibres of the vagus and splanchnic nerves.

Firstly, the initial target site appears to be the DMNV followed closely by the SN. In one brain from the earliest group of 91dpi, PrP^d was present in small amounts in the DMNV but lacking in the SN. Even though PrP^d was mostly present in both DMNV and SN, when the relative amount of PrP^d was compared, the DMNV was consistently more heavily labelled than the SN. As the amount of PrP^d present in a specific area served as an indicator of the timing of deposition this indicated that PrP^d was deposited in the DMNV before the SN.

The DMNV contains the neuronal cell bodies of vagal efferent (motor) fibres leaving the brain. Vagal fibres running to the brain (vagal afferents) have their cell bodies in the nodose ganglion but these do not terminate here and run on to the SN where they synapse with interneurones that project directly to vagal motor neurones of the DMNV (Card *et al.*, 1993, Standish *et al.*, 1994). The vagus nerve innervates the gastrointestinal tract including the stomach, small intestine and

parts of the large intestine so the most plausible explanation for PrP^d deposition in the DMNV and SN is by spread of ingested 263K scrapie after uptake from the alimentary tract. Therefore, neuroanatomically, the sequence of target areas can best be explained by infection spreading along autonomic vagal efferents to the DMNV and subsequently to the SN. This would require the infectious agent to travel in a retrograde direction towards the cell body, a mode of spread that has several precedents in neurotropic viruses such as pseudorabies virus (Card *et al.,* 1993, Standish *et al.*, 1994) and Herpes Simplex Virus Type 1 (Krinke & Dietrich 1990). However, the infectious agent could travel from the gastrointestinal tract directly to the SN along visceral vagal afferents. The agent could also travel from the pharynx, larynx and tongue via the other cranial nerves such as the hypoglossal, facial and trigeminal but primary spread along these routes is not suggested by the targeting or timing of PrP^d deposition. The possible routes by which 263K scrapie reaches the brain from the GI tract are illustrated in Figure 2.9.

Secondly, PrP^d immunolabelling of DRG was found only after PrP^d was firmly established in grey matter of the associated thoracic segment. In several cases, DRG were negative for PrP^d but the corresponding cord segment was positive but there were no instances where the reverse was seen. Sympathetic (motor) efferents of splanchnic nerve branches leave the thoracic cord and synapse in the prevertebral ganglia before reaching the alimentary tract targets. Splanchnic efferents travelling towards the cord have their cell bodies in the sensory neurones of the DRG. As thoracic grey matter rather than DRG was labelled first, initial spread along sympathetic rather than sensory fibres is indicated but the data supporting this is fairly limited and a more far-reaching study is required to ascertain this.

2.3.3 The temporal sequence of targeting to spinal cord suggests multiple points of entry via splanchnic nerve branches

Entry via the thoracic portion of the spinal cord indicated that the infectious agent (or PrP^d, its surrogate marker) had travelled along the nerves supplying the GI tract i.e. the splanchnic nerve. The splanchnic nerve is highly branched and descending branches give rise to the greater, lesser and lumbar splanchnic nerves. The greater splanchnic nerve branches leave the cord from segments T5-9, synapse in the coeliac ganglion and then travel on to supply the stomach, small intestine, spleen, adrenal, kidney and liver. Lesser splanchnic nerves leave cord segments at T7-13, synapse in the superior mesenteric ganglion and innervate the ascending colon. The lumbar branches leave via T13, L1 and 2, synapse in the inferior mesenteric ganglion and supply descending colon, sigmoid colon and rectum. Studies examining the segmental distribution of retrogradely labelled sympathetic preganglionic neurones (IML neurones –see below) showed

Figure 2.9 Hypothesis of neural spread: 263K scrapie is likely to reach the CNS via nerves supplying the mesentery, i.e. vagus or splanchnic, by -
1) Retrograde spread along autonomic (efferent) fibres to neuronal cell bodies in DMNV and intermediolateral nucleus (IML) via coeliac/mesenteric ganglion complex (CMGC)
2) Anterograde spread along sensory (afferent) fibres to SN and dorsal horn via nodose ganglia (NG) and dorsal root ganglia (DRG)

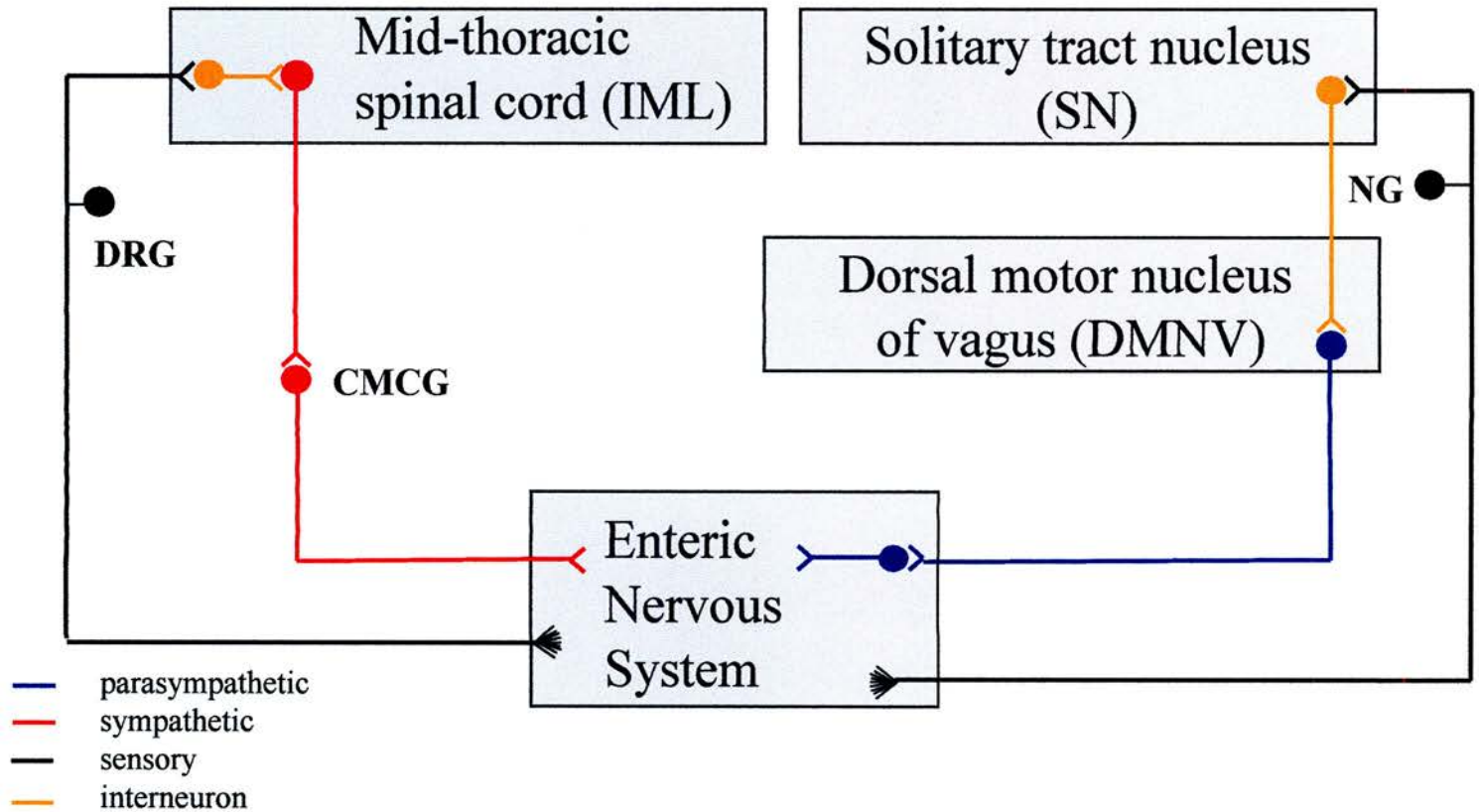

that most peripheral sympathetic ganglia received a dominant input from a single thoracic or lumber spinal cord segment. Also, the more caudally located peripheral ganglia received input from neurones located more caudally (Strack *et al.*, 1988). Although the sections of cord constituted multiple segments of cord, this rostro-caudal topographical organisation was suggested in the results. The location and timing of PrP^d appearance shows that the greater splanchnic nerve branches are significant conduits in early peripheral pathogenesis. Consequently, after oral infection uptake of the infectious agent is most likely to occur from the stomach and small intestine but branches supply the ascending colon also probably contribute to the observed thoracic cord invasion.

The pieces of cord taken in this study were dissected from thoracic vertebrae T1-3, T4-6, etc, and these don't always correspond exactly to that of an excised cord. This is because the vertebral column continues to grow after the spinal cord has stopped so that an adult rodent spinal cord terminates at about the first sacral vertebra. Thus, the most caudal cord segments are situated slightly more cranial to the corresponding vertebra. Nevertheless, the pieces correspond closely enough to show that the data supplied in Table 2.2 parallels that of the anatomy.

PrP^d was seen first in segments T4-9 but the amount of deposition was generally greater in T7-9 so it is probable that PrP^d accumulation (and by association, agent replication) occurred in this area before T4-6. However there was very little temporal separation between the appearance of the protein in T4-9 and in adjacent segments located cranially of caudally to this. The close timing of events could be explained by there being multiple points of entry to the thoracic cord. Access via a number of nerve roots would fit with the highly branched anatomy of the splanchnic nerve. Nevertheless, the temporal delay observed in PrP^d reaching the most caudal and cranial segments might be the consequence of cell-to-cell spread between neurones situated in adjacent segments. In either event, the most likely sites for access and spread are via neurones of the intermediolateral cell column (IML) as these nuclei contain the cell bodies of outgoing splanchnic nerve fibres and form internal links with other IMLs located caudally and rostrally (Rubin & Purves 1980).

2.3.4 Orally-transmitted 263K spreads along defined synaptically-linked neuronal populations

As with targeting *to* the CNS, the pattern of spread *within* the CNS was equally precise. The temporal sequence of targeted sites and the ultimate pattern of PrP^d accumulation were extremely consistent. Spread occurred in a caudal (medulla) to rostral (forebrain) direction with early

targets containing substantially greater accumulations than the most rostrally situated parts of the forebrain and olfactory lobes. The explanation for this is probably not that these areas are privileged (non-infectable) sites but that before the olfactory lobe was reached, key neurones in, for example, the thalamus were terminally disabled causing the animal's death. The pattern of spread from the medulla to prominent nuclei in the cerebellum, pons, midbrain and thalamus (Figure 2.10) followed well-established neuroanatomical pathways (Andrezik & Beitz 1985, Flumerfelt & Hrycyshyn 1985). Even though timing varied between individuals, the location of PrP^d deposition was invariable; occurring in distinct neuronal groups in the (approximate) order** listed is Table 2.1. This consistency is significant as it shows that PrP^d deposition does not occur randomly. Further, the location of the sites and the sequence in which targeting was observed (Figure 2.11) closely reproduces that seen in the transneuronal retrograde spread of the pseudorabies neurotropic virus after intragastric administration of the virus to rats (Enquist *et al.*, 1994). This observation strongly suggests that spread of 263K scrapie also occurred along synaptically linked neuronal pathways.

2.3.5 The physical appearance and cellular location of PrP^d followed a temporal sequence. The disease-associated changes that were visualised in and around individual neurones was a new finding. As illustrated in Figure 2.7, the subtle changes in physical appearance and cellular location of PrP^d that were observed early in the incubation period followed a distinct temporal sequence that was consistent with a progressive pathological process. The earliest pathology was observed as intraneuronal PrP^d inclusions. Inclusion-containing neurones were frequently found in the most recent sites of PrP^d deposition but absent thereafter suggesting that this is a transitory stage of PrP pathology.

The most obvious (and extensively reported) form of PrP pathology is the widely distributed extracellular accumulations of granular PrP^d that are seen in advanced stages of the disease process. Intraneuronal PrP^d is an end-stage pathological feature in the brains of natural and experimental scrapie or BSE infected sheep (Foster *et al.*, 1996, Ryder *et al.*, 2001, Jeffrey *et al.*, 2001b) or cows with BSE (Wells & Wilesmith, 1995). In addition, punctate neurone–associated extracellular PrP^d has been reported early in the pathogenesis of other strains of scrapie such as ME7 and 87V (Bruce *et al.*, 1989,94a, McBride *et al.*, 1998) but the intracellular and membrane-

** Due to their close proximity and the rapidity with which sequential PrP^d-labelled sites appeared, it would be difficult to separate the various nuclei into a precise temporal order without using large numbers of animals. However, this is perhaps unnecessary, because retrograde labelling experiments have shown that these are linked neuroanatomically (Loewy 1995, Card 1994, Enquist 1994).

associated forms were not apparent. These discrepancies may be due to the various PrP antibodies recognising different epitopes but another possibility is that, as previously suggested, they reflect differential PrP processing between strains (Jeffrey *et al.*, 2001b, Gonzales *et al.*, 2003). Only one antibody, 3F4, was used in this study so this possibility couldn't be assessed here. However, in this model a range of PrP pathology was consistently observed but neurones exhibiting the types of PrP^d illustrated in Figure 2.7B-E were only prominent in early stages of the incubation period. It is, therefore, possible that the pattern of pathology associated with individual neurones reflects the underlying biochemical changes in the cell. For example, the focal cell-surface PrP^d and the compartmentalised intracellular PrP^d that follows may represent an *in-vivo* equivalent of the membrane 'rafts' (Vey *et al.*, 1996) and the subsequent trafficking within endosomes/lysosomes.

It is unclear whether the 'reactive' neurones described in section 2.2.4ii are disease specific because, apart from an increased staining intensity, they resembled PrP-labelled uninfected neurones. Without appropriate antibodies that can discriminate between normal and abnormal forms of PrP, the qualitative difference in PrP expression observed in reactive neurones can only be speculative. The observed staining may reflect, for example, early conformational changes between normal and disease-associated forms, differences in PrP glycosylation or PrP^C upregulation in response to cellular stress. Similarly labelled neurones have also been seen in normal mice at sites of injury; around the needle track of intracerebrally mock-infected mice (P. McBride, unpublished observation) or areas of anoxia-induced stroke (McLennan *et al*, manuscript in preparation) perhaps signifying that PrP^C performs a protective role in these situations. New evidence indicates that PrP^C responds to various forms of physiological stress including the damage caused by exogenous copper, hydrogen peroxide and oxidative stress (Herms *et al.*, 1999, Brown *et al.*, 1997a,b, Guentev *et al.*, 2000, Wong *et al.*, 2001). Taken together these studies support a neuroprotective function. Even so, reactive neurones were only observed in brains of scrapie-challenged hamsters during a short phase either before or concurrent with the first appearance of PrP^d–labelled cells and it may be that these are exhibiting the very earliest stages of PrP cellular pathology.

In this study, as with other rodent models (Bruce *et al.*, 1989, 94a, McBride *et al.*, 1998), the greatest abundance of PrP^d was found in or around neurones but from the earliest stages of disease, PrP^d was also associated with a variety of glial cells including astrocytes and microglia. The involvement of glia in TSE pathogenesis is discussed in Chapter 6.

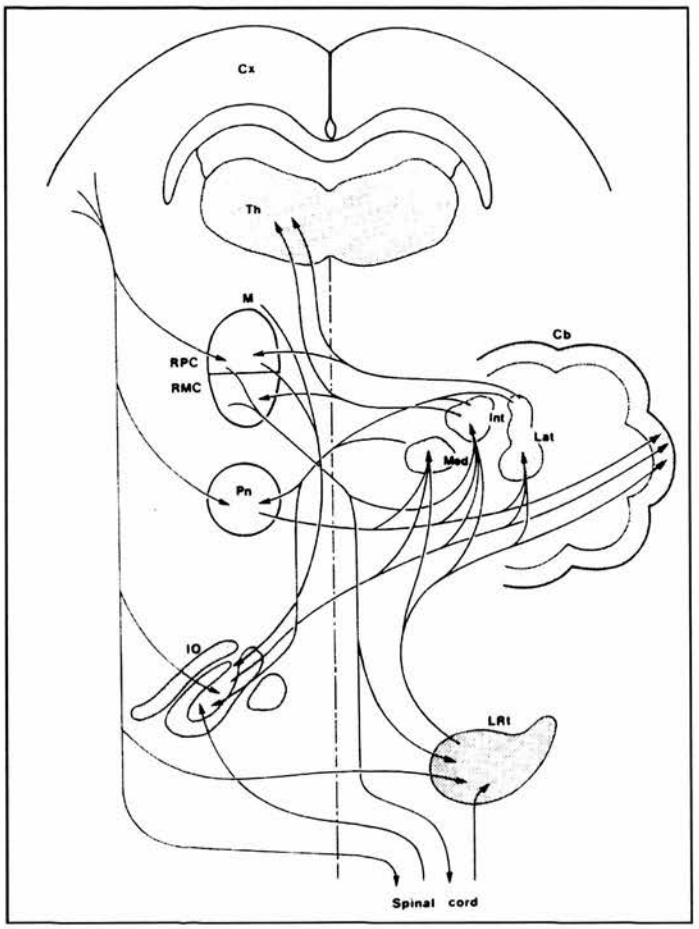

Figure 2.10
The main connections of the precerebellar nuclei and red nucleus in the rat as derived by retrograde labelling. Diagram shows possible connecting pathways by which 263K scrapie could spread from one area to another.

Cb, cerebellum; Cx, cortex; Int, interposed nucleus; IO, inferior olive; Lat, lateral nucleus; LRt, lateral reticular nucleus, M, midbrain; Med, medial nucleus; Pn, pontine nuclei; RMC, red nucleus - magnocellar division; RPC, red nucleus - parvocellular division; Th, thalamus.

From 'The Rat Nervous System', Volume 2, 1985. Edited by George Paxinos. Academic Press

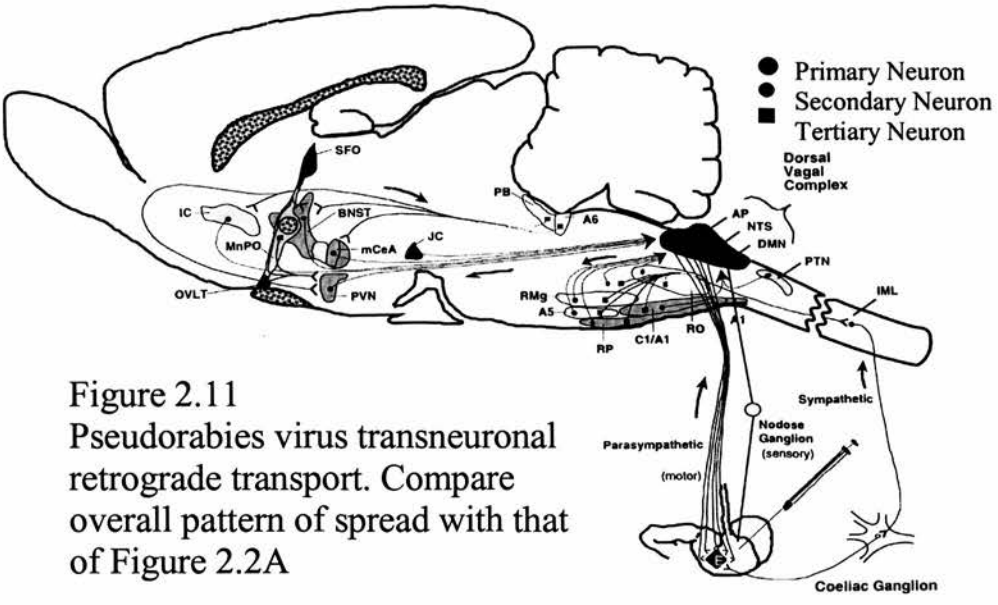

Figure 2.11
Pseudorabies virus transneuronal retrograde transport. Compare overall pattern of spread with that of Figure 2.2A

Reproduced from Enquist *et al.*, 1994

2.4 Summary

The aim of this study was to use immunocytochemistry to identify the early sites of abnormal PrP deposition in the brain and spinal cord and then map the location of subsequent accumulations as the incubation period progressed. As well as providing some new insights into the cellular pathology elicited by oral 263K infection, results have indicated the probable routes by which the 263K agent reaches the brain and spinal cord once it has been taken up from the gastrointestinal tract. Identification of initial PrP^d target sites demonstrated conclusively that the peripheral nervous system and specifically, the vagus nerve are important in dissemination of infectious agent after peripheral infection. There is now strong evidence implicating the vagus nerve as the link between the brain and the gut and indirect evidence that the splanchnic nerve was the spinal cord conduit. In the next chapters studies are undertaken that examine the detail of vagal and splanchnic nerve circuitry in an attempt to elucidate the involvement of these nerves after oral infection of 263K scrapie.

Chapter 3: Neuroanatomical routing hypothesis: Pilot experiments

3.0 Introduction

In Chapter 2, the location and temporal sequence of PrP^d deposition was determined in brain and spinal cord of hamsters that had been orally exposed to 263K scrapie.

Results indicated that after being taken up by the gastrointestinal tract, 263K scrapie reached the brain by spreading along the vagus nerve. The earliest sites for PrP^d deposition were situated in the medulla - in the DMNV and SN. Both these regions innervate the gastrointestinal tract. The GI tract is also supplied by the splanchnic nerve via neurones that originate in the intermediolateral cell column (IML), a nucleus situated in mid to lower segments of thoracic spinal cord. In the cord, PrP^d was first found around grey matter neurones of mid-thoracic segments but due to the plane of section it was not possible to establish the precise neuronal populations involved. Therefore, even though the IML could not be specifically identified, splanchnic nerve participation was strongly suggested but more definitive evidence of IML involvement was required.

In addition to the clear evidence involving the vagus nerve in peripheral spread of the 263K agent, there was some data that provided clues into the possible direction of early spread. The timing and sequence of deposition suggested that PrP^d was present in the DMNV prior to the SN. Also, although DRG had not been excised specifically, the ganglion was sometimes present attached to the cord segment by its corresponding nerve root. PrP^d was present in a number of DRG sections but only after deposition was established in the associated cord segment. Taken together, the data suggested that initial spread might have occurred along efferent (motor) rather than afferent (sensory) fibres.

Although the study described in Chapter 2 focused only on the target sites in the CNS, the data generated provided enough information to hypothesise further about the neuroanatomical routing of infection after the agent has gained access to the gastrointestinal tract. This hypothesis was described diagrammatically in Figure 2.9.

In order to establish splanchnic nerve involvement and to verify this hypothesis of spread, it would be necessary to use the same rodent model of oral challenge to look for the presence of PrP^d in both the CNS and the PNS components identified as being potentially involved in the

routing of 263K scrapie. This, in turn, would depend on being able to;

1) Identify and dissect out such components at post mortem
2) Ensure the presence and correct orientation of all excised tissues/CNS areas on the microscope slide
3) Fix and process the tissues to preserve both PrP protein and cellular morphology
4) Identify the various tissue components/regions and cell types and interpret findings using microscopy

As the points listed above presented practical difficulties, a pilot experiment using uninfected hamsters was undertaken to establish if the proposed plan of work was realistic.

The aim of this Chapter is to describe the procedures carried out in the pilot study, how they were devised, why they were necessary and the degree of success that was achieved.

3.1 Identification and dissection of rodent tissues

The proposed plan required the successful removal of brain, spinal cord with DRG attached, small intestine, spleen, salivary glands, left and right nodose ganglion (NG), left and right vagus nerve and the coeliac and mesenteric ganglion complex (CMGC) from groups of orally-infected hamsters culled throughout the incubation period.

Removal of brain, spleen and salivary glands was not problematical due to existing experience of rodent post-mortem procedure therefore these organs were not included in the dissection trials. However, neither my collaborator, Dr. Michael Beekes, nor myself had experience in PNS micro-dissection so were taught to locate, recognise and excise the tissues by Dr. Walter Schulz-Schaeffer of Göttingen University in two sessions at the Robert Koch Institute in Berlin. Assistance was also sought from neuroanatomy books that included; Stereotaxic Atlas of the Golden Hamster Brain: Edited by Morin and Wood, Academic Press; The Rat Nervous System, Volume 2, Hindbrain and Spinal cord, Edited by George Paxinos, Academic Press; Grays Anatomy, Thirty-Eighth Edition, Churchill Livingstone. Due to the small size of the tissues, *in situ* identification and removal required a dissecting microscope and specialised surgical instruments.

Spinal cord and DRG: As one of the main aims of the project was to compare the amount of PrP^d deposition found in spinal cord segments with corresponding DRGs, the cord had to be

removed intact along with DRGs and connecting nerve roots (Figure 3.1). Access to DRG is impeded because the spinal cord and DRG are in close proximity to one another and tightly surrounded by bones of the vertebral column. Using the dissecting microscope, the encapsulating bones had to be carefully snipped away with small bone nippers. The nerve roots are approximately 0.05mm in diameter and very delicate. If these are cut the DRG become separated from the cord and cannot be retrieved. Each of the twenty-one cord segments and forty-two DRG had to be exposed and sequentially removed by working up the length of the vertebral column. Details of spinal cord/DRG dissection are provided in Appendix 1.1.

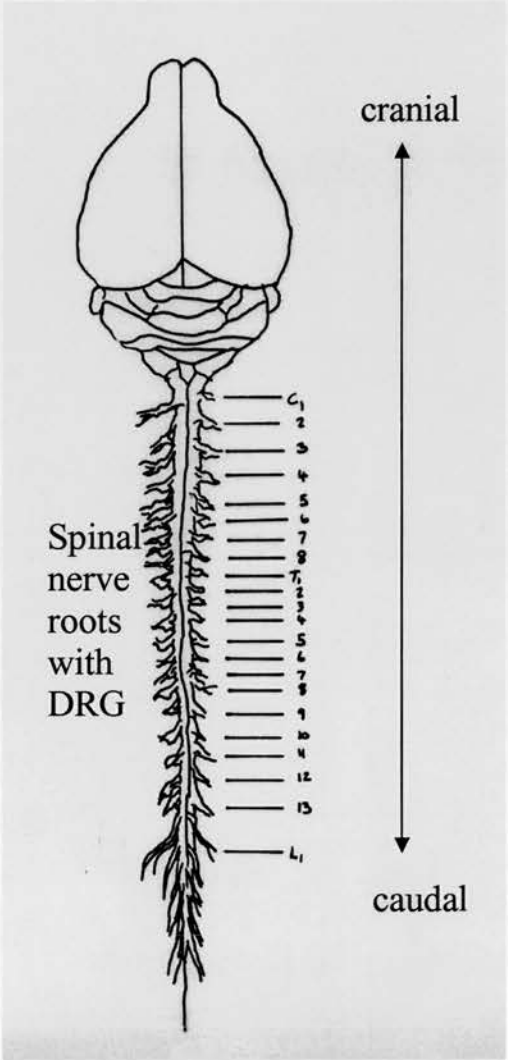

Figure 3.1 Diagrammatic representation of the hamster brain and spinal cord. The eight cervical and thirteen thoracic segments are shown giving rise to a pair of spinal nerves and dorsal root ganglion.

Vagus nerve and NG: Similar difficulties existed for vagus nerve and NG removal. The vagus runs almost the length of the body; arising in the medulla oblongata and coursing down to the base of the abdomen, supplying the heart, lungs, stomach, liver, pancreas, spleen, and several portions of the gastrointestinal tract on its way. For this study, only the cervical portion of the vagus was to be removed. This lies in the neck and runs closely parallel to the carotid artery. An initial difficulty was learning to locate and recognise the vagus among the many other nerves present in the neck. Its small size and delicate nature also presented an obstacle to excision. The ganglion contains the cell bodies of the vagus nerve so it was important that this was also dissected out. However, the NG is embedded in, and protected by a pocket of bone situated near the ear socket making an undamaged removal a difficult and lengthy procedure. Details of vagus nerve/NG dissection are provided in Appendix 1.2.

CMGC: The most difficult component to locate and dissect was the CMGC. The cervical vagus, NG and DRG are small but, with experience, can be recognised using the dissecting microscope. The CMGC cannot be seen even when using the microscope and had to be identified using associated organs and blood vessels as cues. The CMGC lies on the abdominal aorta, adjacent to the kidney and adrenal gland. It is supported on one side by the superior and inferior mesenteric arteries and the coeliac artery and on the other side by the renal artery and ovarian/testicular arteries (Figure 3.2). There are three major ganglia in the CMGC; the coeliac ganglion and the superior and inferior mesenteric ganglia. In larger species these may be removed individually but in rodents, the ganglia are so closely connected that they cannot be separated and must be excised as one entity. The CMGC was dissected out attached to the complex of blood vessels described above and in Appendix 1.3.

Small intestine: Pieces of small intestine were being included in the proposed study because they contain ganglia and nerves of the enteric nervous system (ENS) and gut-associated lymphoid tissue (GALT). It was of interest to include Peyer's patches (PP) and mesenteric lymph nodes because in several rodent models of scrapie the LRS has been shown to play a key role in TSE peripheral pathogenesis. Although PP and ganglia would be present in a chosen sample of GI tract, it was reasoned that a better representation of the 'in vivo' anatomy would be achieved if jejunum and ileum could be dissected out and preserved in a manner that maintained the natural structure of the gut loop formations. The nerves, blood and lymphatic vessels that supply the gut loops run together in branching cords. Mesenteric lymph nodes are often located at the centre of the loops. All these components are supported by a fragile membrane of connective tissue that spans the loop and holds the structure together (see Figure 3.5A). The practicalities of gut loop

Figure 3.2 Location of the coeliac and mesenteric ganglion complex (CMGC) and associated blood vessels of a female rodent. Adapted from 'The rat nervous system, Volume 2, Hindbrain and Spinal Cord', 1985, Edited by George Paxinos

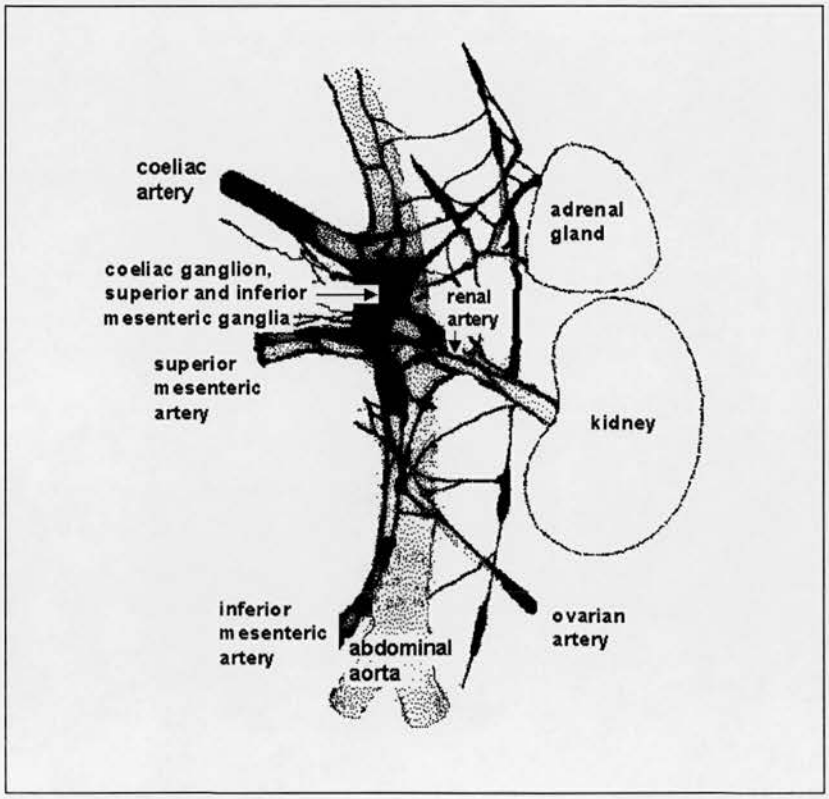

removal were tested in the pilot study. Jejunal and ileal gut loops were carefully removed and mounted on card for immobilisation during fixation. After fixation, the gut contents were gently flushed out using a syringe. During processing the pieces were further supported by filter paper 'envelopes'.

3.2 Trimming, orientation, embedding and cutting of tissues

For the project to provide the desired information, it was necessary that each piece of tissue was present for PrP immunolabelling and microscopic assessment. In the pilot study the presence or absence of any tissue could be ascertained using H&E staining. Prior to this, it was necessary to establish how tissues should be trimmed (sliced up), oriented and embedded in wax so as to be identifiable on the finished microscope slide. As there were a number of tissues with some sub-divided into several pieces, it was essential to devise methods that a) ensured the correct area

and/or maximum amount of tissue was present for microscopic assessment; b) minimised the amount of section cutting and immunolabelling. Trimming, orientation and cutting schedules had to be established for all tissues but different procedures were needed for different tissues.

3.2.1 Trimming, orientation and embedding

Brain: After removal, the fixed brains were placed in a commercial brain-slicing matrix (SEMAT, St Albans) and trimmed throughout their length into two-millimetre thick coronal slices using a series of thin blades (Figures 3.3A-D & 3.6C). The matrix is a plastic block with a brain shaped indentation in which vertical slicing grooves are equally spaced at 1mm intervals. Use of the matrix helped to ensure that brain slices were vertical, symmetrical and of equal thickness. Each piece was then secured in an embedding cassette to prevent movement, processed and embedded in paraffin wax. Using this method, the whole of the brain could be represented in the correct plane and orientation in only one wax block (Figure 3.3E-G).

Spinal cord: Histological preparation is illustrated in Figures 3.4 & 3.5E. The excised fixed spinal cord comprised at least 21 segments (8 cranial and 13 thoracic) plus some of the lumbar portion. DRGs were attached to either side of each segment by nerve roots. Firstly, the cord was laid out flat on its ventral surface and with the aid of the dissecting microscope, bone fragments were gently removed to avoid damage to tissues and the microtome blade during section cutting. Dorsal and ventral nerve roots were cut free from the meningeal membranes that bound roots and cord closely together. The DRG were then spread out at each side of the cord. Vertical cuts were made between each pair of DRG. The pieces were placed caudal end downwards and marked on the cranial surface with India ink. Each piece was then put into a labelled six-division cassette and processed. At embedding the pieces were removed in the appropriate sequence from the cassettes and laid out in the coronal plane with DRG downwards in rows according to the following formula. Starting with cervical segment one (C1), the pieces were placed, inked surface uppermost, in the metal embedding mould in relation to their original position in the intact cord. i.e. C1 was followed by C2, etc. Each row sequentially decreased in number; row one contained 7 pieces (C1-C7), row two had 6 pieces (C8- T5) and so on. In this way, each piece had its own unique location in a particular row (Figure 3.5E&F). Once all the pieces were in position, the embedding mould was cooled slightly to immobilise the pieces and then filled with hot wax. By using this methodology, the separated pieces were brought together in one wax block so that each segment could be identified under the microscope by its position in the block.

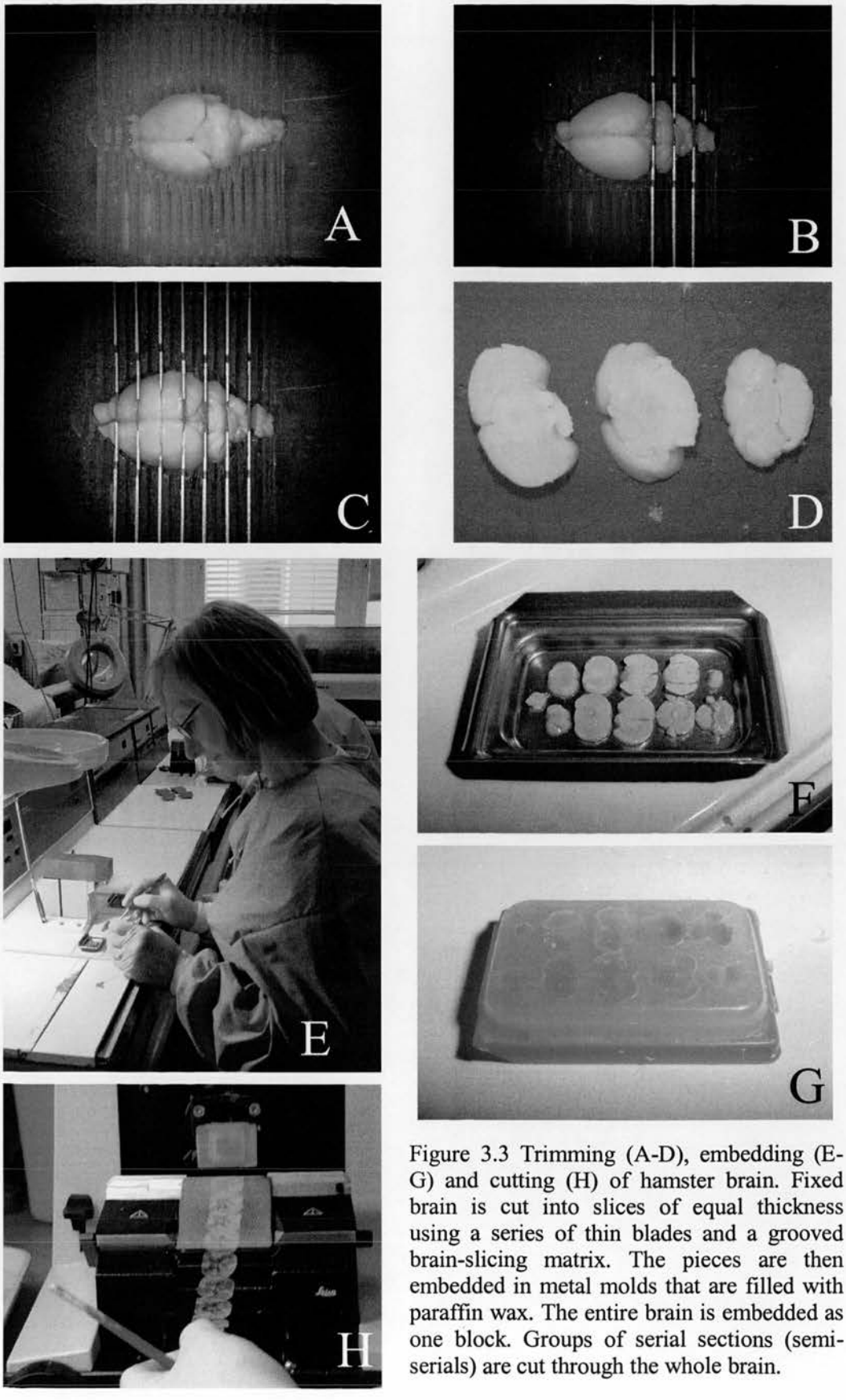

Figure 3.3 Trimming (A-D), embedding (E-G) and cutting (H) of hamster brain. Fixed brain is cut into slices of equal thickness using a series of thin blades and a grooved brain-slicing matrix. The pieces are then embedded in metal molds that are filled with paraffin wax. The entire brain is embedded as one block. Groups of serial sections (semi-serials) are cut through the whole brain.

Figure 3.4 Spinal cord; trimming (A-C) marking (D, E), processing (F) and embedding (G,H)

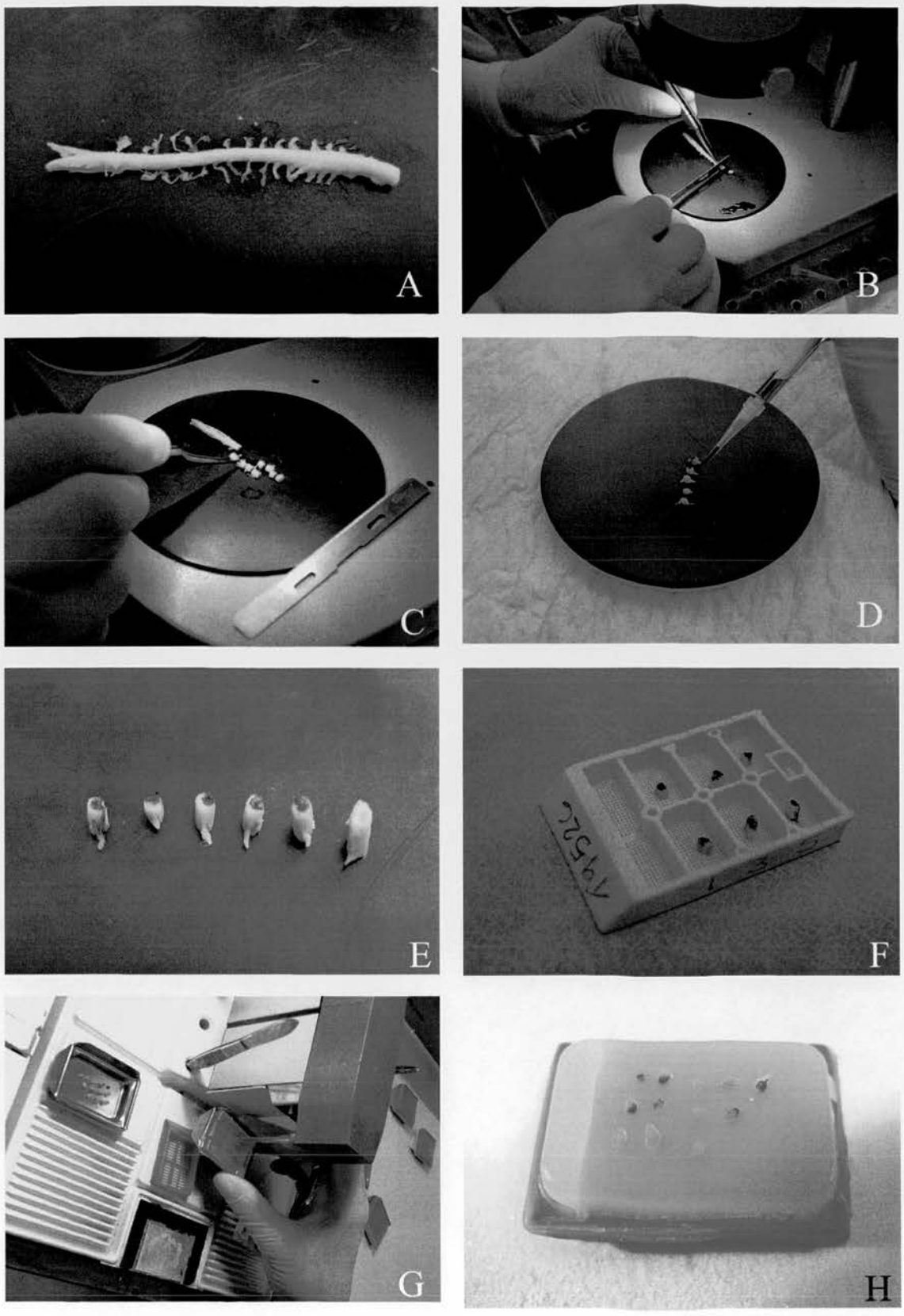

Figure 3.5 Methods employed to orient and embed tissue; diagrammatic representation (A,C,E,G) and results (B,D,F,H)

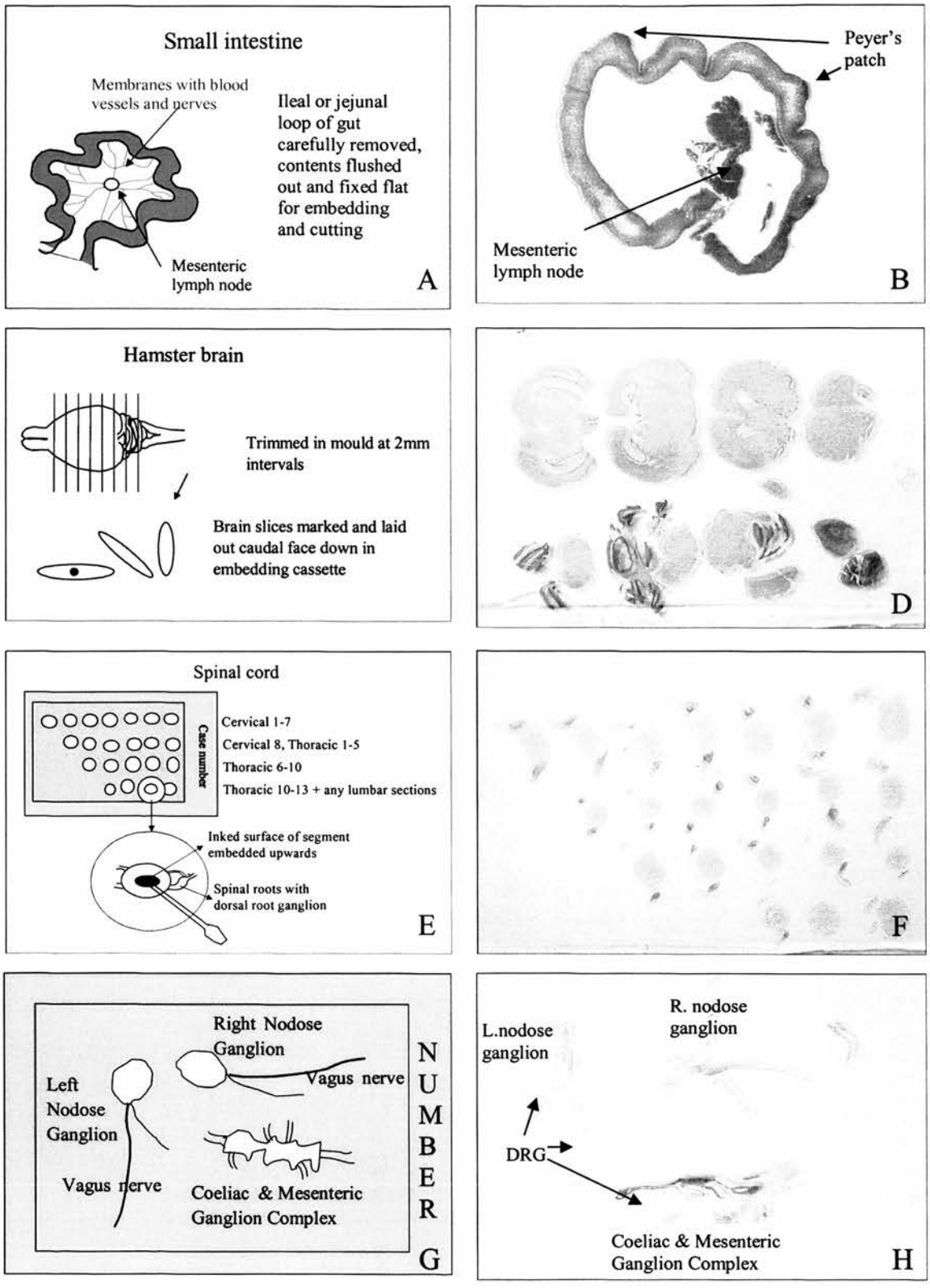

Ganglia: The tissues of the PNS could be processed immediately without the need for trimming but their small size was problematical. The fixed nodose ganglia/vagus nerve complex was so small (less than 0.25mm in diameter), opaque and difficult to see that it was liable to be inadvertently discarded with the fixative or washed through the holes of the cassette during processing. In an effort to ensure their continued existence, the pieces were made more visible by being weakly stained with haematoxylin and processed within fine nylon mesh envelopes.

To reduce the need to cut each tissue individually, it was desirable that both left and right NG and the CMGC be incorporated into the one block. However, the left and right NG are indistinguishable from one another macroscopically and microscopically. To avoid the pieces being mixed up, after being gently removed from the supporting card, each was positioned and oriented in the embedding mould in the layout shown in Figure 3.5G. The left NG was placed in the vertical plane on the left side of the embedding mould with the right NG positioned to its right lying horizontally above, and parallel to, the CMGC. It was important that the right NG was not placed on the right side of the mould because cut sections may be rotated while being mounted on the glass slides. If this happened, left and right could not be distinguished from one another and their individual identities would be lost.

3.2.2 Cutting schedules.

For the CNS, the final complement of sections had to be representative of the entire brain and spinal cord. The aim with the PNS was to ensure that as many sections as possible contained the required components. The ENS is distributed all along the gut wall but care would be needed to make sure that the separate, and much smaller, mesenteric lymph nodes were present on at least some of the gut sections. It was desirable that the major part of each tissue was examined. However, serially sectioning each block would be an overwhelming and unnecessary amount of work. The pilot study was used to test the validity of using an alternative option that would cut down on section cutting without (hopefully) the loss of important tissue. Groups of serial sections taken at regular intervals throughout the tissue (semi-serials) were therefore cut from all tissues. CNS or PNS tissues from two hamsters were sectioned at six microns, the standard thickness used in our laboratory (Figure 3.4H). Brain and small intestine sections were cut at intervals of approximately 200μm, i.e. every 36 sections; spinal cord at 150μm, i.e. every 24 sections and ganglia at intervals of 80μm, i.e. every 14 sections. Six consecutive sections were taken at each interval. In the proposed study these would be used for PrP immunocytochemistry, PET blotting or kept as spares. In the pilot these were either stained with H&E to check tissue integrity and morphology or stained with cresyl violet/luxol fast blue (CV/LFB) to help identify

the various neuroanatomical groups of neurones. One hamster brain was cut serially so that it could be used to check the legitimacy of using semi-serial replacements and to judge the feasibility of further extending the intervals.

3.3 Fixation and immunolabelling trials.

Previous studies had established tissue processing and immunolabelling protocols that gave sensitive detection of PrP in the CNS. The ICC method used (the indirect two-step peroxidase method) had produced good staining in mouse brain and hamster brain and spinal cord from early and late stages of the incubation period (Bruce *et al.*, 1989,94a, Beekes *et al.*, 1998, McBride *et al.*, 1998). Although this procedure had not been applied to the range of tissues described above, it allowed adequate labelling of PrP^d in the DRG so it was likely that the existing methodology would also be suitable for other PNS components. However, a stronger immunolabelling reaction product would be beneficial. Beside this, the original fixation schedules employed a short fixation period (less than 12 hours) while in the present study, practical considerations necessitated a three-day delay from the start of fixation before tissues could be processed and embedded. Therefore, before embarking on the new study, it was necessary to establish whether the longer fixation time would adversely affect PrP detection. Two fixation schedules and two immunolabelling methods were compared.

3.3.1 Fixation trials.

Fixation trials were carried out on periodate-lysine-paraformaldehyde (PLP)-fixed sections of brain from inbred mice or Syrian hamsters. The rodents were intracerebrally injected with brain homogenates of ME7 (12 mice), 22A (4 mice) or 263K (4 hamsters) scrapie or normal brain homogenate (7 mice). At clinical end-point of disease or equivalent, animals were culled by perfusion with PLP under terminal anaesthesia.

Brains were removed and either immersion fixed in PLP for 5 hours and transferred to 70% ethanol for the remainder of a 4-day period *or* immersed in PLP for the entire 4-day period (with regular changes of fixative). The tissues were then trimmed, immersed in 70% ethanol and processed overnight in an automatic tissue processor (Leica TP1050). Tissues were embedded in fresh wax the following morning. Sections of six microns thick were cut. The effects of short or prolonged fixation on PrP were assessed by the Peroxidase anti-Peroxidase (PAP) method. Brain sections from known positive end-point cases served as controls for the methodology.

3.3.2 ICC trials

Two ICC methods were used to visualise and compare the sensitivity of PrP detection. These were; the indirect two-step peroxidase that had been used in the previous study and the PAP method that, by incorporating an additional step, increases signal detection. For this trial, in addition to sections from intracerebrally-infected hamsters and mice, brain sections from the previous time-course study of orally or mock-challenged hamsters were used. The PrP antibodies used were, 1B3 (Farquhar *et al.*, 1989), a rabbit anti-mouse polyclonal (for mice) and 3F4 (Kascsak *et al.*, 1987), a mouse monoclonal (for hamsters). Details of both methods are described in Appendix 2.

3.4 Summary of trials undertaken

On the trips to Berlin and subsequently at NPU, dissections were performed in which brain, spinal cord with DRG, left and right vagus nerve with NG, CMGC, and intestinal loops were taken into formal saline fixative, processed, and embedded. The tissues from six hamsters were used to check the presence, integrity and cellular preservation of the desired pieces of tissue or to establish the most appropriate way to trim, cut and embed the pieces for future studies. All tissues were stained with the histological dyes H&E or CV/LFB. Separate tissues from infected rodents were fixed in PLP for differing periods of time and immunolabelled by either the indirect or PAP methods.

3.5 Results

3.5.1 Dissections

On examination of H&E and CV/LFB stained sections, all tissues had been successfully removed including the macroscopically invisible CMGC (Figures 3.5B,D,F,H & 3.6E). The strategy to remove gastrointestinal tissue as 'loops' also worked very well. The loops appeared intact and included easily identifiable mesenteric lymph nodes and Peyer's patches (Figure 3.5B). Microscopically, all the desired tissue elements were present (Figure 3.6E) and morphologically well preserved (Figure 3.6E). This finding was welcome because inadequate penetration of fixative was a possible consequence of preparing gut in this manner.

Even though the tissues were small and hard to excise all were relatively undamaged. This outcome was important because excessive tissue damage can result in falsely positive immunolabelling (P. McBride, unpublished observation). In most cases spinal cord segments

were in good condition but a few suffered scissor damage. This was considered a consequence of relative inexperience and an occurrence that would be rectified with practise*. It was hoped that it would be possible to remove the cord with both or at least one DRG remaining attached. In practice, the cord was always obtained intact with most DRG present (Figure 3.5A). Given the difficulty of these procedures, results were better than expected.

3.5.2 Trimming, orientation and embedding

The approaches adopted to identify and embed separate tissues and parts of tissues achieved their objectives of reducing the amount of cutting and immunolabelling. The sub-divided and re-amalgamated cord segments were easily identified by their unique position in a particular row (Figure 3.5E&F). For brain, individual identification was unnecessary, as each piece was different. The advantage to using the layouts described in section 3.2.1 was that whole spinal cord or brain was available for viewing in one block. The positioning of ganglia and spinal cord permitted each piece to be individually identified by its relative location to the others both macroscopically and under the microscope (Figures 3.5F, H). As a result, these layouts were adopted as standards and reproduced for each animal.

3.5.3 Section cutting

Assessment was carried out using H&E staining and CV/LFB. In combination, CV aids the identification of neuroanatomical groups by differentiating types of cells by morphology and staining properties while LFB demonstrates nerve processes. In order to adopt the trial cutting intervals used in the pilot experiment as standards, it was essential that all tissues were present on sufficient numbers of sections and that the correct anatomical areas were represented. By comparing H&E-stained semi-serials with the serial sections, it was found that, in general, the selected intervals would supply sufficient sections to provide the desired information.

Morphological differences between sensory and autonomic ganglia were clearly seen even when only a cluster of neurones was present (Figure 3.6 D&F). All three ganglia (left and right NG plus respective vagus nerves, and the CMGC) were found on every section from individual hamsters a high percentage of the time. The CMCG was almost always present on each slide, but fairly regularly, only one of the two NG was present. To increase the inclusion of NG, the

* This was shown to be the case. Removal of the spinal cord/DRG complex was overwhelmingly successful. In the main project segements were mostly undamaged. Almost 100% of DRG were excised from each animal at all timepoints. All but one NG and all CMCG were present and intact.

interval between each group of semi-serials would need to be reduced. This would result in the production of more sections than necessary but by using H&E staining as a screening device, only sections adjacent to those containing ganglia need be immunolabelled.

For the brain and spinal cord, all major areas were present and no particular group of neurones (referred to as nuclei) appeared to be absent from the stained sections. Large neuronal groups of the thalamus, red nucleus and pons could be identified and tracked in their entirety through the appropriate brain levels. Smaller brainstem nuclei such as DMNV and SN (Figure 3.7A-D), and the IML of the spinal cord (Figure 3.7E-F) were also identified in the stained sections. The various nuclei could be located in the plane of the coronal sections and traced dorsally and ventrally in sections from adjacent intervals. These results promoted confidence in the methods employed. Nonetheless, the DMNV, SN and IML are very small focal nuclei whose presence would be crucial to the success of the designed study. It was, therefore, very important that they were available for assessment from every animal in the experiment.

As a result of these findings, it was considered prudent to modify the cutting intervals used in the pilot. In future, sections of brain and spinal cord would be cut and stained at intervals of 100μm, and ganglia at 60μm. For small intestine intervals between sections would remain at 200μm but only 5 sets of sections would be cut and stained. Also, instead of retaining 6 consecutive sections from each set of sections, 10 sections would be taken at each interval. Of these, one would be stained with CV/LFB, two each would be used for PrP ICC and PET blotting and the remaining 5 kept as spares to allow for repeat runs, staining artifacts or the occasional human error.

3.5.4 Fixation trials

Extended fixation in PLP proved to be detrimental to good PrP preservation/detection. In short-fixed brain sections, the different forms of PrP pathology (Bruce *et al.*, 1989,94a, Beekes *et al.*, 1998, McBride *et al.*, 1998) were present and strongly immunolabelled throughout all regions of the brain (Figure 3.8A&B). In sections from all brains fixed for 4 days in PLP, PrP immunolabelling was very much reduced or even absent compared to that seen in brains fixed for only 5 hours in PLP (Figure 3.8C&D). Diffuse PrP^d was particularly weakly stained with only a few punctate deposits remaining. Only amyloid plaques and large PrP aggregates remained easily identifiable. Brain sections from known positive controls showed the typical range and distribution of PrP pathology (data not shown).

Figure 3.6 CV/LFB and H&E staining in hamster CNS, PNS and ileum. A and B; spinal cord cervical segments 2 and 3 with attached DRG, C and D; low and high power views of coeliac and mesenteric ganglion complex - cells are predominantly motor neurones with smaller glia, E; left nodose ganglion containing sensory neurones and no neuropil, F; ileum - muscle layers, orange-pink, submucosa, pale pink, villi, dark pink, myenteric (short arrows) and submucosal (long arrow) enteric ganglia,

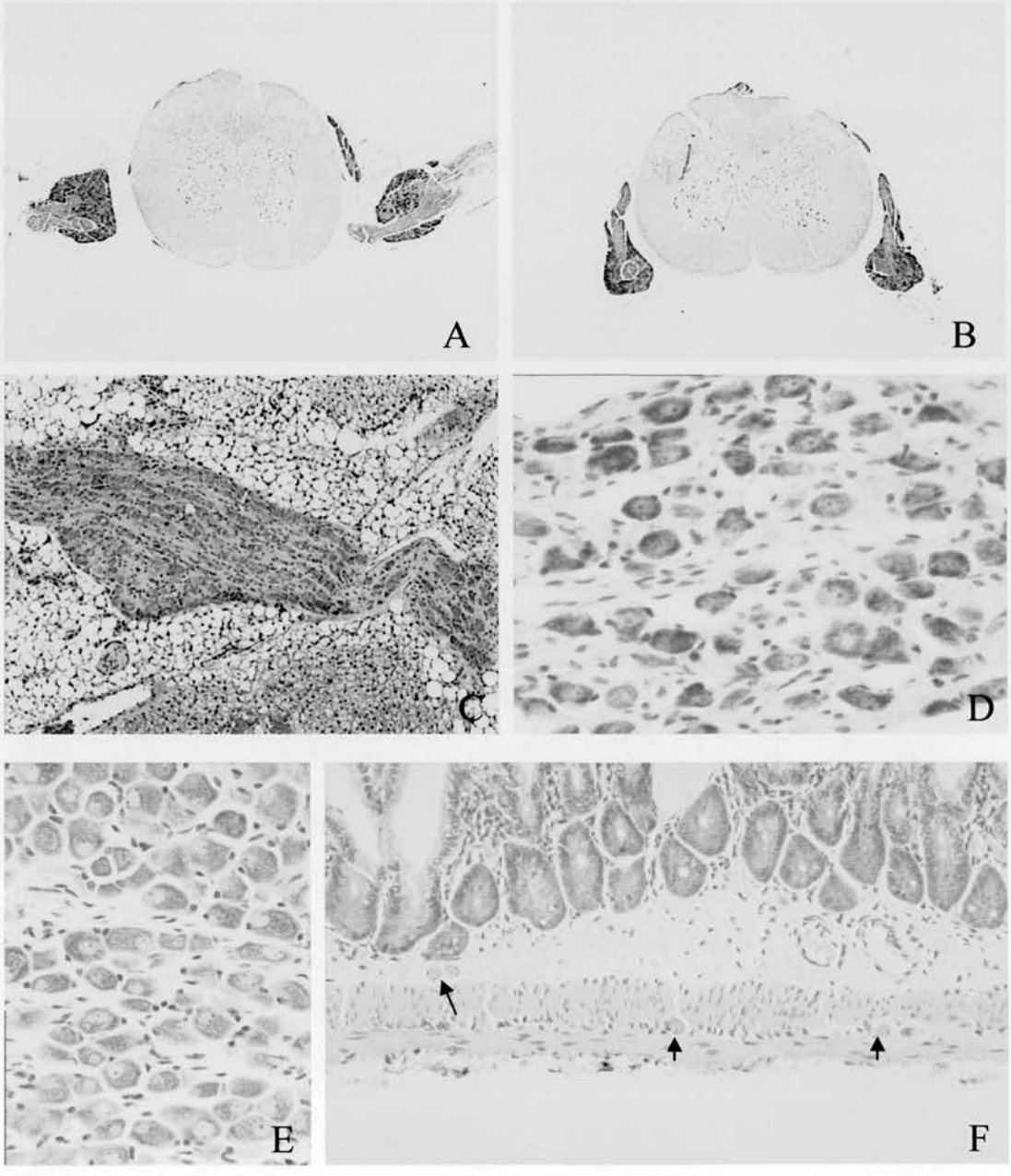

Figure 3.7 Cresyl violet/luxol fast blue staining of CNS. Coronal sections of caudal medulla (A-C) and thoracic spinal segment T7 (D-F) from an uninfected hamster. Cell bodies are shades of purple and nerve fibres are turquoise. A variety of neuronal populations can be identified. A: Several brainstem nuclei are present, DMNV (arrowheads), solitary tract nucleus (SN), area postrema (AP) and hypoglossal nucleus (HN), B: Higher power of A showing the differing morphologies and staining properties of individual cells, C: DMNV motor neurones (oval), D: Low power view of thoracic segments showing inner grey matter 'butterfly' of cell bodies and surrounding white matter fibres. Boxes contain neurones of the intermediolateral cell column (IML) and ventromedial nucleus of the ventral horn (VMN) that are magnified in E and F.

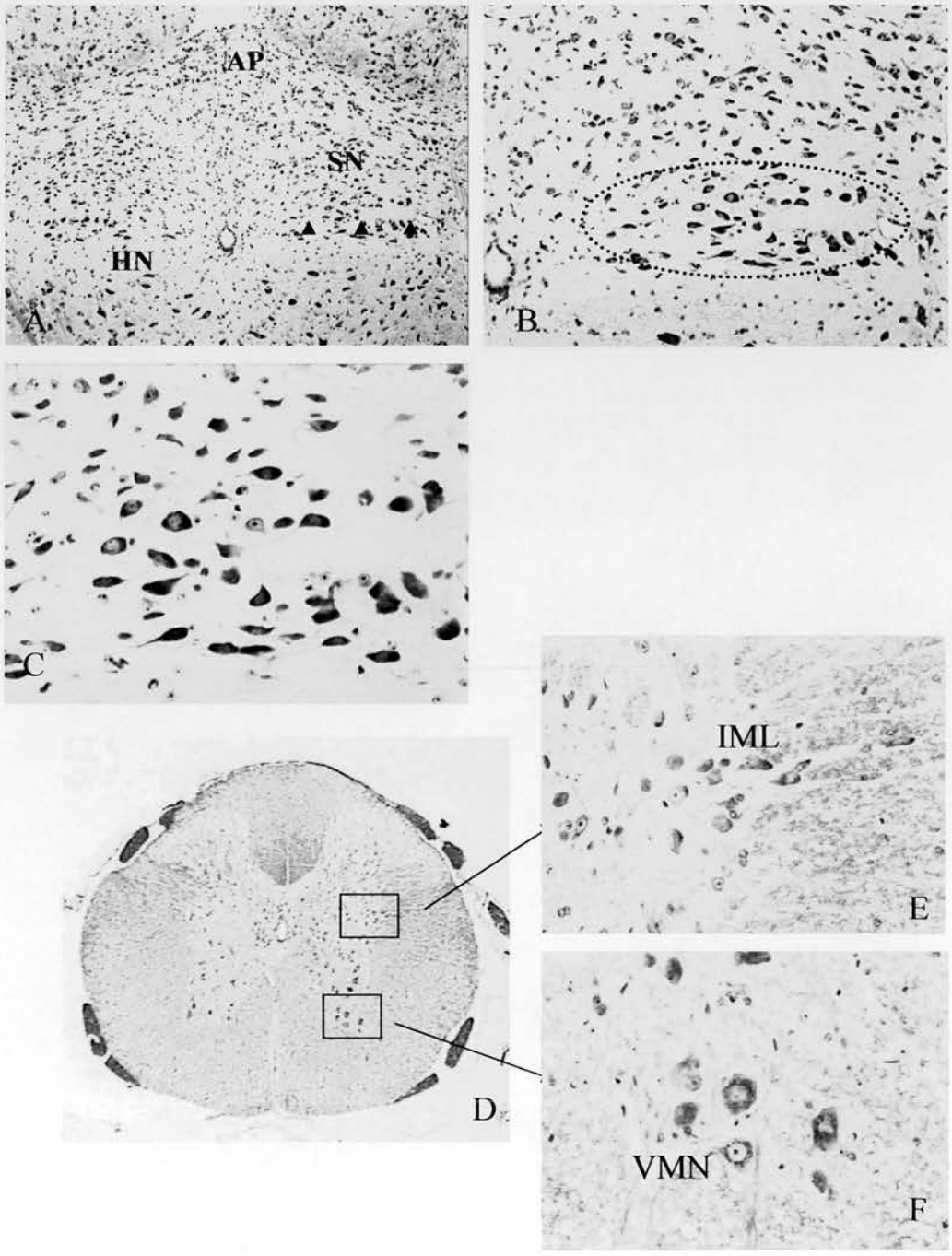

3.5.5 Immunolabelling trials

Comparison of the indirect and PAP immunolabelling methods on brain section from intracerebrally infected hamsters or mice showed that, while both worked well on all sections, the PAP method gave the best results. PrP^d accumulated in the same brain areas with each method but the deposits were darker stained in PAP-labelled sections (Figure 3.9). There appeared to be more abnormal PrP present with the PAP method but this may be due to the more intensely stained reaction product giving better contrast and being easier to see. With both methods, neurones with the appearance typical of PrP^C were occasionally seen (not shown).

Figure 3.8 Duration of fixation. Effect of short (A&B) or long (C&D) fixation with periodate-lysine-paraformaldehyde (PLP). PrP^d (brown granular deposits) is very much reduced in tissue section fixed for 4 days compared to overnight. Disease-associated PrP in medulla/cerebellum (A&C) and thalamus (B&D) of hamsters terminally-affected by 263K scrapie.

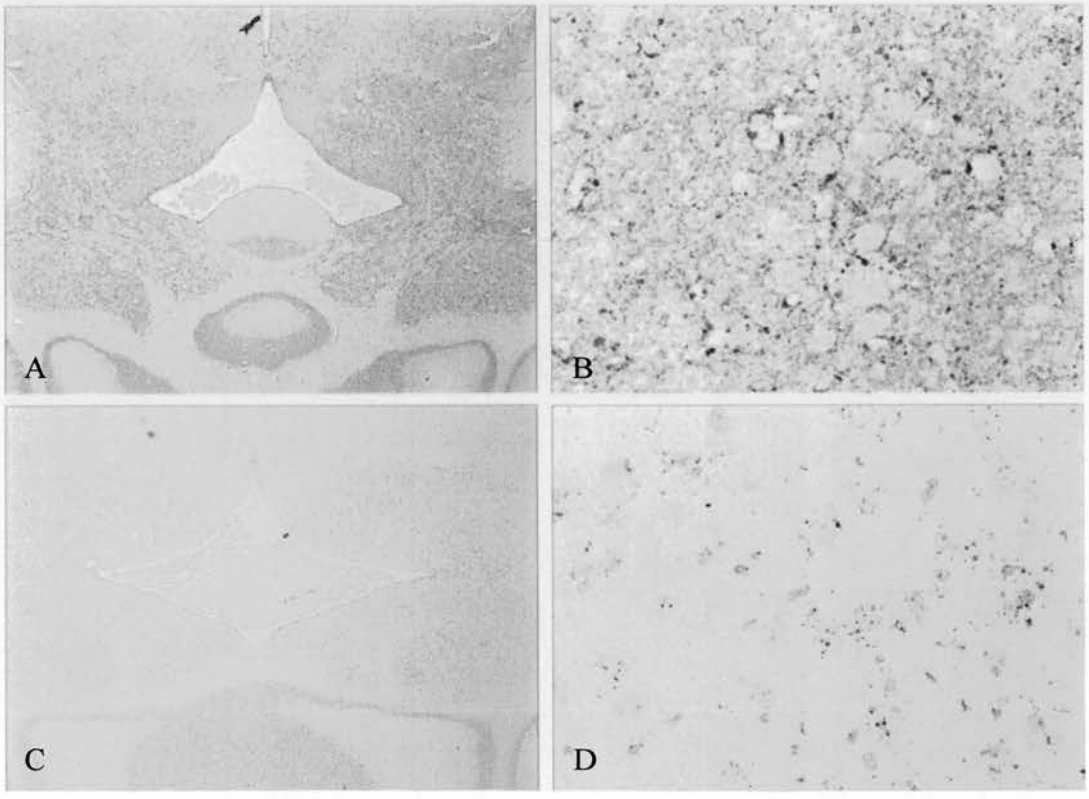

Figure 3.9 Comparison of indirect (right column) and peroxidase anti-peroxidase [PAP] (left column) methods of immunolabelling on adjacent sections of brain from a mouse terminally ill with 87V scrapie. A variety of PrP pathology (brown deposits) and brain area are compared. A: amyloid plaques in the cerebral cortex, B: punctate deposits in the CA2 region of the hippocampus, C: diffuse deposition in the thalamus and D: medulla (midline raphe nucleus at the 4th ventricle). Both methods are adequate but the PAP method gives stronger staining.

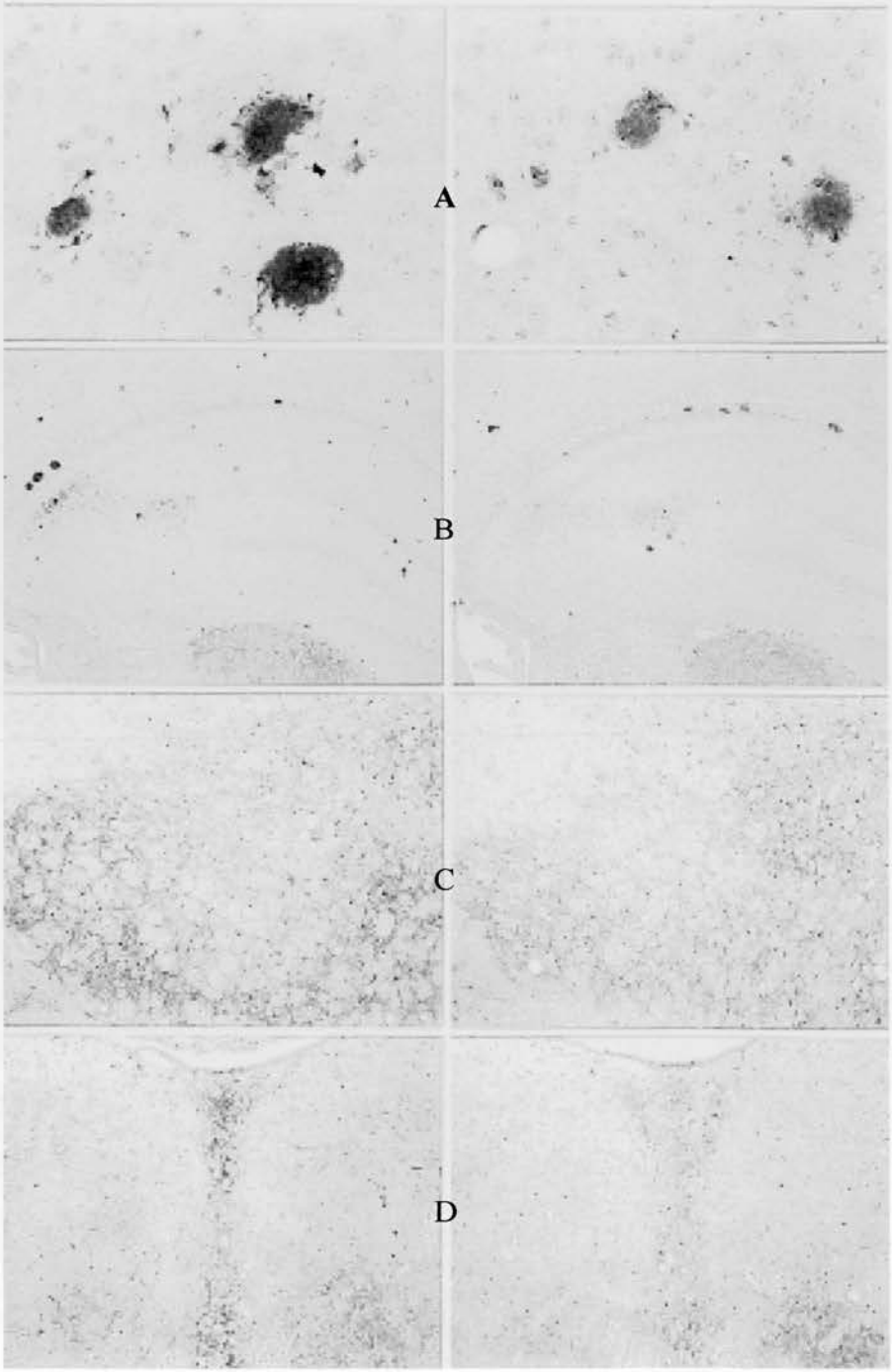

3.6 Discussion

This Chapter describes the strategies used to dissect specific parts of the hamster CNS and PNS and the methods devised to allow these tissues to be displayed for staining and viewing on a microscope slide. It was realised at the outset that the procedures would be complex and technically demanding but these had to be successfully achieved if experiments to elucidate the neuroanatomical pathways of TSE spread were to proceed. In practice, most of the difficulties were overcome and in the main, the methodologies were adopted as being fit for the planned study. The problems encountered were ultimately beneficial as solutions could be sought during the trials and so be avoided in the future.

There was a concern that the micro-dissection of peripheral nervous tissue could not be achieved on small rodents. This was unfounded but some practice was required to become sufficiently competent. It was essential to become familiar with the relevant anatomy and to be able to locate the PNS components with confidence. Attaining the ability to recognise the tissues *in situ* and the expertise to remove them without damage was only possible by using a dissecting microscope and magnifying lamp. The micro-dissections needed great care, manual dexterity and concentration – clumsy use of instruments could destroy valuable material. They also required having to work in the same position for long periods of time which was time consuming and physically tiring.

Other factors were crucial to achieving a successful outcome. It was pivotal that the correct pieces were located and removed undamaged but they also had to be well preserved. Tissues had to be removed accurately but quickly, before the onset of autolysis. This was particularly important for the GI tract as digestive enzymes augment autolysis. For this reason perfusion fixation was the method of choice. Tissues fixed by perfusion are preserved 'from the inside out' via the blood supply as opposed to immersion fixation where excised tissues are fixed by diffusion from the surrounding liquid.

The factors outlined above were common to the dissection of all the tissues but certain tissues had additional specific problems. To obtain comprehensive data from spinal cord, it was desirable that all segments plus their corresponding DRGs were available for viewing on one microscope slide. This was a difficult procedure which, to my knowledge, has not been attempted (or published) previously. The vertebral column encases both spinal cord and DRG so the aim could possibly have been achieved more easily by excising the whole vertebral column and cutting between individual vertebrae. Each section would comprise the spinal cord with

spinal nerve roots linked to DRG surrounded by the interlocking bones of the vertebral arch. It could be assumed that intact segments would present a more realistic view of the '*in-vivo*' relationship between the various components. Three factors argue against employing this strategy:

1) The bones of the vertebrae are locked tightly together. In order to cut between them the column would have to be decalcified requiring several hours immersion in e.g. strong acid or chelating agents. These processes are damaging to soft tissues so tissue matrix preservation and cellular morphology would suffer. While some loss of preservation may be tolerable for general histology it would not be acceptable for PLP-fixed tissues processed for ICC as the subsequent immunolabelling results in high background (signal-to-noise) and uninterpretable analysis.
2) During decalcification the differing tissue elements shrink disproportionately. Consequently, the hard bone shrinks relatively little compared to the softer nervous tissue and the natural close contact is not maintained in the resulting block.
3) All vertebral column segments do not exactly correspond to spinal cord segments. After birth the spinal cord grows at a slower rate than does the vertebral column so that in adulthood, the cord is shorter than the column. As a result the more caudal spinal roots have to descend below the corresponding piece of cord to reach their exit point through the relevant foramen. Therefore, a cut segment of vertebral column may not contain its corresponding DRG.

The points outlined above support the decision to dissect out the cord and attached DRG from the surrounding bone of the column even though this is a lengthy procedure. The technique allows each segment to be represented with its corresponding DRG – a factor considered crucial for the project's success.

Many lessons were learned from the pilot experiments that prevented technical errors and helped to save time, materials and experimental animals. Success was due to many elements including careful planning and execution of the various stages. Sometimes simple schemes proved effective. For instance, by enclosing the smallest tissues in nylon mesh envelopes they were protected during processing and prior staining with haematoxylin allowed them to be seen and manipulated more easily. The idea to embed pieces of GI tract as loops rather than the more customary linear tubes also proved effective. Enteric ganglia run the length of the gut and are present between the muscle layers of any chosen piece but PP are present only at irregular intervals along the small intestine. Both elements could have been present in linear pieces but in

loops these were available along with their associated nerves, blood vessels and draining mesenteric lymph nodes.

A number of potential problems were identified during tissue processing. Often pieces of tissue were indistinguishable from one another and if mixed up, could not be re-identified. Mix-ups could occur at any stage after trimming but were particularly likely to occur during wax embedding. It was found that tissues could float from position through inadequate cooling but if cooled for too long, air bubbles would form causing sectioning difficulties.

A logistical problem arose from the desire to embed multiple pieces of tissue in the same cassette. Individual identity could have been achieved by embedding in separate cassettes but this would have been very labour intensive. This was overcome by devising methods to mark and track the pieces during processing and by embedding each tissue piece according to pre-planned layouts. The procedures were fairly complex but the resulting single block outweighed the time and effort. The strategies greatly reduced the number of final blocks and, in turn, reduced the amount of section cutting and immunolabelling.

Cutting semi-serials at defined intervals instead of serial sectioning was a large factor in reducing section preparation. Accurate representation of CNS anatomy was the main consideration when deciding on CNS cutting intervals. It was necessary to ensure the presence of small groups of neurones within the larger whole. Conversely, with the PNS any problems were due to the small component size and ensuring the threadlike ganglia were retained during processing and were present on a sufficient number of slides. With either CNS or PNS, the various neuronal groups and cell types were identified and differentiated from one another by using CV/LFB dyes. The DMNV and IML are restricted to specific locations in brain and thoracic spinal cord, respectively. These and other important brain stem nuclei were almost always present in CV/LFB-stained sections. This finding was crucial as frequent absence would have had been a serious setback. The subsequent identification of these structures was key to proving the hypothesis of spread.

One important outcome of the pilot trials was to show that it was not possible for one individual to carry out the perfusions, dissections and histological preparations. Dissection of the four animals (the number that would be culled at each time point) took two and a half days and spinal cord preparation, another day. Preparation of the other tissues, processing and embedding required the rest of the week. As the histological and immunocytochemical expertise lay at NPU,

it was decided that the scrapie infections and dissections would be carried out at the Robert Koch Institute and the rest of the procedures (including microscopical analysis) performed at NPU. This division of labour also allowed a direct comparison with the study described in Chapter 2. The techniques carried out here were in the main novel and ambitious but as much of the information regarding peripheral pathogenesis of 263K scrapie derives from our previous studies using orally-challenged hamsters, failure to establish the necessary expertise would have been disappointing and a setback to future research. The success of the pilot experiments provided reasonable optimism that the planned experimental objectives could be achieved. It was now possible to test the hypothesis of neuroanatomical spread. Chapter 4 describes the work of this experiment.

Chapter 4: Oral spread of 263K scrapie: Neuroanatomical routing from the gastrointestinal tract to the CNS

4.0 Introduction

Although the ultimate target of infection is the central nervous system (CNS), there is mounting evidence that in natural (Groschup *et al.*, 1996, van Keulen *et al.*,1999), and experimental (Kimberlin *et al.*,1983b, Baldauf *et al.*,1997, Groschup *et al.*,1999) scrapie, BSE (Wells *et al.*,1998) and vCJD (Haïk *et al.*, 2003) the PNS plays a key role in conveying the TSE agent to the brain and spinal cord from sites of uptake in the alimentary tract. Regardless of the initial mechanisms of uptake from extraneural sites, spread of infection to the brain and spinal cord follows a similar trend in many peripherally infected rodent models of scrapie including this model of oral challenge. Infectivity (Kimberlin & Walker 1982,86,89b, Beekes *et al.*,1996) and protease-resistant PrP (Beekes *et al.*,1996, Baldauf *et al.*,1997) are detected earliest in hindbrain and mid-thoracic spinal cord. Subsequent spread of infection occurs in both cranial and caudal directions (Kimberlin & Walker 1982, 89b, Beekes *et al.*,1996, Baldauf *et al.*,1997). The immunocytochemical detection of PrP^d described in Chapter 2 supported these findings and provided additional evidence that after oral challenge, 263K scrapie is routed to the brain and spinal cord independently. In the brain, the first target site for PrP^d accumulation was the DMNV followed shortly afterwards by the SN, and in the spinal cord PrP^d was first found between thoracic segments 4 and 9.

Targeting to these specific sites is consistent with transit along the vagus and splanchnic nerves supplying the viscera. Identification of the initial cerebral target sites showed that the vagus nerve was a primary pathway to the brain in this model and strongly implicated the splanchnic nerve as the conduit between the gastrointestinal tract and the spinal cord. Also, data drawn from the temporal sequence of PrP^d deposition provided significant indicators that initial spread may have occurred along autonomic rather than sensory fibres of these nerves. Bearing this and the neuroanatomical pathways that link the CNS to the GI tract in mind, it was possible to hypothesise the route and manner by which the agent would need to travel to reach these initial CNS target sites. The data suggested that, after ingestion, the 263K scrapie spreads in a retrograde direction, along autonomic PNS fibres and ganglia supplying the mesentery i.e. along sympathetic and parasympathetic efferents of the splanchnic and vagus nerves (Figure 4.1). If this were the case, the DMNV and the splanchnic preganglionic neurones of the intermediolateral cell column (IML) would be primarily involved. Here autonomic prevertebral ganglia (CMGC) would be intermediate relay points. Spread could also take place along the sensory afferent fibres and in this scenario, the SN and dorsal horn would be the initial targets for PrP^d deposition with the

Figure 4.1 Neural pathways that link the gastrointestinal tract with brain and spinal cord. Circuitry has been simplified to show major routes only. The infectious agent may reach the CNS by spreading along efferent (motor) or afferent (sensory) fibres of vagus or splanchnic nerves. Efferent fibres of the vagus have their nerve cell bodies in the DMNV and synapse with neurones of the ENS in ganglia of the submucosal and myenteric plexuses in the wall of the alimentary tract. The nerve cells of vagal afferent fibres are located in the NG and directly innervate the alimentary canal. These fibres run to the SN where they synapse with interneurones projecting to the DMNV. The cell bodies of splanchnic efferents are located in the IML, and synapse with CMGC neurones that, in turn, innervate the GI tract. Afferent fibres of the splanchnic nerve originate in the DRG, run through the CMGC and directly innervate target organs such as the alimentary canal.

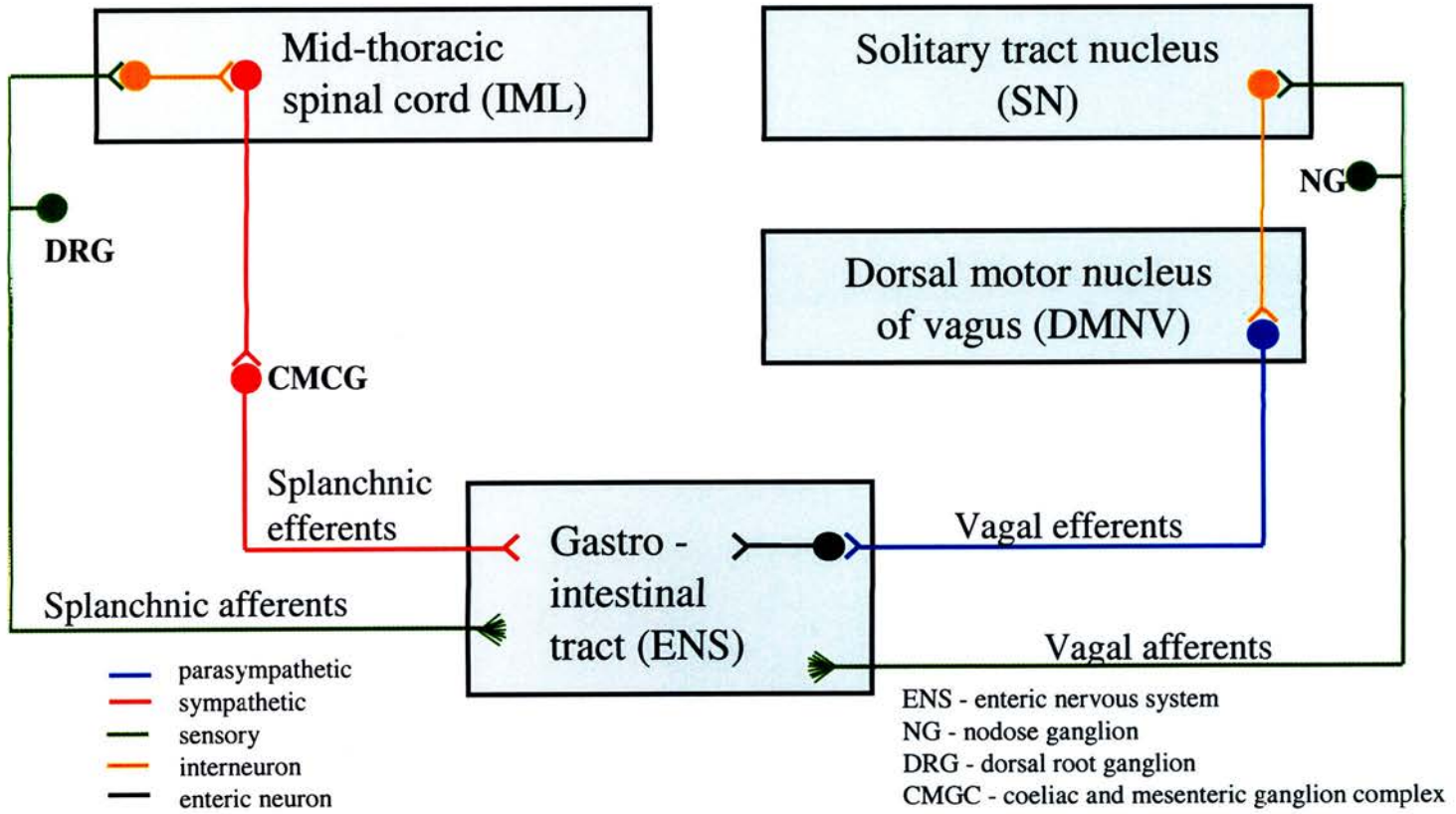

respective sensory neurones of NG and DRG being the intermediaries. Intramural ganglia of the enteric nervous system are also possible sites in which infectivity (PrP^d) could be replicated. Spread could, however, be more indiscriminate and occur simultaneously along both sensory and motor fibres.

To investigate this hypothesis it was necessary to assess the involvement of these nerves in the oral pathogenesis of 263K scrapie. This chapter describes a second time-course experiment in the same rodent model of oral challenge. The aim was to undertake a detailed examination of vagus and splanchnic nerve circuitry focusing on tissues previously identified as being potentially relevant to infectious spread in this model. Specific components of the PNS were examined for the presence of PrP^d along with brain and spinal cord with which they form relay circuits. Jejunum and ileum were included in the study as they contain ganglia of the enteric nervous system (ENS) that forms synaptic links with both nerves. The technical difficulties involved in this undertaking and their resolution were outlined in Chapter 3.

Tissues were collected at points throughout the incubation period and ICC was used to identify the location and temporal sequence of PrP^d in tissue sections. In addition, in collaboration with Dr. Walter Schulz-Schaeffer of the University of Göttingen, Germany, Paraffin Embedded Tissue (PET) blotting was carried out on adjacent sections. This technique employs pretreatments that involve incubating sections for several hours in proteinase K and guanidine to destroy cellular PrP. Thereafter, only the PK-resistant fractions (PrP^{Sc}) remain available for immuno-detection (Schulz-Schaeffer *et al.*, 2000a).

There is little or no data reporting how much infectivity exists in nerves and ganglia after oral TSE infection. For this reason, selective bioassays were also carried out to assess the level of infectivity in two key PNS components, the cervical vagus nerve and the coeliac and mesenteric ganglion complex (CMGC). Such information provides comparisons with the PrP^d deposition and can offer clues to mechanisms of agent transportation and spread. The identity of extraneural reservoirs of infection is also important from a wider perspective as these provide potential sites for early diagnosis and cross-contamination of, for example, surgical instruments.

Using these approaches, it was possible to identify the precise temporal sequence and location of PrP^d (and PrP^{Sc}) deposition in the CNS, PNS and ENS and thereby to define the neuroanatomical pathways involved in early pathogenesis. In addition, data from the

bioassays showed that only minimal levels of infectivity existed in the nerves while substantially higher amounts were contained in autonomic ganglia.

4.1 Materials and Methods

4.1.1 Experimental design

Outbred Syrian hamsters were fed individual food pellets doused with 100µl of a 10% hamster brain homogenate from 263K scrapie-infected donors or uninfected controls as previously described in Chapter 2. For ICC studies, four or five hamsters were culled by CO_2 inhalation at specific time points throughout the incubation period; 56, 62, 69, 76, 83, 90, 97, 104, 111, 118, 126, 132 days post infection (dpi) or at clinical end-point of disease (159±4 [S.E.] dpi). Two mock-challenged hamsters, similarly fed with normal brain homogenate, were sacrificed at 161dpi.

For bioassay experiments, specimens were taken from five terminally ill and two mock-challenged hamsters. Only tissues from end-point cases were subject to bioassay. Previous studies using mice have shown low or undetectable levels of infectivity from peripheral tissues assayed from preclinical stages of disease (M. Bruce, personal communication). As bioassays are lengthy experiments involving the use of many animals and the presence of infectivity in endpoint tissues had not been established, the inclusion of early timepoint tissues could not be justified at this stage.

4.1.2 Histological procedures

Hamsters were transcardially perfused with periodate-lysine-paraformaldehyde (PLP). Dissections were then carried out as described in Chapter 3.1 and Appendix 1. The brain and CMGC were removed from all hamsters. Spinal cord with attached DRG, jejunum, ileum (adjacent to the ileocaecal sphincter), spleen, salivary gland (with associated lymph nodes) and left and right NG with attached cervical vagus nerve were included from 69dpi to endpoint of disease. After perfusion, tissues were immersed for 5 hours in PLP, transferred to 70% alcohol for a further 48 hours, processed over 6 hours in an enclosed tissue processor and embedded in paraffin wax according to the procedures described in Chapter 3.3.1. Prior to processing and embedding, brains were trimmed coronally into 2mm thick slices using a brain-slicing mould. Spinal cords were sliced coronally between nerve roots to provide individual cervical, thoracic and sometimes lumbar segments with corresponding left and right DRG. Pieces were marked on their cranial surface with Indian ink, numbered and processed separately but embedded, in sequence, in one block. Six micron sections of brain and spinal cord with attached DRG were taken at 100 micron intervals for PrP immunocytochemistry and cresyl violet/luxol fast blue (CV/LFB) histochemistry. On other tissues these procedures were carried out either on serial sections or at 50 micron intervals.

4.1.3 Immunocytochemistry

Immunostaining was carried out according to the ABC method* using the 3F4 mouse anti-hamster PrP monoclonal antibody or normal serum and diaminobenzidine to visualise the reaction product. Sections were pretreated with formic acid for 10 minutes to enhance PrP visualisation. To ensure antibody specificity adjacent sections were incubated with normal serum in place of primary antibody. Similarly treated sections from mock-challenged hamsters served as control tissue. (Full method is described in Appendix 2)

4.1.4 Paraffin-Embedded Tissue (PET) blotting

Sections were mounted on nitrocellulose membranes (0.45 micron pore size: Bio-Rad Laboratories, Hemel Hempstead, Herts, England), dried flat at room temperature (approx. 2hrs.) and incubated overnight at 37^{0}C. PET blotting was carried out according to Schulz-Schaeffer et al. (Schulz- Schaeffer *et al.*, 2000a). After washing in TBS with 0.05% Tween 20, sections were digested with 250μg/ml proteinase K (PK) in PK buffer (10mM/L Tris-HCl, pH 7.8; 100mM/L NaCl; 0.1% [w/v] Brij 35) for 8hrs. at 55^{0}C. Sections were then treated with with 3M guanidine isothiocyanate to denature PrP^C. Immunostaining was carried out using 3F4 mouse anti-hamster monoclonal antibody to label PrP and NBT/BCIP to visualise the reaction product. PET blots were analysed using a dissecting microscope.

4.1.5 Quantification of PrP^d

Deposition was assessed in ICC sections using light microscopy according to the following criteria:

\+ Punctate PrP^d on the membrane (surface) or within very few cells (neurones or glia). Visible only at high power (x40 objective).

++ Punctate and granular PrP^d deposited diffusely within or in the adjacent neuropil of several individual cells or localised neuronal groups. Visible using x20 or x40 objectives.

+++ Granular PrP^d accumulated fairly extensively in and around substantial numbers of grouped cells and associated with a number of groups. Obvious using x4 or x10 objective.

++++ Aggregated and/or granular PrP^d greatly accumulated in several distinct neuroanatomical regions or ganglia and diffusely distributed throughout the CNS. Easily seen at low power with x2 or x4 objectives.

---

* The PAP method was replaced by ABC method as further immunolabelling trials showed that ABC gave greater sensitivity of PrP detection

4.1.6 Infectivity bioassays

Vagus nerve and CMGC samples were removed from two terminally ill animals (S1 and S2) and two mock-infected controls. From another three terminally ill hamsters (S3-S5) only vagus nerve samples were taken. To avoid the inclusion of ganglion cell bodies left and right portions (of approximately 1 cm in length) of cervical vagus were removed at a position that was remote from the NG and carefully separated from surrounding tissue. The CMGC was removed attached to the abdominal aorta between the coeliac, superior mesenteric, left renal and right renal arteries. Two 0.5cm pieces from the abdominal artery cranially and caudally adjacent to the CMGC were also sampled. Samples were washed three times in Tris-buffered saline (TBS: 10 mM Tris-HCl, 133 mM NaCl, pH 7.4), incubated at 37°C for 1.5 hr. in 200µl TBS containing 0.25% (w/v) collagenase [Boehringer Mannheim] and 0.025% (w/v) $CaCl_2$ and heated to 80°C for 10 min. The volume was adjusted to 500µl with TBS. 50µl aliquots were inoculated intracerebrally into groups of 5 recipient hamsters. Infectivity titres were estimated from the incubation periods using dose-response curves as previously described (Beekes *et al.*, 1996). The experiment was terminated at 370dpi. Infectivity assays were carried out at the Robert Koch Institute by Michael Beekes.

4.2 Results

To accurately reflect the distribution of PrP^d, ICC, PET blots and CV/LFB histochemistry (to aid neuroanatomical identification) were carried out on series of adjacent sections cut either serially or at intervals through each tissue. Tissues comprised components of splanchnic sympathetic/CNS/sensory (CMGC – IML - DRG) or vagal parasympathetic/CNS/sensory (DMNV – SN - NG) relay circuits and the ileal and jejunal ENS. Diagrammatic representation of the major pathways forming the inter-linking circuitry is shown in Figure 4.1.

4.2.1 Physical appearance of PrP

The cellular appearance of PrP^d and PrP^C was identical to that described in Chapter 2. PrP pathology was marked by characteristic punctate, granular or aggregated accumulations in and around neurones of neuroanatomically distinct CNS regions and peripheral or enteric ganglia of the ENS (Figure 4.2). In tissue sections of 263K-challenged hamsters, the earliest PrP^d was punctate deposition localised at the surface and in the adjacent neuropil of neurones and, sometimes, neuroglia (Figure 4.2A-C). In NG and DRG, PrP^d appeared as intensely stained granular inclusions within a proportion of ganglion neurones and adjacent satellite cells (Figure 4.2D). Labelling of CMGC was similar to the sensory ganglia in initial appearance and progressive accumulation but, probably reflecting differences in anatomy, extracellular labelling of CMGC neuropil was also evident from early stages (Figure 4.2E).

In mock-infected controls, PrP^C was seen only in some neuronal cell bodies, mostly of the brainstem and grey matter of spinal cord. PrP^C was non-granular, labelled less intensely and differed in appearance from any of the (largely extracellular) granular forms of PrP^d (see Chapter 2, Figure 2.7A)

4.2.2 Early temporal and spatial deposition of PrP^d in enteric, splanchnic and vagus nerve relays

The extent of PrP^d accumulation varied between individuals culled within any time-point but the site and sequence of deposition was consistent. PrP^d was found earlier and with more frequency in autonomic components of the circuitry compared to sensory components. In the splanchnic nerve circuitry, PrP^d was found in the CMGC and IML prior to DRG and in the vagal circuitry, in the DMNV before NG. The ENS contains autonomic and sensory NS networks. Table 4.1 summarises the temporal and spatial deposition of PrP^d in enteric, splanchnic and vagal relays.

4.2.2i ENS

PrP^d was found from the earliest available time point (69dpi) to end-point of disease in and around neurones of the myenteric and submucosal ganglia of ileum and jejunum of all four hamsters (Figure 4.2C, 4.3A&B). At this stage of the incubation, deposits were generally fairly abundant and associated with several but not all ganglia. As the incubation period progressed, accumulations increased in individual ganglia and the number of affected ganglia also increased (Figure 4.3C&D, 4.4A).

4.2.2ii Splanchnic nerve circuitry (CMGC –IML - DRG)

PrP^d was observed in the CMGC of all four hamsters at the first time point of 56dpi, (Table 4.1). Initial deposits were few but PrP^d accumulated rapidly. By 76dpi deposition was substantial and by 90dpi PrP^d was detected throughout most of the complex (Figure 4.4B). In spinal cord, PrP^d was invariably seen in the IML at 69dpi, the earliest time point at which cord was available. Deposition was present in thoracic cord segments 3-8 with the greatest amounts in the IML of segments 5, 6 & 7 (Figure 4.4C,D). PrP^d was not detected in DRG until 76dpi when one or two positive cells were observed in mid-thoracic DRG in two out of four hamsters. In later timepoints, deposition remained either absent or scant and was always less than that of the corresponding IML (Figure 4.4E). In all cases PrP^d was found in DRG only after accumulations were fairly widespread within the corresponding cord segment.

4.2.2iii Vagus nerve circuitry (DMNV – SN - NG)

In the brain, the first PrP^d deposits were seen in and around neurones of the DMNV at 62dpi (two out of four brains) and the commissural nucleus of the SN (one out of four brains). In

both areas deposition was minimal but was greater in the DMNV. In later time-points accumulations were typically heavier in the DMNV compared to the SN (Figures 4.5A-C). PrP^d was either low or undetected in NG until 90dpi (Figure 4.5D). At 69, 76 and 83 dpi, PrP^d was found in only a few cells per ganglion and at 90dpi there were only moderate numbers of positively labelled cells. As with the DRG (and in contrast to the CMGC), accumulation was slow and at endpoint of disease several neurones remained unlabelled (Figure 4.5E).

4.2.3 Subsequent pattern of PrP^d accumulation in the PNS and CNS

Subsequent to the IML, PrP^d was observed in intermediate zone (69dpi), around the central canal and then (76dpi) extending from the IML into the adjacent white matter along processes of radial glia (Figure 4.4D). This pattern of early spread is consistent with distribution of PrP^d along the other sympathetic preganglionic neurones that form links with the IML (Cabot 1990). Specifically, these are the intercalated nucleus in the intermediate zone, the central autonomic nucleus located around the central canal and the lateral funicular nucleus whose dendrites extend into the white matter of the lateral funiculus. Accumulations became progressively greater in the initial sites and generally more widespread, firstly within the medial portion of the dorsal grey matter and next within the ventral horn. Concurrent with this, PrP^d appeared in the IML of thoracic segments located cranial and caudal to those first affected. The presence of PrP^d in these latter sites is also consistent with dendritic field of IML-linked neurones within the transverse plane of the same segment and the 'ladder-like' attachments with IML 'nests' in adjacent segments that are located longitudinally (Cabot 1990). This pattern of spread continued with increasing incubation and at late stages of disease, all infected hamsters showed marked granular deposition of PrP^d throughout the brain and grey matter 'butterfly' of all spinal cord segments (Figure 4.6).

Once accumulation was established in the DMNV and commissural portion of the SN, PrP^d was observed in medial and central regions of the SN and then in other specific brainstem nuclei, notably those of the medullary reticular formation (76dpi), vestibular complex, pons and red nucleus (83dpi). Labelling was then rapidly disseminated to several other sites throughout the brain. (Areas affected and pattern of spread are illustrated in Table 2.1 and Figure 2.2 of Chapter 2).

Throughout the incubation period, the sequence and spatial precision of targeting was consistent. The final PrP^d distribution pattern was identical in all spinal cords (Figure 4.6) brains (Figure 4.7) and ganglia. In autonomic and sensory ganglia, the number of PrP^d inclusions and affected cells increased with incubation but even at late-stage disease a

proportion of neurones remained unlabelled although the percentage of unlabelled cells was higher in sensory ganglia, i.e. DRG and NG (Figure 4.2D, 4.4E, 4.5D&E). PrP^d was mostly absent from vagus, splanchnic or spinal nerve roots but a tiny amount was found in the vagus and splanchnic nerve of one terminally-ill hamster (Figure 4.8A&B). Staining was absent from tissues when normal serum replaced PrP antibody.

Although the dissecting microscope does not provide the resolution necessary to view cellular detail in PET blots, aggregations of protease-resistant PrP (PrP^{Sc}) were found in specific neuroanatomical areas of infected hamsters only. In all tissue specimens, at all time points, PrP^{Sc} was seen in the same sites as PrP^d was observed in adjacent ICC-labelled sections (Figure 4.9A&B) indicating that the disease-specific deposits seen with ICC are proteinase K resistant. However, in PET blots, deposits were stained more intensely and were more easily detected at low power than the corresponding ICC-labelled deposits. (Compare Figures 4.9A and B with 4.4C and 4.5A). These findings appear to show that the sensitivity of antigen detection is better with the PET blot than that of ICC. However, it may be that the superior contrast and heavy blue-black chromagen makes the positive labelling more easily seen. Either way, the strong reaction product, the ability to detect small amounts of PrP^{Sc} and the fact that a slice of tissue can be quickly viewed makes PET blotting a useful complementary technique.

Table 4.1 Presence of PrP^d (No.affected/No.in group) in ENS and splanchnic and vagus nerve relays after ingestion of 263K scrapie

DPI/[1]	Enteric ganglia	CMGC	mid-T IML	mid-T DRG	DMNV	SN	Right NG	Left NG
56	nd	4/4	nd	nd	0/4	0/4	nd	nd
62/63	nd	4/4	nd	nd	2/4	1/4	nd	nd
69	4/4	4/4	4/4	0/4	4/4	1/4	1/4	0/4
76	4/4	4/4	4/4	2/4	4/4	1/4	3/4	1/2*
83	4/4	4/4	4/4	3/4	3/3*	3/3*	3/4	2/4
90	4/4	4/4	4/4	3/4	4/4	3/4	3/4	4/4

[1] Early timepoints; incubation period ~160dpi: nd: not done; * 4 in group; area not present in other animals

Figure 4.2 Appearance of PrP^d (brown granular deposition) in CNS, PNS and ENS of a 263K orally-challenged hamster. The earliest deposition (A-C) is localised within, at the surface and in the adjacent neuropil of neurons and glia. A: DMNV at 76dpi;B: A single neuron with associated glia (arrows) in the CMGC at 56dpi; C: Myenteric (Auerbach's) plexus at 69dpi. In sensory ganglia, PrP^d is confined to cell bodies and associated satellite cells(arrows) throughout the incubation period but in sympathetic ganglia PrP^d is commonly deposited on neuronal membranes and accumulates progressively in the neuropil. D; DRG with satellite glia (arrows) and E; CMGC at endpoint of disease. Scale bars A,C, E=30μm; B=12.5μm D=25μm.

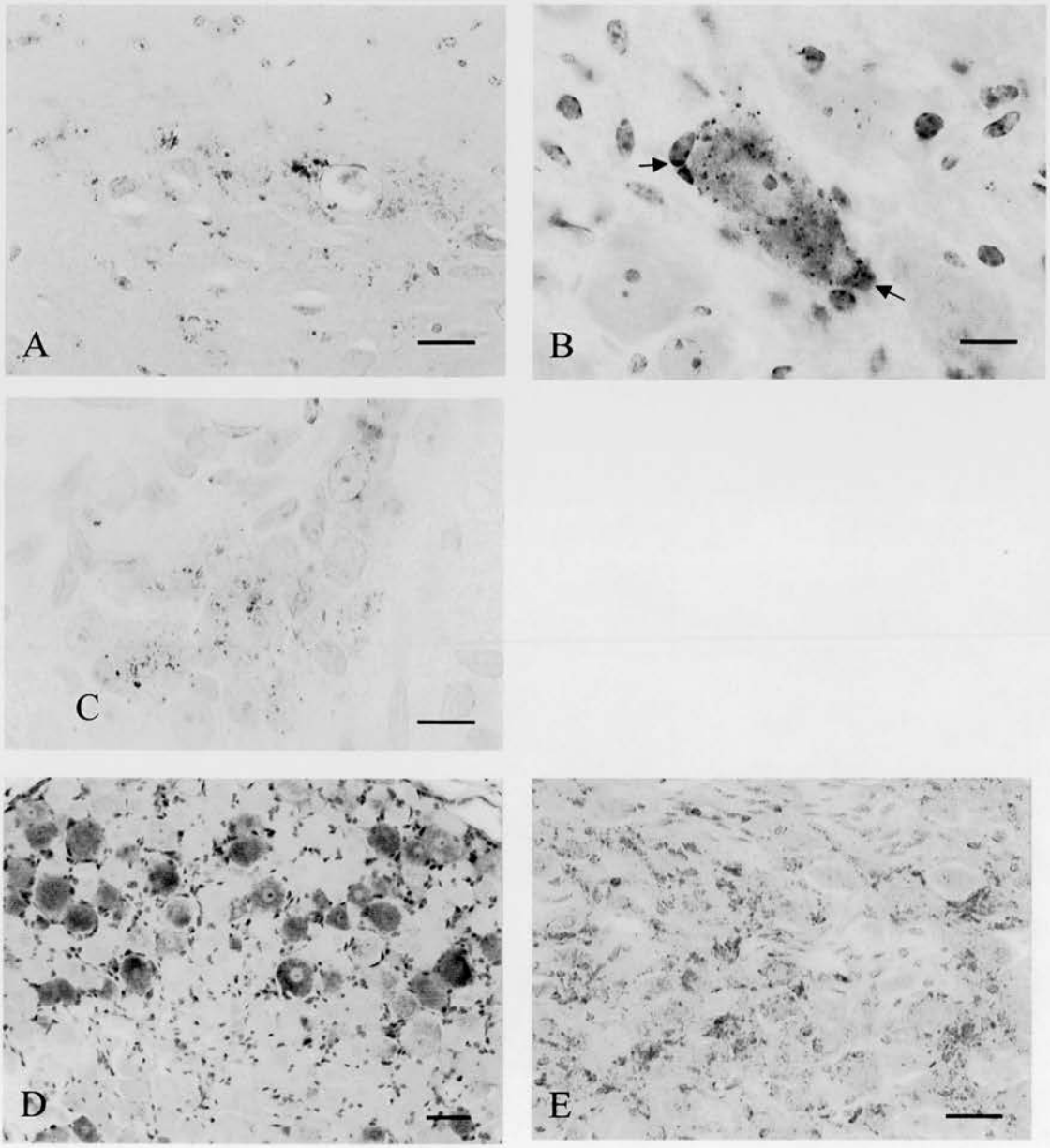

Figure 4.3 Immunolabelling of PrP^d (brown granular deposition) in ileal ENS ganglia of 263K orally challenged hamsters, culled early (A,B) and late (C,D) in the incubation period. Myenteric (hatched arrowheads) and submucosal (open arrowheads) plexus at 69dpi (A&B); and 126dpi (C&D). Scale bars: A,C = 20μm, B,D = 10μm.

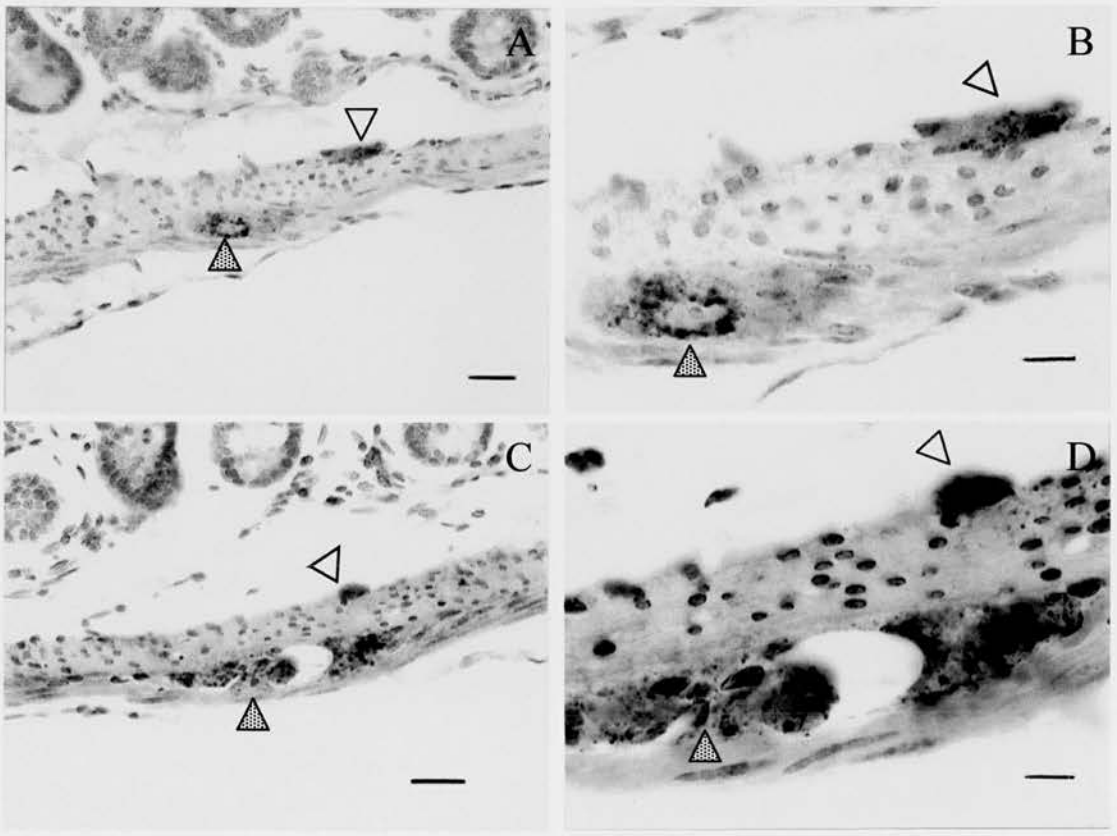

Figure 4.4 PrP^d in the ENS and splanchnic nerve circuitry of the same hamster 90 days after oral challenge with 263K scrapie. A; Myenteric plexus, B; CMGC, C,D; Spinal cord segment T5, D; Detail of IML showing PrP^d accumulating around IML neurones and tracking through the white matter along radial glia, E; DRG sensory neurones with satellite glia (arrows). PrP^d deposition is already extensive in the ENS and CMGC at this stage of the incubation but is minimal in DRG. Scale bars: A,D,E = 20μm; B = 50μm; C = 100μm

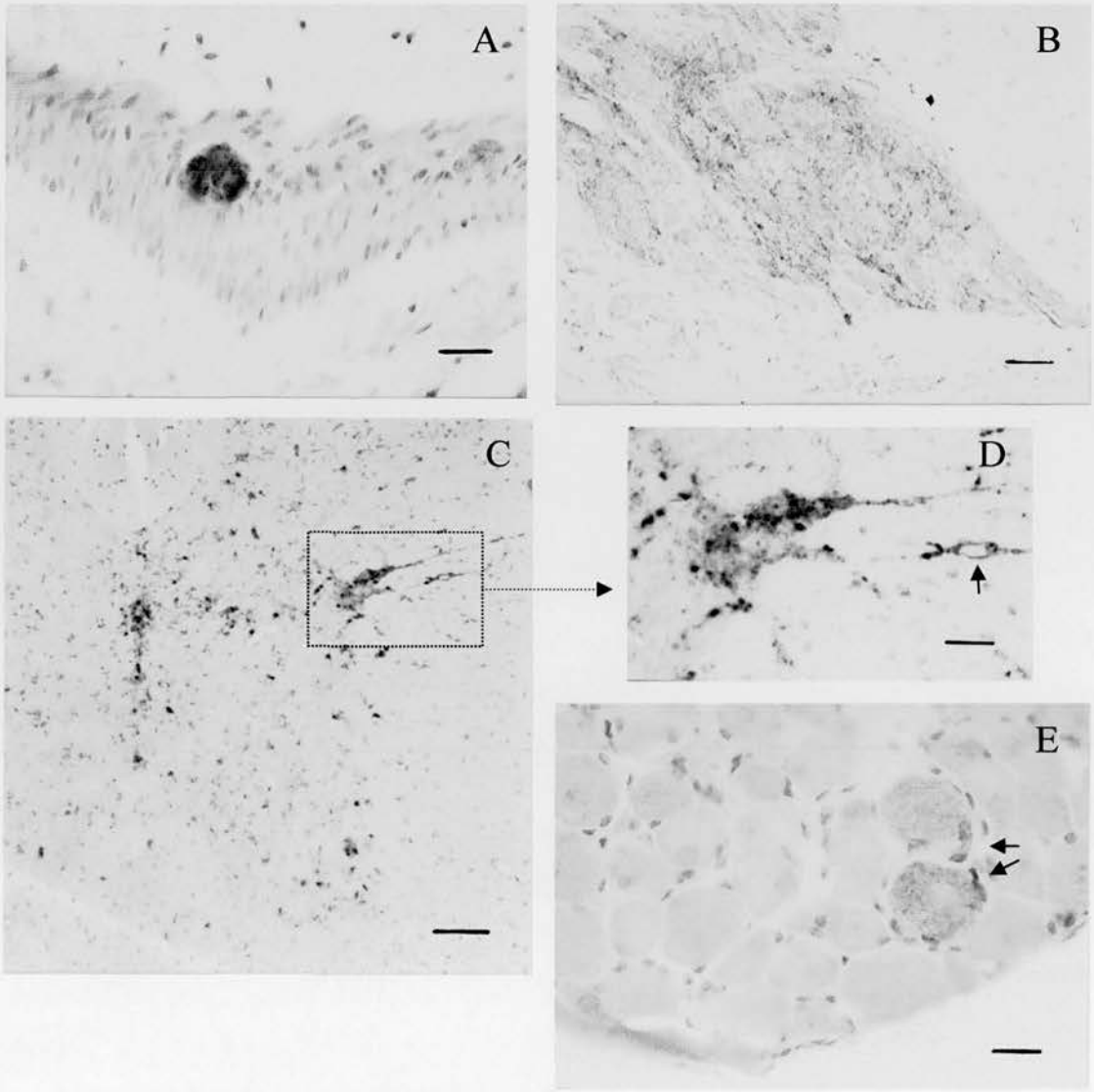

Figure 4.5 PrP^d deposition in the vagus nerve circuitry of hamsters orally-challenged with 263K scrapie. Sequential accumulation in DMNV-SN complex (A-C) and NG (D and E). A;76dpi, Band C; 90dpi. The amounts of PrP^d vary between individuals culled at any time point but the sequence and site of deposition is consistent. PrP^d is more abundant in the DMNV than in the adjacent SN. The area postrema and underlying hypoglossal nucleus are largely unlabelled. D; Right NG at 90dpi - labelling is scant. E; Right NG at end-stage of disease - many neurones are unlabelled. Scale bars: A-C=300μm, D, E=30μm

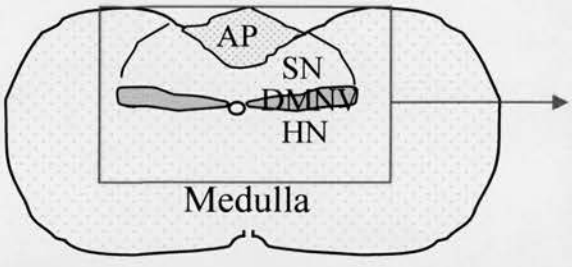

AP; Area Postrema, SN; Solitary tract nucleus, DMNV; Dorsal nucleus of the vagus nerve, HN; Hypoglossal nucleus.

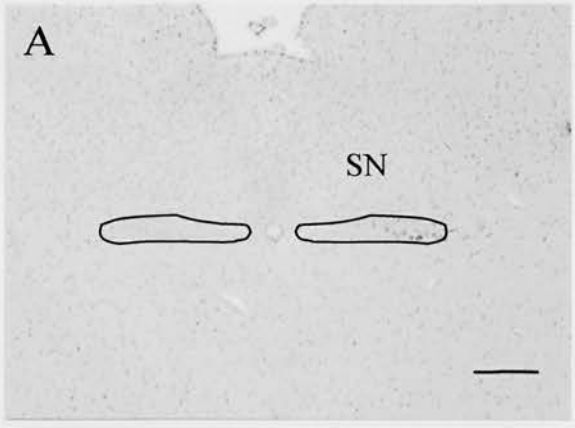

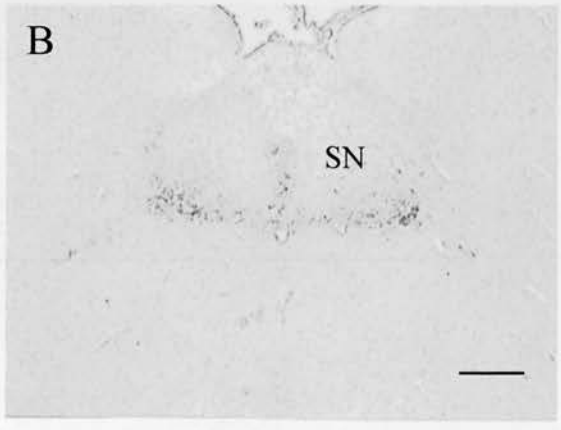

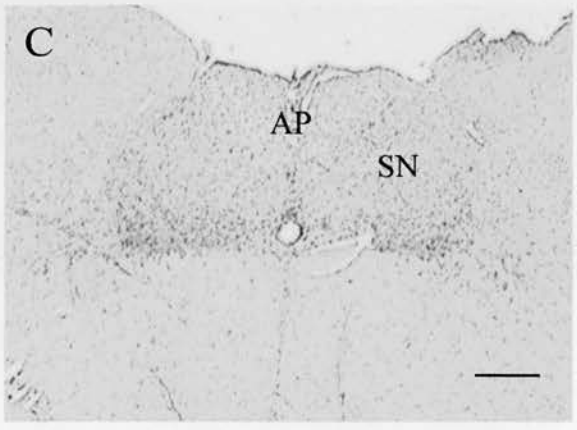

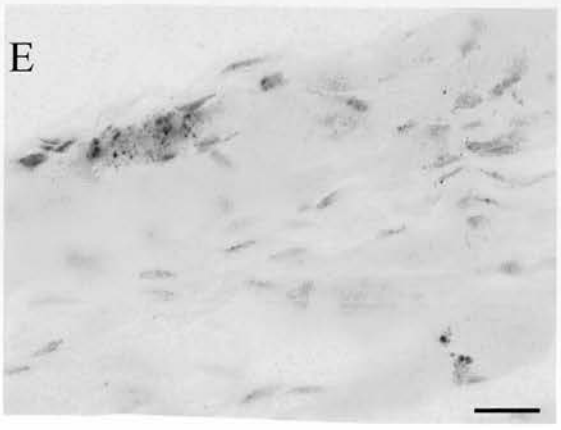

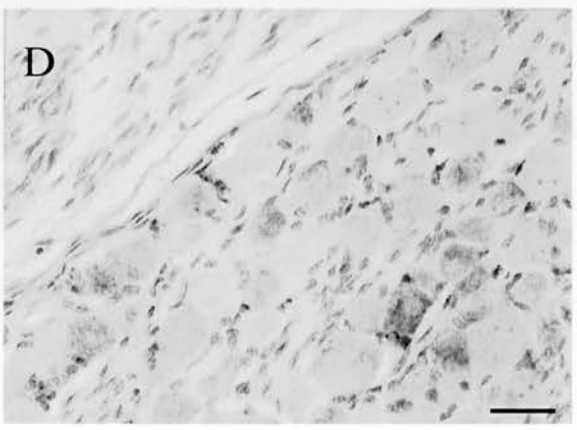

Figure 4.6 Pattern of PrP^d deposition in spinal cord of terminally-affected hamster orally challenged with 263K. Sections, A-F, are from cervical (C) or thoracic (T) segments and are presented in cranial to caudal direction. PrP^d is abundant throughout the entire grey matter 'butterfly' but the white matter is relatively spared. Deposition is particularly obvious around neurones of the IML (arrow), the first site of PrP accumulation. Scale bar = 700μm

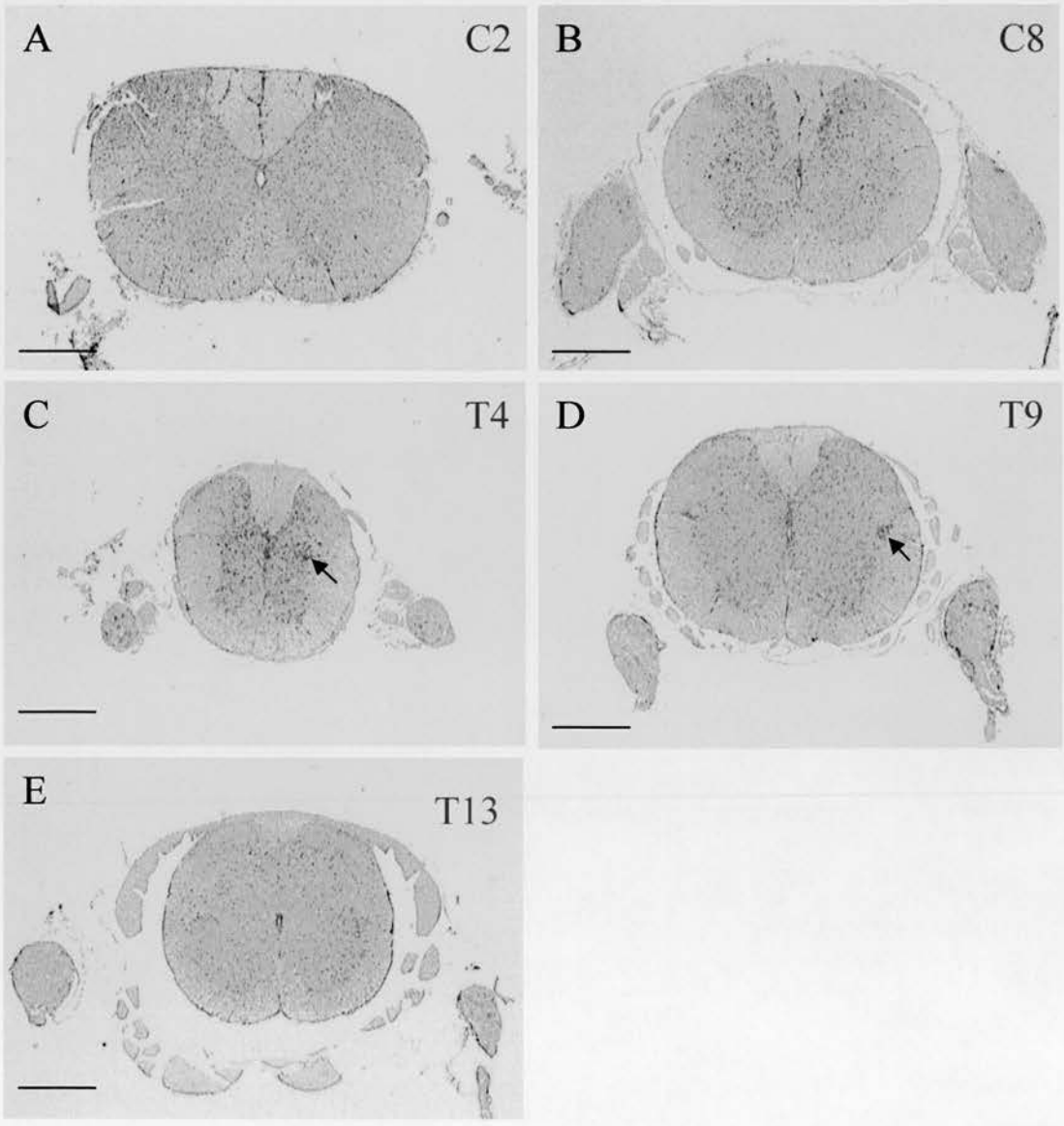

Figure 4.7 Pattern of PrP^d (brown labelling) in terminally-affected brain of hamster orally challenged with 263K scrapie. Distribution is shown in in coronal slices (A - H) throughout the brain in a caudal (medulla) to rostral (forebrain) direction. Scale bars: A = 400μm, B-H = 800μm

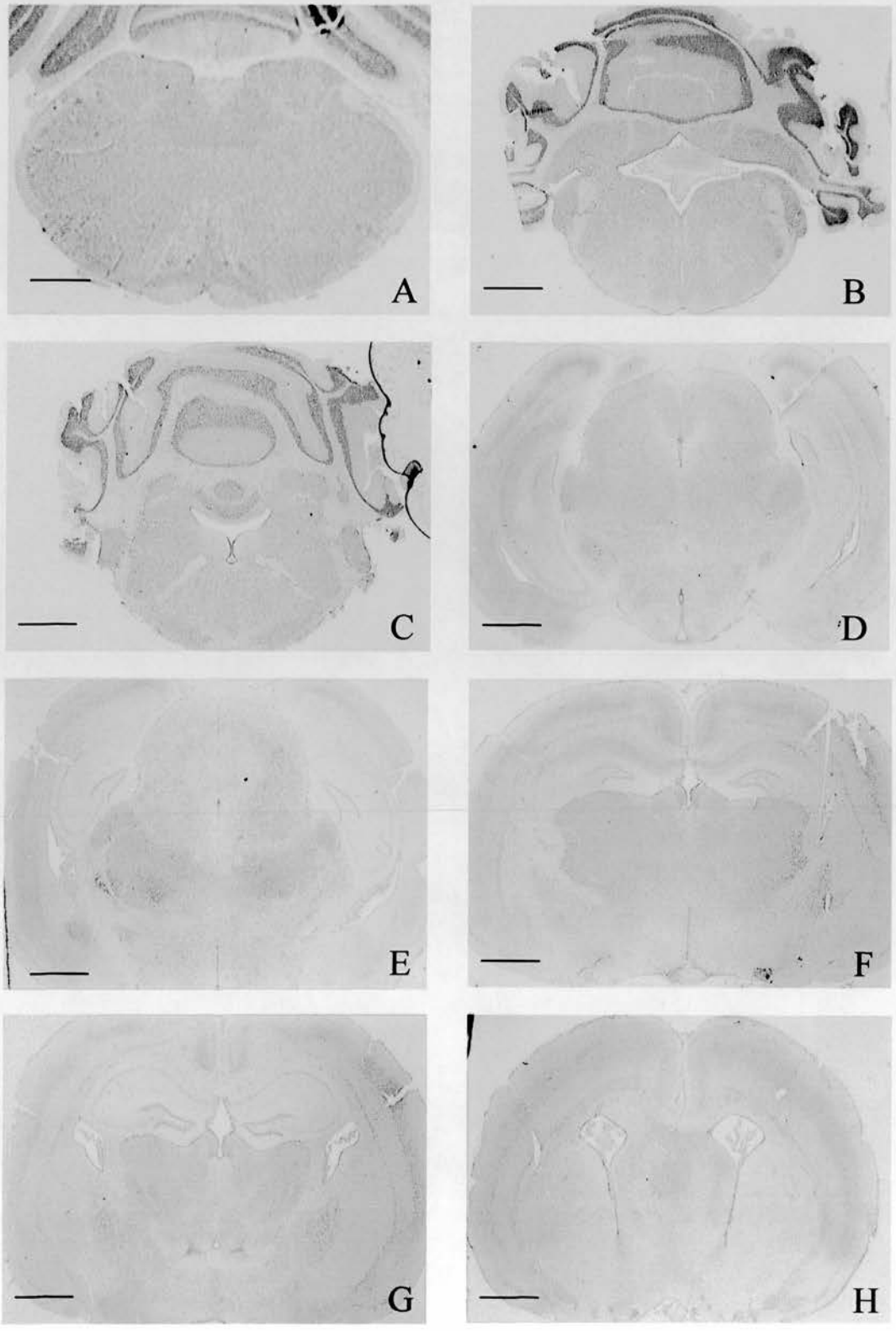

Figure 4.8 PrP^d in the (A) vagus and (B) splanchnic nerve of a terminally-ill hamster orally challenged with 263K scrapie. PrP^d is scant, and in splanchnic nerve may be glia-associated. Scale bars = 12.5μm

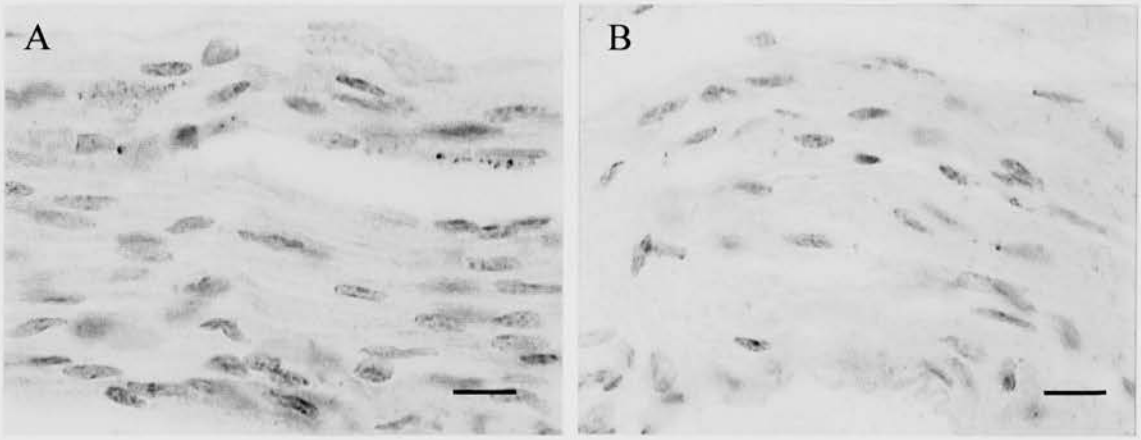

Figure 4.9 Early PrP^d deposition in the DMNV and IML of hamsters orally challenged with 263K scrapie, as demonstrated by PET blot (A and C) and ICC (B). A and B; adjacent sections of DMNV (arrowheads) at 76dpi, C; IML at 90dpi. Specimens are adjacent or nearly adjacent sections to those shown in Figures 4C and 5A. Scale bars: A, B = 1mm, C = 200μm

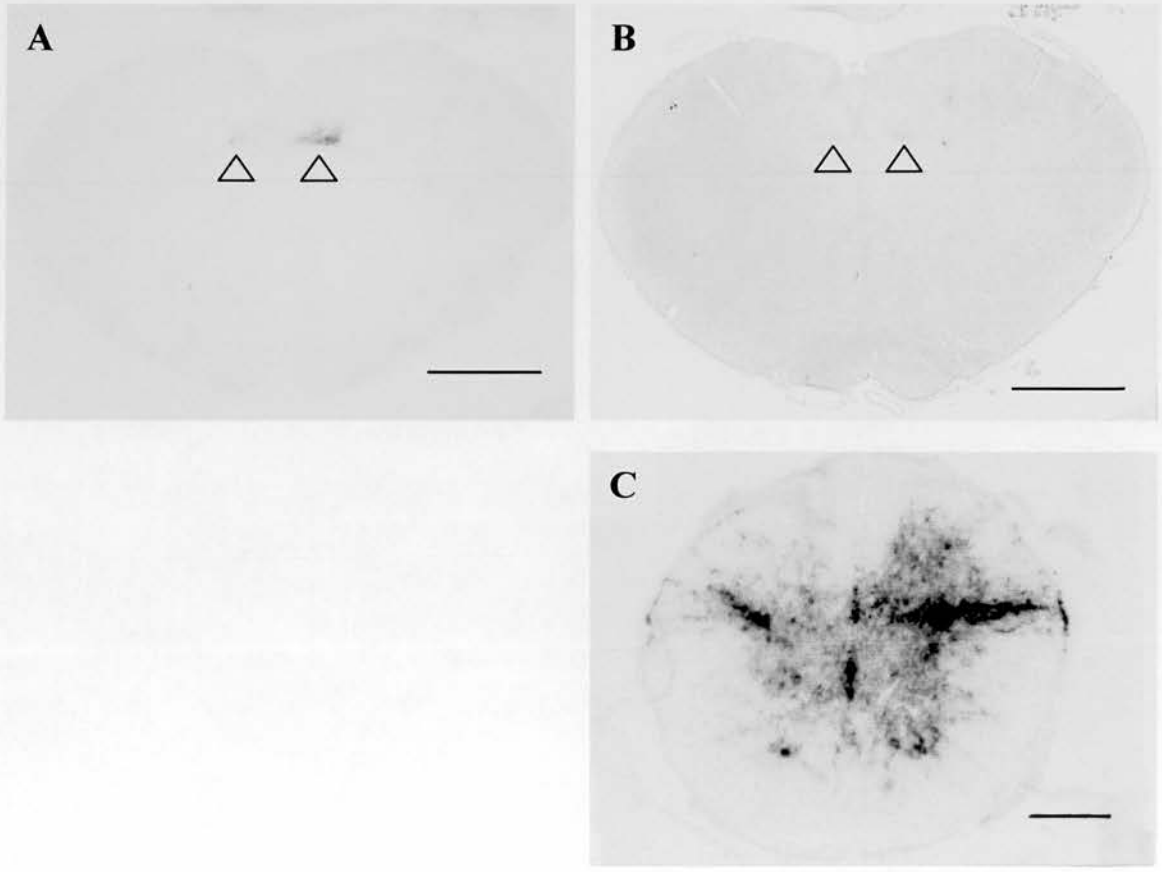

4.2.4 Dynamics of PrP^d accumulation during the incubation period

The amount of PrP^d present was quantified to establish the relative amount of protein in different tissues (Table 4.2). The amount of PrP^d present in each splanchnic or vagal component was scored and compared within and between individual animals across the incubation period. Scores were initially low, i.e. '+' or '++', in all tissues. PrP^d accumulated over time by being detected in a) increasing quantity and number of neurones within a target site, and b) an increasing number of target sites. At the earliest timepoints, PrP^d was present in some relay components, notably those nearest the source of uptake i.e. the GI tract, but absent in others. With increasing time, PrP^d appeared and progressively accumulated in a stepwise manner along the linked pathways. Eventually, deposition was detected in all components of vagal or splanchnic circuitry (Table 4.1, Figures 4.4 and 4.5) but the first targets contained relatively more PrP^d than subsequent ones. When amount of protein in the vagal components of an individual hamster was compared to that in the splanchnic nerve at the same timepoint, less PrP^d was observed in vagal circuitry, i.e. scores were consistently lower in DMNV-SN-NG than the CMGC-IML-DRG. Higher scores were achieved at earlier timepoints in the splanchnic nerve circuitry. Rapid accumulation was particularly apparent in the enteric ganglia and CMCG where scores rose to and were maintained at high levels from the earliest stages of detection.

4.2.5 Scrapie infectivity in the vagal and splanchnic nerve circuitry

Two PNS components, the cervical vagus and CMGC, were analyzed by bioassay for presence of infectivity. Samples of vagus nerve were excised from a position remote from the NG to avoid the inclusion of ganglion cell bodies. Both were obtained from endpoint cases only. The reason for this was explained in section 4.1.1.

The results for the vagus samples are summarised in Table 4.3. Mortality and incubation time of the recipients in the bioassays demonstrate a low but consistent presence of infectivity in the cervical vagal nerve trunks. The estimated amount of infectivity was approximately 10^2 $ID_{50i.c.}$, corresponding to about 10^5 $ID_{50i.c.}$ per gram of tissue.

Infectivity levels in the two CMGC samples (Table 4.4) were higher (approximately 10^3 and 10^4 $ID_{50i.c.}$) even though this represented only a minor constituent of the homogenised tissue sample. Absolute disassociation between the CMGC and aorta is very difficult because the ganglia are invisibly small and adhere closely and at intervals along the much larger aorta. Two pieces from the abdominal artery were also sampled from the same animals. Artery samples were located cranially or caudally adjacent to the CMGC. The trace levels of

infectivity detected from these control specimens probably originate from residual CMGC nervous tissue.

Table 4.2 Quantification of PrP^d. Relative amount and progressive accumulation of PrP^d deposition* in the ENS and splanchnic and vagus nerve relays after ingestion of 263K scrapie

DPI/hamster[1]		Enteric ganglia	CMGC	mid-T IML	mid-T DRG	DMNV	SN	Right NG	Left NG
56	**1**	nd	+	nd	nd	-	-	nd	nd
	2	nd	+	nd	nd	-	-	nd	nd
	3	nd	+	nd	nd	-	-	nd	nd
	4	nd	+	nd	nd	-	-	nd	nd
62/63	**1**	nd	++	nd	nd	-	-	nd	nd
	2	nd	+	nd	nd	+	-	nd	nd
	3	nd	++	nd	nd	-	-	nd	nd
	4	nd	++	nd	nd	+	+	nd	nd
69	**1**	+	++	+/++	-	+	-	-	-
	2	++	++	+/++	-	+	-	+	-
	3	++	++	+	-	++	++	-	-
	4	++	++	+	-	+	-	-	-
76	**1**	+++	++	+++	+	+	-	-	NP
	2	+++	+++	+	-	+	-	+	+
	3	+++	+++	++	+	++	+	+	-
	4	+++	+++	++	-	+	-	+	NP
83	**1**	+++	+++	+++	+	++	++	+	-
	2	+++	+++	++	-	NP	NP	+	-
	3	++++	++++	+++	+	++	++	+	+
	4	+++	+++	+++	+	++	+	-	+
90	**1**	+++	++++	+++	++	++	++	+	+
	2	++	++++	++	+	+	+	-	+
	3	+++	+++	+/++	-	+	-	+	+
	4	+++	++++	++++	++	+++	++	+	+

* Semi-quantified according to described criteria; [1]Early timepoints; incubation period ~160dpi; nd: not done, NP = not present

Table 4.3 Detection of infectivity in cervical trunks of the vagus nerve by bioassay

Donor	Sample	Mortality	Incubation time		Estimated titre[1]
			Range[days]	Mean[days ± S.E.]	[$ID_{50i.c.}$/sample]
S1	Left V.	5/5	119-292	162±30	$10^{1.3}$
S1	Right V.	5/5	117-155	126±7	$10^{2.7}$
S2	Left V.	5/5	117-239	144±22	$10^{1.8}$
S2	Right V.	5/5	117-180	134±11	$10^{2.3}$
S3	Left V.	5/5	120-260	151±25	$10^{1.6}$
S3	Right V.	5/5	131-222	167±18	$10^{1.3}$
S4	Left V.	5/5	131-183	159±10	$10^{1.5}$
S4	Right V.	5/5	127-152	139±4	$10^{2.0}$
S5	Left V.	5/5	124-242	153±20	$10^{1.6}$
S5	Right V.	5/5	145-274	190±21	$<10^{1.2}$

50µl aliquots of homogenized left and right vagus (V) from terminally-ill 263K orally-challenged hamsters were i.c. inoculated into groups of five recipients. Recipients similarly inoculated with vagus from donors previously orally mock-infected with normal brain homogenate showed no clinical signs of scrapie. Experiment was terminated at 370 dpi.

[1] Values refer to the total amount of infectivity in one equivalent of excised tissue, i.e. the entire donor sample, and calculated by applying mean incubation time to a dose response curve.

Table 4.4 Detection of infectivity in the coeliac and superior mesenteric ganglion complex and adjacent parts of the abdominal aorta

Donor	Sample	Mortality	Incubation time		Estimated titre[1]
			Range[days]	Mean[days ± S.E.]	[$ID_{50i.c.}$/sample]
S1	CMGC	5/5	100-107	104±1	$10^{4.1}$
S1	Cran. A.	1/5	318	-	-
S1	Caud. A.	1/5	156	-	-
S2	CMGC	5/5	107-128	118±4	$10^{3.1}$
S2	Cran. A.	1/5	230	-	-
S2	Caud. A.	5/5	120-240	171±24	$10^{1.2}$

50µl aliquots of homogenized CMGC and cranially (cran.) / caudally (caud.) adjacent artery (A.) from terminally-ill 263K orally-challenged donors were i.c. inoculated into groups of five recipients. Recipients similarly inoculated with CMGC from donors previously orally mock-infected with normal brain homogenate showed no clinical signs of scrapie. Experiment was terminated at 370 dpi.

[1] Values refer to the total amount of infectivity in one equivalent of excised tissue, i.e. in the entire donor sample, and calculated by applying mean incubation time to a dose response curve.

4. 3 Discussion

This study used immunocytochemisty, PET blotting and selective infectivity assays to determine the temporal sequence and location of scrapie infection in the splanchnic and vagal neural circuitry of orally challenged hamsters. While bioassays provide the gold standard for detection of scrapie agent *per se*, ICC and PET blot analyses facilitate studies on the spread of infection by using disease-associated forms of PrP (PrP^d/PrP^{Sc}) as surrogate markers for infectivity. A close correlation between infectivity and PrP^{Sc} has been previously established in this animal model (Beekes *et al.*,1996, Baldauf *et al.*,1997) where one infectious unit was estimated to contain approximately of 10^6 molecules of PrP^{Sc} (see Chapter 1.1).

The PrP antibodies that are currently available are unable to discriminate between host and disease-associated forms of PrP in histologically processed tissues. As was shown in previous chapters of this thesis and in other studies using mice (Bruce *et al.*, 1989, 94a, McBride *et al.*,1998), it is possible to distinguish PrP^d from PrP^C by differences in morphological appearance and distribution. However, until now there was no formal proof that the disease-associated PrP detected by ICC corresponded to protease-resistant PrP^{Sc}. PET blot pretreatments destroy PrP^C leaving only the PK-resistant fraction (Schulz-Schaeffer *et al.*, 2000a). Here, the deposits visualised by ICC were consistent with the PrP^{sc} immunostaining in adjacent PET blots, even at early stages of incubation. This provides strong evidence that the PrP^d detected by our ICC method is PrP^{Sc}.

Based on the previous study examining the pathogenesis of 263K scrapie after oral challenge, it was proposed that the infectious agent reaches its initial CNS target sites by spreading in a retrograde direction along autonomic PNS pathways supplying the gastrointestinal tract, i.e. along sympathetic and parasympathetic efferents of the splanchnic and vagus nerve. Large parts of the alimentary canal, in particular the oesophagus, stomach, small intestine and ascending colon are innervated by these two nerves (Dockray 1999, Furness 1999) which contain fibres of sensory and motor (efferent) neurones. Efferent fibres of the vagus have their nerve cell bodies in the DMNV and synapse with neurones of the ENS in ganglia of the submucosal and myenteric plexuses that are located in the wall of the alimentary canal. The sensory fibres of the vagus nerve have their origin, i.e. their nerve cell bodies, outside the brain in the NG and these directly innervate the alimentary canal. The sensory fibres do not terminate in the NG but run to the SN where they synapse with interneurones projecting to the DMNV. In this way, the sensory and motor parts of the vagus nerve form a neuronal circuit involving the solitary tract nucleus.

With regard to splanchnic nerve neuroanatomy, splanchnic efferents have their origin in the IML of the spinal cord and synapse with neurones in the CMGC and these, in turn, innervate the wall of the gastrointestinal tract. The sensory fibres originate outside the spinal cord in the DRG, run through the CMGC and directly innervate target organs such as the alimentary canal. Sensory splanchnic neurones can project directly or via spinal cord interneurones to efferent splanchnic neurones in the IML forming a linked circuit.

With this neuroanatomy in mind, the location, timing and progressive accumulation of PrP^d revealed by this study strongly support and expand the hypothesis of spread proposed in Chapter 2 Figure 2.9. PrP^d appeared and accumulated in a predictable temporal sequence in specific sites that accurately reflect the described autonomic and sensory relays. PrP^d was always present in the CMGC and IML before the corresponding DRG. The same holds true with respect to the DMNV and NG.

The results also show that, at least in this animal model, the ENS may be a key portal of entry of the infectious agent into the splanchnic and vagus nerves. PrP^d was found in submucosal and myenteric ganglia in early stages of infection. In several species including rats, vagal, splanchnic and ENS innervation of the alimentary canal has a complex neuroanatomy (Dockray 1999, Furness 1999). The ENS ganglia contain cell bodies of intrinsic motor, sensory and interneurones. Vagal efferents synapse on intrinsic ENS neurones whose cell bodies are predominantly located in myenteric ganglia. Vagal afferents are thought to project to the myenteric plexus and to the mucosa.

From the splanchnic nerve, efferent fibres target myenteric ganglion cells and also directly supply gastrointestinal blood vessels. Afferent splanchnic terminals are located in the myenteric plexus, the mucosa, smooth muscle and around submucosal blood vessels. Therefore, from the observations reported here, the most likely explanation for splanchnic or vagal neuroinvasion is via myenteric ENS ganglia. These neuronal relays provide a common denominator for retrograde spread of agent along splanchnic and vagal efferents as well as for centripetal spread via the corresponding afferents. However, neuroinvasion may occur via intestinal nerve terminals not linked to ENS ganglia or projections from other visceral tissues.

The findings suggest that after uptake from gastrointestinal mucosa, the infectious agent primarily spreads by two neuroanatomical pathways: 1) along the vagus nerve to the DMNV in brain and, 2) along the splanchnic nerve to the IML of mid-thoracic spinal cord. Intramural ganglia of the gut and the CMGC are respective intervening relay points. From

the DMNV and IML, the infectious agent probably travels along interneurones and sensory afferents to the SN-NG and DRG, respectively (Figure 4.10). The reproducibility and topographical precision of PrP deposition indicates that spread is not random but occurs in a stepwise fashion along the synaptically linked neuronal populations. The data indicates that initial spread occurs in a retrograde direction along efferent motor pathways of both nerves. This mode and pattern of spread has several precedents and shows striking similarities to that of conventional neurotropic viruses, such as herpes simplex virus type 1 (Krinke & Deitrich 1990, Gesser & Koo 1996), reovirus isolate T3C9 (Morrison *et al.*,1991) and pseudorabies virus (Card *et al.*,1990). However, dual efferent and sensory spread to the brain is also possible as PrP^d was found in the DMNV and NG but not the SN of some hamsters (see Table 4.1). The sequential pattern of PrP^d deposition and passage through functionally linked neurones shown here is also similar to spread through gustatory pathways after injection into the tongue (Bartz *et al*, 2003) or infectivity measurements of visual pathway components shown by Scott *et al* 1992 after infection of the eye.

The study did not reveal any evidence for haematogenous spread of infection to the brain. PrP^d was not detected early in infection at sites with an impaired blood-brain-barrier such as the area postrema (see Figure 4.5) or the choroid plexus. In addition, routing via the blood would not be consistent with the observed selectivity of targeting.

One way for PrP^d to spread along peripheral nerves is by the established retrograde axonal transport mechanisms. Several studies have reported that scrapie speads within the nervous system by means of axonal pathways (Kimberlin & Walker 1980, Fraser & Dickinson 1985) and the suggested rate of spread (0.5-2mm/day) is consistent with that of slow axonal transport of cytoskeletal proteins or retrograde locomotion of specific axonal proteins (Kimberlin & Walker 1982, Brady 1991, Scott *et al.*, 1992). It has been claimed that PrP^C can be transported in an anterograde (Borchelt *et al.*, 1994) or retrograde (Moya *et al.*, 2004) direction along peripheral nerve axons and PrP^{Sc} (PrP^d) in a retrograde direction (Bartz *et al.*, 2002). Transportation *per se* was not formally established in this study but the evidence presented here would be compatible with this. While an abundance of PrP^d was detected in association with cell bodies of CNS neurones or peripheral ganglia, deposition in nerves (cell processes) was minimal or undetected even at terminal stages of disease. The low levels of infectivity found at end-stage disease in vagus nerve compared to that of brain or CMGC is a further indication that in nerve fibres the agent is in transit rather than being actively replicated. Similar findings and conclusions were reported for infectivity assays of optic nerve (Fraser & Dickinson 1985, Scott *et al.*, 1992.)

Nevertheless, a domino-like mode of spread along nerves by sequential conversion of PrP^C to PrP^{Sc} (Glatzel & Aguzzi 2000) cannot be ruled out at present. PrP^d has been reportedly visualised in an extra-axonal compartment of the vagus nerve of sheep using light microscopy (Groschup *et al.*, 1999). There are difficulties in accurately determining the subcellular compartmentalisation of tissue constituents by light microscopy but the precise location of PrP^d within sciatic nerve has been determined using electron microscopy. PrP^C was present, localised to the Schwann cell membrane, in transgenic mice that overexpress PrP five to seven times that of wild-type mice (Follet et al., 2002). Infection of the Schwann cell line MSC-80 with the Chandler strain of scrapie resulted in the production of PrP^{Sc} and these cells were capable of transmitting disease to mice (Follet et al., 2002). In this and the previous study PrP^d deposition was associated with glia (satellite [Schwann] cells in peripheral ganglia, astrocytes in brain and radial glia in spinal cord) which sometimes 'tracked' along networks of glial cell processes. Theoretically, scrapie agent could spread from cell to cell along peripheral nerves but this is not compatible with the predictability of spread or the precise targeting of PrP^d to specific groups of neurones.

Infection via the oral route is strongly indicated (but not formally proven) in vCJD, BSE and natural scrapie. Disease-specific PrP is found in the DMNV as a characteristic feature of vCJD (Ironside 2000) and early BSE infection (Schulz-Schaeffer 2000b), natural and experimental scrapie (Foster *et al.*, 1996, Ryder *et al.*, 2001, Begara-McGorum *et al.*, 2002, Ligios *et al.*, 2002) and BSE of sheep (Foster *et al.*, 2001, Ligios *et al.*, 2002, Jeffrey *et al,* 2001b). In addition, the mode of spread along vagal and splanchnic pathways described here is very similar to those reported in sheep with natural scrapie (van Keulen *et al.*, 2000). As the pattern of PrP^d deposition in these non-experimental infections closely resembles that observed in orally-transmitted hamster scrapie, the findings presented here provide new indirect evidence that vCJD in man, BSE in cattle and natural scrapie in sheep were caused by ingestion of TSE agent. These findings for experimental 263K hamster scrapie strongly indicate that after oral challenge, infection of the CNS occurs via the splanchnic and vagus nerves. As similar pathogenic mechanisms are likely to operate in other orally acquired TSEs, this work provides baseline information about the peripheral routing of infection and a rodent model in which to study it.

Figure 4.10 Pictorial representation of the neural pathways used in the oral routing of 263K scrapie. Initial spread (arrows) occurs in a retrograde direction along sympathetic and parasympathetic fibres of the splanchnic and vagus nerves. Enteric and abdominal ganglia (CMGC) have an early involvement in pathogenesis.

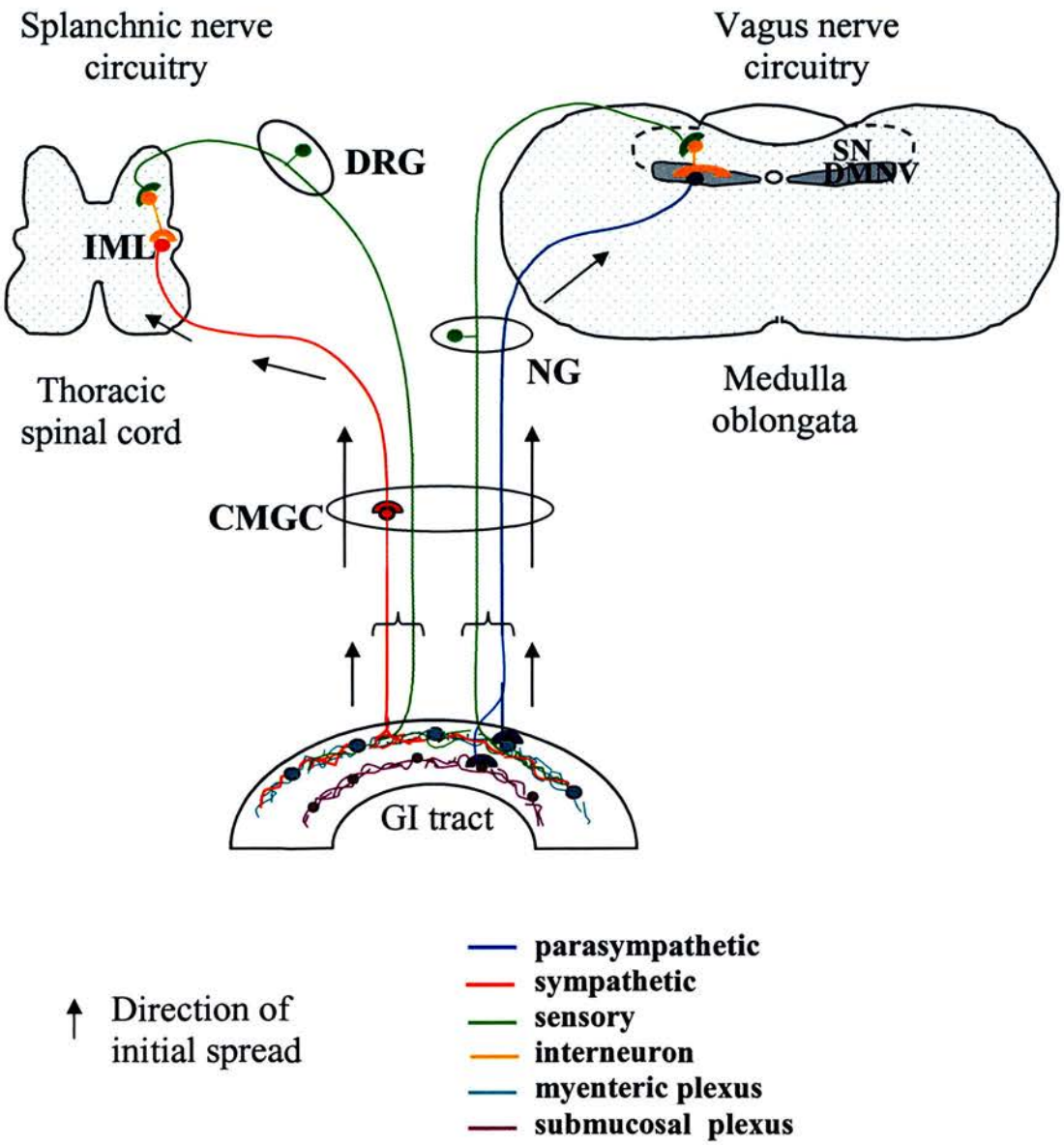

Chapter 5: Disease-specific PrP in the gastrointestinal tract: Involvement of gut-associated lymphoid tissue and the enteric nervous system.

5.0 Introduction

The gastrointestinal tract (GI) contains a variety of components that may be involved in uptake, transport, or replication of infectious agent (see Figure 5.7). These are found in the enteric nervous system and gut-associated lymphoid tissue (GALT) that includes Peyer's patches (PP), single lymphoid follicles and mesenteric lymph nodes (MLN). Overlying the PP is the follicle-associated epithelium (FAE), a single cell layer of specialised mucosal epithelium whose intercellular spaces are sealed by tight junctions. Embedded within and under this layer are M (microfold) cells, intraepithelial lymphocytes and dendritic cells (DC). DC and FAE form part of the immune defence and response mechanisms that protect the mucosa against pathogens. DC squeeze through the tight junctions to monitor the mucosal surface for antigens and return by the same route. M cells deliver foreign material from the gut lumen to lymphoid cells by transepithelial transport. The lymphoid follicle is separated from the epithelium by a dome containing B cells, T cells, antigen-presenting DC and phagocytosing macrophages. The follicle has a B lymphocyte-rich peripheral zone and a germinal centre. B cells support a network of follicular dendritic cells (FDC) and these, in turn, can support scrapie replication (Brown *et al.* 1999). PP are interspersed between villi whose covering epithelium is specialised for digestion and absorption of ingested materials. Epithelial cells are in close contact with blood and lymphatic vessels contained within the lacteal of the villus. These elements are innervated by the intrinsic interlinked ganglionated plexuses of the ENS. Extrinsic fibres of the PNS connect the ENS with the CNS.

The data presented in the previous chapter provided evidence that after oral challenge the 263K agent spreads to the CNS from sites in the GI tract. The neural conduits linking these tissues are likely to be the vagus and splanchnic nerve. Ganglia of the ENS were identified as probable key portals of entry of the infectious agent into these nerves. It has long been assumed that natural scrapie is transmitted orally (Diringer *et al.*, 1994) and that the infectious agent gains access to its host via the alimentary tract (Hadlow & Kennedy, 1982). In naturally infected sheep, PrP^{Sc} is first detectable in GALT (Heggebo *et al.*, 1999, Andreoletti *et al.*, 2000) but peripheral and enteric ganglia are also involved at an early stage (van Keulen *et al.*, 2000). The precise identity of the GI tract cells in which the infectious agent may reside, accumulate or undergo replication is not established although FDCs of the GALT and enteric neurones are candidates. In order to elucidate the relationship between the

ENS and LRS in our model system, spleen, lymph nodes and GALT were included in the study. The presence, location and cellular involvement of PrP^d were investigated using ICC examination of small intestine where components of both GALT and ENS are in close association.

5.1 Materials and methods

Experimental design was as described in Chapter 4. Briefly, outbred Syrian hamsters were fed individual 263K-doused food pellets and sacrificed at specific time points throughout the incubation period; 56, 62, 69, 76, 83, 90, 97, 104, 111, 118, 126, 132 days post infection (dpi) or at clinical end-point of disease (159±4 [S.E.] dpi). Two mock-challenged hamsters, similarly fed with normal brain homogenate, were sacrificed at 161dpi. For this part of the project small intestine (with associated mesenteric lymph nodes), spleen and salivary gland (with associated lymph nodes) were investigated from 69dpi to endpoint of disease. The intestinal specimens comprised 2cm of jejunum and 2cm of ileum, adjacent to the duodenum and ileocaecal sphincter, respectively. Histological procedures and ICC were carried out according to the previously described protocols.

5.2 Results

5.2.1 PrP immunolabelling in lymphoid tissues of orally-challenged hamsters

The presence of PrP^d in spleen, gut associated lymphoid tissue and salivary gland is presented in Table 5.1. The table shows the lymphoid tissues that contained PrP^d and the ratio of hamsters in which PrP^d was detected at successive time points throughout the incubation period. The appearance of PrP^d in enteric ganglia is also shown as a comparison with the LRS.

In the GI tract PrP^d was found in lymphoid tissue of all hamsters from the earliest time point (69dpi) to end-point of disease. The majority of PrP^d was found in PP but the protein was also present in some single follicles in the gut wall. PrP^d was most obvious in germinal centres associated with cells previously identified as FDC (McBride *et al.*, 1992, Brown *et al.*, 1999) and tingible body macrophages (Brown *et al.*, Jeffrey et al., 2000). PrP^d was also found in 'dome' macrophages and in a proportion of cells in the FAE. Due to the lack of specific antibodies these cells could not identified unambiguously but their distribution and morphology was consistent with that of M cells (Davis & Owen 1997) but PrP^d may also have been associated with non-M cell mucosal epithelium. Labelling was also seen in DC that reside underneath the FAE in close contact with M cells but not in the similarly located lymphocytes (Neutra *et al.*, 2001),[Figure 5.1]. Corresponding, though generally weaker and less widespread staining of FDC was also found in MLN (Figure 5.2). MLN were not always

present but when PP and associated MLN were compared, deposition was more limited in MLN - both in amount of PrP^d observed and in the numbers of follicles involved. At all time-points some PP lymphoid follicles were unlabelled.

PrP^d was not observed in any of the four spleens from hamsters culled at 69dpi. At the next time point of 76dpi, PrP^d was detected in one of the four spleens but deposition was very scant and only present in the germinal centre of one of the many white pulp follicles. PrP^d was also detected in only one of the four spleens taken at the subsequent time points of 83 and 97dpi but in these slightly greater accumulations were observed. At 111dpi all spleens showed some positive labelling but only one of these had substantial amounts of deposition. At terminal stages of disease, when deposition in individual follicles was heaviest and most widespread, many follicles remained unlabelled. PrP^d was associated with FDC networks and tingible body macrophages.

No PrP^d deposition could be detected in either mucous or serous secreting portions of salivary gland at any time point throughout the incubation period but it was detected in the FDC network of contiguous submaxillary lymph nodes as incubation period progressed (Figure 5.2). As with spleen, PrP^d labelling was absent in lymph nodes from the early time points and found only in a proportion of other timepoints until 126dpi. Thereafter all salivary gland-associated lymph nodes were consistently positive but as with other lymphoid tissue a proportion of individual follicles within the nodes were negative (Table 5.1).

At 69dpi many PPs contained substantial accumulations of PrP^d as illustrated by the intense labelling and extensive distribution. This indicated that PrP^d was likely to be present even earlier than this. By comparison, MLN had less PrP^d deposition at 69dpi (Figure 5.2) and in spleen and submaxillary lymph noses PrP^d was undetected. The presence and amount of accumulated PrP^d in these lymphoid organs continued to lag behind that of the PP for a considerable time. The order of appearance is consistent with uptake of agent first from PP, with spread via lymph to nearby draining MLN. The short delay in reaching lymph nodes of the salivary glands and spleen would fit with subsequent circulation through lymphatic and blood interconnections.

In uninfected animals some PrP labelling was seen in FDC but not tingible body macrophages of spleen, PP and mesenteric lymph nodes but the labelling was less intense and lacked the granularity of PrP^d. From its appearance the labelling was consistent with that of PrP^C. With all tissues, including those from scrapie-infected hamsters, staining was absent when normal serum replaced the 3F4 primary antibody.

Table 5.1 Presence of PrP^d in the LRS and ENS during the incubation period of 263K-fed hamsters

Tissue \ Dpi	69	76	83	97	111	126	~160 End-point
	No. affected/No. in group*						
GALT*	4/4	2/2	4/4	3/3	1/1	2/2	3/3
SPLEEN	0/4	1/4	1/4	1/4	3/3	4/4	5/5
SALIVARY GLAND	0/4	nd	0/4	0/4	0/4	0/4	0/5
LYMPH NODE (in sal. gland)	0/4	nd	2/4	3/4	3/4	4/4	5/5
ENTERIC GANGLIA	4/4	4/4	4/4	4/4	4/4	4/4	5/5

nd - not determined, * - 4 or 5 hamsters were culled at each timepoint; GALT was only present in the proportion of animals shown

5.2.2 PrP immunolabelling in the ENS of orally-challenged hamsters

PrP^d was found from the earliest time point (69dpi) to end-point of disease in and around neurones of the myenteric and submucosal plexuses of ileum and jejunum in all hamsters (Table 5.1). In accordance with findings for the CNS, the amount of PrP^d and the number of ganglia affected varied between individuals but at 69dpi deposits were already more abundant in amount than was observed in initial sites of deposition in brain or spinal cord. This indicated that accumulation was at a more advanced stage than in CNS and that initial deposition had occurred somewhat earlier than this time point. Labelling was more intense and deposits more widespread in ganglia of the ileum compared to the jejunum, possibly signifying that PrP^d was taken up from the lumen either more readily or preferentially at this part of the small intestine. According to data presented in Chapter 4, portals of entry for the infectious agent may lie in various parts of the alimentary tract including the oesophagus, stomach, small and large intestine. Only small sections of jejunum and ileum were included in this study so the range of samples needs to be widened to include these and other GI tissues.

Physical appearance of ganglia-associated PrP^d was also similar to that observed in the CNS and presented as punctate and granular deposits. Accumulations increased as the incubation period progressed (see Table 4.1 and Figures 4.2 and 4.3 of previous Chapter) i.e. deposition

became more abundant around individual ganglia and their associated nerve fibres. Nerve fibres could be visualised by the punctate labelling along their length (Figure 5.3) and these were more frequently observed with time. This delineating effect was presumably a manifestation of PrP^d accumulation at synaptic boutons - it corresponds with accounts of nerve fibre distribution in the circular muscle of small intestine (Furness *et al.*, 1999)

PrP^d was also observed on structures indistinguishable from nerves in PP situated above the muscularis and submucosa. These fibres appeared to extend from the heavily labelled enteric plexus to lymphocytes of the overlying PP (Figure 5.4). If this image is an accurate *in vivo* representation it demonstrates direct contact between FDC-containing lymphoid tissue and the ENS. Both vagal and splanchnic fibres synapse on ENS neurones providing the subsequent connections to the CNS.

5.2.3 Temporal relationship between PrP^d deposition in PP and ENS

Samples of gut from early stages of incubation were examined to find evidence of a temporal separation in the emergence of PrP^d in PP and enteric ganglia. As was stated above and shown in Table 5.1, PrP^d was observed in both PP and ENS at the earliest timepoint of 69dpi. This finding was contrary to expectations that PrP^d would not be detected at this time - (discussed further in section 5.3). Nonetheless, as was also observed in previous Chapters, there was variation in the extent of PrP immunolabelling between animals and also within tissues from individuals. Therefore although PrP^d was detected in both LRS and ENS components in all animals, in individual animals the protein was occasionally found in some tissue elements but not others. The segregation of labelling probably indicated differences in the timing of onset of PrP^d deposition in individual PP.

In animals with extensive PrP labelling throughout the GI samples, PrP^d was found in all cell types described above i.e. enteric neurones, FDCs, macrophages and cells of the FAE that included DCs and probably M cells (Figure 5.1A&B). In these situations the degree of deposition was such that it was not possible to determine which tissue elements had been labelled primarily. However, in tissues with low levels of deposition, it could be seen that some cell types were more strongly immunolabelled than others. In these cases the FAE was not or only weakly labelled but the underlying DCs (identified by location and morphology), FDCs and macrophages were PrP^d positive (Figure 5.1C).

FAE was positively labelled on many occasions but staining was more obvious when PrP^d was present in other PP components. PrP^d could only be detected by viewing under oil immersion at the highest magnification so it is possible that PrP^d was regularly undetected.

In one PP, in which the FDC network exhibited the weakly stained, non-granular appearance indicative of PrP^C, only dome macrophages and possibly a few DCs were positive. There was little evidence of FAE involvement although this may reflect reduced sensitivity of detection in epithelial cytoplasm. The entire ENS was negative (Figure 5.5). This suggests that PrP^d is present in the dome of the PP prior to the germinal centre and that *en route* to FDCs and enteric neurones, PrP^d can become phagocytosed by macrophages. As well as DC, macrophages are found within the intraepithelial pocket formed by M cell cytoplasm (Neutra *et al.*, 2001) so conceivably, this could occur by direct uptake from FAE, contact with mobile DCs involved in PrP^d transportation or by diffusion of cell-free PrP^d between the various cell populations. The involvement of dome epithelium is not clear.

It was noticeable that as overall PP labelling became heavier, i.e. deposition more abundant in germinal centres, a greater number of PrP^d-positive DCs were observed. DCs were also distributed more widely within the PP. Initially DCs were commonly seen below the dome FAE but were later seen near the base of the mucosal crypts (Figure 5.6). DC may play an early and important role in transporting PrP^d around the PP and possibly further afield. Their presence in the mucosa in close proximity to the lacteal lymphatic vessels may be a significant indicator that migration of PrP^d-tagged DC takes place *in vivo*.

Enteric ganglia were often positive at early stages of incubation but intensity of labelling of these was not noticeably stronger than that of FDC networks and in some cases PrP^d deposition around ganglia was less than that observed in the lymphocyte populations abutting the muscularis mucosa (in which the ENS is located). Many ganglia were unlabelled but in some cases, ganglia directly below PP were more heavily labelled than those more distal to PP (Figure 5.4A) though this was not observed invariably. PrP^d deposition was heavier and more widespread in ileal ganglia. While the relative amounts of PrP^d in enteric ganglia and overlying PP could not be correlated, PP are more frequent in ileum than other parts of the intestine (Neutra *et al.*, 2001) so this may indicate that PrP^d presence in GALT contributes to this result.

Taken together these results suggest that a variety of lymphoid cells are sequentially involved in the cellular processing of PrP^d and that in some cell populations this precedes invasion of enteric neurones. However, the opportunity to assess these early events was hindered by the small number of cases in which low-level staining was present so further investigation is required for clarification.

Figure 5.1 PrP^d labelling in Peyer's patch of 263K-fed hamsters.
A: Low power view showing PP anatomy and the location of differing cell types with which PrP^d is associated (126dpi), B: PrP^d in follicle associated epithelium (FAE) layer (arrowheads) at 111dpi. A macrophage (arrow) and a dendritic cell (DC - open arrow) are present beneath the FAE, C; Macrophages (arrows) and DCs (open arrows) in dome region (83dpi), D; High power of DCs beneath the FAE layer (83dpi), E; Germinal centre with FDC network (endpoint of disease). A few macrophages (arrows) and DCs (open arrows) are also present. Bar, A,C = 40um, B = 12.5um, D = 15um, E = 20um.

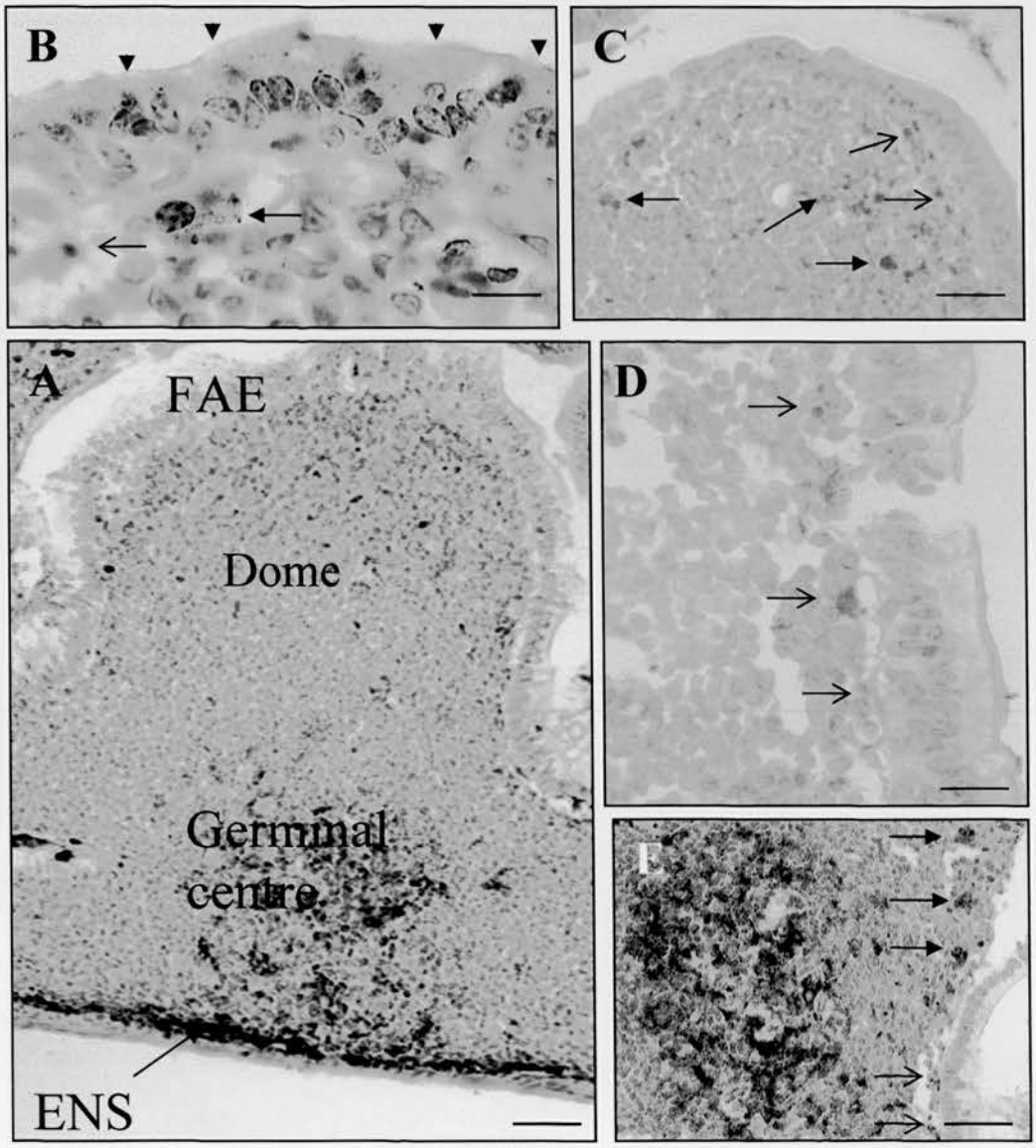

Figure 5.2 PrP^d in mesenteric (A-C) and submaxillary (D) lymph nodes of 263K-fed hamsters. A; Low and B; higher power views of node at 111dpi, C; 97dpe, and D; 126dpi. Relative to incubation time, PrP^d accumulation is less in both mesenteric and submaxillary lymph node than is commonly observed in PP at 69dpi, E. Bar, A = 300μm, B= 40μm, C = 20μm, D = 80μm, E = 100μm.

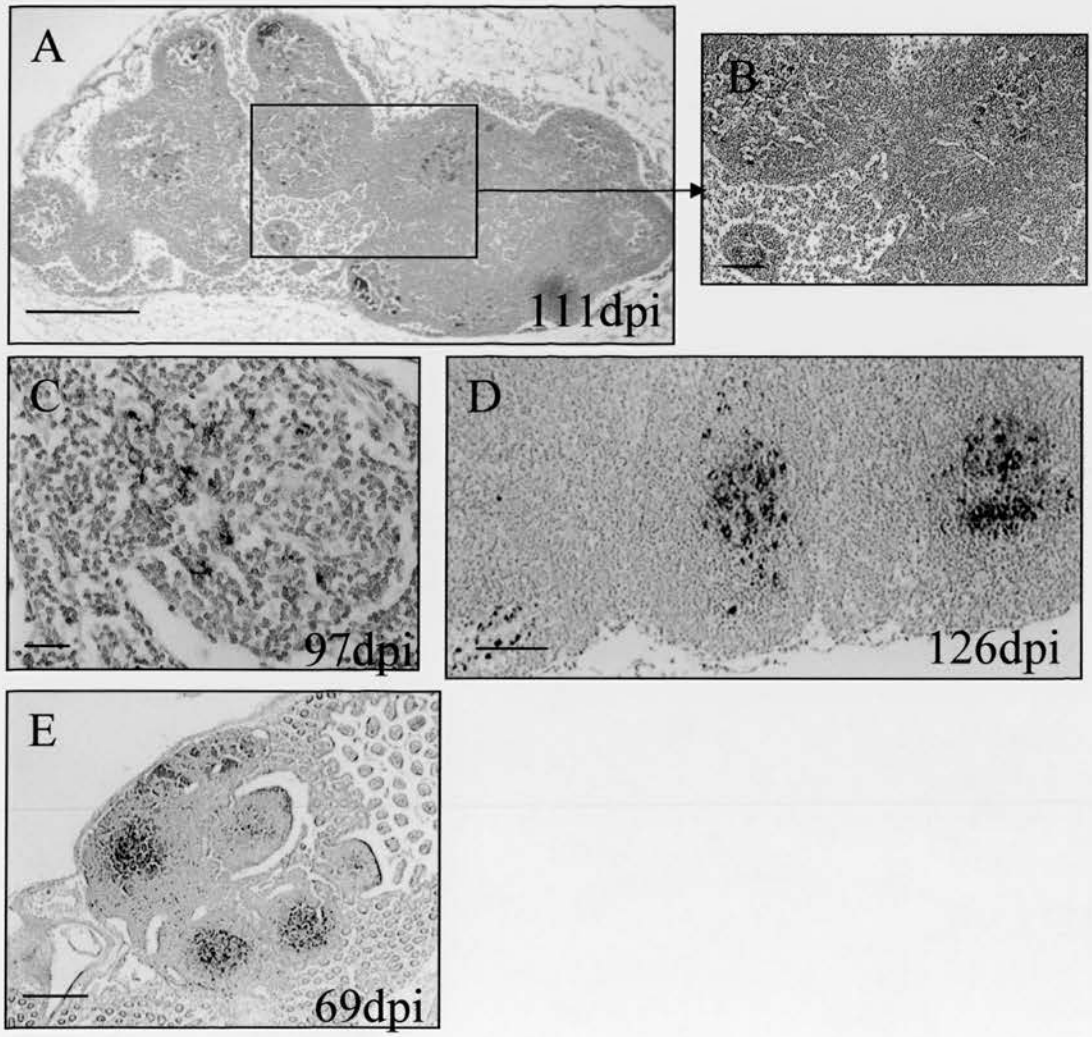

Figure 5.3 PrP^d in the ENS of 263K-orally challenged hamsters Punctate synaptic labelling of nerves (arrowheads) at early (A) and late (B, C) stages of disease. Bar, A, B =10um, C = 20um.

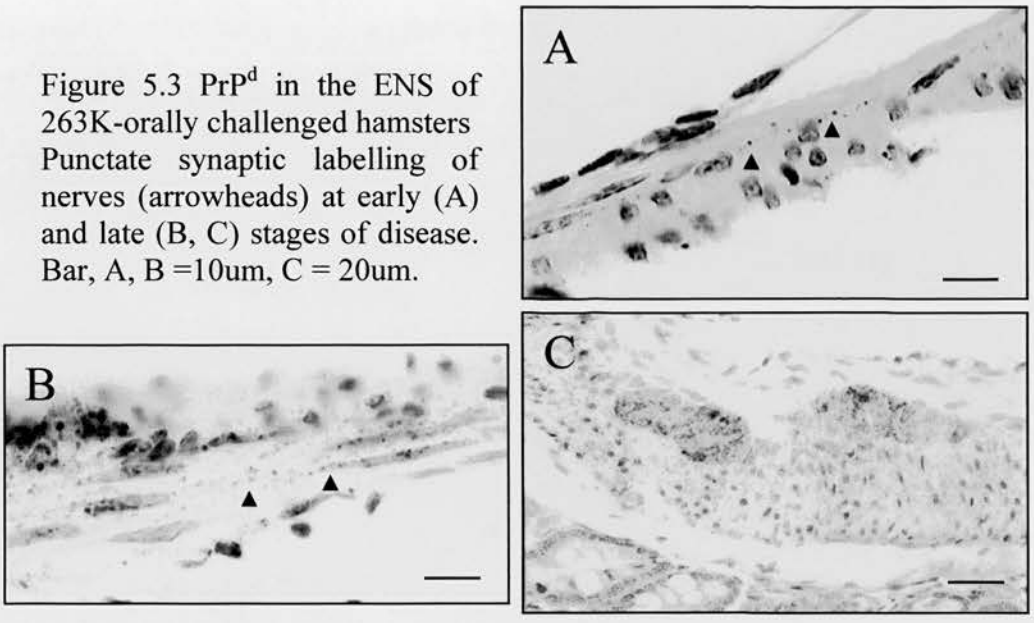

Figure 5.4 Association between PrP^d-labelled nerves and the LRS. Nerve-like structures extend between the neural and lymphocyte domains of PP from hamsters culled at 97dpi (A, B), 126dpi (C, D) and terminal stage (E) of disease. Note: In A, the ENS region directly below germinal centre contains the most positively labelled ganglia. Bar, A = 40um, B, C = 20um, D, E = 10um.

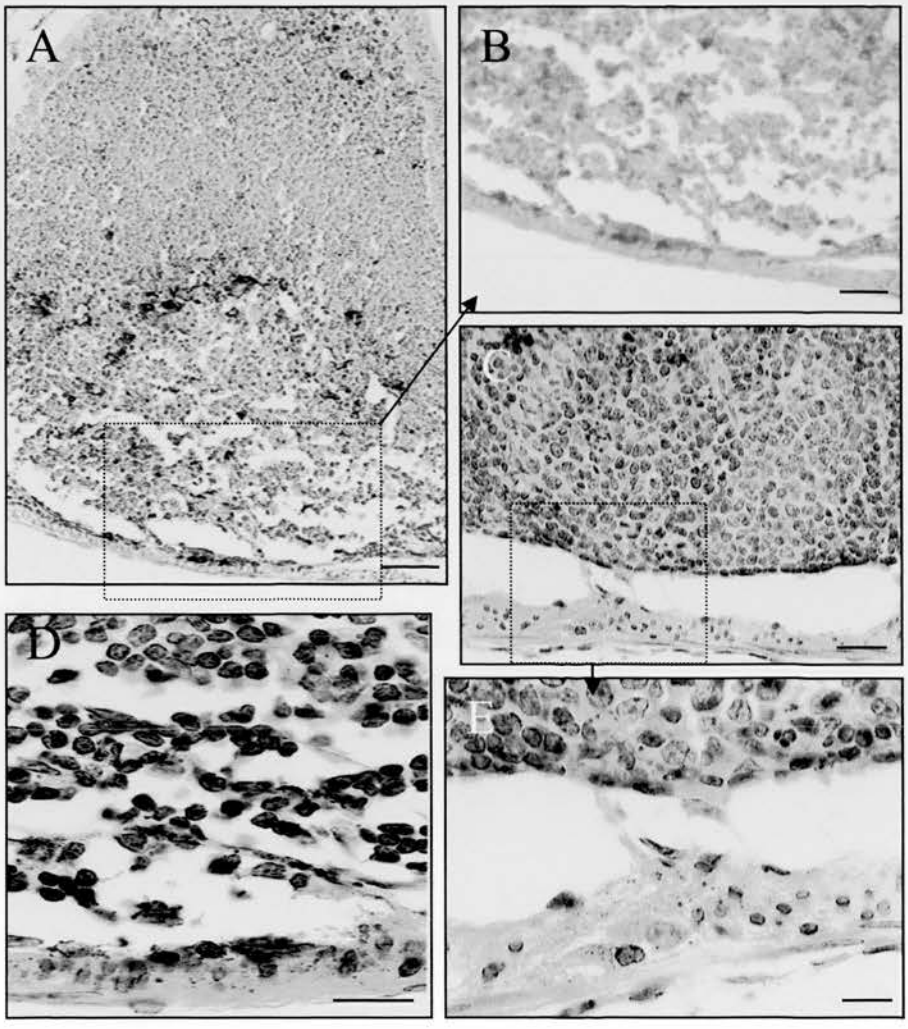

Figure 5.5 Early stages of PrP^d deposition in ileum of hamster culled at 97dpi. A: Peyer's patch with underlying ENS. Detail of dome region (B), FDCs and ENS (C). Cellular components display differential PrP labelling. Macrophages (arrowhead) contain PrP^d while the FDC network shows labelling typical of PrP^C. The FAE (open arrows), enteric ganglia and nerves (closed arrows) are unlabelled. Bar, A = 40μm, B, C = 30μm

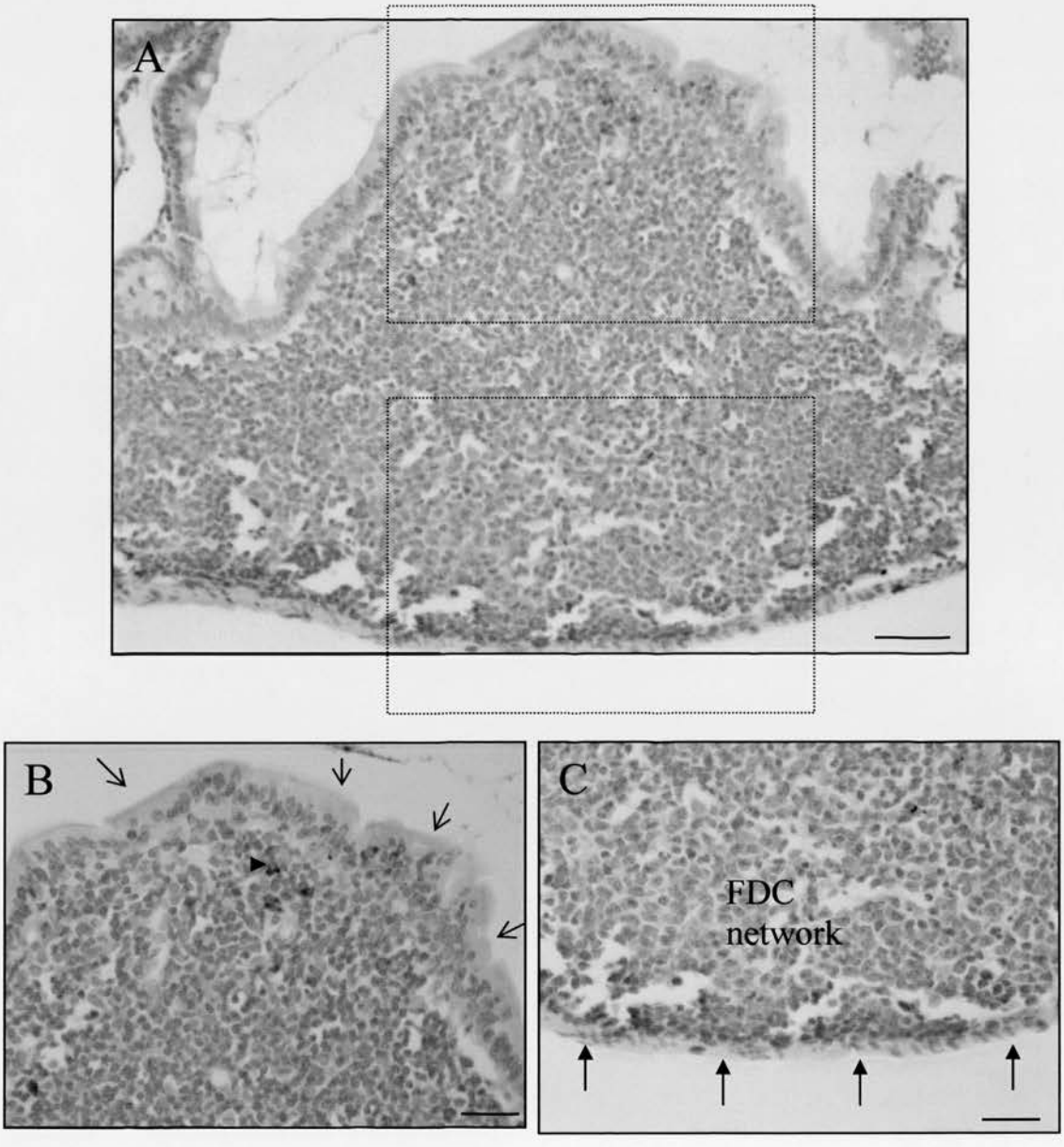

Figure 5.6 Distribution of dendritic cells in Peyer's patch from 263K-fed hamster culled at 83dpi. A, B, C: PrP^d-positive DC are seen in the dome region (arrowheads) and in the base of the PP near mucosal crypts (short arrows). Long arrows indicate their presence in a lacteal of an adjacent villus. B: High power to show DC location below the FAE. Bar, A = 40um, B, C = 30 um, D = 10um .

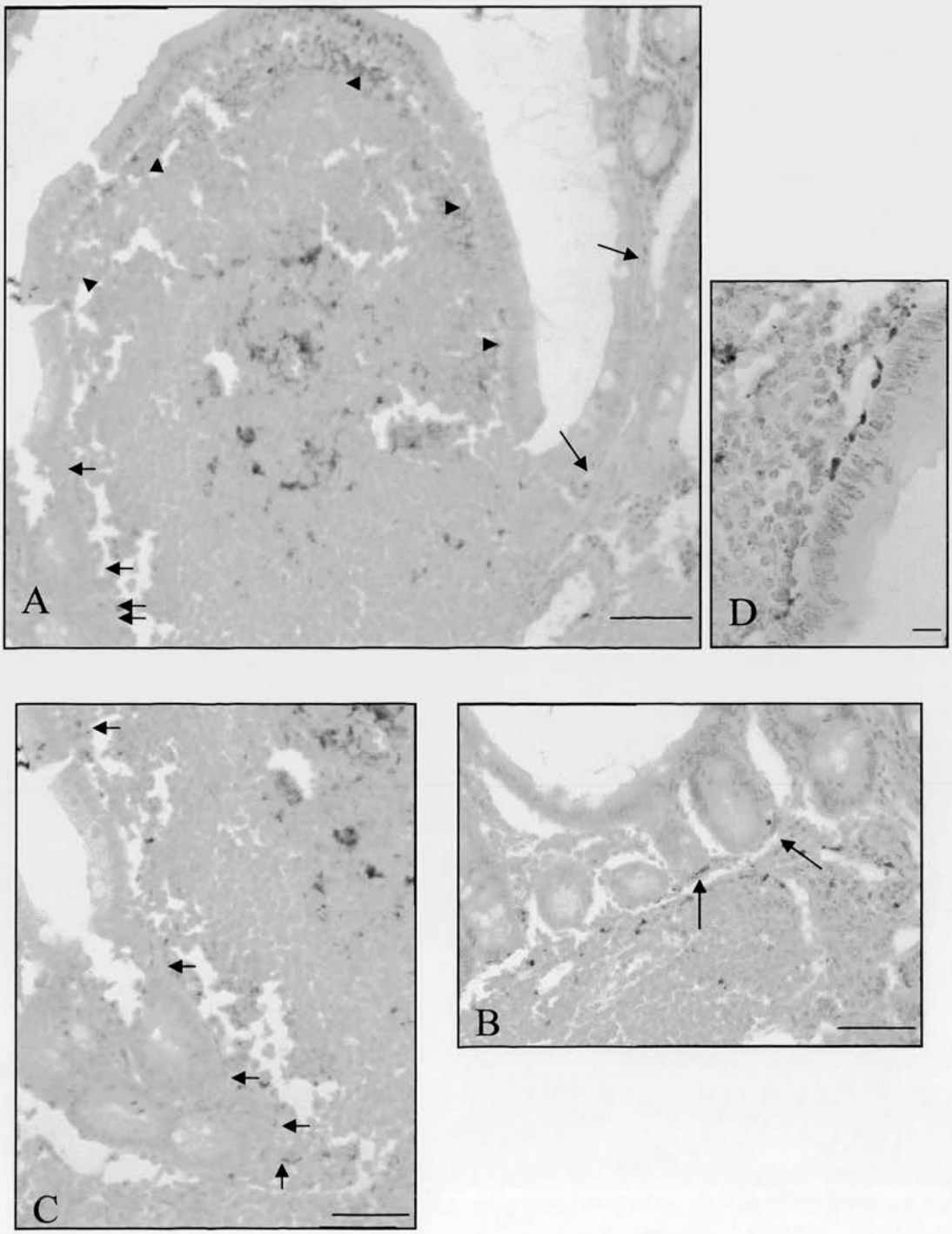

5.3 Discussion

In addition to the PNS and ENS, there is evidence that the lymphoreticular system (LRS) contributes to peripheral pathogenesis in several rodent TSE models (Fraser *et al.*, 96, Lasmezas *et al.*, 96, Brown *et al.*, 99, Maignien *et al.*, 99), sheep with natural scrapie (van Keulen *et al.*, 96,99) and in vCJD (Hilton *et al.*, 1998). Studies using SCID mice or high doses of infectivity have shown that prior replication in lymphoid tissues is not necessary for infection (Fraser *et al.*, 96, Lasmezas *et al.*, 96). However, involvement of the LRS appears to be strain dependent because in BSE infected cows (Somerville *et al.*, 1997b) and sCJD of man (Hill *et al.*, 99) infectivity was not recovered from lymphoid tissues. Also, in experimental scrapie of mice (Kimberlin & Walker 86,89a and the hamster model used in this project, the spleen does not seem to be crucial to neuroinvasion (Beekes *et al.*, 96, Race *et al.*, 2000). In such instances it is commonly proposed that uptake of infection occurs directly via peripheral nerves.

One aim of this chapter was to elucidate the relative contribution of the LRS and ENS in establishing infection in this model. By examining samples of gut from early stages of infection it was hoped that detection of PrP^d in PP and enteric ganglia could be a temporally separated and thus provide indirect evidence for primary involvement of the ENS.

This was only partially achieved due to PrP^d being present in the relevant tissue components at the unexpectedly early time point of 69dpi. The choice of time points was based on results from the first study (described in Chapter 2) which showed that PrP^d could not be detected prior to 91dpi in brain or spinal cord in this model system. It was thought that 69dpi would be early enough to obtain negative results. However, in the second study PrP^d was detected much earlier in the CNS at 62dpi. As preparation of tissues was the same in each study the enhanced detection was probably due to better sensitivity of detection by ICC or a higher titre inoculum.

5.3.1 How may the TSE agent access the LRS and PNS of the GI tract?

Although the data showing temporal segregation between lymphoid and neural components of the PP is limited, the results presented here show that different cell types appear to be sequentially involved in PrP^d uptake/processing/transport after oral infection. The findings showed that PrP^d was present in association with a number of PP components including FAE in which M cells are located, DC, FDC, dome and tingible body macrophages, enteric neurones and their processes but not lymphocytes. The data also appears to show that involvement of the ENS occurs after that of the PP but this must be substantiated using a larger number of samples. The possible routes by which the TSE agent may enter the gastrointestinal tract following oral challenge are represented diagrammatically in Figure 5.7.

Figure 5.7 Possible routes by which the TSE agent may access the gastrointestinal tract

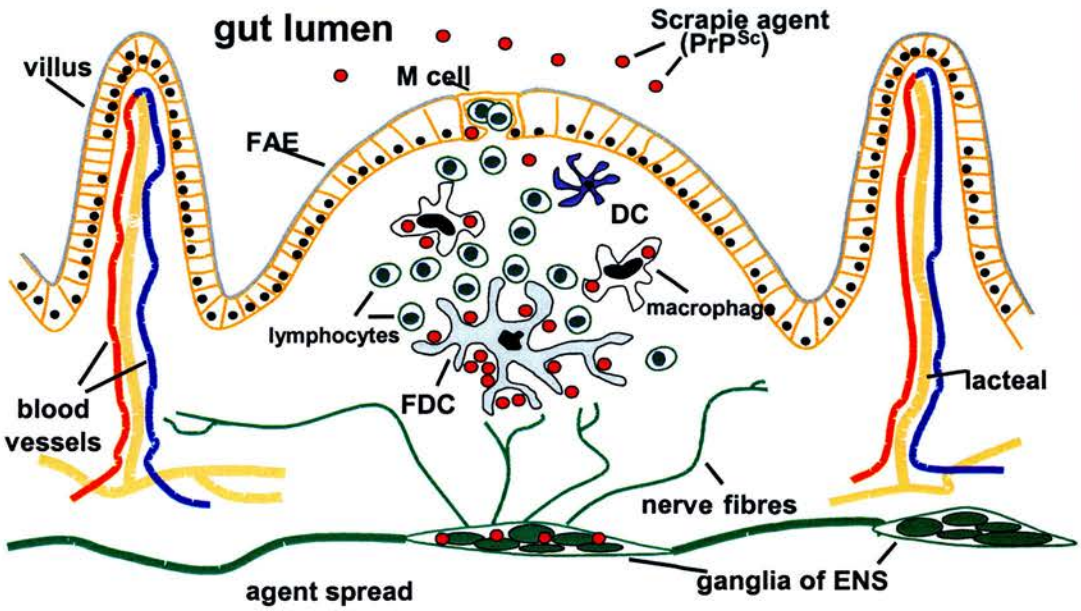

The GI tract contains a variety of cells that may be involved in uptake, transport or replication of infectivity. The TSE agent may enter from the gut lumen via epithelial or dendritic cells to be taken up by macrophages and/or transported in a free state or by e.g. mobile dendritic cells to FDCs for replication and accumulation. The agent may then spread to and accumulate in enteric ganglia before being transferred to the CNS via vagus and splanchnic nerves. The agent may also bind to peripheral nerves either directly or with the aid of cellular intermediaries.

Regardless of whether neuroinvasion occurs after amplification of infectivity in lymphoid tissue or directly via uptake of agent by nerve endings, the site and mode of uptake remain to be explained. After oral challenge disease-specific PrP is found in PP and the ENS of both natural and experimental TSE models. If it is assumed that neurones of the ENS and nerves of PNS are responsible for neuroinvasion, i.e. binding and transportation of agent to the CNS, the identity of the cells that interface with nerve endings remains open.

There is now clear evidence that FDCs have an important role in TSE peripheral pathogenesis. Assisted by complement, FDCs trap antigens that are retained in immune complexes for long periods (Van Rooijen 1980). PrP^C is localised to and PrP^d accumulates on FDC processes and this co-localises with immune complexes in spleen and lymph nodes of normal or scrapie-infected mice (McBride *et al.*, 1992, Brown *et al.*, 1999, Jeffrey *et al.*,

2000). There is now evidence showing that complement may also play a role in fixing and holding PrP^d on mouse spleen FDCs and temporary depletion or genetic deficiency of complement cascade components delay the onset of disease after peripheral challenge (Klein *et al.*, 2001, Mabbott *et al.*, 2001). Crucially, the infectious agent replicates in FCDs in rodent models of experimental scrapie or BSE (Brown *et al.*, 1999, Mabbott *et al.*, 2000a & b, Montrasio *et al.*, 2000) and the reported association of PrP^d with FDCs in many other TSEs including natural and experimental scrapie (Andreoletti *et al.*, 1999,2000, van Keulen *et al* 1999, Heggebo *et al.*, 2000,02.) CWD (Sigurdson *et al.*,1999, Williams *et al.*, 2002) vCJD (Hilton *et al.*, 1998, Hill *et al.*, 1999) and BSE in sheep (Foster *et al.*, 2001, Jeffrey *et al.*, 2001) suggests that these cells fulfil a similar role in these diseases.

Nevertheless FDCs are non-mobile and there appears to be little evidence showing close contact of FDC processes with peripheral nerve endings. The alimentary canal is innervated by sympathetic, parasympathetic and sensory fibres of vagus and splanchnic nerves. Sympathetic noradrenergic fibres of the splanchnic nerve innervate several lymphoid organs including PP, MLN and spleen. Many studies show ramification of adrenergic fibres within lymphocyte domains and synaptic-type contact with lymphocytes and antigen presenting cells of the periarteriolar sheath (Felton *et al.*, 1985,88) but such fibres do not appear to enter the follicles to any great extent (Felton *et al.*,1985, Jolois *et al.*,1997,99) and direct contact between FDCs and nerve endings is lacking (Heinen *et al.,* 1995). In studies examining the proximity of adrenergic nerves to PrP^d-labelled cells in spleens from sheep affected with natural scrapie, tyrosine hydroxylase labelling was seen around blood vessels but there was scant association with (unspecified) immune cells (Bencsik *et al.*, 2001). The lack of direct contact is also supported by very recent experiments carried out at Adriano Aguzzi's laboratory in Zurich. When germinal centres were engineered to re-position mouse FDCs in close contact with tyrosine hydroxylase positive nerves, survival after peripheral infection was shortened (Prinz et al., 2003). However, in addition to adrenergic nerves, there are many other nerves using different neurotransmitters present in these organs including those of sensory and parasympathetic origin (Fink & Weihe 1988). As well as noradrenalin which is synthesised and stored in splanchnic nerve terminals, neuropeptide Y, somatostatin, substance P and vasoactive intestinal peptide have also been observed in lymphoid organs (Straub *et al.*, 98, Madden & Felton 1995).

Despite the convincing evidence for FDC involvement, the mechanisms that permit the infectious agent to be taken up from the gut lumen into PP germinal centres remain to be established. Epithelial M cells, enterocytes, migratory dendritic cells and macrophages may play a part in this.

There is data showing that dendritic cells could provide the connection between FDCs and nerve endings. DCs are mobile and as stated previously sample their environment for antigens and transport them to draining lymph nodes. DCs, therefore, have the ability to move from the gut lumen through the FAE and into the PP making contact with a number of cells including M cells, FDCs, B cells and macrophages. DCs can acquire PrP^{Sc} *in vitro* and transport it, *in vivo,* via lymph to mesenteric lymph nodes after intra-jejunal injection (Huang *et al.*, 2002). They also contain high titres of infectivity and are capable of causing scrapie in RAG-$1^{0/0}$ mice after intravenous injection (Aucouturier *et al.*, 2001). RAG-$1^{0/0}$ mice lack B and T lymphocytes and FDCs and resist scrapie infection by peripheral routes (Klein *et al.*, 1997). The findings presented here support a role for DC in this model. PrP^{d}-labelled DCs were one of the first cell types to show PrP^{d} labelling. Furthermore their distribution pattern was observed to extend within the PP from an initial dome-based location towards the submucosa as PrP^{d} accumulation progressed. As DCs migrate to MLN via lymph, being sited in close proximity to the lacteal lymphatic vessels would place them in an ideal position for further migration to draining lymph nodes. Subsequent lymphocyte trafficking would disseminate agent to other lymphoid populations such as spleen.

The role of M cells is to form an antigenic barrier, of which the first step is pathogen recognition. Pathogens are processed by mucosal macrophages and DC and presented to B and T cells to mount a secretory immune response (Davis & Owen 1997). This scenario presents difficulties for TSEs because as no classical immune response is observed, the agent is not recognised as an antigen *per se*. Nevertheless, M cells have been shown to have the ability to transport the infectious agent across an epithelial monolayer *in vitro* (Heppner *et al.*, 2001) but to date these cells have not been specifically identified *in vivo*. In this study, cells of the FAE contained PrP^{d} at both early and later time points. Protein trafficking through M cells can occur in either direction (Davis & Owen 1997), so it is also conceivable that these cells are involved in transporting PrP^{d} that has undergone germinal centre replication back out of the PP into the lumen. In any case from the evidence presently available it is not clear whether M cells are actively, passively or uninvolved in uptake of PrP^{d} from the gut lumen.

Another possible means of entry is via the epithelium that lines GI tract lumenal surfaces. As well as M cells, PrP^{d} has been reported to be present in mucosal epithelium of lemurs prior to and concurrent with clinical disease after feeding with the BSE agent (Bons *et al.,* 1999) - although M cells were not specifically identified in that study. As epithelial cells line the entire length of the GI tract from oesophagus to rectum, enterocytes vastly outnumber the

pockets of PP-restricted M cells thus providing greater accessibility to the TSE agent. Immunocytochemical and electron microscopical studies have shown PrP^C to be expressed in epithelium of stomach, small and large intestine of human and hamster (Fournier *et al.*, 1998, Pammer *et al.*, 2000, Morel *et al.*, 2003). The rodent and human GI tract is highly innervated (Furness *et al.*, 1999). Nerves (including vagal afferents) course through epithelium parallel to lymphoid vessels in lacteals of villi (Berthoud 1995). PrP^C+ve nerve fibres have also been found in apposition to lymphoid and epithelial cells in the human ileal enteric system (Shmakov *et al.*, 2000). The existence of these relationships raises the possibility that agent could be taken up directly by nerve endings in ileal villi. If PrP^d or the infectious agent can bind directly to nerves this may be a mechanism by which peritoneal nerves become infected after peripheral routes of challenge with neurotropic (highly neuroinvasive) strains or high doses of lymphotropic TSE strains. Exploitation of intramucosal nerve fibres is thought to be the conduit by which neurotropic virus gains access to the enteric nervous system from the gastrointestinal lumen. Herpes Simplex Virus Type 1-infected nerve fibres were seen projecting through the mucosal layer to interact directly with surface epithelial cells (Gesser & Koo 1996).

In this study, the cells in which PrP^d was detected earliest were macrophages located in the dome region of PP. A similar early involvement has been observed in PP of very young lambs from a Romanov flock with natural scrapie (Andreoletti *et al.*, 2000). Other researchers have also reported the participation of macrophages in TSE pathogenesis. Using techniques that temporally deplete macrophage populations, Beringue and co-workers showed that macrophages functioned in the clearance of PrP^{res} (PrP^d) in the early stages of infection with C506M3 scrapie – a strain with a similar pathogenic course to ME7. Chemical depletion of macrophages with clodronate prior to or 28 days after scrapie challenge lead to raised levels of inoculum in spleen and accelerated PrP^d deposition (Beringue *et al.*, 2000). These studies suggest that phagocytosis sequesters PrP^d rendering it no longer available for replication. The capacity of macrophages to reduce infectivity was first reported over twenty years ago (Carp & Callahan, 1982) when macrophages were isolated and cultured with ME7 scrapie. More recently, PrP^d has been found within the lysosomes of tingible body macrophages in spleens of ME7 infected mice (Jeffrey *et al.*, 2000) and in PP macrophages of BSE-fed cattle (Terry *et al.*, 2003). These cells probably acquire PrP^d by ingestion after its release from the surface of FDC processes (Jeffrey *et al.*, 2000, Manuelidis *et al.*, 2000). Macrophages, therefore, exhibit an innate immune response to invasion.

5.3.2 Involvement of the LRS in orally-acquired 263K scrapie

It has long been established that spleen removal around the time of i/p infection prolongs the incubation period in several mouse models of experimental scrapie (Fraser & Dickinson 1970, Fraser *et al.*, 1992b). In contrast, previous data show that agent replication in spleen is not obligatory for disease progression in oral 263K hamster scrapie (Beekes *et al.*, 1996, Race *et al.*, 2000). Splenectomy following intraperitoneal or intragastric challenge of hamsters failed to lengthen the incubation period (Kimberlin & Walker 1986,89a) leading to the suggestion that neuroinvasion can occur directly via peripheral nerves. However, as is shown by findings presented in this thesis, with regard to oral challenge, the spleen may not be the most relevant LRS component on which to base these conclusions. Studies where transgenic mice expressing hamster PrP were peripherally-infected with 263K scrapie confirmed that spleen cells were not required for either agent amplification or transport and that peripheral nerves could support replication independently of LRS involvement (Race *et al.*, 2000). Infectivity (Kimberlin & Walker, 1988,89b) or PrP^{res} (Maignien *et al.*, 1999) is found in Peyer's patches and MLN of mice very shortly after intragastric challenge but only later in spleen. Evidence has been presented here showing that PrP^{d} detection in the LRS of scrapie-fed hamsters also follows this sequence of events. While this data supports the evidence that the spleen does not appear to be crucially involved in pathogenesis after peripherally administered 263K, PP and MLN appear to be involved at an early stage. In this model, rather than providing a site for the extraneural replication necessitated by lymphotropic strains such as ME7 or C506M3, GALT may function as a reservoir of infectious agent which can be taken up by enteric neurones and/or peripheral nerves.

Similar mechanisms may operate with other TSE strains. In cows experimentally infected with BSE, infectivity was not detected in spleen or lymph nodes but was detected in distal ileum at six and ten months post infection (Wells *et al.*, 1994, 96). GALT involvement in pathogenesis was presumed but as the inoculum used in these studies was prepared from intestinal wall, the ENS seems another obvious source for the detected BSE-infectivity particularly since infectivity is not recovered from lymphoid tissues of BSE infected cows (Somerville *et al.*, 1997b).

Even with a relatively early involvement of GALT in 263K-scrapie pathogenesis existing evidence is compatible with the LRS being an optional mediator rather than an obligatory key player of neuroinvasion in this experimental model. Neuro-immune mechanisms may also operate but because 263K scrapie is highly neuroinvasive, the infectious agent probably invades the ENS and PNS either before or concurrent with replication in GALT. However this view will have to be reassessed if the observed temporal lag between the involvement of PP and ENS can be substantiated.

Chapter 6: Discussion

The aims of this study were to discover the early sites of PrP^d accumulation in the CNS and to define the neuroanatomical pathways involved in CNS invasion in hamsters orally-infected with 263K scrapie. The findings have established that the vagus and splanchnic nerves are involved in the routing of 263K from the GI tract to brain and spinal cord in hamsters. They provide good evidence that the infectious agent reached the brain and spinal cord, independently, by autonomic fibres of these nerves. PrP^d was found at early stages of the incubation period simultaneously in vagal and splanchnic nerve cell bodies and components of their circuitry. Such involvement implies that both sympathetic and parasympathetic nerves are important conduits of peripheral spread.

The splanchnic nerve was originally implicated in the spread of peripherally-administered scrapie in mice through infectivity assay data (Kimberlin & Walker 1989a&b) and this has been supported more recently in studies showing an extended incubation period after chemical or immunological sympathectomy of intraperitoneally infected mice (Glatzel *et al.*, 2001). Conversely, mice with sympathetic hyperinnervation of lymphoid organs showed shortened scrapie survival times (Glatzel *et al.*, 2001). The presence of abnormal PrP in sympathetic ganglia of natural, experimental and accidentally transmitted TSEs (Andréoletti *et al.*, 2000, Foster *et al.*, 2001 Groschup *et al.*, 1999, Van Keulen et al., 2000, McBride & Beekes 1999, Haïk *et al*, 2003) suggests that the sympathetic NS may also participate in conveying the agent to the CNS in these diseases. However, conclusions drawn from findings in terminally-ill animals may be unreliable because centrifugal spread from CNS is almost certain to contribute to the observed PrP^d accumulation in peripheral ganglia at late stages of disease.

The pattern of spread along vagal and splanchnic pathways described in Chapter 4 is very similar to that reported for sheep with natural scrapie (van Keulen *et al.*, 2000). It therefore seems possible that as well as the splanchnic nerve, the vagus is important in peripheral pathogenesis. Vagal involvement may be especially pertinent to oral TSE transmission since food digestion and absorption are under vagal control.

The involvement of the vagus nerve has been reported in the pathogenesis of vCJD (Ironside 2000), early BSE infection (Schulz-Schaeffer *et al.*, 2000b), natural and experimental scrapie (Foster *et al.*, 1996, Jeffrey *et al.*, 2001b) and BSE of sheep (Foster *et al.*, 2001, Jeffrey *et al.*, 2001a). In these, and the rodent model used here, DMNV-associated PrP^d deposition was a characteristic and/or early pathological feature. However, the relevance of the DMNV to

the subsequent dissemination of 263K throughout the brain is difficult to determine from these studies. Although the DMNV has neural connections with other brainstem nuclei exhibiting early PrP^d accumulation, these could also be reached by projections arising from the IML that ascend to the brain from the spinal cord (see Figure 4.11). Therefore the observed pattern of agent spread and replication within the brain could originate via either vagus or splanchnic nerve connections. The relative importance of either nerve to disease progression could be investigated by employing procedures that disrupt the autonomic connections between the GI tract and CNS. Surgical or chemical disablement of the vagus and splanchnic nerves may result in lengthened incubation period and/or alterations to the known pattern of PrP^d targeting.

The vagal and splanchnic involvement in oral pathogenesis illustrated here parallels that reported for sheep with natural scrapie (van Keulen et al., 2000). This shows that the described routing is not confined to experimental scrapie of rodents and has a wider relevance for TSE peripheral spread. Nevertheless it is by no means certain that these neural pathways are ubiquitous to all TSE stains or the only conduits involved in peripheral spread. It is therefore important to discover if these nerves feature in the peripheral spread of TSE in other rodent models, especially those such as ME7 in which the LRS has a key role.

In Chapters 4 and 5, data was presented showing that PrP^d is present in enteric nerves and ganglia at an early stage in the incubation period and it is likely that in this experimental model neuroinvasion occurs via their nerve endings. The process by which this happens is unknown but composition and type of nerve may be relevant.

Experiments carried out by Outram in the 1970s implied that immature nerves were vulnerable to scrapie invasion (Outram *et al.*,1973, Outram unpublished). Using doses of scrapie that were lethal to adults, he showed that while some neonatal mice either survived or had extended incubation periods after i/p or subcutaneous challenge, a proportion developed scrapie after incubation periods that were significantly shorter than that of adults. Similar results were obtained more recently using ME7 infection of SCID mice in which the LRS component is compromised (Michelle Ierna, PhD thesis). The lengthened survival times in newborns were shown to relate to FDC maturation and absence of PrP^C, i.e. LRS under-development. Shortened incubations could be explained by direct uptake of the infectious agent by developing nerves. The extent of peripheral innervation is greater in the newborn compared to those in the adult (Brown *et al.*, 1976). PrP^C levels are also high in developing axons and during synaptogenesis (Salès *et al.*, 2000). Either of these factors may facilitate entry of infection or enhance the efficiency of admission. Peripheral nerves remain

underdeveloped until two weeks after birth (Jessen & Mirsky 1999) during which time myelinating Schwann cells are immature and not fully functional. In maturity, these cells encircle and protect the axon from damage and infection (Mirsky & Jessen 1999) so it is possible that access is more easily gained via the compromised myelin sheaths of developing nerves compared to intact ones. This scenario fits well with results showing shortened incubation periods in mice with mechanically or chemically damaged nerves (Kimberlin *et al.*, 1983). Nerve injury has been proposed as a factor in increased access of human poliovirus (Morrison & Fields 1991). Experimental nerve injury causes, among other things, demyelination and hyper-innervation (Mirsky & Jessen 1999) and as was stated above, in experiments designed to show sympathetic nerve involvement, mice with hyperinnervated lymphoid organs succumbed more readily to peripheral challenge with RML scrapie (Glatzel *et al.*, 2001).

While the data presented in this thesis suggests that the LRS does not significantly influence peripheral pathogenesis of the rodent model used in this study, in many models agent replication in lymphoid organs is crucial for successful neuroinvasion. Interaction between immune and neural cells could play an important role in transfer of the infectious agent. The mechanism by which the infectious agent passes from lymphoid tissue to nerve endings has yet to be elucidated but may involve a chemically mediated local interaction between nerves and immune cells. Lymphoid organs are innervated largely by branches of the splanchnic nerve and are under sympathetic nervous system control (Felton *et al.*, 1985, Felton & Felton 1988) but sensory afferent fibres of the vagus nerves are also present (Elfvin *et al.*, 1992, Berthoud & Neuhuber 2000). Cytokines such as IL-1, IL-6 and TNF-alpha released from immune cells can modulate the CNS either directly or via receptors on sensory afferent fibres of the vagus nerve (Stein *et al.*, 1990, Cabot *et al.*, 1997). Studies investigating the nature of the chemical messengers that permit communication between the nervous system and the immune system may provide much needed information about the mode of transmission and avenues for therapeutic intervention.

The vagus nerve communicates with the immune system to provide an effective host defence against pathogens (Goehler *et al.*, 2000) and acts in a T-cell independent manner through Toll-like receptors (TLRs) located in the cell wall of sentinel cells such as dendritic cells (Reis e Sousa *et al.*, 1999). As well as being present in all tissues of the body including skin and the gastrointestinal tract, DCs are also prominently located in the abdominal vagus (Geohler *et al.*, 1999). DCs are capable of internalising pathogens or pathogen-associated particles and were identified in this study associated with PrP^d accumulations in Peyer's patches and the GI lamina propria at early stages of the incubation. When activated, DCs

release cytokines that activate afferent neurons of the sensory vagus (Banchereau & Steinman 1988). Vagal afferents are widely distributed in visceral and the gastrointestinal tract ensuring that pathogenic activation of the immune system is detected early. Interestingly, activation of TLRs (by CpG oligonucleotide treatment) after i/p administration of scrapie to mice was found to almost double the incubation period (Sethi *et al.*, 2002) implying that these molecules may act to bind infectious agent/PrP^d on DCs and other cells of the innate immune system on which they are expressed.

Once access has been achieved the agent travels along peripheral nerves to the brain. In this model the routing follows synaptically linked pathways of splanchnic and vagus nerves but the mode of spread is still a matter for debate. Axonal or non-axonal transport is feasible. Axonal transport of infectivity (Scott *et al.*, 1992, Kimberlin *et al.* 1983c, Kimberlin *et al.*, 1987), and both PrP^C (Borchelt 1994, Rodolfo *et al.*, 1999, Moya *et al.*, 2004) or PrP^{Sc} (Bartz *et al.*, 2002,03) have been reported in CNS and peripheral nerves. In these studies the rate and direction of spread varied. In some studies the rate was reportedly very slow (between 0.5-2mm per day) - a velocity that is compatible with slow anterograde axonal transport (Brady 1981). The direction of trafficking was also variable. Accumulated data from the papers cited above shows that both PrP^C and infection-specific PrP can travel in an anterograde or a retrograde direction and at least in some rodent scrapie models (Scott *et al.*, 1992, McBride *et al.,* 2001, Bartz *et al.*, 2002,03) both transport systems appear to operate simultaneously. Inconsistencies exist between the suggested rates of agent/PrP spread and those for axoplasmic transport of e.g. cytoskeletal proteins, lectins, viruses and tracers such as horseradish peroxidase (Brady 1981, Weiss 1982, Goldstein & Yang 2000). In the studies carried out by Bartz *et al*, 2002, PrP^{Sc} was estimated to spread in a retrograde direction at a rate of approximately 3.3mm per day but this is still much slower that the rate of retrograde axonal transport which varies between 70 to 430mm per day (Goldstein & Yang 2000, Brown 2003). Discrepancies may be due, in part, to the method of assessment. The slow rates of spread measured by infectivity assays are almost certainly inaccurate. Transportation may occur fairly quickly but a major part of the estimated time is probably accounted for by uptake and replication in target neurones. Another possible explanation is that the reduced transport rates observed in TSE-infected rodents reflect infection-induced transport defects. Similar protein transport deficits have been shown in Alzheimer's disease (Morfini *et al.*, 2002) linked to presenilin-1 modulation of motility (Naruse *et al.*, 1998, Cai *et al.*, 2002).

It has been suggested that fast axoplasmic transport is not the primary mechanism by which the TSE agent spreads along nerves. Aguzzi and co-workers propose that 'prions' are not transported within axons but spread along axons ad-axonally, possibly via Schwann cells

(Follet *et al.*, 2002), by the sequential conversion of PrP^{C} molecules into PrP^{Sc} (Glatzel & Aguzzi 2000). A later report from Aguzzi's laboratory appeared to support this theory. Transgenic mice with a fast axonal transport impairment (a consequence of four-repeat human tau over-expression) showed similar incubation times to control mice after intranerval challenge of RML scrapie (Kunzi *et al.,* 2002). However, doubts have been expressed as to the validity of the conclusions drawn from this work (Moya *et al.*, 2004) due to the lack of evidence to show that rapid axonal transport is affected. Although this line of mice displays axonopathy in brain and spinal cord, Moya *et al.*, argue that deviation from normal range of anterograde or retrograde transport velocities was not proven.

Although axonal transportation was not formally established in this study the evidence presented here indicates convincingly that the infectious agent uses axonal pathways to spread through the nervous system. In this respect, the current data supports the old 'slow virus' concept of TSE infection, after which scrapie and related diseases were originally named, i.e. unconventional slow virus encephalopathies. Axonal transport is established as the mechanism by which neurotropic viruses such as Herpes Simplex virus, pseudorabies and Borna disease virus spread between neuronal populations (Cook & Steven 1973, Carbone *et al.*, 1987, Card *et al.*, 1990,93, Gesser & Koo 1996). Initially, Borna disease virus travels in a retrograde direction but in late stages of infection the virus is transported centrifugally by anterograde axonal transport and consequently many tissues become infected (Gosztonyi and Ludwig 1995). The temporal pattern of PrP^{d} deposition was compatible with this scenario and bi-directional transport was also suggested to occur after intraocular (Scott *et al.*, 1992) or sciatic nerve (Bartz *et al.*, 2002) infection.

As well as parallels in transportation and spread, neurotropic viruses share many other features of TSE pathogenesis including strain selectivity, tropism, cell-specific targeting and astrocyte involvement (Krinke & Dietrich 1990, Gesser and Koo 1996, Card & Enquist 1994, Vahine *et al.*, 1978), making neurotropic viruses interesting models to obtain insights into TSE pathogenesis. PrP^{Sc} is derived from a host glycoprotein and given its role in TSE pathogenesis, it is note-worthy that specific glycoproteins also influence the pathogenesis of neurotropic viruses. Differences in pseudorabies virus tropism (Whealy *et al.,* 1993), reduced virulence (Heffner *et al.*, 1993) and neuronal access (Peeters *et al.*, 1993) have been produced by deletion of viral genes encoding particular envelope glycoproteins.

The neurotropic properties of viruses such herpes, polio, pseudorabies, reovirus and Borna disease have long been used to characterise neuronal circuitry and virally-induced pathogenesis. These viruses invade and replicate in neurones and spread through synaptically

linked chains. The sequential pattern of PrP^d deposition through functionally linked neurones shown here is similar to spread through gustatory pathways after injection into the tongue (Bartz *et al*, 2003) or infectivity measurements of visual pathway components shown by Scott *et al* 1992 after infection of the eye. Taken together, the data indicates that these TSE agents also spread in a similar stepwise manner along synaptically linked neuronal populations. Indeed the delineation of vagal and splanchnic neural circuitry exhibited by orally-administered 263K scrapie accurately replicates the transneuronal tracing which would be obtained by intra-gastric administration of a pseudorabies virus (Enquist *et al.*, 1994, Loewy 1995). Further, the correlation between PrP^d and infectivity suggests that the progressive accumulation of PrP^d in the sequentially targeted sites is a consequence of local replication at these locations.

The selectivity of differing strains of the same virus for specific neural populations is particularly interesting. For example, the spread of the enteric reovirus strain T3C9 from the intestinal lumen to the CNS (Krinke & Dietrich 1990, Morrison *et al*, 1991, Morrison & Fields 1991) is remarkably similar to that theoretically possible for TSE agent. Two pathways are known to be exploited by reoviruses; 1) spread into the PP through M cells with infection of enteric ganglia and subsequent spread to brain via the vagus nerve or; 2) via the bloodstream (after accessing draining lymph node and thoracic duct). Both polio and reovirus have been shown to bind selectively to M cells of Peyer's patches then to be transcytosed into and replicate in lymphoid cells of PP and tonsils (Sicinski *et al.*, 1990, Wolf *et al.*, 1981). Some virus is shed into the blood in most systemic infections with enteric viruses and in the latter route skeletal or heart muscle is eventually infected. Low levels of scrapie or sCJD agent have been seen in blood of rodents (Manuelidis *et al.*, 1978, Kuroda *et al.*, 1983, Diringer 1984) and this could account for the low levels of infectivity seen in various tissues after scrapie infection (Eklund *et al* 1967). There is no strong evidence that viraemia contributes significantly to CNS invasion but low level viraemia could explain reports of PrP^d presence in muscle (Bosque *et al.*, 2002, Thomzig *et al.*, 2003). Strain specific viral tropism is determined by factors that include genetic susceptibility to infection and immunocompetence (Mims & White 1984, Tyler & Fields 1990).

Findings from this study indicated selectivity of the 263K agent for particular neuronal subpopulations. For example, in peripheral ganglia, some neurones contained very heavy accumulations of PrP^d but others were completely unlabelled. Such selectivity is a recognised feature of PrP pathology in the brain; PrP^d is targeted to particular neuroanatomical areas and accumulates in a strain specific pattern of distribution (Bruce *et al.*, 1989,94a, DeArmond *et al.*, 1997, Beekes *et al.*, 1998). Scrapie strains, therefore,

recognise and selectively target certain groups of neurones for replication. As has been described above neurotropic viruses also show preferential targeting to specific neuronal populations.

The basis of targeting is not clear and is difficult to clarify in an organ as complex as brain. A more simplified way to investigate the types of neurones that are permissive to infection could be to examine components of the peripheral and enteric rather than the CNS as these are more readily manipulated experimentally. The enteric ganglia may a particularly useful model. The organisation of enteric ganglia is very similar to that of the CNS. Glial cells and neurones are in close relationship and a blood–ganglion-barrier exists similar to the blood-brain-barrier. There are several types of neurones present in the ENS identifiable by their morphological, chemical and electrophysiological properties (Furness 2000, Furness & Sanger 2002). The cell type to which virus initially binds may determine the ultimate course of infection and disease (Morrison & Fields 1991). It is possible that cell specific targeting for e.g. neurotransmitter receptors (Lipkin *et al.*,1988) or cell-attachment proteins (Kauffman *et al.*, 1983) are affected by TSE infection indicating that these are necessary for cell-cell spread or the accessibility of particular nerve fibre pathways (Bodkin & Fields 1989). An understanding of the pathophysiological role of neurotransmitters and their receptors could also suggest therapeutic targets.

In this study, as with other rodent models (Bruce *et al.*, 1989,94a, McBride *et al.*, 1998) the greatest abundance of PrP^d was found in or around neurones but from the earliest stages of disease, PrP^d was associated with a variety of glial cells including astrocytes and microglia. Histopathological studies have linked the distribution and range of glial activation with scrapie strain variation. Experimentally transmitted BSE or vCJD (Brown DA *et al.*, 2003) and mouse-derived BSE strains 301V and 301C (P. McBride unpublished) show a similar glial cell involvement and widespread distribution to 263K scrapie (this thesis, Ye *et al.*, 1998). Others, like ME7 and 87V (Bruce *et al.*, 1994a) or 139H (Ye *et al.*, 1998) have less glial pathology and astrocytic and microglial activation is largely confined to areas of vacuolar and PrP^d deposition. With 22A, 22L and 79A scrapie (Fraser 1979, Deidrich *et al.*, 1991, Bruce *et al.*, 1994a) microglia are upregulated and PrP^d is seen within or as a 'blush' around activated astrocytes but there is no overt association with ependymal or blood vessel linings. The causes of differential glial cell involvement are unknown. Potentially, glial specificity could provide clues to understanding aspects of strain targeting but at present this is being used as a diagnostic tool to differentiate between TSE strains in ruminants (Jeffrey *et al.*, 2001b, Ligios *et al.*, 2002, Gonzales *et al.*, 2003).

PrP^d can accumulate within both astrocytes and microglia (Deidrich *et al*, 1991, Bruce *et al*, 1994, Ye *et al.*, 1998, P. McBride unpublished). In relation to microglia, internalisation probably occurs in response to PrP^d toxicity and triggers the release of cytokines and free radicals whose effects ultimately cause neuronal death (Ye *et al.*, 1998, Bate *et al,* 2001, Brown 2001). Cytokine expression correlates with degree of inflammation and neurological disease (Williams *et al.*, 1997a,b, Brown 2001, Brown *et al.*, 2003). An astrocyte-associated marker of oxidative stress has been shown at late stages of the TSE disease (Andreoletti *et al.*, 2002) but astrocytic involvement may be as a secondary response to the primary microglial reaction (Brown *et al.*, 1996).

As glial activation occurred after PrP^d deposition this indicates that astrocytes, microglia and satellite cells were responding to rather than initiating the related pathology. What is not clear is whether glial activation causes or acts to limit neuronal damage. In the healthy or injured brain, astrocytes function to protect and supply nutrients to neurones. In the aftermath of stroke-induced CNS impairment, astrocytes and microglia release growth factors that promote the growth of axons and dendrites of undamaged neurones in the anoxic region (Gluckman *et al.*, 1992). Astrocytes may also have a beneficial role in Alzheimer's disease through their amyloid-degrading capability (Wyss-Coray *et al.*, 2002) and in pseudorabies infection, glial cells, whose involvement is also secondary to viral infection (Carbone 1991), act to restrict rather than amplify the spread of the virus (Card *et al.*, 1994). In addition, glutamine synthetase (GS), a marker of glial function, has been reported to be increased in the brains of scrapie infected mice (Lazarini *et al.,* 1994) or sheep with natural scrapie (Lefrançois *et al.*, 1994). Since high levels of glutamate are toxic to neurones, GS release by astrocytes is a neuroprotective measure.

Understanding the cells that express PrP^C is necessary to discovering where agent replicates and spreads. PrP^C is present on many cell types including those of the LRS, blood and GI tract that are potentially involved in uptake, replication and dissemination of the infectious agent. PrP^C is also expressed on other cells e.g. heart, lung, salivary gland, adrenal, thymus, pancreas, kidney, skeletal muscle, and those of reproductive system (McBride & Bruce 1993) whose association with TSE pathogenesis is not readily apparent. For TSE infection, there is a requirement for PrP^C expression in the host (Manson *et al.*, 1994b, Beuler *et al.*, 1993, Brandner *et al.*, 1996, Prusiner *et al.*, 93). Nevertheless, competency of expression does not necessarily indicate that a cell is receptive to infection.

Both PrP^C mRNA (Bendheim *et al.,* 1992) and protein (McBride & Bruce 1993) are widely distributed in the body. PrP^d can be found in a variety of cells during the incubation period of

experimental mice (McBride & Bruce 1993, McBride *et al.*, 1992), hamsters (McBride & Beekes 1999, Beekes & McBride 2000) or sheep with natural scrapie (van Keulen *et al*, 1999, Heggebo *et al.*, 2002) and BSE (Jeffrey *et al.*, 2001a). Other than neurones, there is no indication that these cells are fatally injured by TSE infection. PrP-expressing FDCs which can support scrapie replication (Brown *et al*, 1999, Montrasio *et al.*, 2000) are not obviously functionally abnormal. Even at end-stage disease, FDC capacity for immune complex trapping remains intact (McBride *et al.*, 1992) but some structural abnormalities are apparent at the ultrastructural level (Jeffrey *et al.*, 2000). PrP pathology is also found in association with astrocytes. PrP^{C} is expressed by astrocytes and both PrP^{Sc} and PrP^{C} have a great affinity for glial fibrillary acidic protein (GFAP) an astrocyte-specific intermediate filament protein (Oesch *et al.,* 1990). PrP knockout mice expressing hamster PrP under the GFAP promoter can accumulate infectivity and develop scrapie (Raeber *et al.*, 1997). However, the finding that mice devoid of GFAP develop normally and are susceptible to scrapie (Gomi *et al.*, 1995) conflicts with a crucial role for astrocytes in TSE pathogenesis. Certainly, at end stages of scrapie infection in wild-type rodents, astrocytes appear healthy and have retained the ability to respond to trauma, and it is not clear whether the PrP^{d} deposits observed within reactive astrocytes (Deidrich *et al*, 1991, Bruce *et al*, 1994, Ye *et al.*, 1998, P. McBride unpublished observation) are due to replication or phagocytosed accumulations. The documented role for macrophage participation in TSE pathogenesis would suggest the latter applies (Carp & Callahan, 1982, Beringue *et al.*, 2000, Terry *et al.*, 2003).

Collectively, these data suggest that the neurone is the ultimate target of the TSE agent – or at least the only target that succumbs to infection. Indeed, in i/c infected transgenic mice, neurone-specific PrP expression was sufficient to maintain scrapie infection while PrP expression in non-neuronal cells (including glia and those of the LRS) was not (Race *et al.*, 1995). It is not known why neurones are susceptible to TSE infection when PrP^{C} can be found in many other cell types. Compared to neurones, other cells have lower or undetectable levels of PrP mRNA (Oesch *et al.*, 1985, Kretzschmar *et al.*, 1986, Manson *et al.*, 1992) so the level of PrP production and rate of turnover may be relevant to initiating and/or sustaining pathogenesis; but neurone susceptibility is likely to be multifactorial. The characteristics that make (some) neurones vulnerable or resistant to TSE infection may well be an important factor in the selectivity of targeting. Discovering the reasons for the basis of neuronal targeting would help our understanding of these diseases and provide a means of pursuing avenues of therapeutic intervention.

Bibliography

Askanas V, Bilak M, King Engel W, Leclerc A, Tomé F. 1993. Prion protein is strongly immunolocalized at the postsynaptic domain of human normal neuromuscular junctions. *Neurosci. Lett.* 159:111-114

Alper T, Cramp WA, Haig DA, Clarke MC. 1967. Does the agent of scrapie replicate without nucleic acid? *Nature* 214:764-766

Aguzzi A and Weissmann C. 1997. Prion research: the next frontiers. *Nature.* 389:795-798

Andréoletti O, Berthon P, Grosclaude J, Delaunay T, Guerrucci S, Schelcher F, Lantier F, Elsen J-M. 1999. Immunohistochemical detection of the ovine PrP protein in the central nervous and lymphoid systems. *In Characterization and Diagnosis of Prion Diseases in Animals and Man.*Tubingen, Germany, 23-25 September 1999. Symposium proceedings, p 122

Andréoletti O, Berthon P, Marc D, Sarradin P, Grosclaude J, van Keulen L, Schelcher F, Elsen J-M, Lantier F. 2000. Early accumulation of PrPSc in gut-associated lymphoid and nervous tissues of susceptible sheep from a Romanov flock with natural scrapie. *J.Gen. Virol.* 81:3115-3126

Andréoletti O, Levavasseur E, Uro-Coste E, Tabouret G, Sarradin P, Delisle M-B, Berthon P, Salvayre R, Schelcher F, Negre-Salvayre A. 2002. Astrocytes accumulate 4-hydroxynonenal adducts in murine scrapie and human Creutzfeldt-Jakob disease. *Neurobiol. Dis.* 11:386-393

Andrezik JA and Beitz AJ. 1985. *In* The Rat Nervous System, vol.2, pp221-250. G. Paxinos (Ed). Reticular formation, central gray and related tegmental nuclei. Sidney: Academic Press

Armstrong RA, Cairns NJ, Ironside JW, Lantos PL. 2003. Does the neuropathology of human patients with variant Creutzfeldt-Jakob disease reflect haematogenous spread of the disease? *Neurosci. Lett.* 348:37-40

Aucouturier P, Geissmann F, Damotte D, Saborio GP, Meeker HC, Kascsak R, Kascsak R, Carp RI, Wisniewski T. 2001. Infected splenic dendritic cells are sufficient for prion transmission to the CNS in mouse scrapie. *J.Clin. Invest.* 108:703-708

Baldauf E, Beekes M, Diringer H. 1997. Evidence for an alternative direct route of access for the scrapie agent to the brain bypassing the spinal cord. *J. Gen. Virol.* 78:1187-1197

Banchereau J and Steinman RM. 1998. Dendritic cells and the control of immunity. *Nature* 392: 245-252

Barron RM, Thomson V, Jamieson E, Melton DW, Ironside J, Will R, Manson JC. 2001. Changing a single amino acid in the N-terminus of murine PrP alters TSE incubation time across three species barriers. *EMBO J.* 20:5070-5078

Bartz JC, Kincaid AE, Bessen RA. 2002. Retrograde transport of transmissible mink encephalopathy within descending motor tracts. *J. Virol.* 76:5759-5768

Bartz JC, Kincaid AE, Bessen RA. 2003. Rapid prion neuroinvasion following tongue infection. *J. Virol.* 77:583-591

Basler K, Oesch B, Scott M, Westaway D, Walchi M, Groth DF, McKinley MP, Prusiner SB, Weissmann C. 1986. Scrapie and cellular PrP isoforms are encoded by the same chromosomal gene. *Cell* 46:417-428

Bate C, Reid S, Williams A. 2001. Killing of prion-damaged neurones by microglia. *Neuroreport* 12:2589-2594

Beekes M, Baldauf E, Diringer H. 1996. Sequential appearance and accumulation of pathognomonic markers in the central nervous system of hamsters orally infected with scrapie. *J. Gen. Virol.* 77:1925-1934.

Beekes M, McBride PA, Baldauf E. 1998. Cerebral targeting indicates vagal spread of infection in hamsters fed with scrapie. *J.Gen.Virol.* 79:601-607

Beekes M and McBride PA. 2000. Early accumulation of pathological PrP in the enteric nervous system and gut-associated lymphoid tissue of hamsters orally infected with scrapie. *Neurosci. Lett.* 278:181-184

Begara-McGorum I, Gonzalez L, Simmons M, Hunter N, Houston F, Jeffrey M. 2002. Vacuolar lesion profile in sheep scrapie: factors influencing its variation and relationship to disease-specific PrP accumulation. *J. Comp. Pathol.* 127:59-68

Bell JE, Gentleman SM, Ironside JW, McCardle L, Lantos PL, Doey L, Lowe J, Fergusson J, Luthert P, McQuaid S, Allen IV. 1997. Prion protein immunocytochemistry – U.K. five centre consensus report. *Neuropathol. Appl. Neurobiol.* 23:25-35

Bencsik A, Lezmi S, Baron T. 2001. Autonomous nervous system innervation of lymphoid territories in spleen; A possible involvement of noradrenergic neurons for prion neuroinvasion in natural scrapie. *J. Neurovirol.* 7:447-453

Bendheim PE, Barry RA, DeArmond SJ, Stites DP, Prusiner SB. 1984. Antibodies to a scrapie prion protein. *Nature* 310:418-421

Bendheim PE, Brown HR, Rudelli RD, Scala LJ, Goller NL, Wen GY, Kascsak RJ, Cashman NR, Bolton DC. 1992. Nearly ubiquitous tissue distribution of the scrapie agent precursor protein. *Neurology* 42:149-156

Beringue V, Demoy M, Lasmézas CI, Gouritin B, Weingarten C, Deslys J-P, Andreux J-P, Couvreur P, Dormont D. 2000. Role of spleen macrophages in the clearance of scrapie agent early in pathogenesis. *J. Pathol.* 190:495-502

Berthoud HR, Kressel M, Raybould HE, Neuhuber WL. 1995. Vagal sensors in the rat duodenal mucosa: distribution and structureas revealed by in vivo Dil-tracing. *Anat. Embryol.* 191:203-212

Berthoud HR and Neuhuber WL. 2000. Functional and chemical anatomy of the afferent vagal system. *Autonom. Neurosci: Basic and Clinical* 85:1-17

Blättler TS, Brandner A.J, Raeber MA, Klein M, Voigtlander T, Weissmann C, Aguzzi A. 1997. PrP-expressing tissue required for transfer of scrapie infectivity from spleen to brain. *Nature* 389:69-73

Bodkin DK and Fields BN. 1989. Growth and survivial of reovirus in intestinal tissue: role of the L2 and S1 genes. *J. Virol.* 63:1188-1193

Bolton DC, McKinley MP, Prusiner SB. 1982. Identification of a protein that purifies with the scrapie prion. *Science* 218:1309-1311

Bons N, Mestre-Frances N, Belli P, Cathala F, Gajdusek DC, Brown P. 1999. Natural and experimental oral infection of nonhuman primates by bovine spongiform encephalopathy agents. *Proc. Natl. Acad. Sci. USA* 96:4046-4051

Bons N, Lehmann S, Nishida N, Mestre-Frances N, Dormont D, Belli P, Delacourte A, Grassi J, Brown P. 2002. BSE infection of the small short-lived primate Microcebus murinus. *Comp. Rend. Biol.* 325:67-74

Borchelt DR, Scott M, Taraboulos A, Stahl N, Prusiner SB. 1990. Scrapie and cellular prion proteins differ in their kinetics of synthesis and topology in cultured cells. *J.Cell Biol.* 110:743-752

Borchelt DR, Koliatsos VE, Guarnieri M, Pardo CA, Sisodia SS, Price DL. 1994. Rapid anterograde axonal transport of the cellular prion glycoprotein in the peripheral and central nervous systems. *J. Biol. Chem.* 269:14711-14714

Bosque PJ, Ryou C, Telling G, Peretz D, Legname G, DeArmond SJ, Prusiner SB. 2002. Prions in skeletal muscle. *Proc. Natl. Acad. Sci. USA.* 99:3812-3817

Bounhar Y, Zhang Y, Goodyer CG, LeBlanc A. 2001. Prion protein protects human neurones against Bax-mediated apoptosis. *J. Biological Chem.* 276:39145-39149

Bradley R. 1996. Bovine spongiform encephalopathy: distribution and update on some transmission and decontamination studies. *In*: Bovine Spongiform Encephalopathy: the BSE dilemna. pp.11-27 CJ Gibbs, (Ed.) Springer-Verlag, New York,

Brady ST. 1991. Molecular motors in the nervous system. *Neuron* 7:521-533

Brandner S, Isenmann S, Raeber A, Fischer M, Sailer A, Kobayashi Y, Marino A, Weissmann C, Aguzzi A. 1996. Normal host prion protein necessary for scrapie-induced neurotoxicity. *Nature* 379:339-343

Brenner HR, Herczeg A, Oesch B. 1992. Normal development of nerve-muscle synapses in mice lacking the prion protein gene. *Proc. R. Soc. Lond. B. Biol. Sci.* 250:151-155

Brown A. 2003. Axonal transport of membranous and nonmembranous cargoes: a unified theory. *J. Cell. Biol.* 160:817-821

Brown AR, Webb J, Rebus S, Walker R, Williams A, Fazakerley JK. 2003. Inducible cytokine gene expression in the brain in the ME7/CV mouse model of scrapie is highly restricted, is at a strikingly low level relative to the degree of gliosis and occurs only late in disease. *J. Gen. Virol.* 84:2605-2611

Brown DA, Bruce ME, Fraser JR. 2003. Comparison of the neuropathological characteristics of bovine spongiform encephalopathy (BSE) and variant Creutzfeldt-Jakob disease (vCJD) in mice. *Neuropathol. Appl. Neurobiol.* 29:262-272

Brown DR, Schmidt B, Kretzschmar H. 1996. A neurotoxic prion protein fragment enhances proliferation of microglia but not astrocytes in culture. *Glia* 18:59-67

Brown DR, Qin KF, Herms JW, Madlung A, Manson J, Strome R, Fraser PE, Kruck T, von Bohlen A, Schulz-Schaeffer W, Giese A, Westaway D, Kretzschmar H. 1997a. The cellular prion protein binds copper *in vivo*. *Nature* 390:684-687

Brown DR, Schulz-Schaeffer WJ, Schmidt B, Kretzschmar H. 1997b. Prion protein-deficient cells show altered response to oxidative stress due to decreased SOD-1 activity. *Exp. Neurol.* 146:104-112

Brown DR, Schmidt B, Groschup MH, Kretzschmar HA. 1998. Prion protein expression in muscle cells and toxicity of a prion protein fragment. *Eur. J. Cell Biol* 7:29-37

Brown DR. 2000. PrP^{Sc}-like prion protein inhibits the function of cellular prion protein. *Biochem. J.* 352:511-518

Brown DR. 2001. Microglia and prion disease. *Microscopy research and technique* 54:71-80

Brown DR, Nicholas RS, L Canevari. 2002. Lack of prion protein expression results in a neuronal phenotype sensitive to stress. *J. Neurosci. Res.* 67:211-224

Brown KL, Stewart K, Ritchie DL, Mabbottt NA, Williams A, Fraser H, Morrison WI, Bruce ME. 1999. TSE replication in lymphoid tissues depends on PrP-expressing follicular dendritic cells. *Nature Medicine* 5:1-5

Brown KL, Ritchie DL, McBride PA, Bruce ME. 2000. Detection of PrP in extraneural tissues. *Micro. Res. Tech.* 50:40-45

Brown MC, Jansen JKS, van Essen D. 1976. Polyneuronal innervation of skeletal muscle in new-born rats and its elimination in maturation. *J. Physiol.* 261:387-422

Brown P, Rowher RG and Gajdusek DC. 1986. Newer data on the inactivation of scrapie virus or Creutzfeldt-Jakob disease virus in brain tissue. *J. Infect. Dis.*153:1145-1148

Brown P and Gajdusek DC. 1991. Survival of scrapie virus after 3 years interment. *Lancet* 337:269-270

Brown P, Preece MA, Will RG. 1992. "Friendly fire" in medicine hormones, homografts and Creutzfeldt-Jakob disease. *Lancet* 340:24-27

Bruce ME and Fraser H. 1976. Cerebral amyloidosis in scrapie in the mouse: effect of agent strain and mouse genotype. *Neuropathol. Appl. Neurobiol.* 2:471-478

Bruce ME. 1981. Serial studies on the development of cerebral amyloidosis and vacuolar degereration in murine scrapie. *J.Comp.Path.* 91:589-597

Bruce ME and Dickinson AG. 1987. Biological evidence that scrapie agent has an independent genome. *J.Gen.Virol.* 68:79-89

Bruce ME, McBride PA, Farquhar CF. 1989. Precise targeting of the pathology of the sialoglycoprotein, PrP, and vacuolar degeneration in mouse scrapie. *Neurosci. Lett.* 102: 1-6

Bruce ME and Fraser H. 1991. Scrapie strain variation and its implications. *Curr. Top. Microbiol. Immunol.* 172:126-134

Bruce ME, McConnell, Fraser H, Dickinson AG. 1991. The disease characteristics of different strains of scrapie in *Sinc* congenic mouse lines: implications for the nature of the agent and host control of pathogenesis. *J. Gen. Virol.* 72:595-603

Bruce ME, McBride PA, Jeffrey M, Scott JR. 1994a. PrP in pathology and pathogenesis in scrapie-infected mice. *Mol. Neurobiol.* 8:105-112

Bruce ME, Chree A, McConnell I, Foster J, Pearson G, Fraser H. 1994b. Transmission of bovine spongiform encephalopathy and scrapie to mice: strain variation and the species barrier. *Phil. Trans. R. Soc. Lond.* B343:405-411

Bruce, ME, Will RG, Ironside JW, McConnell I, Drummond D, Suttie A, McCardle L, Chree A, Hope J, Birkett C, Cousens S, Fraser H, Bostock CJ. 1997. Transmissions to mice indicate that 'new variant' CJD is caused by the BSE agent. *Nature* 389:498-501

Büeler H, Fischer M, Lang Y, Bluethmann H, Lipp H-P, DeArmond SJ, Prusiner SB, Aguet M, Weissmann C. 1992. Normal development and behaviour of mice lacking the neuronal cell-surface PrP protein. *Nature* 356:577-582

Büeler H, Aguzzi A, Sailer A, Greiner R-A, Autenreid P, Aguet M, Weissmann C. 1993. Mice devoid of PrP are resistant to scrapie. *Cell* 73:1339-1347

Cabot JB. 1990. *In* Central Regulation of Autonomic Functions, pp45-67. AD Loewy and KM Spyer (Eds), Sympathetic preganglionic neurons: Cytoarchitecture, Ultrastructure and Biophysical Properties. New York: Oxford University Press

Cabot PJ, Carter L, Gaiddon C, Zhang Q, Schaefer M, Loeffler JP, Stein C. 1997. Immune cell-derived beta-endorphin: Production, release and control of inflammatory pain in rats. *J. Clin. Invest.* 100:142-148

Cai D, Leem JY, Greenfield JP, Wang P, Kim BS, Wang R, Lopes LO, Kim SH, Zheng H, Greengard P, Sisodia SS, Thinakaran G, Xu H. 2002. Presenilin-1 regulates intracellular trafficking and cell surface delivery of beta-amyloid precursor protein. *J. Biol. Chem.* 278:3446-3454

Carbone KM, Duchala CS, Griffin JW, Kincaid AL, Narayan O. 1987. Pathogenesis of Borna disease in rats: Evidence that intra-axonal spread is the major route for virus dissemination and the determinant for disease incubation. *J.Virol.* 61:3431-3440

Carbone KM, Moench TR, Lipkin W. 1991. Borna disease virus replicates in astrocytes, Schwann cells and ependymal cells in persistently infected rats: Location of viral genomic and messenger RNAs by in situ hybridisation. *J. Neuropathol. Exp. Neurol.* 50: 205-214

Card JP, Rinaman L, Schwaber JS, Miselis RR, Whealy ME, Robbin AK, Enquist LW. 1990. Neurotropic properties of pseudorabies virus: uptake and transneuronal passage in the rat central nervous system. *J. Neurosci.* 10:1974-1994

Card JP, Rinaman L, Lynn RB, Lee B-H, Meade RP, Miselis RR and Enquist LW. 1993. Pseudorabies virus infection of the rat central nervous system: ultrastructural characterization of viral replication, transport and pathogenesis. *J. Neurosci.* 13:2515-2539

Card JP and Enquist LW. 1994. Use of pseodorabies virus for definition of synaptically linked populations of neurones. *Meth. Mol. Gen.* 4:363-382

Carleton A, Tremblay P, Vincent JD, Lledo PM. 2001. Dose-dependent, prion protein (PrP)-mediated facilitation of excitatory synaptic transmission in the mouse hippocampus. *Pflugers Arch.* 442:223-229

Carlson GA, Kingsbury DT, Goodman PA, Coleman S, Marshall ST, DeArmond S, Westaway D and Prusiner SB. 1986. Linkage of prion protein and scrapie incubation time genes. *Cell* 46:503-511

Carp RI. 1982. Transmission of scrapie by oral route: Effect of gingival scraification. *Lancet* 1:170-171

Carp RI and Callahan SM. 1982. Effect of mouse peritoneal macrophages on scrapie infectivity during extended in vitro incubation. *Intervirology* 17:201-207

Carp RI, Moretz RC, Wisniewski HM. 1984. Development of amyloid plaques in a scrapie agent-mouse strain combination with a short incubation period. J. *Neuropathol. Neurol.* 43:314-320

Casaccia P, Ladogana A, Xi YG, Pocchiari M. 1989. Levels of infectivity in the blood throughout the incubation period of hamsters peripherally injected with scrapie. *Arch. Virol.* 108:145-149

Cashman NR, Loertscher R, Nalbantoglu J, Shaw I, Bolton DC, Bendheim PE. 1990. Cellular isoform of the scrapie agent protein participates in lymphocyte activation. *Cell* 61:185-192

Caughey B, Race R, Chesebro B. 1988. Detection of prion protein mRNA in normal and scrapie-infected tissues and cell lines. *J. Gen. Virol.* 69:711-716

Caughey B and Raymond GJ. 1991. The scrapie-associated form of PrP is made from a cell-surface precursor that is both protease-sensitive and phospholipase-sensitive. *J. Biol. Chem.* 266:18217-18223

Cervenakova L, Goldfarb LG, Garruto R, Lee HS, Gajdusek DC, Brown P. 1998. Phenotype-genotype studies in kuru: implications for new variant Creutzfeldt-Jakob disease. *Proc. Natl. Acad. Sci. USA* 95:13239-13241

Chandler RL. 1961. Encephalopathy in mice produced by inoculation with scrapie brain material. *Lancet* 1:1378-1379

Chandler RL. 1963. Experimental scrapie in the mouse. *Res. Vet. Sci.* 4:276-285

Chesebro B, Race R, Wehrly K, Nishio J, Bloom M, Lechner D, Bergstrom S, Robbins K, Mayer L, Keith JM, Garon C, Haase A. 1985. Identification of scrapie prion protein-specific messenger-RNA in scrapie-infected and uninfected brain. *Nature* 315:331-333

Clarke MC and Kimberlin RH. 1984. Pathogenesis of mouse scrapie: distribution of agent in the pulp and stroma of infected spleens. *Vet. Microbiol.* 9:215-255

Cole S and Kimberlin RH. 1985. Pathogenesis of mouse scrapie: Dynamics of vacuolation in brain and spinal cord after intraperitoneal infection. *Neuropath. Appl. Neurobiol.*11:213-217

Collee JB and Bradley R. 1997a. BSE: A decade on. 1. *Lancet* 349:636-641

Collee JB and Bradley R. 1997b. BSE: A decade on. 2. *Lancet* 349:715-721

Colling SB, Collinge J, Jefferys JGR. 1996. Hippocampal slices from prion protein null mice: disrupted Ca^{2+}-activated K^{+} currents. *Neurosci. Lett.* 209:49-52

Collinge J, Whittington MA, Sidle KCL, Smith CJ, Palmer MS, Clarke AR, Jefferys JGR. 1994. Prion protein is necessary for normal synaptic function. *Nature* 370:295-297

Collinge J, Sidle KCL, Meads J, Ironside J, Hill AF. 1996. Molecular analysis of prion strain variation and the aetiology of 'new variant' CJD. *Nature* 383:685-690

Collinge J. 1999. Investgation of variant Creutzfeldt-Jakob disease and other human prion diseases with tonsil biopsy samples. *Lancet* 353:183-189

Colm H and Knight R. 2002. Clinical features of variant Creutzfeldt-Jakob disease. *Rev. Med. Virol.* 12:143-150

Cook ML and Steven JG. 1973. Pathogenesis of herpetic neuritis and ganglionitis in mice: evidence for intra-axonal transport of infection. *Infect. Immun.* 7:272-288)

Cuillé J and Chelle PL. 1939. Experimental transmission of trembling to the goat. *CR Seances Acad Sci* 208:1058-1060

Curtis J, Errington M, Bliss T, Voss K, MacLeod N. 2003. Age-dependent loss of PTP and LTP in the hippocampus of PrP-null mice. *Neurobiol. Dis.* 13:55-62

Davis IC and Owen RL 1997. The immunopathology of M cells. *Springer Semin. Immunopathol.* 18:421-448

Dawson M, Warner R, Nolan A, McKeown B, Thomson J. 2003. 'Complex' PrP genoytpes identified by the National Scrapie Plan. *Vet. Record* 152(24):754-755

DeArmond SJ, McKinley PM, Barry RA, Braunfield MB, McColloch JR, Prusiner SB. 1985. Identification of prion amyloid filaments in scrapie-infected brain. *Cell* 41:221-235

DeArmond SJ, Mobley WC, DeMott DL, Barry RA, Beckstead JH and Prusiner SB. 1987. Changes in the localisation of brain prion proteins during scrapie infection. *Neurology* 37:1271-1280

DeArmond SJ, Kristensson K, Bowler RP. 1992. PrP^{Sc} causes nerve cell death and stimulates astrocyte proliferation: a paradox. *Prog. Br. Res.* 94:437-446

DeArmond SJ, Sanchez H, Yehiely F, Qui Y, Ninchak-Casey A, Daggett V, Camerino AP, Cayetano J, Rogers M, Groth D, Torchia M, Tremblay P, Scott M, Cohen RE, Prusiner SB.1997. Selective neuronal targeting in prion disease. *Neuron* 19:1337-1348

Deidrich J, Bendheim P, Kim YS, Carp RI, Haase AT. 1991. Scrapie-associated prion protein accumulates in astrocytes during scrapie infection. *Proc .Natl. Acad. Sci. USA* 88:375-379

Deiner T. 1973. Similarities between the scrapie agent and the agent of potato spindle tuber disease. *Ann. Clin. Res.* 5:268-278

Dickinson AG, Meikle VMH, Fraser H. 1968. Identification of a gene which controls the incubation period of some strains of scrapie in mice. *J. Comp. Path.* 78:293-299

Dickinson AG, Meikle VHM, Fraser H. 1969. Genetical control of the concentration of ME7 scrapie agent in the brain of mice. *J. Comp. Path.* 79:15-22

Dickinson AG and Meikle VMH. 1971. Host-genotype and agent effects in scrapie incubation: change in allelic interaction with different strains of agent. *Mol. Gen. Genet.* 112:73-79

Dickinson AG and Fraser H. 1977. Scrapie pathogenesis in inbred mice: an assessment of host control and response involving many strains of agent. In *Slow Virus Infections of the Central Nervous System,* pp3-14, V. ter Meulen & M. Katz, Eds. New York: Springer-Verlag.

Dickinson AG and Fraser H. 1979. An assessment of the genetics of scrapie in sheep and mice. In *Slow Transmissible Diseases of the Nervous System.* Vol. 1 pp 387- 405. Edited by SB Prusiner, WJ Hadlow, New York. Academic Press.

Dickinson AG and Outram G.1979 The scrapie replication-site hypothesis and its implications for pathogenesis. In *Slow Transmissible Diseases of the Nervous System.* Vol. 1 pp 13-31. Edited by SB Prusiner, WJ Hadlow, New York. Academic Press.

Dickinson AG and Outram GW. 1988. Genetic aspects of unconventional virus infections: the basis of the virino hypothesis, pp63-83. *In* G. Bock, and R. Marsh (Eds.) Novel infectious agents and the central nervous system (Ciba Foundation Symposium vol 135). Wiley, Chichester.

Diringer H, Hilmert H, Simon D, Werner E, Ehlers B. 1983a. Towards purification of the scrapie agent. *Eur. J. Biochem.* 134:555-560

Diringer H, Gelderblom H, Hilmert H, Ozel M, Edelbluth C, Kimberlin RH. 1983b. Scrapie infectivity, fibrils and low molecular weight protein. *Nature* 306:476-478

Diringer H. 1984. Sustained viraemia in experimental hamster scrapie. *Arch. Virol.* 82:105-109

Diringer H. 1991. The concept of virus-induced amyloidosis. *Eur. J. Epidemiol.* 7:562-566

Diringer H, Beekes M, Oberdieck U. 1994. The nature of the scrapie agent – the virus theory. *Ann. NY Acad. Sci.* 724:246-258

Dockray GJ 1999. The brain-gut axis, pp 67-81. *In*: T. Yamada (Ed.) Textbook of Gastro-enterology, 3rd ed. Lippincott, Williams & Wilkins, Philadelphia, New York, Baltimore.

Ehlers B, Rudolph R, Diringer H. 1984. The reticuloendothelial system in scrapie pathogenesis. *J. Gen. Virol.* 65:423-428

Eklund CM, Kennedy RC, Hadlow WJ. 1967. Pathogenesis of scrapie virus infection in the mouse. *J. Infect. Dis.* 117:15-22

Elfvin L-G, Aldskogius H, Johansson J. 1992. Splenic primary sensory afferents in the guinea-pig demonstrated with anterogradely transported wheat-germ agglutinin conjucated to horseradish peroxidase. *Cell Tissue Res.* 269:229-234

Enquist LW, Miselis RR, Card JP. 1994. Specific infection of rat neuronal circuits by pseudorabies virus. *Gene Therapy* 1:S10

Farquhar CF, Somerville RA, Ritchie LA. 1989. Post-mortem immunodiagnosis of scrapie and bovine spongiform encephalopathy. *J. Virol. Meth.* 24:215-221

Farquhar CF, Dornan J, Somerville RA, Tunstell AM, Hope J. 1994. Effect on *Sinc* genotype, agent isolate and route of infection on the accumulation of protease-resistant PrP in non-central nervous system tissues during the development of murine scrapie. *J. Gen. Virol.* 75:495-504

Felton DL, Felton SY, Carlson SL, Olschowka JA, Livnat S. 1985. Noradrenergic and peptidergic innervation of lymphoid tissue. *J. Immunol.* 135:755-765

Felton DL and Felton SY. 1988. Sympathetic noradrenergic innervation of immune organs. *Brain Behav. Immun.* 2:293-300

Fink T and Weihe E. 1988. Multiple neuropeptides in nerve supplying mammalian lymph nodes: messenger candidates for sensory and autonomic neuroimmunomodulation. *Neursci. Lett.* 90:39-44

Flumerfelt BA and Hrycyshyn AW. 1985. Precerebellar nuclei and red nuclesus. *In* The Rat Nervous System, vol.2, pp. 221-250. Edited by G. Paxinos. Sidney: Academic Press

Follet J, Lemaire-Vieille C, Blánquet-Gossard F, Podevin-Dimster V, Lehmann S, Chauvin J-P, Decavel J-P, Varea R, Grassi J, Fontès M, Cesbron J-Y. 2002. PrP expression and replication by Schwann cells: Implications in prion spreading. *J. Virol.* 76:2434-2439

Ford MJ, Burton LJ, Li H, Graham CH, Frobert Y, Grassi J, Hall SM, Morris RJ. 2001. A marked disparity between the expression of prion protein and its message by neurones of the CNS. *Neuroscience* 111: 533-551

Foster JD, Wilson M and Hunter H. 1996. Immunolocalisation of the prion protein (PrP) in the brains of sheep with scrapie. *Vet. Record* 139:512-515

Foster JD, Parnham DW, Hunter N, Bruce M. 2001. Distribution of the prion protein in sheep terminally affected with BSE following experimental oral transmission. *J. Gen. Virol.* 82:2319-2326

Fournier J-G, Escaig-Haye F, Billette de Villemeur T, Robain O, Lasmézas C, Deslys J-P, Dormont D, Brwon P. 1998. Distribution and submicroscopic immunogold localization of cellular prion protein (PrPc) in extracerebral tissues. *Cell Tissue Res.* 292:77-84

Fournier J-G, Escaig-Haye F, Grigoriev V. 2000. Ultrastructural localization of prion proteins: physiological and pathological implications. *Microscop. Res. Tech.* 50:76-88

Fraser H and Dickinson AG. 1970. Pathogenesis of scrapie in the mouse: the role of the spleen. *Nature* 226:462-463

Fraser H and Dickinson AG. 1973. Scrapie in mice: agent-strain differences in the distribution and intensity of grey matter vacuolation. *J. Comp. Path.* 83:29-40

Fraser H. 1976. The pathology of a natural and experimental scrapie. *Frontiers of Biology* 44:267-305

Fraser H and Dickinson AG. 1978. Studies of the lymphoreticular system in the pathogenesis of scrapie: the role of the spleen and thymus. *J. Comp. Path.* 88:563-573

Fraser H. 1979. Neuropathology of scrapie: the precision of the lesions and their diversity. In *Slow Transmissible Diseases of the Nervous System.* Vol. 1 pp 387-405. Edited by SB Prusiner, WJ Hadlow, New York. Academic Press.

Fraser H and Dickinson AG. 1985. Targeting of scrapie lesions and spread of agent via the retino-tectal projection. *Brain Research* 346:32-41

Fraser H and Farquhar CF. 1987. Ionising radiation has no influence on scrapie incubation period in mice. *Vet. Microbiol.* 13:211-223

Fraser H, Davies D, McConnell I, Farquhar CF. 1989. Are radiation-resistant, post-mitotic, long-lived (RRPMLL) cells involved in scrapie replication? In *Unconventional Virus Diseases of the Central Nervous System,* pp 561-564, Edited by LA Court, D. Dormont, P. Brown & DT Kingsbury. Fauntenay-aux-Roses: Commisariat à l'Énergie Atomique.

Fraser H, Bruce ME, Chree A, McConnell I, Wells GA. 1992a. Transmission of bovine spongiform encephalopathy and scrapie to mice *J. Gen. Virol.* 73:1891-1897

Fraser H, Bruce ME, Davies D, Farquhar CF, McBride PA. 1992b. The lymphoreticular system in the pathogenesis of scrapie, pp308-317. *In* S.B. Prusiner, J. Collinge, J. Powell, and B. Anderton (Eds.) Prion Diseases of Humans and Animals, Ellis Horwood, Chichester.

Fraser H, Pearson GR, McConnell I, Bruce ME, Wyatt JM, Gruffydd-Jones TJ. 1994. Transmission of feline spongiform encephalopathy to mice. *Vet. Rec.* 134:44927.

Fraser H, Brown KL, Stewart K, McConnell I, McBride PA, Williams A. 1996. Replication of scrapie in spleens of SCID mice follows reconstitution with wild-type mouse bone marrow. *J. Gen.Virol.* 77:1935-1940

Fraser J. 2002. What is the basis of transmissible spongiform encephalopathy induced neurodegeneration and can it be repaired? *Neuropathol. Appl. Neurobiol.* 28:1-11

Furness J.B, Bornstein JC, Kunze WAA, Clerc N. 1999. The enteric nervous system and its extrinsic connections, pp11-35. *In* T. Yamada (Ed.) Textbook of Gastroenterology, 3rd ed. Lippincott, Williams & Wilkins, Philadelphia, New York, Baltimore.

Furness JB. 2000. Types of neurons in the enteric nervous system *J. Auton. Nerv. Syst.* 81:87-96

Furness JB and Sanger GJ. 2002. Intrinsic nerve circuits of the gastrointestinal tract: identification of drug targets. *Curr. Op. Pharm.* 2:612-622

Gajdusek CA. 1977. Unconventional viruses and the origin and disappearance of kuru. *Science* 197:943-960

Gesser RM and Koo SC. 1996. Oral inoculation with herpes simplex virus type 1 infects enteric neurons and mucosal nerve fibers within the gastrointestinal tract in mice. *J.Virol.* 70:4097-4102

Gibbs CJ Jr. and Gajdusek CA. 1972. Isolation and characterization of the subacute spongiform virus encephalopathies of man: kuru and Creutzfeldt-Jakob disease. *J. Clin. Pathol.* 25:84-96

Glatzel M and Aguzzi A. 2000. Peripheral pathogenesis of prion diseases. *Microbes and infection* 2:613-619

Glatzel M. Heppner FL, Albers KM, Aguzzi A. 2001. Sympathetic innervation of lymphoreticular organs is rate limiting for prion neuroinvasion. *Neuron* 31:25-34

Gluckman P, Klempt N, Guan J, Mallard C, Sirimanne E, Dragunown S, Klempt M, Singh D, Williams C, Nikolics K. 1992. A role for IGF-1 in the rescue of CNS neurons following hypoxic ischemic injury. *Biochem. Biophys. Res. Commun.* 182:593-599

Goehler LE, Gaykema RPA, Nguyen KT, Lee JL, Tilders FJH, Maier SF, Watkins LR. 1999. Interleukin-1B in immune to nervous system link. *J. Neurosci.* 17:2799-2806

Goehler LE, Gaykema RPA, Hansen MK, Anderson K, Maier SF, Watkins LR. 2000.Vagal immune-to-brain communication: a visceral chemosensory pathway. *Auton. Neurosci: Bas. & Clin.* 85:49-59

Gohel C, Grigoriev V, Escaig-Haye F, Lasmézas CI, Deslys J-P, Langeveld J, Alaboune M, Hantai D, Fournier J-G. 1999. Ultrastructural localization of cellular prion protein (PrPc) at the neuromuscular junction. *J. Neurosci. Res.* 55:261-267

Goldstein LS and Yang Z. 2000. Microtubule-based transport systems in neurons: the roles of kinesins and dyneins. *Ann. Rev. Neurosci.* 23:39-71

Gomi H, Yokoyama T, Fujimoto K, Ikeda T, Katoh A, Itoh T, Itohara S. 1995. Mice devoid of glial fibrillary acidic protein develop normally and are susceptible to scrapie prions. *Neuron* 14:29-41

Gonzalez L, Martin S, Jeffrey M. 2003. Distinct profiles of PrPd immunoreactivity in the brain of scrapie- and BSE-infected sheep: implications on differential cell targeting and PrP processing. *J. Gen. Virol.* 84:1339-1350

Goodfield J. 1997. Cannibalism and kuru. *Nature* 387:841

Gordon WS. 1946. Advances in veterinary research. *Vet. Res.* 58:516-520

Gosztonyi G and Ludwig H. *In* Borna disease. 1995. Koprowsik H and Lipkin I (Eds) Borna disease – Neuropathology and Pathogenesis pp39-73. Berlin, Springer Berlag

Graner E, Mercadante AF, Zanata SM, Forlenza OV, Cabral ALB, Veiga SS, Juliano MA, Roesler R, Walz R, Minetti A, Izquierdo I, Martins VR, Brentani RR. 2000. Cellular prion protein binds laminin and mediates neuritogenesis. *Mol.Brain Res.* 76:85-92

Griffith JS. 1967. Self-replication and scrapie. *Nature* 215:1043-1044

Groschup MH, Weiland F, Straub OC, Pfaff E. 1996. Detection of scrapie agent in the peripheral nervous system of a diseased sheep. *Neurobiol. Dis.* 3:191-195

Groschup MH, Beekes M, McBride PA, Hardt M, Hainfellner JA, Budka H. 1999. Deposition of disease-associated prion protein involves the peripheral nervous system in experimental scrapie. *Acta Neuropathol.* 98:453-457

Guentchev M, Voigtlander T, Haberler C, Groschup MH, Budka H 2000. Evidence for oxidative stress in experimental prion disease. *Neurobiol. Dis.* 7:270-273

Hadlow WJ, Eklund CM, Kennedy RC, Jackson TA, Whitford HW, Boyle CG. 1974. Course of experimental scrapie virus infection in the goat. *J. Infect. Dis.* 129:559-567

Hadlow WJ, Kennedy RC, Race RE. 1982. Natural infection in Suffolk sheep with scrapie virus. *J Infect. Dis.* 146:657-664

Hadlow WJ and Karstad L. 1986. Transmissible encephalopathy of mink in Ontario. *Can. Vet.* 9:193-196

Haïk S, Peyrin JM, Lins L, Rosseneu MY, Brasseur R, Langeveld JP. Tagliavini F, Deslys JP, Lasmézas C, Dormont D. 2000. Neurotoxicity of the putative transmembrane domain of the prion protein. *Neurobiol. Dis.* 7:644-656

Haïk S, Faucheux BA, Sadovitch V, Privat N, Kemeny J-L, Perret-Liaudet A, Hauw J-J. 2003. The sympathetic nervous system is involved in variant Creutzfeldt-Jakob disease. *Nat. Med.* 9:1121-1123

Hartsough GR and Burger D. 1965. Encephalopathy of Mink. Epizootioligic and clinical observations *J. Infect. Dis.* 115:387-392

Heffner S, Kovaks F, Klupp BG, Mettenleiter TC. 1993. Glycoprotein gp50-negative pseudorabies virus: a novel approach toward a non-spreading live herpesvirus vaccine. *J. Virol.* 67:1529-1537

Heggebo R, Press C McL, Gunnes G, Lie KI, Tranulis MA, Ulvund M, Groschup MH, Landsverk T. 2000. Distribution of prion protein in the ileal Peyer's patch of scapie-free lambs and lambs naturally and experimentally exposed to the scrapie agent. *J. Gen. Virol.* 81:2327-2337

Heggebo R, Press C McL, Gunnes G, Gonzales L, Jeffrey M. 2002. Distribution and accumulation of PrP in gut-associated and peripheral lymphoid tissue of scrapie-affected Suffolk sheep. *J. Gen. Virol.* 83:479-489

Heggebo R, Gonzales L, Press C McL, Gunnes G, Espenes A, Jeffrey M. 2003. Disease-associated PrP in the enteric nervous system of scrapie-affected Suffolk sheep. *J. Gen. Virol.* 84: 1327-1338

Heinen E, Bosseloir A, Bouzahzah F. Follicular dendritic cells: origin and function. 1995. *Curr. Top. Microbiol. Immunol.* 201:15-47

Heppner F, Christ AD, Klein MA, Prinz M, Fried M, Kraehenbuhl JP, Aguzzi A. 2001. Transepithelial prion transport by M cells. *Nat. Med.* 7:967-977

Herms JW, Kretzschmar HA, Titz S, Keller BU. 1995. Patch-clamp analysis of synaptic transmission to cerebellar Purkinje cells of prion protein knockout mice. *Eur. J. Neurosci.* 7:2508-2512

Herms J, Tings T, Gall S, Madlung A, Giese A, Siebert H, Schurmann P, Windl O, Brose N, Kretzschmar H. 1999. Evidence of presynaptic location and function of the prion protein. *J. Neurosci.* 19:8866-8875.

Hill AF, Desbruslais M, Joiner S, Sidle KCL, Gowland I, Collinge J, Doey LJ, Lantos P. 1997. The same prion strain causes vCJD, *Nature* 389:448-450

Hill AF, Butterworth RJ, Joiner S, Jackson G, Rossor MN, Thomas DJ, Frosh A, Trolley N, Bell JE, Spencer M, King A, Al-Sarraj S, Ironside JW, Lantos PL, Collinge J. 1999. Investigation of variant Creutzfeldt-Jakob disease and other human prion diseases with tonsil biopsy samples. *Lancet* 253:183-189

Hill AF, Butterworth RJ, Joiner S, Jackson G, Rossor MN, Thomas DJ, Frosh A, Trolley N, Bell JE, Spencer M, King A, Al-Sarraj S, Ironside JW, Lantos PL, Holada K, Vostal JG. 2000. Different levels of prion protein (PrPc) expression on hamster mouse and human blood cells. *Br. J.Haematol.* 110:472-480

Hilton DA, Fathers E, Edwards P, Ironside JW, Zajicek J. 1998. Prion immunoreactivity in appendix before clinical onset of variant Creutzfeldt-Jakob disease *Lancet* 352:703-704

Houston F, Foster JD, Chong A, Hunter N, Bostock CJ. 2000. Transmission of BSE by blood transfusion in sheep. *Lancet* 356:999-1000

Huang F-P, Farquhar CF, Mabbottt NA, Bruce ME, MacPherson GG. 2002. Migrating intestinal dendritic cells transport PrP^{Sc} from the gut. *J. Gen. Virol.* 83:267-271

Hunter GAD. 1979. The enigma of the scrapie agent: Biochemical approaches and the involvement of membranes and nucleic acids. In *Slow Transmissible Diseases of the Nervous System.* Vol. 1 pp 365-385. Edited by SB Prusiner, WJ Hadlow, New York. Academic Press.

Hunter N, Dann JC, Bennett AD, Somerville RA, McConnell I, Hope J. 1992. Are *Sinc* and the PrP gene congruent? Evidence from PrP gene analysis in *Sinc* congenic mice. *J. Gen. Virol.* 73:2751-2755

Hunter N, Moore L, Hosie BK, Dingwall WS, Greig A. 1997a. Association between natural scrapie and PrP genotype in a flock of Suffolk sheep in Scotland. *Vet. Record.* 140:59-63

Hunter N, Goldmann W, Foster JD, Cairns D, Smith G. 1997b. Natural scrapie and PrP genotype: case-control studies in British sheep. *Vet. Record* 141:137-140

Ierna M. 2001. An investigation of scrapie pathogenesis in neonatal mice with special reference to germinal centre maturation. PhD thesis, University of Edinburgh.

Ingrosso L, Pisani R, Pocchiari M. 1999. Transmission of the 263K scrapie strain by the dental route. *J. Gen. Virol.* 80:3043-3047

Ironside JW. 2000. Pathology of variant Creutzfeldt-Jacob disease. *Arch. Virol. (Suppl)* 16:143-151

Jeffrey M, Goodsir CM, Bruce M, McBride P, Scott JR, Halliday W. 1994. Correlative light and electron microscopy studies of PrP localisation in 87V scrapie. *Br. Res.* 656:329-343

Jeffrey M, Goodsir CM, Bruce ME, McBride PA Scott JR. 1997. *In vivo* toxicity of prion protein in murine scrapie: ultrastructural and immunogold studies. *Neuropathol. Appl. Neurobiol.* 23:93-101

Jeffrey M, McGovern G, Goodsir CM, Brown KL, Bruce ME. 2000. Sites of prion protein accumulation in scrapie-infected mouse spleen revealed by immune-electron microscopy. *J.Pathol.* 191:323-332

Jeffrey M, Ryder S, Martin S, Hawkins SAC, Terry L, Berthelin-Baker C, Bellworthy SJ. 2001a. Oral inoculation of sheep with the agent of Bovine Spongiform Encephalopathy (BSE). 1. Onset and distribution of disease-specific PrP accumulation in brain and viscera. *J. Comp. Path.* 124:280-289

Jeffrey M, Martin S, Gonzalez L, Ryder S, Bellworthy SJ, Jackman R. 2001b. Differential diagnosis of infections with the bovine spongiform encephalopathy (BSE) and scrapie agents in sheep. *J Comp. Path.* 125:271-284

Jessen KR and Mirsky R. 1999. Schwann cells and their precursors emerge as major regulators of nerve development. *TINS* 22:402-410

Jolois O, Farquhar C, Brown K, Ritchie D, Heinen E, Bruce M. 2001. Does spleen innervation influence TSE pathogenesis? Abstract of the Internat. Soc. Neuroimmunol. 6th Internat. Congress, Edinburgh 3-7 September.

Jolois O, Antoine N, Collin S, Heinen E. 1999. Analysis of contacts between nerve fibres and the lymphoid cells in the spleen and Peyer's patches. Abstract. 13th International Conference on Lymphoid Tissue in Immune Reactions. Geneva. Aug. 1-6.

Kascsak RJ, Rubenstein R, Merz PA, Carp RI, Wisniewski HM, Diringer H. 1985. Biochemical differences among scrapie-associated fibrils support the biological diversity of scrapie agents. *J. Gen.Virol.* 66:1715-1722

Kascsak RJ, Rubenstein R, Mertz PA, Tonna-Demasi M, Fersko C, Carp RI, Wisniewski HM, Diringer H. 1987. Mouse polyclonal and monoclonal antibody to scrapie-associated fibril protein. *J. Virol.* 61:3688-3693

Kauffman RS, Wolf JL, Finberg R, Trier JS, Fields BN. 1983. The σ1 protein determines the extent of spread of reovirus from the gastrointestinal tract of mice. *Virology* 124:403-411

Kimberlin RH and Walker CA. 1977. Characteristics of a short incubaion model of scrapie in the Golden hamster. *J. Gen.Virol.* 34:295-304

Kimberlin RH and Walker CA. 1979. Pathogenesis of mouse scrapie: Dynamics of agent replication in spleen, spinal cord and brain after infection by different routes. *J. Comp. Path.* 89:551-562

Kimberlin RH and Walker CA. 1980. Pathogenesis of mouse scrapie: Evidence for neural spread of infection to the CNS. *J.Gen.Virol.* 51:183-187

Kimberlin RH and Walker CA. 1982. Pathogenesis of mouse scrapie: Patterns of agent replication in different parts of the CNS following intraperitoneal infection. *J.R. Soc. Med.* 75:618-624

Kimberlin RH, Walker CA, Millson GC, Taylor DM, Robertson PA, Tomlinson AH, Dickinson AG. 1983a. Disinfection studies with two strains of mouse-passaged scrapie agent. Guidelines for Creutzfeldt-Jakob and related agents. *J. Neurol. Sci.* 59:355-369

Kimberlin RH, Field H, Walker CA. 1983b. Pathogenesis of mouse scrapie: Evidence for spread of infection from central to peripheral nervous system. *J. Gen.Virol.* 64:713-716

Kimberlin RH, Hall SM, Walker CA. 1983c. Pathogenesis of mouse scrapie: Evidence for direct neural spread of infection to the CNS after injection of sciatic nerve. *J. Neurol. Sci.* 61:315-325

Kimberlin RH and Walker CA. 1986. Pathogenesis of scrapie (strain 263K) in hamsters infected intracerebrally, intraperitoneally or intraocularly. *J. Gen.Virol.* 67:255-263

Kimberlin RH, Cole S, Walker CA. 1987. Pathogenesis of scrapie is faster when infection is intraspinal instead of intracerebral. *Microbial Pathogenesis* 2:405-415

Kimberlin RH and Walker CA. 1988. Pathogenesis of experimental scrapie, pp37-62. *In* G. Bock, and R. Marsh (Eds.) Novel infectious agents and the central nervous system (Ciba Foundation Symposium vol 135). Wiley, Chichester.

Kimberlin RH and Walker CA. 1989a. The role of the spleen in the neuroinvasion of scrapie in mice. *Virus Res.* 12:201-212

Kimberlin RH and Walker CA. 1989b. Pathogenesis of scrapie in mice after intragastric infection. *Virus. Res.* 12:213-220

Kirkwood JK, Wells GAH, Wilesmith JW, Cunningham AA, Jackson SI. 1990. Spongiform encephalopathy in an Arabian oryx (Oryx leucoryx) and a greater kudu (Tragelaphis strepsiceros). *Vet. Record* 127:418-420

Kitamoto T, Ogomori K, Tateishi J, Prusiner SB. 1987. Formic acid pretreatment enhances immunostaining of cerebral and systemic amyloids. *Lab.Invest.* 57:230-236

Kitamoto T, Muramoto T, Mohri S, Doh-Ura K, Tateishi J. 1991. Abnormal isoform of prion protein accumulates in follicular dendritic cells in mice with Creutzfeldt-Jakob Disease. *J. Virol.* 65:6292-295

Klamt R, Dal-Pizzol F, Conte da Frota ML, Walz R, Andrades ME, da Silva EG, Brentani RR, Izquierdo I, Fonseca Moreira JC. 2001. Imbalance of antioxidant defence in mice lacking cellular prion protein. *Free Radic. Biol. Med.* 30:1137-1144

Klein MA, Frigg R, Raeber AJ, Flechsig E, Raeber AJ, Lakinke U, Bluethmann H, Bootz F, Suter M, Zinkernagel RM, Aguzzi A. 1997. A crucial role for B cells in neuroinvasive scrapie. *Nature* 390:687-690

Klein MA, Kaeser PS, Schwarz P, Weyd H, Xenarios I, Zinkernagel RM, Carrol MC, Verbeek JS, Botto M, Walport MJ, Molina H, Kalinke U, Acha-Orbea H, Aguzzi A. 2001. Complement facilitates early prion pathogenesis. *Nat. Med.* 7:488-492

Kocisko DA, Come JH, Priola SA, Chesebro B, Raymond GJ, Lansbury PT, Caughey B. 1994. Cell-free formation of protease-resistant protein. *Nature* 370:471-474

Kretzschmar HA, Prusiner SB, Stowring LE, DeArmond SJ. 1986. Scrapie prion proteins are synthesised in neurones. *Am. J. Pathol.* 122:1-5

Krinke GJ and Dietrich FM. 1990. Transneuronal spread of intraperitoneally administered herpes simplex virus type 1 from the abdomen via the vagus nerve to the brains of mice. *J.Comp. Path.* 103:301-306

Kunzi V, Glatzel M, Nakano MY, Greber UF, Leuven F. Van, Aguzzi A. 2002. Unhampered prion neuroinvasion despite impaired fast axonal transport in transgenic mice overexpressing four-repeat tau. *J. Neurosci.* 22:4771-7477

Kuroda Y, Gibbs CJ, Jr, Amyx HL, Gajdusek DC. 1983. Creutzfeldt-Jakob disease in mice; Persistent viraemia and preferential replication of virus in low-density lymphocytes. *Infect. Immunol.* 41:154-161

Kuwahara C, Takeuchi AM, Nishimura T, Haraguchi K, Kubosaki A, Matsumoto Y, Saeki K, Matsumoto Y, Yokoyama T, Itohara S, Onodera T. 1999. Prions prevent neuronal cell-line death. *Nature* 400:225-226

Lasmézas CI, Cesbron JY, Deslys JP, Demaimay R, Adjou LT, Rioux R, Lemaire C, Locht C, Dormont D. 1996. Immune system-dependent and system independent replication of the scrapie agent. *J. Virol.* 70:1292-1295

Lasmézas CI, Deslys JP, Robain O, Jaegly A, Beringue V, Peyrin JM, Hauw J, Rossier J, Dormont D. 1997. Transmission of the BSE agent to mice in the absence of detectable abnormal prion protein. *Science* 275: 402-405

Latarjet R. 1979. Inactivation of the agents of scrapie, Creutzfeldt-Jakob disease and kuru by radiations. In *Slow Transmissible Diseases of the Nervous System.* Vol. 1 pp 387-407. Edited by SB Prusiner, WJ Hadlow, New York. Academic Press.

Lazarini F, Boussin F, Deslys JP, Tardy M, Dormont D. 1994. Astrocyte gene expression in experimental mouse scrapie. *J. Comp. Path.* 111:87-98

Lefrançois T, Fages C, Brugère-Picoux J, Tardy M. 1994. Astroglial activity in natural scrapie of sheep. *Microbial Pathogenesis* 17:283-289

Lemaire-Vieille C, Schulze T, Podevin-Dimster V, Follet B, Bailly Y, Blanquet-Grossard F, Decavel JP, Heinen E, Cesbron JY. 2000. Epithelial and endothelial expression of the green fluorescent protein reporter gene under the control of bovine prion protein (PrP) gene regulatory sequences in transgenic mice. *Proc. Natl. Acad. Sci. USA* 97:5422-5427

Liberski PP and Gajdusek CA. 1997. Kuru: forty years later, a historical note. *Br. Pathol.* 7:555-560

Ligios C, Jeffrey M, Ryder SJ, Bellworthy SJ, Simmons MM. 2002. Distinction of scrapie phenotypes in sheep by lesion profiling. *J. Comp. Pathol.* 127:45-57

Lipkin WI, Carbone KM, Wilson MC, Duchala CS, Narayan O, Oldstone MB. 1988. Neurotransmitter abnormalities in Borna disease. *Brain Res.* 475:366-370

Loewy AD. 1995. Pseudorabies virus: a transneuronal tracer for neuroanatomical studies. *In* Viral vectors, Gene therapy and Neuroscience applications, pp349-366. Edited by MG Knipe and AD Loewy: Academic Press Inc, San Diego, Calif.

Mabbottt NA, Brown KL, Manson J, Bruce ME. 1997. T-lymphocyte activation and the cellular form of the prion protein. *Immunol.* 92:161-165

Mabbott NA, Farquhar CF, Brown KL, Bruce ME. 1998. Involvement of the immune system in TSE pathogenesis. *Immunology Today* 19:201-203

Mabbottt NA, Williams A, Farquhar C, Pasparakis M, Kollias G, Bruce ME. 2000a. Tumour Necrosis Factor Alpha-Deficient, but not Interleukin-6-Deficient mice resist peripheral infection with scrapie. *J. Virol.* 74:3338-3344

Mabbottt NA, Mackay F, Minns F, Bruce ME. 2000b. Temporary inactivation of follicular dendritic cells delays neuroinvasion of scrapie. *Nature Medicine* 6:719-720

Mabbott NA, Bruce ME, Botto M, Walport MJ, Pepys MB. 2001. Temporary depletion of complement component C3 or genetic deficiency of C1q significantly delays onset of scrapie. *Nature Medicine* 7:485-487

Madden KS and Felten DL. 1995. Experimental basis for neural-immune interactions. *Physiol. Rev.* 75:77-106

Maignien T, Lasmézas CI, Beringue V, Dormont D, Deslys J-P. 1999. Pathogenesis of the oral route of infection of mice with scrapie an bovine spongiform encephalopathy agents. J. Gen. Virol. 80:3035-3042

Manson JC, McBride PA, Hope J. 1992. Expression of the PrP gene in the brain of *Sinc* congenic mice and its relationship to the development of scrapie. *Neurodegen.* 1:45-52

Manson JC, Clarke AR, Hooper ML, Aitchison L, McConnell I, Hope J. 1994a. 129/Ola mice carrying a null mutation in PrP that abolishes mRNA production are developmentally normal. *Mol. Neurobiol.* 8:121-127

Manson JC, Clarke AR, McBride PA, McConnell I, Hope J. 1994b. PrP gene dosage determines the timing but not the final intensity or distribution of lesions in scrapie pathology. *Neurodegeneration* 3:331-340

Manson J, Hope J, Clarke AR, Johnstone AR, Black CJ, MacLeod NK. 1995. PrP dosage and long term potentiation. *Neurodegeneration* 4:113-114

Manson JC, Jamieson E, Baybutt H, Tuzi NL, Barron R, McConnell I, Somerville R, Ironside J, Will R, Man-Sun S, Melton DW, Hope J, Bostock C. 1999. A single amino acid alteration (101L) introduced into murine PrP dramatically alters incubation time of transmissible spongiform encephalopathy. *EMBO J.* 18: 6855-6864

Manuelidis EE, Gorgacz EJ, Manuelidis LM. 1978. Viraemia in experimental Creutzfeldt-Jakob disease. *Science* 200:1069-1071

Manuelidis L, Sklaviadis T, Manuelidis EE. 1987. Evidence suggesting that PrP is not the infectious agent in Creutzfeldt-Jakob disease. *EMBO J.* 6:341-347

Manuelidis L. 1994. Dementias, neurodegeneration and viral mechanisms of disease from the perspective of human transmissible encephalopathies. *Ann. NY Acad. Sci.* 724:259-281

Manuelidis L, Zaitsev I, Koni P, ZY Lu, RA Flavell, Fritch W. 2000. Follicular dendritic cells and dissemination of Creutzfeldt-Jakob disease. *J. Virol.* 74:8614-8622

Marsh RF, Millar JM, Hanson RP. 1973. Transmissible mink encephalopathy: studies on the peripheral lymphocyte. *Infect. Immun.* 7:352-355

Marsh RF and Hanson RP. 1977. The Syrian hamster as a model for the study of slow virus disease caused by unconventional agents. *Fed. Proc.* 37:2076-2078

Marsh RF and Besson RA. 1993. Epidemiologic and experimental studies on transmissible mink encephalopathy. *Dev. Biol. Stand.* 80:111-118

McBride PA, Bruce ME, Fraser H. 1988. Immunostaining of scrapie cerebral amyloid plaques with antisera raised to scrapie-associated fibrils (SAF). *Neuropathol. Appl. Neurobiol.* 14:325-336

McBride PA, Eikelenboom P, Kraal G, Fraser H, Bruce ME. 1992. PrP protein is associated with follicular dendritic cells of spleens and lymph nodes in uninfected and scrapie-infected mice. *J. Pathol.* 168:413-418

McBride PA and Bruce ME. 1993. PrP protein is widely distributed in tissues from scrapie and normal mice, abstr. 2B07, p. 25. Association of Veterinary Teachers and Research Workers Annual Meeting 1993, Scarborough, U.K.

McBride PA, Wilson MI, Eikelenboom P, Tunstall A, Bruce ME. 1998. Heparan sulphate proteoglycan is associated with amyloid plaques and neuroanatomically targeted PrP pathology throughout the incubation period of scrapie-infected mice. *Exp. Neurol.* 149:447-454

McBride PA and Beekes M. 1999. Pathological PrP is abundant in sympathetic and sensory ganglia of hamsters fed with scrapie. *Neurosci. Lett.* 265:135-138

McBride PA, Schulz-Schaeffer WJ, Donaldson M, Bruce M, Diringer H, Kretzschmar H, Beekes M. 2001. Early spread of scrapie from the gastrointestinal tract to the central nervous system involves autonomic fibers of the splanchnic and vagus nerves. *J.Virol.* 75:9320-9327

McKinley MP, Bolton DC, Prusiner SB. 1983. A protease-resistant protein is a structural component of the scrapie prion. *Cell* 35:57-62

McLean IW and Nakane PK. 1974. Periodate-lysine-paraformaldehyde (PLP): A new fixative. *J. Histochem. Cytochem.* 22:1077-1083

Mertz PA, Somerville RA, Wisneiwski HM, Iqbal K. 1981. Abnormal fibrils from scrapie-infected brain. *Acta. Neuropathol.* 54:63-74

Milhavet O, McMahon HEM, Rachidi W, Nishida N, Katamine S, Mange A, Arlotto M, Casanova D, Riondel J, Favier A, Lehmann S. 2000. Prion infection impairs the cellular response to oxidative stress. *Proc. Natl. Acad. Sci.* 97:13937-13942

Miller JM, Jenny A, Taylor WD, Marsh RF, Rubenstein R, Race RE. 1993. Immunohistochemical detection or prion protein in sheep with scrapie. *J. Vet. Diag. Invest.* 5:309-316

Millson GC and Manning EJ. 1979. The effect of selected detergents on scrapie infectivity. In *Slow Transmissible Diseases of the Nervous System.* Vol. 1 pp 409-423. Edited by SB Prusiner, WJ Hadlow, New York. Academic Press.

Mims CA and White DO. 1984. Viral pathogens and immunology. Blackwell Scientific Publications.

Mirsky R and Jessen KR. 1999. The neurobiology of Schwann cells. *Brain Pathology* 9:293-311

Montrasio F, Frigg R, Glatzel M, Klein MA, Mackay F, Aguzzi A, Weissmann C. 2000. Impaired prion replication in spleens of mice lacking functional follicular dendritic cells. *Science* 288:1257-9.

Moore RC, Redhead NJ, Selfridge J, Hope J, Manson JC, Melton DW. 1995. Double replacement gene targeting for the production of a series of mouse strains with different prion protein gene alterations. *Biotechnology (NY)* 13:999-1004

Moore R, Hope J, McBride P, McConnell I, Selfridge J, Melton K, Manson J. 1998. Mice with gene targeted prion protein alterations show that *Prnp*, *Sinc* and *Prni* are congruent. *Nature Genetics* 18:118-125.

Moore RC, Lee IY, Silverman GL, Harrison PM, Strome R, Heinrich C, Karunaratne A, Pasternak SH, Chishti MA, Liang Y, Mastrangelo P, Wang K, Smit AFA, Katamine S, Carlson GA, Cohen FE, Prusiner SB, Melton DW, Tremblay P, Hood LE, Westaway D. 1999. Ataxia in prion protein (PrP)-deficient mice is associated with upregulation of the novel PrP-like protein dopppel. *J. Mol. Biol.* 292:797-817

Morel E, Fouquet S, Chateau D, Yvernault L, Frobert Y, Pincon-Raymond M, Chambaz J, Pillot T, Rousset M. 2003. The cellular prion protein PrPc is expressed in human enterocytes in cell-cell junctional domains. *J. Biol. Chem.* 10:1074-1080

Morfini G, Pigino G, Beffert U, Busciglio J, Brady ST. 2002. Fast axonal transport misregulation in Alzheimer's disease. *Neuromolecular Med.* 2:89-99

Morrison LA, Sidman RL, Fields BN. 1991. Direct spread of reovirus from the intestinal lumen to the central nervous system through vagal autonomic nerve fibers. *Proc. Natl. Acad. Sci. USA.* 88:3852-3856

Morrison LA and Fields BN. 1991. Parallel mechanisms in neuropathogenesis of enteric virus infections. *J. Virol.* 65:2767-2772

Moya KL, Hässig R, Créminon C, Laffont I, Di Giamberardino L. 2004. Enhanced detection and retrograde axonal transport of PrP^C in peripheral nerve. *J. Neurochem.* 88:155-160

Muramoto T, Kitamoto T, Tateishi J, Goto I. 1993. Accumulation of abnormal prion protein in mice infected with Creutzfeldt-Jakob disease via intraperitoneal route: a sequential study. *Am. J. Pathol.* 143:1470-1479

Nakamura F, Seki I, Kobayashi K, Tanaka M, Fukunaga S. 2002. Immunohistochemical detection of cellular prion protein (PrPc) in the rat central nervous system. *Animal Sci. J.* 73:553-556

Naruse S, Thinakaran G, Luo JJ, Kusiak JW, Tomita T, Iwatsubo T, Qian X, Ginty DD, Price DL, Borchelt DR, Wong PC, Sisodia SS. 1998. Effects of PS1 deficiency on membrane protein trafficking in neurons. *Neuron* 21:1213-1221

Neutra MR, Mantis NK, Kraehenbuhl J-P 2001. Collaboration of epithelial cells with organized mucosal lymphoid tissue. *Nature Immunol.* 2:1004-1009

Niewiadomska M, Kulczycki J, Wochnik-Dyjas D, Szpak GM, Rakowicz M, Lojkowska W, Niedzielska K, Inglot E, Wieclawska M, Glazowski C, Tarnowska-Dziduszko E. 2002. Impairment of the peripheral nervous system in Creutzfeldt-Jakob disease. *Arch. Neurol.* 59:1430-1436

Oesch B, Westaway D, Walchi M, McKinley MP, Kent SBH, Aebersold R, Barry RA, Teplow DB, Tempst DB, Hood LE, Prusiner SB, Weissmann C. 1985. A cellular gene encodes scrapie PrP 27-30 protein. *Cell* 40:735-746

Oesch B, Teplow DB, Stahl N, Serban D, Hood LE, Prusiner SB. 1990. Identification of cellular proteins binding to the scrapie prion protein. *Biochemistry* 29:5848-5855

O'Rourke KI, Huff TP, Leathers CW, Robinson MM, Gorham JR. 1994. SCID mouse spleen does not support scrapie replication. *J. Gen. Virol.* 75:11511-1514

Outram GW, Dickinson AG, Fraser H. 1973. Developmental maturation of susceptibility to scrapie in mice. *Nature* 241:536-537

Pálsson PA. 1979. Rida (scrapie) in Iceland and its epidemiology. In *Slow Transmissible Diseases of the Nervous System.* Vol. 1 pp 357- 366. Edited by SB Prusiner, WJ Hadlow, New York. Academic Press.

Pammer J, Cross HS, Frobert Y, Tschachler E, Oberhuber G. 2000. The pattern of prion-related protein expression in the gastrointestinal tract. *Vichows Arch.* 436:466-472

Pan K-M, Baldwin M, Nguyen J, Gasset M, Serban A, Groth K, Mehlhorn I, Huang Z, Fletterick RJ, Cohen FE. 1993. Conversion of a-helices into b-sheets features in the formation of the scrapie prion proteins. *Proc. Natl. Acad. Sci. USA* 90:10962-10966

Parchi P, Castellani R, Capellari S, Petersen RB, Chen SG, Young K, Farlow M, Trojanowski JQ, Sima A, Ghetti B, Gambetti P. 1995. Protease-resistant prion protein in sporadic Creutzfeldt Jakob disease (CJD): correlation with clinicopathological features and PrP genotype. *J. Neuropathol. Exp. Neurol.* 54:416

Pattison IH and Millson GC. 1961. Experimental transmission of scrapie to goats and sheep by the oral route. *J.Comp. Path.* 71:171-176

Pattison IH, Hoare MN, Jebbett JN, Watson WA. 1972. Spread of scrapie to sheep and goats by oral dosing with foetal membranes from scrapie-affected sheep. *Vet. Rec.* 90:465-468

Pattison IH, Hoare MN, Jebbett JN, Watson WA. 1974. Further observations on the production of scrapie in sheep by oral dosing with foetal membranes from scrapie-affected sheep. *Br. Vet. J.* 130:65-67

Pauly PC and Harris DA. 1998. Copper stimulates endocytosis of the prion protein. *J. Biol.Chem.* 273:33107-33110

Peeters B, Pol J, Geilkens A, Moormann R. 1993. Envelope glycoprotein gp50 of pseudorabies virus is essential for virus entry but is not required for viral spread in mice. *J. Virol.* 67:170-177

Peyrin JM, Lasmézas CI, Haik S, Tagliavini F, Salmona M, Williams A, Ritchie D, Deslys JP, Dormont D. 1999. Microglial cells respond to amyloidogenic PrP peptide by the production of inflammatory cytokines. *Neuroreport* 10:723-729

Prinz M, Heikenwalder M, Junt T, Schwarz P, Glatzel M, Heppner FL, Fu Y-X, Lipp M, Aguzzi A. 2003. Positioning of follicular dendritic cells within the spleen controls neuroinvasion. *Nature* 425:957-962

Prusiner SB, Groth DF, Cochran SP, Masiarz FR, McKinley MP, Martinez HM. 1980. Molecular properties, partial purification, and assay by incubation period measurements of the hamster scrapie agent. *Biochem.* 19:4881-91

Prusiner SB, Bolton DC, Groth DF, Bowman KA, Cochran SP, McKinley MP. 1982a. Further purification and characterization of scrapie prions. *Biochemistry* 21:6942-6950

Prusiner SB. 1982b. Novel proteinaceous infectious particles cause scrapie. *Science* 216:136-144

Prusiner SB, Bolton DC, Bowman K, Cochran SP, Groth D, McKinley MP. 1983a. Properties of a 30,000 mw protein-component of the scrapie prion. *Federation Proc.* 42:845-849

Prusiner SB, McKinley MP, Bowman KA, Bolton DC, Bendheim PE, Groth D, Glenner GG. 1983b. Scrapie prions aggregate to form amyloid-like birefringent rods. *Cell* 35:349-358

Prusiner SB, Groth DF, Bolton DC, Dent SB, Hood LE. 1984. Purification and structural studies of a major scrapie prion protein. *Cell* 38: 27-134

Prusiner SB, Cochran AP, Alpers MP. 1985. Transmission of scrapie in hamsters. *J. Infect. Dis.* 152:971-978

Prusiner A, Scott M, Foster D, Westaway D, DeArmond S. 1990. Transgenetic studies implicate interactions between homologous PrP isoforms in scrapie prion replication. *Cell* 63:673-686

Prusiner SB. 1991. Molecular biology of prion diseases. *Science* 252:1515-1522

Prusiner SB, Groth D, Serban A, Koehler R, Foster D, Torchia M, Burton D, Yang SL, DeArmond SJ. 1993. Ablation of the prion protein (PrP) gene in mice prevents scrapie and facilitates production of anti-PrP antibodies. *Proc. Natl. Acad. Sci. USA* 90:10608-10612

Prusiner SB and Scott MR. 1997. Genetics of prions. *Ann. Rev. Gen.* 31:139-175

Puchtler H, Sweat F, Levine M. 1962. On the binding of Congo red by amyloid. *J. Histochem. Cytochem.* 10:355-364

Race RE, Priola SA, Bessen RA, Ernst D, Dockter J, Rall GJ, Mucjke L, Chesebro B, Oldstone MB. 1995. Neurone-specific expression of a hamster prion protein minigene in transgenic mice induces susceptibility to hamster scrapie agent. *Neuron* 15:1183-1191

Race R, Oldstone M, Chesebro B. 2000. Entry versus blockade of brain infection following oral or intraperitoneal scrapie administration: Role of prion protein expression in peripheral nerves and spleen. *J.Virol.* 74:828-833

Raeber AJ, Race RE, Brandner S, Priola SA, Sailer A, Bessen RA, Mucke L, Manson J, Aguzzi A, Oldstone MBA, Weissmann C, Chesebro B. 1997. Astrocyte-specific expression of hamster prion protein (PrP) renders PrP knockout mice susceptible to hamster scrapie. *EMBO J.* 16:6057-6065

Reis e Sousa C, Sher A, Kaye P. 1999. The role of dendritic cells in the induction and regulation of immunity to microbial infection. *Curr. Opin. Immunol.* 11:392-399

Ritchie DL, Brown KL, Bruce ME. 1999. Visualisation of PrP protein and follicular dendritic cells in uninfected and scrapie infected spleen. *J. Cell. Pathol.* 1:3-10

Roberts GW, Lofthouse R, Brown R, Crow TJ, Prusiner SB. 1986. Prion protein immunoreactivity in human transmissible dementias. *N. Eng. J. Med.* 315:1231-5

Rodolfo K, Hassig R, Moya KL, Frobert Y, Grassi J, Giamberardino L, di. 1999. A novel cellular prion protein isoform present in rapid anterograde axonal transport. *Neuroreport* 10:3639-3644

Rowher RG, Brown PW, Gadjusek DC. 1979. The use of sedimentation to equilibrium as a step in the purification of the scapie agent. In *Slow Transmissible Diseases of the Nervous System.* Vol. 1 pp 465-477. SB Prusiner, WJ Hadlow, (Eds.) New York. Academic Press.

Rowher RG. 1984. Scrapie infectious agent is virus-like in size and susceptibility to inactivation. *Nature.* 308:658-662

Rohwer RG. 1991. The scrapie agent: 'a virus by any other name'. *Curr. Top. Microbiol. Immunol.* 172: 195-232

Rubenstein R, Mertz PA, Kascsak RJ, Scalici CL, Papini MC, Carp RO, Kimberlin RH. 1991. Scrapie-infected spleens: Analysis of infectivity, scrapie-associated fibrils, and protease-resistant proteins. *J. Infect. Dis.* 164:29-35

Rubin E and Purves D. 1980. Segmental organisation of sympathetic preganglionic neurones in the mammalian spinal cord. *J. Comp.Neurol.* 192: 163-174

Ryder SJ, Spencer YI, Bellerby PJ, March SA. 2001. Immunohistochemical detection of PrP in the medulla oblongata of sheep: the spectrum of staining in normal and scrapie-affected sheep. *Vet. Rec.* 148:7-13

Sakaguchi S, Katamine S, Nashida N, Moriuchi R, Shigematsu K, Sugimoto T, Nakatani A, Kataoka Y, Houtani T, Shirabe S, Okada H, Hasegawa S, Miyamoto T, Noda T. 1996. Loss of cerebellar Purkinje cells in aged mice homozygous for a disrupted PrP gene. *Nature* 380:528-531

Salès N, Rodolfo K, Hassig R, Di Giamberardino L, Traiffort E, Ruat M, Frétier P, Moya KL. 1998. Cellular prion protein localization in rodent and primate brain. *Eur. J. Neurosci.* 10:2464-2471

Salès N, Hassig R, Rodolfo K, Faucheux B, Di Giamberardino L, Moya KL. 2002. Developmental expression of the cellular prion protein in elongating axons. *Eur. J. Neurosci.* 15:1163-1177

Sanchez-Alavez M, Huitron-Resendiz S, Gallegos R, Gombart L, Carr J, Steffensen S, Chesebro B, Oldstone MB, Criado J, Henriksen SJ. 2000. Role of neuronal PrP in the sleep/wake cycle. (Abst.) *30th Ann. Meet. Soc. Neurosci.* New Orleans, USA. 4-9 Nov.

Schreuder BEC, van Keulen LJM, Vromas MEW, Langeveld JP, Smits MA. 1998. Tonsillar biopsy and PrP^{Sc} detection in the preclinical diagnosis of scrapie. *Vet. Rec.* 142:564-568

Schulz-Schaeffer WJ, Tschöke S, Kranefuss N, Dröse W, Hause-Reitner D, Giese A, Groschup MH, Kretzschmar HA. 2000a. The paraffin-embedded tissue blot detects PrP^{Sc} early in the incubation time in prion diseases. *Am. J. Pathol.* 156:51-56

Schulz-Schaeffer WJ, Fatzer R, Vandevelde M, Kretzschmar HA. 2000b. Detection of PrP^{Sc} in subclinical BSE with the paraffin-embedded tissue (PET) blot. *Arch. Virol. (Suppl)* 16:173-180

Scott M, Foster D, Mirenda C, Serban D, Coufal F, Walchli M, Torchia M, Groth D, Carlson G, DeArmond SJ, Westaway D, Prusiner SB. 1989. Transgenic mice expressing hamster prion protein produce species-species scrapie infectivity and amyloid plaques. *Cell* 59:849-857

Scott JR and Fraser H. 1989. Enucleation after intraocular scrapie injection delays the spread of infection. *Br. Res.* 504:301-305

Scott JR, Davies D, Fraser H. 1992. Scrapie in the central nervous system: neuroanatomical spread of infection and *Sinc* control of pathogenesis. *J.Gen.Virol.* 73:1637-1644

Sethi S, Lipford G, Wagner H, Kretzschmar H. 2002. Post exposure prophylaxis against prion disease with a stimulator of innate immunity. *Lancet* 360:229-30

Sicinski P, Rowinski J, Warchol JB, Jarzabek Z, Gut W, Szczygiel B, Bielecke K, Koch B. 1990. Poliovirus type 1 enters the human host through intestinal M cells. *Gastroenterology* 98:56-58

Sigurdson CJ, Williams ES, Miller MW, Spraker TR, O'Rourke KI, Hoover EA. 1999. Oral transmission and early lymphoid tropism of chronic wasting disease PrP^{res} in mule deer fawns (Odocoileus hemionus) *J. Gen. Virol.* 80:2757-2764

Šimák J, Holada K, D'Agnillo F, Janota J, Vostal JG. 2002. Cellular prion protein is expressed on endothelial cells and is released during apoptosis on membrane microparticles found in human plasma. *Transfusion* 42: 334-342

Shaked GM, Fridlander G, Meiner Z, Taraboulos A, Gabizon R. 1999. Protease-resistant and detergent-insoluble prion protein is not necessarily associated with prion infectivity. *J. Biolog. Chem.* 274:17981-86

Shmakov A, McLennan N, McBride P, Farquhar C, Bode J, Rennison K, Ghosh S. 2000. Cellular prion protein is expressed in the human enteric system. *Nat. Med.* 6:840-850

Somerville RA, Mertz PA, Carp RI. 1986 Partial copurification of scrapie-associated fibrils and scrapie infectivity. *Intervirology* 25:48-55

Somerville RA and Ritchie LA. 1989. Are scrapie-associated fibrils a pathological product of infection? In *Unconventional Virus Diseases of the Central Nervous System,* pp 521-535, LA Court, D. Dormont, P. Brown & DT Kingsbury, (Eds.) Fauntenay-aux-Roses: Commisariat à l'Énergie Atomique.

Somerville RA and Dunn AJ. 1996. The association between PrP and infectivity in scrapie and BSE-infected mouse brain. *Arch. Virol.* 141:275-289

Somerville RA, Chong A, Mulqueen O, Birkett CR, Wood SCER and Hope J. 1997. Biochemical typing of scrapie strains. *Nature* 386:564

Somerville RA, Birkett CR, Farquhar CF, Hunter N, Goldmann W, Dornan J, Grover D, Hennion RM, Percy C, Foster J, Jeffrey M. 1997b. Immunodetection of PrP^{Sc} in spleens of some scrapie-infected sheep but not BSE-infected cows. *J. Gen. Virol.* 78:2389-2396

Somerville RA. 1999. Host and transmissible spongiform encephalopathy agent strain control glycosylation of PrP. *J. Gen.Virol.* 80:1865-1872

Somerville RA, Oberthur RC, Havekost U, MacDonald F, Taylor DM, Dickinson AG. 2002. Characterisation of Thermodynamic diversity between TSE agent strains. *J Biol. Chem.* 277 (13): 11084-11089

Standish A, Enquist LW, Schwaber JS 1994. Innervation of the heart and its central medullary origin defined by viral tracing. *Science.* 263:232-234

Stein C, Hassan AH, Przewlocki R, Bramsch C, Peter K, Herz A. 1990. Opiods from immunocytes interact with receptors on sensory nerves to inhibit nociception in inflammation. *Proc. Natl. Acad. Sci. USA* 87:5935-5939

Strack AM, Sawyer WB, Marubio LM, Loewy AD. 1988. Spinal origin of sympathetic preganglionic neurones in the rat. *Br. Res.* 455:187-191

Straub RH, Westermann J, Schölmerich J, Falk W. 1998. Dialogue between the CNS and the immune system in lymphoid organs. *Immunology Today* 19:409-413

Taylor DM, McConnell I and Fernie K. 1996a. The effect of dry heat on the ME7 strain of mouse-passaged scrapie agent. *J. Gen.Virol.* 77:3161-3164

Taylor DM, McConnell I, Fraser H. 1996b. Scrapie infection can be established readily through skin scarification in immunocompetent but not immunodeficient mice. *J. Gen. Virol.* 77:1595-1599

Taylor DM. 1999. Bovine spongiform encephalopathy and human health. *Vet. Rec.* 125:413-415

Taylor DM, Fernie K, Steele PJ, McConnell I, Somerville RA. 2002. Thermostability of mouse-passaged BSE and scrapie is independent of host PrP genotype: Implications for the nature of the causal agents. *J. Gen.Virol.* 83:3199-32024

Telling GC, Scott M, Foster D, Yang S-L, Torchia M, Sidle KCL, Collinge J, DeArmond SJ, Prusiner SB. 1994. Transmission of Creutzfeldt-Jakob disease from humans to transgenic mice expressing chimeric human-mouse prion protein. *Proc. Natl. Acad. Sci. USA* 91:9936-9940

Telling GC, Scott M, Mastrianni J, Gabizon R, Torchia M, Cohen FE, DeArmond SJ, Prusiner SB. 1995. Prion propagation in mice expressing human and chimeric PrP transgenes implicates the interaction of cellular PrP with another protein. *Cell* 83:79-90

Terry LA, Marsh S, Ryder SJ, Hawkins SAC, Wells GAH, Spencer YI. 2003. Detection of disease-specific PrP in the distal ileum of cattle exposed orally to the agent of bovine spongiform encephalopathy. *Vet. Rec.* 152:387-392

Thomzig A, Kratzel C, Lenz G, Krüger D, Beekes M. 2003. Widespread PrP^{Sc} accumulation in muscles of hamsters orally infected with scrapie. *EMBO reports* 4:530-533

Tobler I Gaus SE, Deboer T, Achermann P, Fischer M, Rulicke T, Moser M, Oesch B, McBride PA, Manson JC. 1996. Altered circadian activity rhythms and sleep in mice devoid of prion protein. *Nature* 380:639-642

Tyler KL and Fields BN. 1990. *In* Virology, 2nd ed., BN Fields (Ed.) pp191-239 Pathogenesis of viral infections. Raven Press, New York

Vahine A, Nystrom B, Sandberg M, Hamberger A, Lyck E. 1978. Attachment of herpes simplex virus to neurones and glial cells. *J. Gen. Virol.* 40: 359-371

Van Keulen LJM, Schreuder BEC, Meloen RH, Poelen-van den Berg M, Mooij-Harkes G, Vromans MEW, Langeveld JPM. 1995. Immunohistochemical detection and localisation of prion protein in brain tissue of sheep with natural scrapie. *Vet. Pathol.* 32:299-308

Van Keulen LJM, Schreuder BEC, Meloen RH, Mooij-Harkes G, Vromans MEW, Langeveld JPM. 1996. Immunohistochemical detection of prion protein in lymphoid tissues of sheep with natural scrapie. *J. Clin. Microbiol.* 34:1228-1231

Van Keulen LJM, Schreuder BEC, Vromans MEW, Langeveld JPM, Smits MA. 1999. Scrapie-associated prion protein in the gastro-intestinal tract of sheep with natural scrapie. *J. Comp. Path.* 121:55-63

Van Keulen LJM, Schreuder BEC, Vromans MEW, Langeveld JPM, Smits MA. 2000. Pathogenesis of natural scrapie in sheep. *Arch. Virol.* 16:57-71

Van Rooijen N. 1980. Immune complex trapping in lymphoid follicles: a discussion on possible functional implication, pp 281-290. *In*: Manning MJ, (Ed.) Phylogeny of Immunological Memory. Amsterdam: Elsevier

Vey M, Pilkuhn S, Wille H, Nixon R, DeArmond SJ, Smart EJ, Anderson RWG, Taraboulos A, Prusiner SB. 1996. Subcellular colocalization of the cellular and scrapie prion proteins in caveolae-like membranous domains. *Proc, Natl. Acad, Sci. USA*, 93:14945-14949

Weiss DG. 1982. General properties of axoplasmic transport, pp 1-14. *In* D.G. Weiss & A. Gorio (Eds.) Axoplasmic Transport in Physiology and Pathology. Berlin, Springer-Verlag

Weissmann C. 1991. A 'unified theory' of prion propagation. *Nature* 352: 679-683

Wells GAH, Scott AC, Johnson CT, Gunning RF, Hancock RD, Jeffrey M, Dawson M, Bradley R. 1987. A novel progressive encephalopathy in cattle. *Vet. Rec.* 121:419-420

Wells GAH, Dawson M, Hawkins SAC, Green RB, Francis ME, Simmons MM, Austin AR, Horigan MW. 1994. Infectivity in the ileum of cattle challenged orally with bovine spongiform encephalopathy, *Vet. Rec.* 135:40 – 41

Wells GAH and Wilesmith JW. 1995. The neuropathology and epidemiology of Bovine Spongiform Encephalopathy. *Br. Pathol.* 5:91-103

Wells GAH, Dawson M, Hawkins SAC, Austin AR, Green RB, Dexter I, Horigan MW, Simmons MM. 1996. Preliminary observations on the pathogenesis of experimental bovine spongiform encephalopathy (BSE), pp28. *In*: Gibbs C.J. Jnr (ed.), Bovine Spongiform Encephalopathy; The BSE Dilemma, Serono Symposia USA, Norwell. Massachusetts. Springer-Verlag, New York.

Wells GAH, Hawkins SAC, Green RB, Austin AR, Dexter I, Spencer YI, Chaplin MJ, Stack MJ, Dawson M. 1998. Preliminary observations on the pathogenesis of experimental bovine spongiform encephalopathy (BSE): An update. *Vet. Rec.* 142:103-6

Wells GAH, Hawkins SAC, Austin AR, Ryder SJ, Done SH, Green RB, Dexter I, Dawson M, Kimberlin RH. 2003. Studies of the transmissibility of the agent of bovine spongiform encephalopathy to pigs. *J. Gen.Virol.* 84:1021-1031

Westaway DA and Prusiner SB. 1986. Conservation of the gene encoding the scrapie prion protein. *Nuc. Acids Res.* 14:2035-2044

Westaway D, Goodman PA, Miranda CA, McKinley MP, Carlson GA, Prusiner SB. 1987. Distinct prion strains in short and long incubation period mice. *Cell.* 51:651-662

Whealy ME, Card JP, Robbins AK, Bubin JR, Rziha H-J, Enquist LW. 1993. Specific pseudorabies virus infection of the rat visual system requires both gI and gp63 glycoproteins. *J. Virol.* 67:3786-3797

Wilesmith JW, Ryan JBM, Atkinson JM. 1991. Bovine spongiform encephalopathy: epidemiological studies on the origin. *Vet. Rec.* 129:199-203

Wilesmith JW, Ryan JBM, Hueston WD, Hoinville LJ. 1992. Bovine spongiform encephalopathy: epidemiological features 1985-1990. *Vet. Rec.* 130:90-94

Wiley CA, Burrola PG, Buchmeier MJ, Wooddell MK, Barry RA, Prusiner SB, Lampert PJ. 1987. Immuno-gold localization of prion filaments in scrapie-infected hamster brains. *Lab. Invest.* 57:646-656

Will RG, Knight RSG, Zeidler M, Stewart G, Ironside JW, Cousens SN, Smith PG. 1996. Reporting of suspect new variant Creutzfeldt-Jakob disease. *Lancet* 349:874

Wille H, Prusiner SB, Cohen FE. 2000. Scrapie infectivity is independent of amyloid staining properties of the N-terminally truncated prion protein. *J.Struct. Biol.* 130:323-338

Williams A, VanDam AM, Ritchie D, Eikelenboom P, Fraser H. 1997a. Immunocytochemical appearance of cytokines, prostaglandin E-2 and lipocortin-1 in the CNS during the incubation period of murine scrapie correlates with progressive PrP accumulations. *Br. Res.* 754:171-180

Williams A, Lucassen PJ, Ritchie D, Bruce M. 1997b. PrP deposition, microglial activation and neuronal apoptosis in murine scrapie. *Exp. Neurol.* 144:433-438

Williams ES and Young S. 1980. Chronic wasting disease of captive mule deer: spongiform encephalopathy. *J Wildlife Dis.*16:89-98

Williams ES and Millar MW. 2002. Chronic wasting disease in deer and elk in North America. *Revue Sci.Tech. OIE* 21:305-316

Wolf JL, Rubin D, Finberg R, Kauffman RS, Sharpe AH, Trier JS, Fields BN. 1981. Intestinal M cells: A pathway for entry of reovirus into the host. *Science* 212:471-472

Wong B-S, Liu T, Li R-L, Pan T, Petersen RB, Smith MA, Gambetti P, Perry G, Manson JC, Brown DR, Sy M-S. 2001. Increased levels of oxidative stress markers detected in the brains of mice devoid of prion protein. *J. Neurochem.* 76: 565-572

Wopfner F, Weidenhofer G, Schneider R, Brunn A von, Gilch S, Schwarz TF, Werner T, Schatzl M. 1999. Analysis of 27 mammalian and 9 avian PrPs reveals high conservation of flexible regions of the prion protein. *J. Mol.Biol.* 289:1163-1178

Wyss-Coray T, Loike JD, Brionne TC, Lu E, Anankov R, Yan F, Silverstein SC, Husemann J. 2003. Adult mouse astrocytes degrade amyloid-beta in vitro and in situ. *Nat. Med.* 4:453-457

Ye X, Scallet AC, Kascsak RJ, Carp RI. 1998. Astrocytosis and amyloid deposition in scrapie-infected hamsters. *Br. Res.* 809: 277-287

Zlotnik I and Rennie JC. 1962. The pathology of the brain of mice inoculated with tissue from scrapie sheep. *J. Comp. Path.* 72: 360-365

Appendix 1: Dissection protocols

1.1 - Dissection of spinal cord and DRG removal

1. Remove skin, open torso and remove heart, lungs and abdominal viscera.
2. Remove overlying chest muscles to expose ribs.
3. Excise the entire spinal column by cutting up either side. Leave the proximal stumps of the ribs attached to aid subsequent identification of cervical and thoracic regions. (Thoracic cord segment one lies adjacent to first rib).
4. Using the dissecting microscope, lay spinal column dorsal side up with cervical portion to the north. Anchor the cervical portion with tape or pins and starting from sacral end, remove top layer of bone to expose cord.
5. Once bone has been removed cut as close as possible with bone cutters around DRGs then pull nerves through to cord side.
6. Work systematically up the cord removing DRGs from each side before going on to the next segment.

1.2 - Dissection of cervical vagus nerve and nodose ganglion

1. Lie hamster face downwards on a dissecting board. Snip hair from head, neck and snout. Snip down mid back then peel back skin almost down to tail
2. Turn hamster over. Cut away exterior tissue from neck and remove arms from shoulder by cutting through the tendons holding joints in place. There should be no necessity to cut through bones. Snip off any protruding ribcage.
3. Remove legs to prevent the tendency of the torso to roll out of position.
4. Lie torso on its back with the head on left of the working area. Roll up a piece of tissue and use this to prop up the animal so that the torso lies on its side with neck facing upwards. Remove exterior fat and salivary glands and any other connective tissue to expose muscle. All muscle groups around neck area should be intact. Remove ear socket. The ear cavity remains exposed.
5. Gently remove the first muscle encountered – the sternocleidomastoid (most southerly of group) by delicately paring away with scalpel (No 11). The accessory nerve can now be seen running in an east-west direction embedded in the underlying levator scapulae muscle. Carefully cut the distal end of this nerve and retain it by folding it back on top of muscle. Snip off rest of same muscle below.
6. Remove next muscle, the scalenus medius – lies above the first one in an east/west direction. Then remove the smaller digastric muscle lying under and higher up (small muscle). Vagus is under this lying next to the large carotid artery that travels in a

north/south direction. Remove the tiny hyoid muscle at northern end of this and take away excess tissue down to bone.

7. Remove carotid by stripping it away from nerve. Approximately 1cm of vagus nerve can now be removed.

To remove nodose ganglion:

8. Ganglion lies surrounded by bone at ear socket. Carefully cut away at bone at position where the trio of nerves (vagus, accessory and laryngeal) entering nodose converge. This takes some time and you must ensure that the nerves are held together and away from bone cutters
9. Gently pull out the ganglion attached to a section of vagus nerve. This will emerge with some bone attached. Leave the stumps of the other two nerves attached as to remove them would damage the ganglion.
10. Lay the excised tissue on a glass slide. With the aid of a dissecting microscope, tease away bone pieces.
11. Attach to a small piece of card to maintain shape and protect against damage if histology is required.

1.3 - Removal of coeliac-mesenteric ganglion complex (CMGC)

1. Remove skin from abdomen. Remove entire liver carefully without destroying surrounding structures – particularly oesophagus and aorta. Cut connections liver has with surrounding tissue. Remove lower ribs and skin.
2. Lie torso on right side with the head pointing towards the right of the working area. Push aside the lungs. The aorta can be observed running down inside the chest cavity. Remove diaphragm and follow aorta down to left kidney.
3. Push the exposed intestines towards the back for easier access to region around kidneys. Remove any superficial fat. Three vessels (4 ,5, 6 in diagram) can be seen running from the kidneys to mesentery and aorta in a north/south direction.
4. Two blood vessels (1, 2) connecting the mesentery to the aorta should now be apparent. Free these gently from the associated connective tissue with scalpel but do not cut.
5. Take a hold of aorta (3) at right hand side and free it from surrounding tissue. Cut it at right but keep a hold of this end. All further dissections lie to the left of this cut.
6. Still holding onto aorta, cut from underneath to release aorta from deeper mesenteric connections and follow aorta caudally to beyond the kidney. Vessels 4, 5 & 6 are still attached.
7. Free vessels 4, 5 & 6 from each other and surrounding connections. Cut these at southern end (close to kidney) and then cut vessels 1 & 2 (northern end) and left side of aorta.

CMGC lies attached to and spanning this structure of supporting vessels.

8. Maintaining its shape, attach the entire complex (CMGC + BVs) to a small piece of card to for protection during fixation and processing

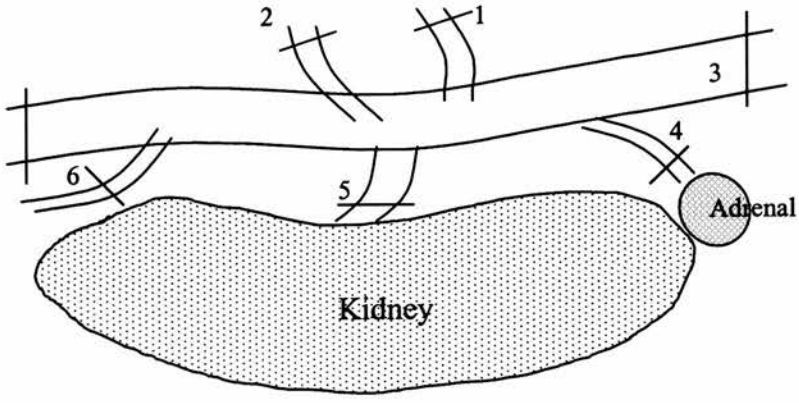

1: Coeliac artery

2: Superior mesenteric artery

3: Abdominal aorta

4: Suprarenal artery

5: Renal artery

6: Ovarian/testicular artery

____ Sites where vessels are cut

Appendix 2: Immunocytochemistry methods and reagents

2.1 Indirect, PAP and ABC methods for immunolabelling hamster PrP.

Indirect Method

1. Take sections to water i.e Remove paraffin wax by immersion in xylene, graded alcolohols (IMS 99) and water – 5 mins.
2. Immerse in 98 % Formic Acid 10 mins.
3. Wash in water.
4. 1% H_2O_2 in methanol 10 mins
5. Wash in water then 5 mins in PBS/BSA
6. Block in normal donkey serum (1/20 dilution) - 15 mins.
7. Tap off serum and apply primary antibody i.e.1B3 rabbit anti-mouse polyclonal at 1/400 for one hour at room temp. Apply normal rabbit serum (1/1000) to adjacent sections and known positive control.
8. Wash 3x5mins in PBS/BSA buffer (see below)
9. Incubate in peroxidase conjugated donkey anti-rabbit 1/100 for 1hour.
10. Wash PBS/BSA 3x5 mins.
11. Incubate in DAB (see below) for 5-10 mins.
12. Counterstain with haematoxylin 30 secs – 1min. Blue nuclei in Scott's tap water.
13. Dehydrate in alcohol, clear in xylene and mount in DPX.

PAP Method

Follow directions of Indirect Method to 7.

8. Wash 3x5mins in PBS/BSA buffer (see below)
9. Incubate in donkey anti-rabbit 1/40 for 1hour
10. Wash PBS/BSA 3x5 mins.
11. Apply rabbit PAP 1/100 for 1 hour
12. Wash PBS/BSA 3x5 mins.
13. Incubate in DAB (see below) for 5-10 mins.
14. Counterstain with haematoxylin 30 secs – 1min. Blue nuclei in Scott's tap water.

15 Dehydrate in alcohol, clear in xylene and mount in DPX.

ABC Method

Follow directions of Indirect Method to 5.

6. Block in normal rabbit serum (1/20 dilution) - 15 mins.

7. Tap off serum and apply primary antibody i.e.3F4 mouse anti-hamster monoclonal, 1/400 for one hour at room temp. Apply normal mouse serum (1/1200) to adjacent sections and known positive control.
8. Wash 3x5mins in PBS/BSA buffer (see below).
9. Incubate in rabbit anti-mouse biotinylated (Jacksons)1/200 for 1hour.

NB: At this point make up Avidin- Biotin-Complex (ABC) –10µl A + 10µl B to PBS/BSA 1ml buffer. This must be prepared at least 30mins before use.

10. Wash PBS/BSA 3x5 mins.
11. Incubate in ABC for 30 mins.
12. 3x5min washes in PBS/BSA DAB for 5-10mins.
13. Counterstain with haematoxylin 30 secs – 1min. Blue in Scott's tap water
14. Dehydrate in alcohol, clear in xylene and mount in DPX.

2.2 Immunolabelling Reagents

PBS/BSA wash buffer

Dissolve 5g BSA (bovine serum albumin) in 250mls stock PBS (10x PBS)
Top up to 2500ml with distilled water.

10x PBS

400g Sodium Chloride
10g Potassium Chloride
57.5g DiSodium Hydogen Orthophosphate
10g Potassium DiHydrogen Orthophosphate
5 litres of deionised water

1% PBS/BSA –antibody diluent

1g BSA in 100ml PBS

Methanol/H_2O_2

232 ml methanol + 8mls H_2O_2

DAB chomagen

1g 3,4,3,4, Tetra amino biphenyl hydrochloride
40 ml de-ionised water

Scott's Tap Water

8.75g Sodium Hydrogen Carbonate
50g Magnesium Sulphate
2500 tap water

Paraformaldehyde-Lysine-Periodate (PLP) fixative

Stock solutions

Phosphate buffer (0.05M) pH 74.
7.10g Disodium hydrogen orthophosphate anhydrous **(soln. A)**
500 ml de-ionised water
7.80 Sodium dihydrogen orthophosphate dihydrate **(soln. B)**
500 ml de-ionised water

To make up 400mls of phosphate buffer (0.05M)
Add **324mls** of **soln. A** to **76 mls** of **soln. B** and adjust to pH 7.4 using soln A to increase the pH or soln B to decrease the pH. Use this to make the **Working Solution (WS)** for PLP.

40% Sodium hydroxide (w/v) (NaOH)
40g Sodium Hydroxide
100ml Deionised water

8% Paraformaldehyde
40g parformaldehyde
500ml Deionised water
Add 40g of Paraformaldehyde to 500mls of deionised water, heat to 60-65°C in the fumecupboard, add approximately 1 ml of 40% NaOH dropwise until the precipitate clears. Allow the solution to cool before labelling the bottle with the pre-printed label and store for up to 2 months in the fridge at 2-8°C.

- **Preparation of Working Solution (WS) for PLP**

Column A	Column B	Column C
Working Solution (WS) (ml)	0.05M Phosphate buffer (ml)	8% paraformaldehyde (ml)
50	37.5	12.5
100	75	25
200	150	50
300	225	75
350	262.5	87.5
400	300	100
500	375	125
750	562.5	187.5
1000	750	250

To make the above amounts of Working Solution (column A) measure the appropriate amounts of columns B and C, mix thoroughly and store in the fridge at 2-8°C. Label container with the pre-printed label and store for up to 2 weeks in the fridge at 2-8°C. Discard after two weeks if unused.

- **Final Preparation of PLP fixative:** This solution must be used within 10-12 hours.

(50 mls is sufficient for the fixation of 5 tissues in individual polypots.)

Working Solution (WS)(ml)	Sodium m-periodate (0.1M)	D L-Lysine monohydrochloride (0.075M)
50ml	0.108g	0.69g
100ml	0.216g	1.37g
200ml	0.432g	2.74g
300ml	0.648g	4.11g
350ml	0.756g	4.80g
400ml	0.864g	5.48g
500ml	1.080g	6.85g
750ml	1.620g	10.28g
1000ml	2.16g	13.70g

To the appropriate amount of working solution add the appropriate amounts of sodium m-periodate and DL-Lysine then mix well.

Appendix 3: References

Beekes M, McBride PA, Baldauf E. 1998. Cerebral targeting indicates vagal spread of infection in hamsters fed with scrapie. *J. Gen. Virol.* 79:601-607

McBride PA and Beekes M. 1999. Pathological PrP is abundant in sympathetic and sensory ganglia of hamsters fed with scrapie. *Neurosci. Lett.* 265:135-138

Beekes M and McBride PA. 2000. Early accumulation of pathological PrP in the enteric nervous system and gut-associated lymphoid tissue of hamsters orally infected with scrapie. *Neurosci. Lett.* 278:181-184

Wilson MI, McBride PA. 2000. Technical aspects of tracking scrapie infection in orally dosed rodents. *J. Cell Pathol.* 5:17-22

McBride PA, Schulz-Schaeffer WJ, Donaldson M, Bruce M, Diringer H, Kretzschmar H, Beekes M. 2001. Early spread of scrapie from the gastrointestinal tract to the central nervous system involves autonomic fibers of the splanchnic and vagus nerves. *J.Virol.* 75:9320-9327

Journal of General Virology (1998), **79**, 601–607. Printed in Great Britain

Cerebral targeting indicates vagal spread of infection in hamsters fed with scrapie

Michael Beekes,[1] Patricia A. McBride[2] and Elizabeth Baldauf[1]

[1] Robert Koch-Institut, Bundesinstitut für Infektionskrankheiten und nicht übertragbare Krankheiten, FG 123, Nordufer 20, 13353 Berlin, Germany

[2] Institute for Animal Health, BBSRC/MRC Neuropathogenesis Unit, Ogston Building, West Mains Road, Edinburgh EH9 3JF, UK

The pathogenesis of scrapie and other transmissible spongiform encephalopathies (TSEs) following oral uptake of agent is still poorly understood and can best be studied in mice and hamsters. The experiments described here further extend the understanding of the pathways along which infection spreads from the periphery to the brain after an oral challenge with scrapie. Using TSE-specific amyloid protein (TSE-AP, also called PrP) as a marker for infectivity, immunohistochemical evidence suggested that the first target area in the brain of hamsters orally infected with scrapie is the dorsal motor nucleus of the vagus nerve (DMNV), rapidly followed by the commissural solitary tract nucleus (SN). The cervical spinal cord was affected only after TSE-AP had been deposited in the DMNV, SN and other medullary target areas. For the first time, these results demonstrate conclusively that, in our animal model, initial infection of the brain after oral ingestion of scrapie agent occurs via the vagus nerve, rather than by spread along the spinal cord.

Introduction

Following the BSE epidemic in Great Britain and the recent emergence of a new CJD variant, transmissible spongiform encephalopathies (TSEs) are a matter of great public concern. The oral route of infection is the epidemiologically most relevant pathway for natural transmission of scrapie and related diseases within and between different species (Diringer *et al.*, 1994). However, little is known about the pathogenesis of TSEs following uptake of infectious agent via the gastrointestinal tract. Previous approaches addressing the dynamics of scrapie pathogenesis by tracing the spread of agent after a parenteral or intragastric challenge in small rodents revealed that infection enters the CNS at the thoracic spinal cord and then spreads rostrally to the brain (Kimberlin & Walker, 1979, 1982, 1986, 1989). However, preliminary observations by Kimberlin & Walker (1982), Muramoto *et al.* (1993) and van Keulen *et al.* (1995) also indicate an alternative spreading pathway, possibly along the vagus nerve. While the existence of an access to the brain bypassing the spinal cord was corroborated recently (Baldauf *et al.*, 1997), the precise anatomical identity of the bypass remained the subject of speculation. Due to the close association between infectivity and TSE-specific amyloid protein (TSE-AP, also called PrP; McKinley *et al.*, 1983) established in our animal model (Beekes *et al.*, 1996; Baldauf *et al.*, 1997), spread of infection in hamsters can be investigated by tracing the deposition of TSE-AP. In the study described here, we used immunohistochemistry to identify the presence and anatomical location of TSE-AP as an indicator for the spread of infection to and within the brain of hamsters orally challenged with scrapie. This approach allowed an exact localization of the initial cerebral target areas and provided strong evidence for the vagus nerve as the primary pathway to the brain in our model animals.

Author for correspondence: Michael Beekes.
Fax +49 30 4547 2609. e-mail BeekesM@rki.de

Methods

■ Oral infection of outbred Syrian Golden hamsters with scrapie (strain 263K) was performed as described previously (Baldauf *et al.*, 1997). Four animals were sacrificed at 84, 91, 98, 105, 113, 119, 126 and 133 days post-infection (p.i.), and also at 156 days p.i. (terminal stage of disease). Four uninfected controls were sacrificed after having reached an age of between 180 and 210 days. Brain and vertebral column were removed. Two of the brains from each group were dissected mid-sagitally, the two others were dissected coronally into five segments. The spinal column

0001-5204

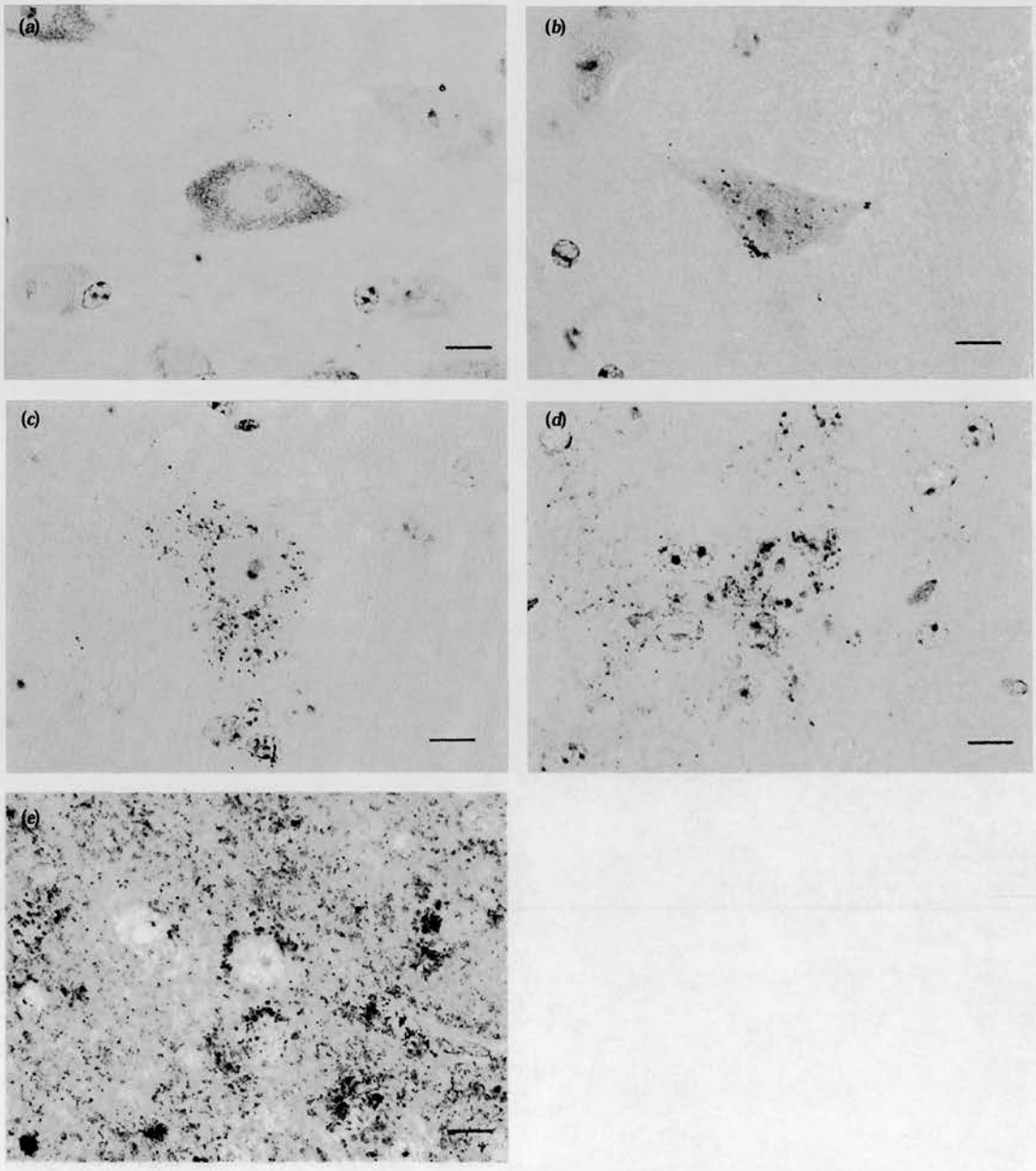

Fig. 1. Immunohistochemical appearance of TSE-AP in the CNS. (*a*) Unaffected control. Cellular precursor protein (homogeneous brown staining) within neurons. Some neurons remain unstained. (*b*) Early stage of infection. Punctuate deposits of abnormal protein appear within and on cell surface of individual cells. (*c*) Inclusions progressively increase in number and staining intensity. (*d*) As incubation period advances, heavier deposits accumulate around cells and appear scattered in the neuropil. (*e*) Terminal stage of disease. TSE-AP deposition is consolidated within the neuropil. Bar, 10 μm.

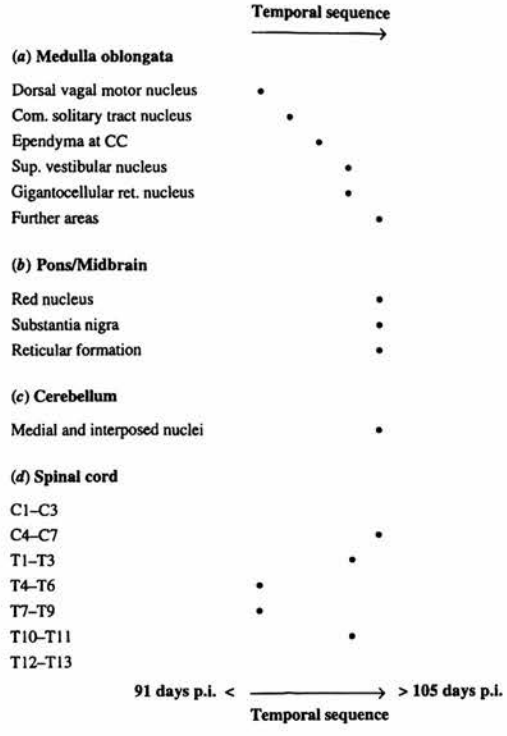

Fig. 2. Early target areas in the CNS found to be affected between 91 and 105 days p.i. Dots indicate the temporal sequence of TSE-AP deposition. Spinal cord segments C1–C3 and T12–T13 showed no immunostaining for the pathological protein until 105 days p.i. (*a*) 'Further areas' in the medulla oblongata: IO and DAO, PRN, LPGN, SpVN and MVN. (*b*) 'Reticular formation': RaN and PoN.

was dissected transversally into segments corresponding to vertebrae C1–C3, C4–C7, T1–T3, T4–T6, T7–T9, T10–T11 and T12–T13 and the spinal cord was removed. Tissue samples were fixed in paraformaldehyde–lysine–periodate (2% paraformaldehyde in final concentration), dehydrated over 6 h and embedded in paraffin wax. Serial and/or semi-serial sections were cut at 6 μm. Immunostaining was carried out according to the peroxidase antiperoxidase (PAP) and/or ABC method using MAb 3F4 (Kascsak *et al.*, 1987) to label TSE-AP and its normal precursor and diaminobenzidine (DAB) to visualize the reaction product. Prior to immunostaining, sections were pretreated with formic acid (98%) for 10 min to enhance staining. Adjacent sections were stained with cresyl violet (0·1%) and haematoxylin and eosin to facilitate neuroanatomical identification.

Results

TSE-AP presented as granular accumulations of immunoreactive material within or around neurons. These infection-specific deposits could be clearly distinguished from the normal precursor protein and were absent in uninfected control animals (Fig. 1).

As in previous studies (Beekes *et al.*, 1996; Baldauf *et al.*, 1997), formation of TSE-AP in the CNS was first seen at 91 days p.i., but onset varied between individuals. However, the sequence of areas targeted in the brain and spinal cord was remarkably consistent (Figs 2 and 3 *a–f, g–l*).

The first area showing deposition of TSE-AP in the brain was the dorsal motor nucleus of the vagus nerve (DMNV; Fig. 4 *a*), followed by the commissural solitary tract nucleus (SN) and ependymal linings of the adjacent central canal (CC; Fig. 4 *b*). Positive immunostaining extended caudally to the area postrema (AP) although the AP was itself negative. Shortly after detection in the DMNV and SN (Fig. 4 *c*), TSE-AP appeared in the superior vestibular nucleus (SVN) and in the gigantocellular nucleus (GN) of the reticular formation.

Subsequently, TSE-AP was seen in other nuclei of the medulla [spinal and medial vestibular nuclei (SpVN, MVN), parvocellular reticular nucleus (PRN), inferior and dorsal accessory olives (IO, DAO), lateral paragigantocellular nucleus (LPGN); Fig. 4 *d*], in the pons and midbrain [red nucleus (RN), substantia nigra, raphe and pontine nuclei of the reticular formation (RaN, PoN)] and in the cerebellum [medial and interposed nuclei (MCN, ICN); Fig. 4 *e*]. The rapid spread of infection did not allow the identification of a clear temporal sequence in these later target areas. The trend of further spread was in a caudal to rostral direction. At 113 days p.i., TSE-AP could be detected for the first time in the ventromedial thalamic nucleus (VmTN) and by 119 days p.i. it was seen in the medial geniculate nucleus (MGN) and throughout the thalamus (Fig. 4 *f*) and hypothalamus. At this time TSE-AP also appeared in the parietal, cingulate (CCo) and frontal cortex (FCo). At 133 days p.i. deposition of TSE-AP had spread considerably within individual areas. By 156 days p.i., when the disease reached its clinical stage, the pathological protein was widespread throughout all brain areas except the olfactory lobes.

In the spinal cord, the first deposition of TSE-AP appeared in and around the neuronal cell bodies of the grey matter between vertebrae T4–T9. Timing of appearance coincided with that in the brain: the first deposition was seen at 91 days p.i. in the same cases and with corresponding relative amounts as had been identified in the brain. Subsequent spread within the spinal cord (Fig. 2) occurred in a rostral and caudal direction as reported previously (Kimberlin & Walker, 1979, 1982, 1986, 1989; Beekes *et al.*, 1996; Baldauf *et al.*, 1997). However, TSE-AP was found in the cervical spinal cord (C1–C3) only after it had been identified in a number of target areas in the medulla.

Discussion

These findings suggest that the onset of infection in the medulla oblongata is not accounted for by rostral spread along the grey matter of the spinal cord. Early infection of the DMNV and SN via white matter tracts also appears to be unlikely as no tracts directly link the thoracic spinal cord with

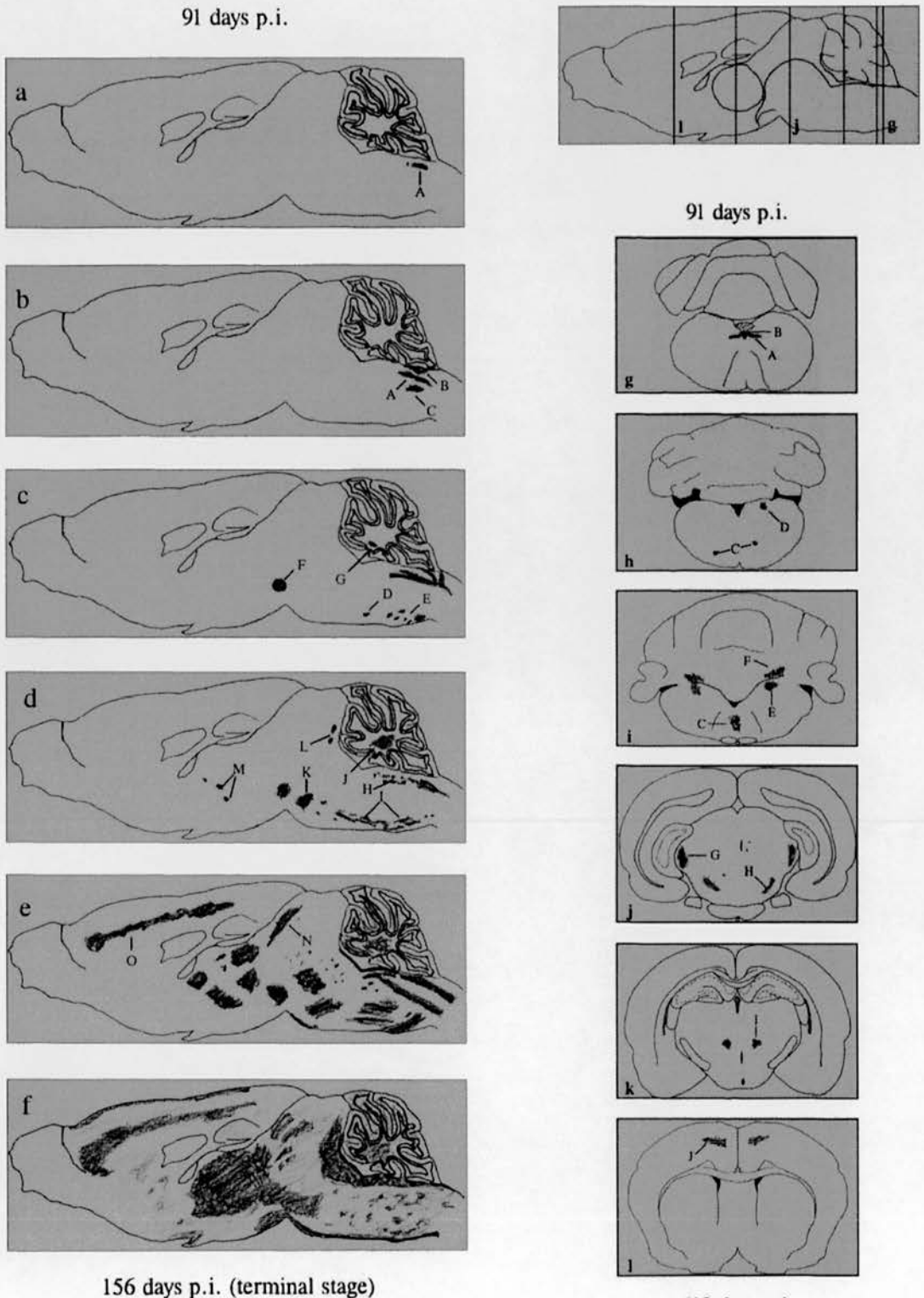

Fig. 3. For legend see facing page.

these medullary nuclei. Thus, the initial appearance of TSE-AP in the DMNV and SN strongly indicates that infection enters the brain via anatomical projections outside the CNS. Spread via parasympathetic efferent or associated afferent fibres of the vagus nerve (cranial nerve X) best fits the observed sequence of initial target areas in the medulla oblongata. Vagal efferents and afferents have their respective nerve cell bodies in the DMNV and in the nodosal ganglion (NG). However, the afferent fibres do not terminate in the NG but run to the solitary tract nucleus where they synapse with perikarya of interneurons directly projecting to vagal motor neurons in the DMNV (see Card *et al.*, 1993; Standish *et al.*, 1994). Efferents and afferents of this vagal circuit innervate the heart and the lung and visceral organs of the digestive system such as the stomach, pancreas, small intestine and ascending colon.

Therefore, neuroanatomically, the sequence of target areas can best be explained by a retrograde spread of infection along parasympathetic vagal efferents to the DMNV and subsequently to the solitary tract nucleus as described for pseudorabies virus (Card *et al.*, 1993; Standish *et al.*, 1994). However, direct spread to the SN along visceral vagal afferents from the gastro-intestinal tract or along afferents of the vagus and other cranial nerves from the pharynx (IX, X), larynx (X) and tongue (VII, IX, X) is also possible, but not suggested by the observed timing of events.

Other areas showing early deposition of TSE-AP in the brain, i.e. the SVN, GN and ependymal linings of the CC and fourth ventricle, may well be infected via neuronal pathways originating or terminating in the DMNV and SN. The onset of infection observed in target areas located within the vestibular nuclei could be explained by spread from the DMNV and SN along fibres of the vestibulo-autonomic reflex (Balaban & Beryozkin, 1994; Ito & Honjo, 1990). Projections from the GN to pancreatic parasympathetic neurons originating in the DMNV (Loewy *et al.*, 1994) could account for spread to the GN. Early deposition of TSE-AP in the ependyma of the CC at the fourth ventricle could possibly also be explained by projections to or from the DMNV (Navaratnam & Lewis; 1975) and SN. However, these areas lie anatomically adjacent to one another (Fig. 3*g*) and direct cell-to-cell spread also appears possible. In any case, subsequent spread of infection from the early target sites in the medulla to prominent nuclei in the pons, midbrain, cerebellum and thalamus seems to follow well-established neuroanatomical pathways (Andrezik & Beitz, 1985; Flumerfelt & Hrycyshyn, 1985).

The findings reported here expand our understanding of scrapie invasion of the CNS which, until recently (Baldauf *et al.*, 1997), focused predominantly on the spinal cord (Kimberlin & Walker, 1979, 1982, 1986, 1989). Our results indicate an important role of the autonomic nervous system in the spread of infection and striking similarities between the routing pathways of scrapie agent and pseudorabies virus (Card *et al.*, 1993; Standish *et al.*, 1994). Further studies will be necessary to investigate more thoroughly the relationship between TSEs and neurodegenerative diseases caused by conventional viruses.

Most recently, Blättler *et al.* (1997) reported that neuroinvasion of the scrapie agent is dependent on 'PrP expression' in a tissue compartment interposed between the lymphoreticular system and the CNS. The findings outlined above strongly point to the vagus nerve as an integral part of this compartment.

We would like to extend our special thanks to Prof. Dr H. Diringer for critical reading of the manuscript and for helpful discussion. The skilful technical assistance of Ms M. Wilson is gratefully acknowledged. This work was supported by grants to H. Diringer from the European Union, the Bundesministerium für Bildung, Wissenschaft, Forschung und Technologie, and the Hertie-Stiftung.

Fig. 3. (*a–f*) Sequence of cerebral target areas observed in semi-serial mid-sagittal sections. Deposition of TSE-AP (shaded regions) is represented in brain maps of selected individual slices covering the range between first appearance (91 days p.i.) and terminal accumulation (156 days p.i.). A, DMNV; B, SN; C, PRN; D, GN; E, IO; F, RN; G, MCN; H, SpVN, MVN and SVN; I, medullary and pontine reticular nuclei (IO, GN, PoN); J, MCN and ICN; K, retrorubral field; L, central grey matter; M, ventrolateral thalamic nucleus and VmTN; N, superior colliculus; and O, CCo (layers 4 and 5). (*g–l*) Initial target areas at different coronal levels. Deposition of TSE-AP (shaded regions) is represented in brain maps of selected individual slices demonstrating the caudal to rostral spread observed between 91 and 119 days p.i. A, DMNV; B, SN; C, GN; D, SpVN; E, SVN; F, MCN and ICN; G, MGN; H, retrorubral field; I, VmTN; and J, CCo and FCo (layers 4 and 5).

Fig. 4. Immunolabelling of TSE-AP (brown staining) in various target areas of the brain. Photographs were taken from selected slices of brains from individual animals sacrificed at different times p.i. (*a*) and (*b*), Earliest target sites. DMNV (*a*) and SN (larger arrowheads) and CC (smaller arrowhead) (*b*) at 91 days p.i. Bar, 20 μm. (*c*) Accumulation in the DMNV (larger arrowheads) and in the SN (smaller arrowheads) later in incubation period, 126 days p.i. Bar, 200 μm. (*d*) Deposition in several medullary nuclei, 119 days p.i. Bar, 400 μm. (*e*) Cerebellar target sites in the MCN and ICN (larger arrowheads) and portions of the granular layer (smaller arrowheads), 119 days p.i. Bar, 200 μm. (*f*) Widespread brainstem deposition at terminal stage of disease particularly in the thalamus (larger arrowheads) and RN (smaller arrowheads), 156 days p.i. Bar, 400 μm.

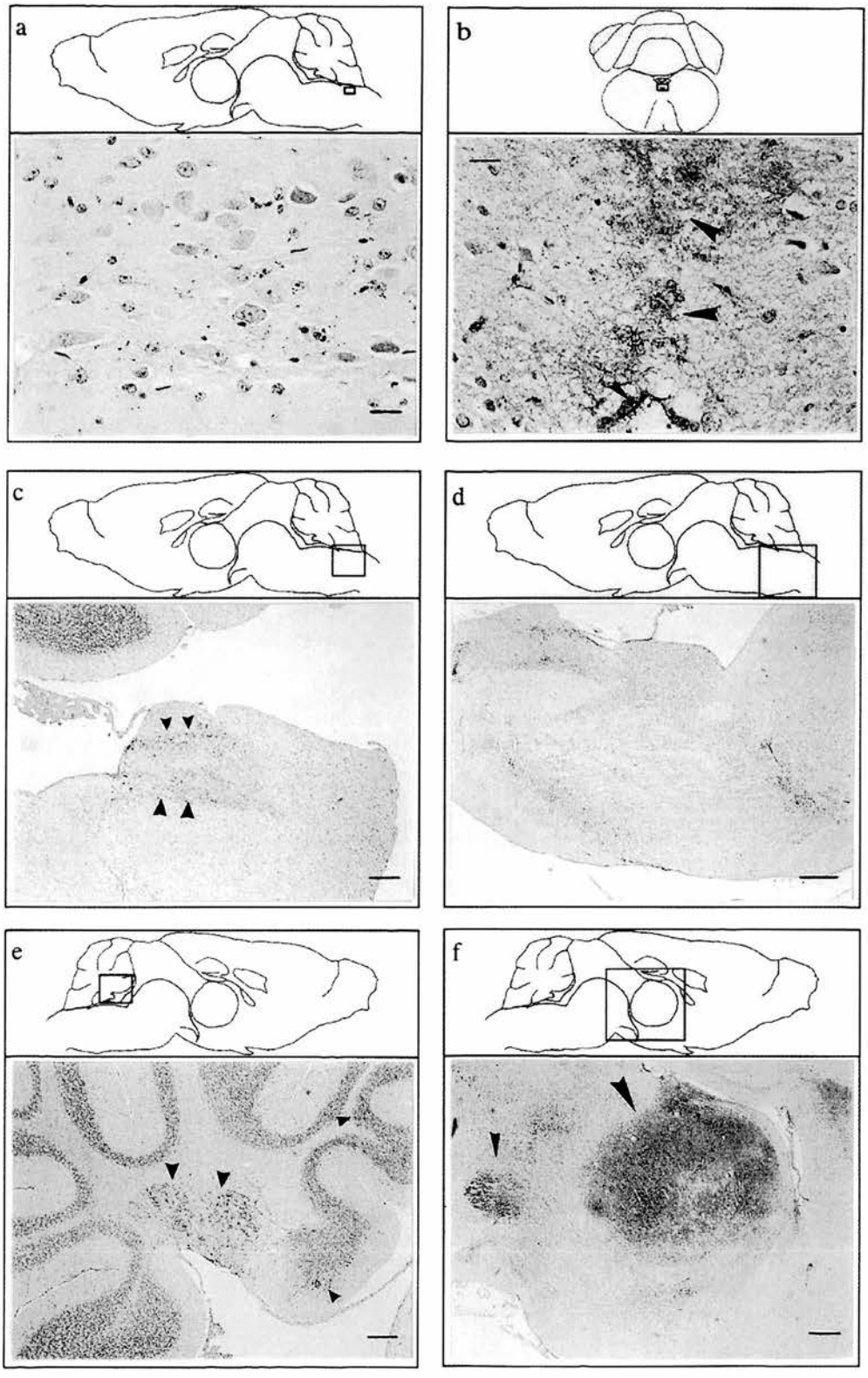

Fig. 4. For legend see page 605.

References

Andrezik, J. A. & Beitz, A. J. (1985). Reticular formation, central gray and related tegmental nuclei. In *The Rat Nervous System*, vol. 2, pp. 1–28. Edited by G. Paxinos. Sidney: Academic Press.

Balaban, C. D. & Beryozkin, G. (1994). Vestibular nucleus projections to nucleus tractus solitarius and the dorsal motor nucleus of the vagus nerve: potential substrates for vestibulo-autonomic interactions. *Experimental Brain Research* **98**, 200–212.

Baldauf, E., Beekes, M. & Diringer, H. (1997). Evidence for an alternative direct route of access for the scrapie agent to the brain bypassing the spinal cord. *Journal of General Virology* **78**, 1187–1197.

Beekes, M., Baldauf, E. & Diringer, H. (1996). Sequential appearance and accumulation of pathognomonic markers in the central nervous system of hamsters orally infected with scrapie. *Journal of General Virology* **77**, 1925–1934.

Blättler, T., Brandner, S., Raeber, A. J., Klein, M. A., Voigtländer, T., Weissmann, Ch. & Aguzzi, A. (1997). PrP-expressing tissue required for transfer of scrapie infectivity from spleen to brain. *Nature* **389**, 69–72.

Card, J. P., Rinaman, L., Lynn, R. B., Lee, B.-H., Meade, R. P., Miselis, R. R. & Enquist, L. W. (1993). Pseudorabies virus infection of the rat central nervous system: ultrastructural characterization of viral replication, transport, and pathogenesis. *The Journal of Neuroscience* **13**, 2515–2539.

Diringer, H., Beekes, M. & Oberdieck, U. (1994). The nature of the scrapie agent: the virus theory. *Annals of the New York Academy of Sciences* **724**, 246–258.

Flumerfelt, B. A. & Hrycyshyn, A. W. (1985). Precerebellar nuclei and red nucleus. In *The Rat Nervous System*, vol. 2, pp. 221–250. Edited by G. Paxinos. Sidney: Academic Press.

Ito, J. & Honjo, I. (1990). Central fiber connections of the vestibulo-autonomic reflex arc in cats. *Acta Oto-Laryngologica* **110**, 379–385.

Kascsak, R. J., Rubenstein, R., Merz, P. A., Tonna-Demasi, M., Fersko, R., Carp, R. I., Wisniewski, H. M. & Diringer, H. (1987). Mouse polyclonal and monoclonal antibody to scrapie-associated fibril protein. *Journal of Virology* **61**, 3688–3693.

Kimberlin, R. H. & Walker, C. A. (1979). Pathogenesis of mouse scrapie: dynamics of agent replication in spleen, spinal cord and brain after infection by different routes. *Journal of Comparative Pathology* **89**, 551–562.

Kimberlin, R. H. & Walker, C. A. (1982). Pathogenesis of mouse scrapie: patterns of agent replication in different parts of the CNS following intraperitoneal infection. *Journal of the Royal Society of Medicine* **75**, 618–624.

Kimberlin, R. H. & Walker, C. A. (1986). Pathogenesis of scrapie (strain 263K) in hamsters infected intracerebrally, intraperitoneally or intraocularly. *Journal of General Virology* **67**, 255–263.

Kimberlin, R. H. & Walker, C. A. (1989). Pathogenesis of scrapie in mice after intragastric infection. *Virus Research* **12**, 213–220.

Loewy, A. D., Franklin, M. F. & Haxhiu, M. A. (1994). CNS monoamine cell groups projecting to pancreatic vagal motor neurons: a transneural labeling study using pseudorabies virus. *Brain Research* **638**, 248–260.

McKinley, M. P., Bolton, D. C. & Prusiner, S. B. (1983). A protease-resistant protein is a structural component of the scrapie prion. *Cell* **35**, 57–62.

Muramoto, T., Kitamoto, T., Tateishi, J. & Goto, I. (1993). Accumulation of abnormal prion protein in mice infected with Creutzfeldt–Jakob disease via intraperitoneal route: a sequential study. *American Journal of Pathology* **143**, 1470–1479.

Navaratnam, V. & Lewis, P. R. (1975). Effects of vagotomy on the distribution of cholinesterases in the cat medulla oblongata. *Brain Research* **100**, 599–613.

Standish, A., Enquist, L. W. & Schwaber, J. S. (1994). Innervation of the heart and its central medullary origin defined by viral tracing. *Science* **263**, 232–234.

van Keulen, L. J. M., Schreuder, B. E. C., Meloen, R. H., Poelen-van den Berg, M., Mooij-Harkes, G., Vromans, M. E. W. & Langeveld, J. P. M. (1995). Immunohistochemical detection and localization of prion protein in brain tissue of sheep with natural scrapie. *Veterinary Pathology* **32**, 299–308.

Received 12 September 1997; Accepted 16 October 1997

ELSEVIER

Neuroscience Letters 265 (1999) 135–138

Neuroscience Letters

Pathological PrP is abundant in sympathetic and sensory ganglia of hamsters fed with scrapie

Patricia A. McBride[a,*], Michael Beekes[b]

[a]Institute for Animal Health, Neuropathogenesis Unit, Ogston Building, West Mains Road, Edinburgh EH9 3JF, UK
[b]Robert Koch-Institut (P31), Nordufer 20, 13353 Berlin, Germany

Received 11 January 1999; received in revised form 1 March 1999; accepted 1 March 1999

Abstract

Although the ultimate target of infection is the CNS, there is evidence that the peripheral nervous system (PNS) is involved in the pathogenesis of Transmissible Spongiform Encephalopathies (TSEs). We used immunocytochemistry to identify the presence of pathological accumulations of a host protein, PrP, in the CNS and PNS (sensory and autonomic ganglia) of hamsters orally infected with 263K scrapie. All hamsters showed pathological deposition of PrP in most brain areas, along the length of the spinal cord, in nodose (NG) and dorsal root (DRG) ganglia and in the coeliac mesenteric ganglion complex (CMGC). In one case, scant deposition was observed along a few axons of the vagus nerve. This finding suggests that, after oral challenge, TSE infectious agent uses neural pathways and ganglia of the peripheral nervous system to reach target sites in the CNS.

Keywords: Hamster scrapie; Peripheral nervous system; PrP; Neuroanatomical targeting; Routing of infection

The need to identify how oral infection of TSE leads to CNS disease has become scientifically and politically important following the emergence of bovine spongiform encephalopathy (BSE), a new variant of CJD (vCJD) and the demonstration that the two are linked [4,9], presumably through consumption of BSE-contaminated beef.

There is evidence that the PNS is involved in the spread of infection to the CNS in natural [7] and experimental scrapie [3,12,15], experimental CJD [17], and BSE [18]. The presence of infectious agent in peripheral nerve ganglia in preclinical stages of disease in cows orally-infected with BSE [18] raised concern and contributed towards the British government's decision to ban the sale of beef-on-the-bone in December 1997. We now report that abnormal PrP (prion protein), the protein marker for TSE infection, is abundant within sensory (DRG, NG) and sympathetic (CMGC) PNS components of hamsters orally-infected with scrapie.

Five outbred Syrian hamsters were orally-infected with scrapie by being fed single pellets doused with 100 μl of a 10% 263K brain homogenate. Two hamsters were similarly mock-challenged with normal brain homogenate. At the terminal stage of disease at 159 ± 6 days post infection, all hamsters were sacrificed and perfused with periodate lysine paraformaldehyde (PLP) [16]. Brain, cervical and thoracic spinal cord with attached DRG, left and right NG with attached vagus nerve and the CMGC were removed, left overnight in PLP then 48 h in 70% alcohol. Brains were sliced through coronally. Spinal cords were sliced coronally to provide individual segments with corresponding left and right DRGs. Immunocytochemistry was performed on semi-serial, paraffin-embedded tissues according to the ABC method using 3F4 mouse anti-hamster PrP monoclonal antibody [10] and diaminobenzidine (DAB) to visualise the reaction product. Prior to immunostaining, sections were pretreated with formic acid for 10 min to enhance visualisation of PrP. Cresyl violet/luxol fast blue histochemistry was carried out on adjacent sections to aid neuroanatomical identification.

All scrapie-infected hamsters showed marked granular deposition of pathological PrP in most brain areas and along the length of the spinal cord as previously described [3]. Strong immunoreactivity was seen in several brainstem nuclei including the dorsal motor nucleus of the vagus nerve (DMNV) and adjacent solitary tract nucleus (SN) and throughout the entire 'butterfly' of dorsal and ventral horn gray matter of each cervical and thoracic spinal cord segment (Fig. 1).

Immunolabelling of PNS components showed that in all

* Corresponding author. Tel.: +44-131-667-5204; fax: +44-131-668-3872.
E-mail address: tricia.mcbride@bbsrc.ac.uk (P.A. McBride)

0304-3940/99/$ - see front matter
PII: S0304-3940(99)00223-2

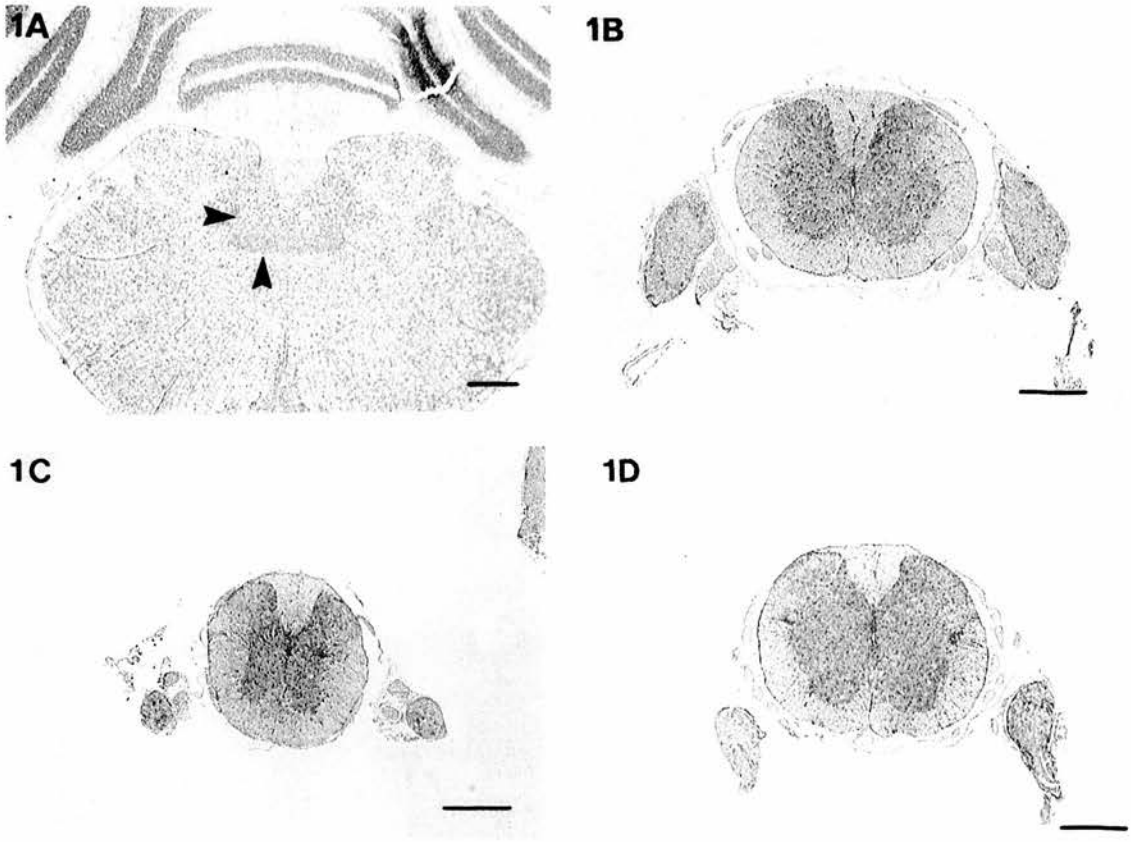

Fig. 1. Immunolabelling of pathological PrP (brown granular accumulations) in CNS of a hamster terminally affected with 263K scrapie. (A) Cerebellum and medulla. Labelling is particularly strong around DMNV and SN (arrows) Scale bar, 250 μm. (B) cervical (C8), (C) thoracic (T4), (D) thoracic (T9) segments of spinal cord. PrP labelling is seen primarily in 'butterfly' of dorsal and ventral horn gray matter. Note: Pathological PrP is also seen in attached DRGs. Scale bar, 650 μm.

NG and DRG, PrP was seen as intensely stained pathological granular inclusions within a substantial proportion of ganglion cells and adjacent satellite cells (Fig. 2A,B). Ganglia of the CMGC showed additional extracellular staining (Fig. 2C).

Mostly, PrP immunolabelling was not found in either vagus nerve or spinal nerve roots. However, in one section from a single case, scant punctate deposition was observed along a few axons of the vagus nerve (Fig. 3).

In brain and spinal cord from mock-challenged hamster, PrP immunolabelling was present only in a small proportion of neuronal cell bodies. PrP was more weakly stained and of homogenous appearance, contrasting markedly to 'granular' pathological forms [3]. All ganglia were unlabelled. In all adjacent control sections where normal serum replaced 3F4, staining was absent.

Although the ultimate target of TSE infection is the CNS, there is evidence that the lymphoreticular [5,6,8,11,13] and PNS [3,12,14,15] are involved in the replication and transport of infectious agent after natural or peripheral challenge. However, the relative contributions of the two systems in establishing disease appears to differ between various models. Regardless of the initial pathogenic mechanisms, neural spread of infection to the brain and spinal cord shows a consistent pattern in several peripherally-infected rodent models of scrapie including this model of oral challenge. Initial targeting of infectivity [11–14] and the earliest deposits of pathological PrP [1–3] are localised to mid-thoracic spinal cord. The first target site for abnormal PrP accumulation in the brain is the DMNV followed shortly afterwards by the SN [3]. These data indicated that, after peripheral challenge, scrapie infection may reach the CNS by retrograde spread along autonomic nerves supplying the mesentery, i.e. along sympathetic and parasympathetic efferents of the splanchnic and vagus nerves, respectively. Subsequent spread through the CNS occurs rostrally and caudally [2,3,11,14] and as we now show, at the terminal stage of disease, the NG and CMGC as well as all cervical and thoracic segments of spinal cord and corresponding DRG contain substantial pathological PrP accumulations.

Although the presence of pathological deposits of PrP in such peripheral ganglia at late-stage disease does not establish the direction of spread, i.e. whether infection spreads to the CNS from abdominal nerves or vice versa, the finding fits perfectly into the model of spread outlined above and shows that spread along peripheral nerves is possible and

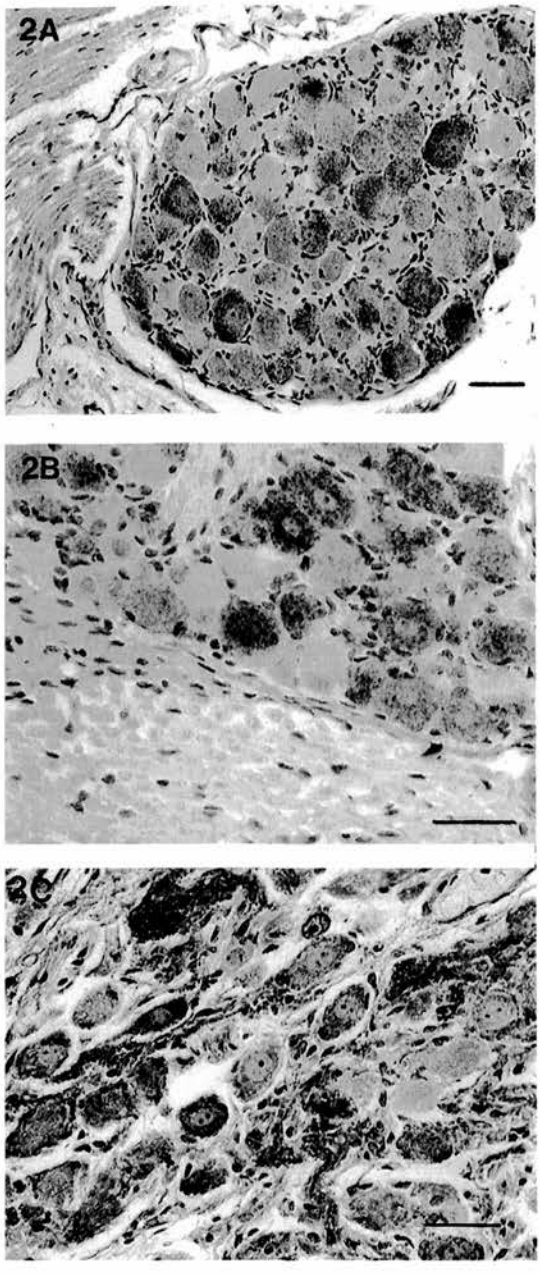

Fig. 2. Immunolabelling of pathological PrP (brown granular accumulations) in PNS of a hamster terminally-affected with 263K scrapie. (A) DRG, (B) NG, (C) CMGC. PrP accumulates within and around a large proportion of individual ganglion and adjacent satellite cells. Scale bar, 50 μm (A), 40 μm (B,C).

occurs during scrapie pathogenesis. Neuroanatomically, infection of the NG and DRG can best be explained by spread of agent from as yet unidentified mesenteric sites via (i) retrograde transport along vagal and splanchnic efferent fibres to neuronal cell bodies in the DMNV and intermediolateral nuclei (IML), respectively, and then via SN or dorsal root interconnections; (ii) direct anterograde transport along sensory (afferent) fibres of the vagus or splanchnic nerves (Fig. 4).

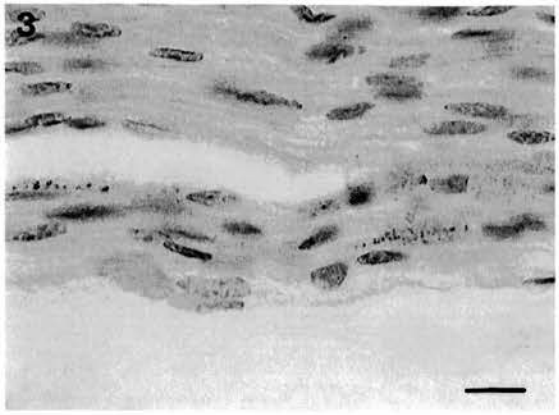

Fig. 3. Immunolabelling of pathological PrP (brown granular accumulations) in PNS of a hamster terminally-affected with 263K scrapie. Pathological PrP deposits along nerve fibres in the cervical vagus nerve. Scale bar, 10 μm.

The finding of pathological PrP in sensory and autonomic ganglia and associated peripheral nerves further strengthens the supposition that, after peripheral challenge, TSE infectious agent uses neuronal pathways and ganglia of the peripheral nervous system to reach target sites in the CNS. Such involvement raises the possibility that nerve fibres and ganglia serve as early reservoirs for infectivity after an oral challenge.

If this is so, findings in our hamster model will also be relevant to peripheral pathogenesis of non-experimental TSEs such as BSE and vCJD.

The skilful technical assistance of Marion Joncic, Stephanie Collishaw and Maura Wilson is gratefully acknowledged. The authors also wish to thank Dr. Walter Schulz-Schaeffer (Institute for Neuropathology, University of Goet-

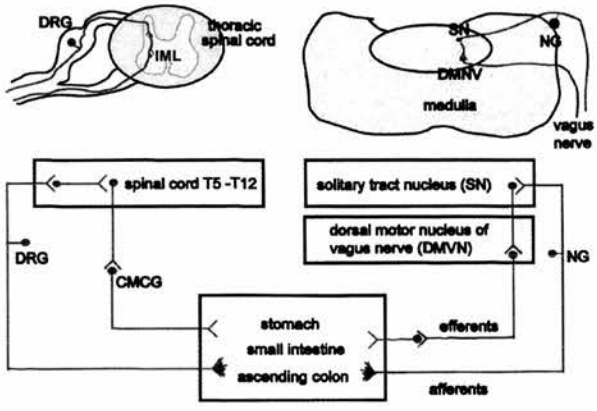

Fig. 4. Schematic representation of possible routes for the spread of infection from mesentery to CNS after oral challenge of 263K scrapie. Available data suggests spread occurs via relevant efferent or afferent nerve fibres and ganglia.

tingen) for demonstration of hamster ganglia dissection. This work was supported, in parts, by grants from the German 'Bundesministerium für Bildung und Forschung' and the German 'Bundesministerium für Gesundheit'.

[1] Baldauf, E., Beekes, M. and Diringer, H., Evidence for an alternative direct route of access for the scrapie agent to the brain bypassing the spinal cord. J. Gen. Virol., 78 (1997) 1187–1197.
[2] Beekes, M., Baldauf, E. and Diringer, H., Sequential appearance and accumulation of pathognomonic markers in the central nervous system of hamsters orally infected with scrapie. J. Gen. Virol., 77 (1996) 1925–1934.
[3] Beekes, M., McBride, P.A. and Baldauf, E., Cerebral targeting indicates vagal spread of infection in hamsters fed with scrapie. J. Gen. Virol., 79 (1998) 601–607.
[4] Bruce, M.E., Will, R.G., Ironside, J.W., McConnell, I., Drummond, D., Suttie, A., McCardle, L., Chree, A., Hope, J., Birkett, C., Cousens, S., Fraser, H. and Bostock, C.J., Transmissions to mice indicate that 'new variant' CJD is caused by the BSE agent. Nature, 389 (1997) 498–501.
[5] Fraser, H., Brown, K.L., Stewart, K., McConnell, I., McBride, P. and Williams, A., Replication of scrapie in spleens of SCID mice follows reconstitution with wild-type mouse bone marrow. J. Gen. Virol., 77 (1996) 1935–1940.
[6] Fraser, H., Bruce, M.E., Davies, D., Farquhar, C.F. and McBride, P.A., The lymphoreticular system in the pathogenesis of scrapie. In S.B. Prusiner, J. Collinge, J. Powell and B. Anderton (Eds.), Prion Diseases of Humans and Animals, Ellis Horwood, Chichester, 1992, p. 308.
[7] Groschup, M.H., Weiland, F., Straub, O.C. and Pfaff, E., Detection of scrapie agent in the peripheral nervous system of a diseased sheep. Neurobiol. Dis., 3 (1996) 191–195.
[8] Hadlow, W.J., Kennedy, R.C. and Race, R.E., Natural infection of Suffolk sheep with scrapie virus. J. Infect. Dis., 146 (1982) 657–664.
[9] Hill, A.F., Desbruslais, M., Joiner, S., Sidle, K.C.L., Gowland, I., Collinge, J., Doey, L.J. and Lantos, P., The same prion strain causes vCJD and BSE. Nature, 389 (1997) 448–450.
[10] Kascsak, R.J., Rubenstein, R., Mertz, P.A., Tonna-Demasi, M., Fersko, R.M., Carp, R.I., Wisniewski, H.M. and Diringer, H., Mouse polyclonal and monoclonal antibody to scrapie-associated fibril protein. J. Virol., 61 (1987) 3688–3693.
[11] Kimberlin, R.H. and Walker, C.A., Pathogenesis of mouse scrapie: patterns of agent replication in different parts of the CNS following intraperitoneal infection. J. R. Soc. Med., 75 (1982) 618–624.
[12] Kimberlin, R.H. and Walker, C.A., Pathogenesis of scrapie (strain 263K) in hamsters infected intracerebrally, intraperitoneally or intraocularly. J. Gen. Virol., 67 (1986) 255–263.
[13] Kimberlin, R.H. and Walker, C.A., The role of the spleen in the neuroinvasion of scrapie in mice. Virus Res., 12 (1989) 201–212.
[14] Kimberlin, R.H. and Walker, C.A., Pathogenesis of scrapie in mice after intragastric infection. Virus Res., 12 (1989) 213–220.
[15] Kimberlin, R.H., Field, H. and Walker, C.A., Pathogenesis of mouse scrapie: Evidence for spread of infection from central to peripheral nervous system. J. Gen. Virol., 64 (1983) 713–716.
[16] McBride, P.A., Wilson, M.I., Eikelenboom, P., Tunstall, A. and Bruce, M.E., Heparan sulphate proteoglycan is associated with amyloid plaques and neuroanatomically targeted PrP pathlogy throughout the incubation period of scrapie-infected mice. Exp. Neurol., 149 (1998) 447–454.
[17] Muramoto, T., Kitamoto, T., Tateishi, J. and Goto, I., Accumulation of abnormal prion protein in mice infected with Creutzfeldt-Jakob disease via intraperitoneal route: a sequential study. Am. J. Pathol., 143 (1993) 1470–1479.
[18] Wells, G.A.H., Hawkins, S.A.C., Green, R.B., Austin, A.R., Dexter, I., Spencer, Y.I., Chaplin, M.J., Stack, M.J. and Dawson, M., Preliminary observations on the pathogenesis of experimental bovine spongiform encephalopathy (BSE): an update. Vet. Rec., 142 (1998) 103–106.

ELSEVIER

Neuroscience Letters 278 (2000) 181–184

Neuroscience Letters

www.elsevier.com/locate/neulet

Early accumulation of pathological PrP in the enteric nervous system and gut-associated lymphoid tissue of hamsters orally infected with scrapie

Michael Beekes[a,*], Patricia A. McBride[b]

[a]Robert Koch-Institut (P31), Nordufer 20, 13353 Berlin, Germany
[b]Institute for Animal Health, Neuropathogenesis Unit, Ogston Building, West Mains Road, Edinburgh EH9 3JF, UK

Received 8 October 1999; received in revised form 22 November 1999; accepted 22 November 1999

Abstract

Infection of the central nervous system (CNS) is a defining feature of scrapie. Several findings suggest that scrapie agent invades the CNS via the splanchnic and vagus nerve after ingestion of infectivity. Here we address the involvement of the enteric nervous system (ENS) and gut-associated lymphoid tissue (GALT) in this pathogenetic process. Immunocytochemistry was used for the detection of pathological PrP in the duodenum and ileum of hamsters fed with 263K scrapie and sacrificed at different stages of incubation. The experiments revealed early infection of various GALT components and of submucosal and myenteric ENS ganglia. These results provide evidence for an important role of the ENS in scrapie neuroinvasion and for centripetal vagal spread of infection from the gut to the brain after oral uptake of agent.

Keywords: Hamster scrapie; Oral infection; Pathogenesis; PrP; Enteric nervous system; Gut-associated lymphoid tissue

Transmissible spongiform encephalopathies (TSEs) such as Creutzfeldt–Jakob disease (CJD) in man, bovine spongiform encephalopathy (BSE) in cattle and scrapie in sheep are infectious and invariably fatal neurodegenerative disorders of the central nervous system (CNS). After the emergence of BSE and 'new variant' CJD (vCJD) and the discovery that the two are linked [5,8], presumably through consumption of BSE-contaminated foodstuffs, the pathogenesis of orally transmitted TSEs has become a matter of great scientific and public interest.

Accumulating data from experimental time-course studies on the pathogenesis of scrapie in rodents strongly suggest that after an intragastric or oral challenge infection spreads from sites in the gastrointestinal tract via the splanchnic and vagus nerve to the spinal cord and brain, respectively [1–3,10,11,15]. Portals of entry for the infectious agent from the alimentary canal into these neuronal circuits may lie in the esophagus, stomach, small intestine and large intestine.

There is a long-standing assumption that natural scrapie in sheep is transmitted by the oral route [6] and that the infectious agent invades its natural host via the alimentary tract [7] but the precise identity of the digestive system tissues and cells in which infectivity is either supported or replicated remains to be established. Deposition of pathological PrP, the protein marker for TSE infection, in myenteric and submucosal plexuses of the gut wall, stomach and caudal esophagus of sheep with clinical signs of natural scrapie suggests that the enteric nervous system (ENS) is involved [20]. However, the presence of pathological PrP in ENS ganglia at late-stage disease does not indicate from which source these sites were infected or to which targets they direct the infectious agent.

To address the involvement of the ENS and non-neural gut components in early pathogenesis, we have carried out a sequential study in hamsters orally challenged with 263K scrapie. Immunocytochemistry was used to determine the timing and location of the deposition of pathological PrP in the duodenum and ileum early in the incubation period and throughout the progression of infection.

Outbred Syrian hamsters were orally infected with 263K scrapie as described elsewhere [15]. Three or four animals were sacrificed at 69, 76, 83, 90, 97, 104, 111, 118, 125, 132 days post infection (dpi), and also at 153 dpi (terminal stage of disease) by CO_2 euthanasia and perfused with periodate

* Corresponding author. Tel.: +49-30-4547-2396; fax: +49-30-4547-2609.
E-mail address: beekesm@rki.de (M. Beekes)

0304-3940/00/$ - see front matter
PII: S0304-3940(99)00934-9

lysine paraformaldehyde (PLP) [14]. Two control animals were fed normal brain homogenate and sacrificed at 161 days after mock-infection. From the small intestine, 2 cm of duodenum and 2 cm of ileum were removed adjacent to the jejunum and the ileocecal sphincter, respectively. The specimens were left overnight in PLP, 48 h in 70% ethanol, dehydrated and embedded in paraffin wax. After pretreatment with formic acid, 6 μm semi-serial sections of gut were immunocytochemically stained for PrP with MAb 3F4 [9] and diaminobenzidine as recently described [15]. Hematoxylin/eosin histochemistry was performed on adjacent sections to facilitate identification of anatomical structures.

Pathological PrP presented as characteristic immunoreactive granular depositions within or around neurons and non-neuronal cells. This pathological form of PrP accumulation differs markedly from the pattern of PrP immunostaining seen in normal brains [3,15] and was absent in mock-infected control animals. No immunostaining was observed in adjacent control sections where normal serum replaced MAb 3F4.

In the duodenal and ileal muscularis and submucosa, pathological PrP was consistently found in myenteric and submucosal plexuses from 69 dpi (Fig. 1a,b), the earliest time point investigated in this study, until the terminal stage of disease. The amount of PrP deposition and the number of ganglia affected varied between individuals. In three out of four hamsters sacrificed at 69 dpi labelling was stronger and more widespread in ganglia of the ileum than in the duodenum, i.e. heavier granular deposition appeared around a greater number of individual ganglion cells with more ganglia affected. At subsequent time points, accumulations of pathological PrP became increasingly more abundant in ENS ganglia (Fig. 1c,d) and their associated nerve fibers (Fig. 2a) and along anatomical structures indistinguishable from nerves in individual lymphoid follicles (Figs. 2b and 3a) and Peyers's patches. At end-point of disease, all ganglia were heavily labelled.

From the earliest time point available (69 dpi), immunostaining for pathological PrP also occurred in gut-associated lymphoid tissue (GALT), i.e. in mesenteric lymph nodes, mucosal lymphoid follicles (Fig. 3a) and Peyer's patches. Labelling was most obvious in follicular dendritic cells (FDCs) (Fig. 3b) within germinal centers but could also be clearly seen at 69 dpi and later in several macrophages of the dome and in cells of the follicle-associated epithelium (Fig. 3c). Although the latter were not specifically identified, their location and morphology was consistent with that of M cells.

Previous time-course studies on the pathogenesis of scrapie in orally infected hamsters revealed strong evidence for vagal spread of infection to the brain and indicated that initial cerebral invasion probably occurs by retrograde transport of agent along parasympathetic efferents to the

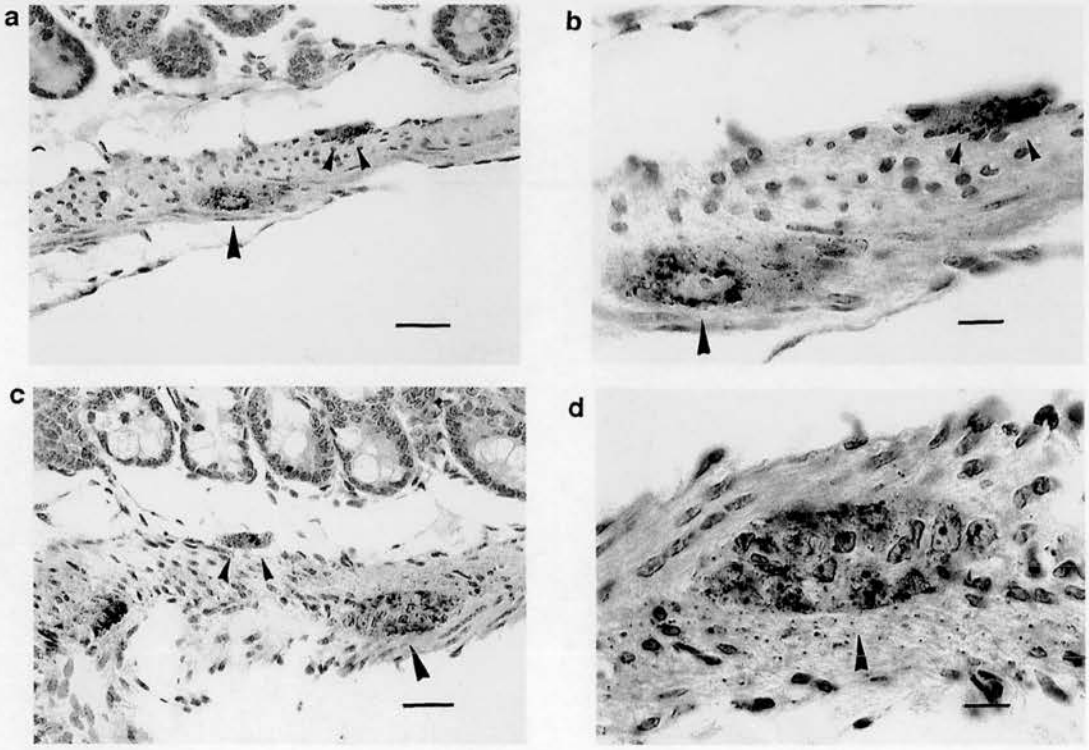

Fig. 1. Immunolabeling of pathological PrP (brown granular accumulations) in ileal ENS ganglia from hamsters sacrificed at different time points after oral infection with 263K scrapie. (a,b) Submucosal (small arrowheads) and myenteric (large arrowheads) plexus at 69 dpi. (c,d) Submucosal (small arrowheads) and myenteric (large arrowheads) plexus at 153 dpi. Scale bar, 30 μm (a,c); 10 μm (b,d).

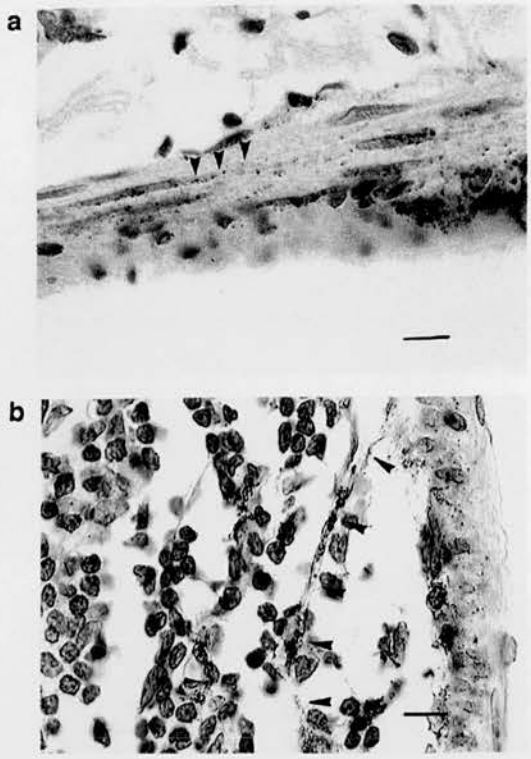

Fig. 2. Immunolabeling of pathological PrP associated with nerve fibres and nerve-like structures in ileum from hamsters terminally affected with 263K scrapie. (a) 'Tracking' along nerve fibres in ileal muscularis. (b) Nerve-like structures extending from the submucosal/muscular layer into an overlying lymphoid follicle. Scale bar, 10 μm.

dorsal motor nucleus of the vagus nerve [3]. Using the same animal model we now report early infection of the ENS and GALT after uptake of 263K scrapie via the gastrointestinal tract.

According to the observed sequential pattern of spread, i.e. the time of onset and the quantitative increase of pathological PrP deposition in intestinal and cerebral [3] target areas, the involvement of myenteric and submucosal plexuses at early stages of incubation is extremely unlikely to result from centrifugal spread of agent. Rather, the observed sequence of events indicates centripetal propagation of infection from the ENS to the brain. Since preganglionic motor fibers of the vagus nerve originating in the dorsal motor nucleus synapse with ENS postganglionic neurons in the gut this further strengthens the evidence for retrograde transport of scrapie agent along vagal efferents. A striking similarity to this pattern of spread is exhibited by reovirus serotype 3, isolate T3C9 [16] which, after oral administration, causes lethal encephalitis in newborn mice. Our findings strongly point to the ENS as an important site for neuroinvasion following ingestion of infectivity. However, the vagus nerve also sends fibers to viscera other than the alimentary tract. If scrapie agent were disseminated by blood or lymphatic drainage to such organs, these may possibly provide additional sites for neural penetration. Further studies will be necessary to address this question.

The same holds true with respect to whether and to what degree neuroinvasion of the ENS depends on GALT and/or other non-neuronal gut components. In our animal model, deposition of pathological PrP in follicle-associated epithe-

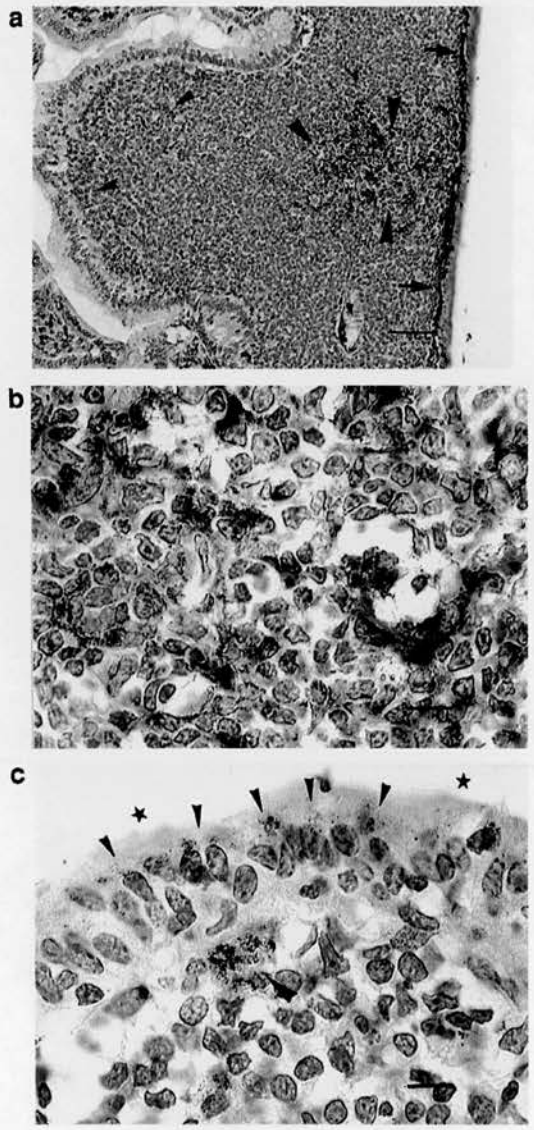

Fig. 3. Immunolabeling of pathological PrP in ileal lymphoid follicles from hamsters sacrificed at different time points after oral infection with 263K scrapie. (a) Individual follicle at 125 dpi. Immunostaining in the 'dome' (small arrowheads) and in the germinal center (large arrowheads) is associated with macrophages and FDCs, respectively. Note heavy labelling of nerve fibres (arrows). (b) Germinal center FDCs at 153 dpi. (c) Macrophage (large arrowhead) of the 'dome' and cells of the follicle-associated epithelium (probably M cells, small arrowheads) at 111 dpi. Stars indicate luminal surface. Scale bar, 50 μm (a); 10 μm (b,c).

lium (probably associated with M cells), macrophages and FDCs of intestinal lymphoid follicles and Peyer's patches occurred at early and late stages of incubation. Previously, pathological PrP was found in lymphoid tissues of the digestive system of sheep with natural scrapie [19] and of lemurs experimentally or accidentally fed with BSE [4]. For the lemurs, the authors reported that the protein could be detected in epithelial cells, M cells, lymphocytes and lymphoreticular tissue compartments of the gastrointestinal tract prior to and concurrent with clinical disease.

At present, the available data suggest three options: GALT and/or other non-neuronal gut components are: (i) obligatory key players; (ii) optional mediators; or (iii) by-standers of neuronal infection after oral uptake of infectivity. Which of these possibilities apply may well depend on the combination of host species, strain of agent, dose or other unknown factors. Although several findings argue against a sole by-stander role of at least the FDCs [12,13,17,18], the mechanisms of neuroinvasion in orally transmitted TSEs have only begun to unfold.

The skilful technical assistance of Marion Joncic, Stephanie Collishaw and Maura Donaldson is gratefully acknowledged. This work was supported by grants of the German 'Bundesministerium für Bildung und Forschung', the German 'Bundesministerium für Gesundheit' and the Biotechnology and Biological Sciences Research Council (BBSRC).

[1] Baldauf, E., Beekes, M. and Diringer, H., An alternative direct route of access for the scrapie to the brain bypassing the spinal cord. J. Gen. Virol., 78 (1997) 1187–1197.
[2] Beekes, M., Baldauf, E. and Diringer, H., Sequential appearance and accumulation of pathognomonic markers in the central nervous system of hamsters orally infected with scrapie. J. Gen. Virol., 77 (1996) 1925–1934.
[3] Beekes, M., McBride, P.A. and Baldauf, E., Cerebral targeting indicates vagal spread of infection in hamsters fed with scrapie. J. Gen. Virol., 79 (1998) 601–607.
[4] Bons, N., Mestres-Frances, N., Belli, P., Cathala, F., Gajdusek, D.C. and Brown, P., Natural and experimental oral infection of nonhuman primates by bovine spongiform encephalopathy agents. Proc. Natl. Acad. Sci. USA, 96 (1999) 4046–4051.
[5] Bruce, M.E., Will, R.G., Ironside, J.W., McConnell, I., Drummond, D., Suttie, A., McCardle, L., Chree, A., Hope, J., Birkett, C., Cousens, S., Fraser, H. and Bostock, C.J., Transmissions to mice indicate that 'new variant' CJD is caused by the BSE agent. Nature, 389 (1997) 498–501.
[6] Diringer, H., Beekes, M. and Oberdieck, U., The nature of the scrapie agent: the virus theory. Ann. N.Y. Acad. Sci., 724 (1994) 246–258.
[7] Hadlow, W.J., To a better understanding of scrapie. Curr. Topics Veter. Med. Animal Sci., 55 (1991) 117–130.
[8] Hill, A.F., Desbruslais, M., Joiner, S., Sidle, K.C.L., Gowland, I., Collinge, J., Doey, L.J. and Lantos, P., The same prion strain causes vCJD and BSE. Nature, 389 (1997) 448–450.
[9] Kascsak, R.J., Rubenstein, R., Merz, P.A., Tonna-Demasi, M., Fersko, R., Carp, R.I., Wisniewski, H.M. and Diringer, H., Mouse polyclonal and monoclonal antibody to scrapie-associated fibril protein. J. Virol., 61 (1987) 3688–3693.
[10] Kimberlin, R.H. and Walker, C.A., Pathogenesis of experimental scrapie. In G. Bock and J. Marsh (Eds.), Novel Infectious Agents and the Central Nervous System, Vol. 135, Ciba Foundation Symposium, Wiley, Chichester, 1988, pp. 37–62.
[11] Kimberlin, R.H. and Walker, C.A., Pathogenesis of scrapie in mice after intragastric infection. Virus Res., 12 (1989) 213–220.
[12] Kimberlin, R.H. and Walker, C.A., The role of the spleen in the neuroinvasion of scrapie in mice. Virus Res., 12 (1989) 201–212.
[13] McBride, P.A., Eikelenboom, P., Kraal, G., Fraser, H. and Bruce, M.E., PrP protein is associated with follicular dendritic cells of spleens and lymph nodes in uninfected and scrapie-infected mice. J. Pathol., 168 (1992) 413–418.
[14] McBride, P.A., Wilson, M.I., Eikelenboom, P., Tunstall, A. and Bruce, M.E., Heparan sulfate proteoglycan is associated with amyloid plaques and neuroanatomically targeted PrP pathology throughout the incubation period of scrapie-infected mice. Exp. Neurol., 149 (1998) 447–454.
[15] McBride, P.A. and Beekes, M., Pathological PrP is abundant in sympathetic and sensory ganglia of hamsters fed with scrapie. Neurosci. Lett., 265 (1999) 135–138.
[16] Morrison, L.A., Sidman, R.L. and Fields, B.N., Direct spread of reovirus from the intestinal lumen to the central nervous system through vagal autonomic nerve fibres. Proc. Natl. Acad. Sci. USA, 88 (1991) 3852–3856.
[17] Raeber, A.J., Klein, M.A., Frigg, R., Flechsig, E., Aguzzi, A. and Weissmann, C., PrP-dependent association of prions with splenic but not circulating lymphocytes of scrapie-infected mice. EMBO J., 18 (1999) 2702–2706.
[18] Scott, J.R., Scrapie pathogenesis. Br. Med. Bull., 49 (1993) 778–791.
[19] van Keulen, L.J.M., Schreuder, B.E.C., Meloen, R.H., Mooij Harkes, G., Vromans, M.E.W. and Langeveld, J.P.M., Immuno-histochemical detection of prion protein in lymphoid tissues of sheep with natural scrapie. J. Clin. Microbiol., 34 (1996) 1228–1231.
[20] van Keulen, L.J.M., Schreuder, B.E.C., Vromans, M.E.W., Langeveld, J.P.M. and Smits, M.A., Scrapie-associated prion protein in the gastro-intestinal tract of sheep with natural scrapie. J. Comp. Pathol., 121 (1999) 55–63.

Journal of Cellular Pathology

Journal of Cellular Pathology 2000
5, 17–22

Paper

Technical aspects of tracking scrapie infection in orally dosed rodents

M. I. Wilson, P. A. McBride

Neuropathogenesis Unit, Institute for Animal Health, Edinburgh, UK

Abstract

The sheep and goat disease scrapie belongs to a group of diseases known collectively as Transmissible Spongiform Encephalopathies (TSEs). These are fatal neurodegenerative diseases, which affect many species, and are transmissible either naturally or experimentally to a number of others. A disease specific protein, known as PrP^{Sc}, PrP^{res} or Prion protein, can be used as a tool for tracking the spread of infection in these diseases. The purpose of this study was to establish protocols, which would enable identification of precise neuroanatomic groups and sensitive detection of PrP in the brain and spinal cord of Syrian hamsters, orally infected with scrapie. Tissue preservation and structure were optimised by varying the length of fixation in periodate-lysine-paraformaldehyde and immersion in 70% alcohol. Precise histological techniques were devised for the trimming, embedding and orientation of the tissues. Two immunocytochemistry methods were used and compared to detect early and terminal stage PrP accumulations in the brain and spinal cord. Histological staining methods were also used to identify the specific cell types involved. The procedures established in this study could be used as standards for detailed investigations of the spread of scrapie infection from the gastro-intestinal tract to the central nervous system.

Keywords

Scrapie; PrP protein; Syrian hamsters; immunocytochemistry

INTRODUCTION

Scrapie is a naturally occurring disease of sheep and goats. It was first recognised over 250 years ago and acquired its name from the unusual behaviour exhibited by clinically affected sheep, i.e. scraping or scratching themselves against fence posts, etc. Scrapie was also the first recognised member of a group of fatal degenerative diseases of the central nervous system (CNS) known as Transmissible Spongiform Encephalopathy (TSE) diseases.

To date, the precise nature of the infectious agent for TSE diseases remains unidentified. Pathological examination reveals vacuolation, gliosis and neuronal loss in the brain and spinal cord. TSEs also result in the accumulation of an abnormal form of a host protein, PrP, sometimes also referred to as PrP^{Sc}, PrP^{res} or Prion protein. Investigative studies in mice have demonstrated that abnormal PrP protein is expressed in several forms. Widespread diffuse type or granular PrP accumulates into the CNS of affected mice throughout the incubation of the disease. These deposits are found within precisely targeted brain areas such as defined neuronal groups; within microglia and in the neuropil. Several types of amyloid PrP plaques can also be found in infected animals. These plaques can be small and diffuse or larger with a fibrillar core.[1]

The role or function of PrP protein in normal animals is not fully understood. However, its

Correspondence to: M. I. Wilson BSc Hons, Neuropathogenesis Unit, Institute for Animal Health, Ogston Building, West Mains Road, Edinburgh EH9 3JF, Scotland.
Research funded by the Biotechnology and Biological Sciences Research Council (BBSRC)

ERRATA: This article was previously published in Volume 4 Issue 3 of this Journal without the figures. The Publisher would like to apologise to the authors.

presence has been shown to be instrumental in the development of clinical disease after infection with scrapie, as PrP gene 'knockouts' do not develop the disease.[2,3] The detection of abnormal PrP provides a useful tool to track the spread of scrapie disease.

The public and political awareness of TSE diseases has been raised by recent scientific revelations concerning Bovine Spongiform Encephalopathy (BSE) in cattle and new variant Creutzfeldt Jakob Disease (nvCJD) in man. Transmission studies of nvCJD into mice results in a pattern of vacuolation in the brain identical to that produced by BSE.[4] This provides very strong evidence that BSE has transmitted from cattle into humans. Epidemiological studies show that the most likely route of transmission of BSE to man is the oral route, through the consumption of infected beef products.[5]

The aim of this study was to establish protocols to investigate the accumulation of abnormal PrP in a hamster model, which could then be used in a subsequent study tracking the spread of scrapie infection from the gastro-intestinal tract to the CNS.

This has involved fixation trials and the establishment of specific trimming, processing and embedding methods for several different tissues. Two immunocytochemistry (ICC) techniques were compared to determine the most sensitive method for labelling the abnormal PrP deposits. Combinations of histological stains were used to identify the specific cell types involved.

METHODS

Experimental Design

Syrian hamsters were orally infected by feeding with 10mg pellets of 263K strain of scrapie brain homogenate. The control hamsters were fed with a 10mg pellet of normal brain homogenate.

At predetermined time points after infection, four hamsters were perfused with periodate-lysine-paraformaldehyde (PLP) under terminal anaesthesia. Culls were carried out at 56 days post infection (dpi) and thereafter at weekly intervals up to terminal stage of the disease at 159 dpi (mean figure). Tissues were dissected out in Berlin, Germany, and transported to Edinburgh for histopathology. This involved a necessary 3-day delay before tissues could be processed. Previous studies using PLP employed only short periods of fixation (<12 hours). A trial was therefore carried out to establish whether tissues fixed for longer times gave equally good results. Immediately after perfusion of the hamster, with PLP fixative, several tissues were dissected out. They were then either:

a. Fixed by immersion in PLP for a further 5 hours then transferred to 70 % alcohol for the remainder of the 3-day period, or
b. Immersed in PLP for the entire 3-day period.

After this, these tissues were trimmed, immersed in 70% alcohol; processed overnight through a series of graded alcohols, xylene and wax, and were embedded the following morning into fresh paraffin wax. Six micron serial sections were cut from the wax blocks, floated out on tap water and mounted onto superfrost plus slides (General Scientific).

A number of tissues were removed from the hamsters for examination. The brain and spinal cord were taken for the purpose of this study, as they are the ultimate target sites for the scrapie infection. The spleen was also taken for a future ICC study as it has been found to be important in some models of scrapie for the early replication or accumulation of the disease.[6,7]

Immunocytochemistry

Two ICC techniques were used to visualise and compare PrP between normal and infected animals. These methods were the indirect two-step peroxidase method and the avidin biotin complex (ABC)-elite peroxidase (Vector laboratories) method. Prior to both methods, the slides were immersed in a solution of 99% formic acid for ten minutes to unmask antigenic sites. Endogenous peroxidase staining was then blocked by a 10 minute pre-treatment with a 1 per cent solution of hydrogen peroxide in methanol. The wash and dilution buffer used throughout was phosphate buffered saline with either 0.2% or 1% bovine serum albumin added respectively. All incubations were carried out in a humidity chamber. A normal rabbit blocking serum (from the Scottish antibody production unit) was used prediluted to 1/20. The primary antibody was an appropriately diluted mouse anti-hamster-PrP monoclonal antibody produced by Michael Beekes at the Robert Koch Institute in Berlin, Germany. A normal mouse serum was applied at an appropriate dilution to adjacent sections as a serum control. Diaminobenzidine (DAB) substrate was used to

visualise the peroxidase staining. The slides were then lightly counterstained with Haematoxylin and were coverslipped with DPX mountant.

The effects of prolonged fixation in PLP or extended incubation in 70% alcohol post fixation were assessed by ICC methods. Tissues, which underwent these treatments, were compared with control tissues, from short fixation regimes in which good PrP immuno-labelling had been obtained.

Histopathological procedures

Protocols were established for the trimming, processing and embedding of the brain and spinal cord. Each brain was sliced in a caudal to rostral direction at 2 mm intervals using a rat brain mould (purchased from SEMAT Ltd., St. Albans) and the slices were laid proximal surface down into a single processing/embedding cassette (Fig. 1). The spinal cords were dissected out, with all dorsal root ganglia (DRG) attached, by the dorsal and ventral nerve roots. Firstly, using a dissecting microscope, tiny fragments of bone were gently removed to prevent scoring during section cutting. The nerve roots were then separated from each other. This involved separating meningeal membranes, which bound roots and cord closely together. The spinal cord was then sliced between each pair of roots from cervical to lumbar regions to form individual segments. Each segment of cord was marked with indian ink on the rostral side, placed in a sequentially numbered cassette for identification and processed according to standard laboratory procedures. The processed segments of cord for each case were then embedded together in one wax block, rostral surface uppermost, using a designated standard pattern (Figs. 2a–d).

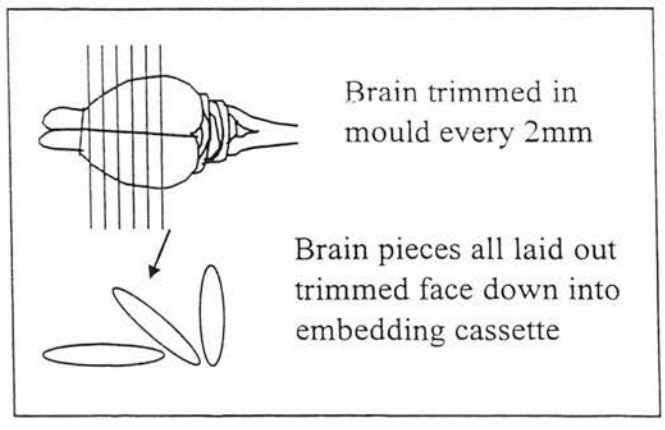

Figure 1. Coronal trimming of the hamster brain.

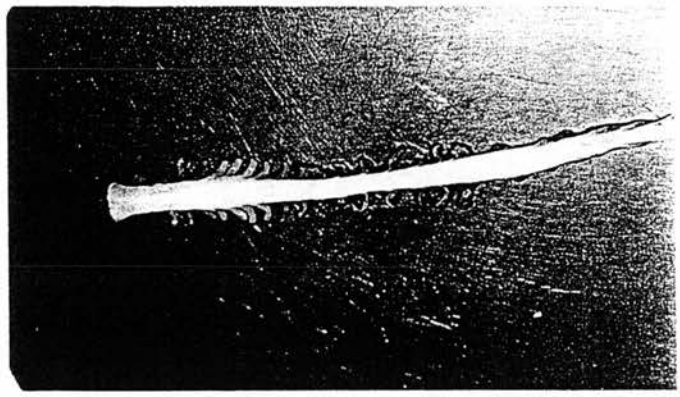

Figure 2a. Intact hamster spinal cord with dorsal root ganglia attached.

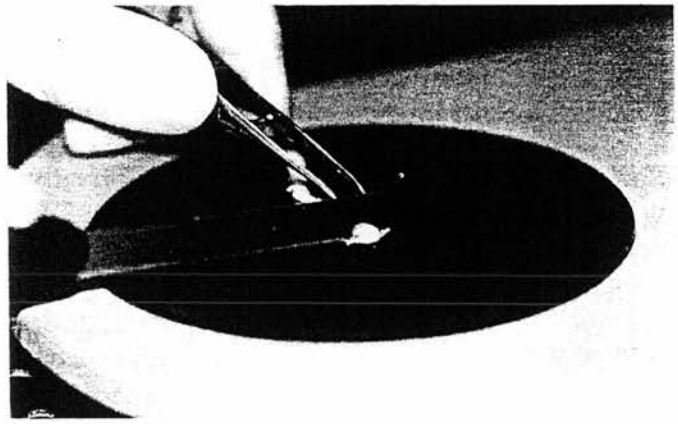

Figure 2b. Spinal cord being trimmed coronally between nerve roots.

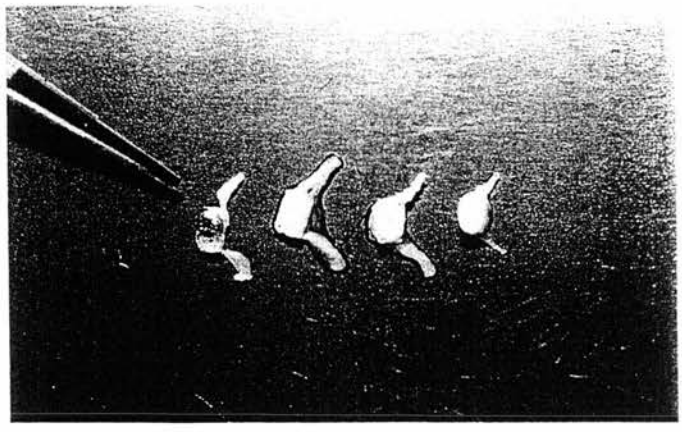

Figure 2c. Trimmed segments of spinal cord being marked with indian ink on the dorsal surface.

Combinations of histological stains were used for cellular recognition. Haematoxylin and Eosin (H&E) was used to assess general cellular morphology and to check the quality of fixation. Luxol Fast Blue (LFB) was combined with Cresyl Violet (CV) to demonstrate myelinated fibres and to identify differing neuronal populations.

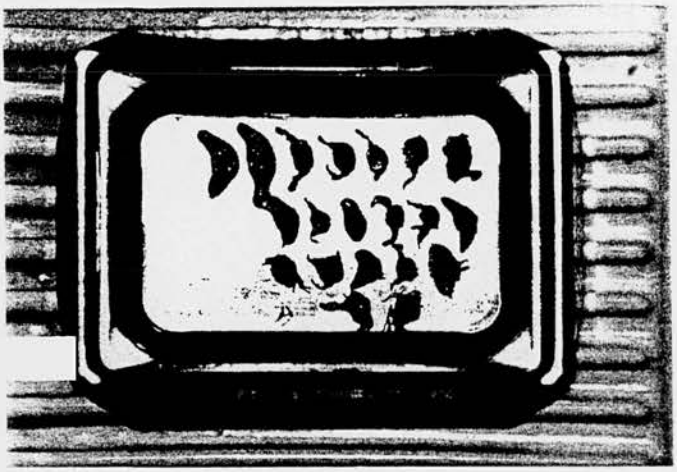

Figure 2d. Cervical and thoracic segments of hamster spinal cord, in an embedding cassette.

RESULTS

The effects of prolonged exposure to PLP fixative, or 70%, alcohol provided unexpected results. Long fixation in PLP (approximately 3 days) was detrimental to PrP demonstration by ICC. The transfer of tissues into 70% alcohol after a short fixation in PLP (5 to 7 hours) substantially improved ICC results. The latter protocol was therefore adopted for use in subsequent experiments.

The routine protocols established for the brain and spinal cord worked very well. Two-millimeter thick coronal slices of brain gave good representation of all major areas on one slide and allowed comparisons between slices within a single section. The preparation and orientation of the spinal cords were highly time consuming and required a great deal of attention to detail. However, every segment of the spinal cord, and most pairs of associated dorsal roots and ganglia, could be identified from cervical through to lumbar. Surprisingly, the spinal cord roots and the DRGs withstood all the histological procedures that they were subjected to, despite their microscopic size and their fragility. The morphology and cellular detail observed with the light microscope in both ICC and conventional histology sections were good.

The indirect two step and ABC elite ICC methods produced excellent labelling of both early deposits and late stage accumulations of PrP. At terminal stage, of the disease, abnormal PrP staining occurred in all sections of brain and spinal cord. All forms of PrP pathology were present and the distribution was as described in a previous study[8] (Fig. 3). Abnormal PrP was also labelled in the DRGs and appeared as small granular inclusions within several neurons and adjacent satellite cells. The indirect two step peroxidase method achieved good immunostaining results with a clear background. However, the ABC elite method was far more sensitive for detecting early deposits and subtle staining. A light brown background also occurred with the ABC method, but this was clearly distinguishable from PrP immunostaining and did not interfere with interpretation of the results.

The histological staining methods employed in this study, produced results appropriate to our aims. H&E demonstrated good cellular morphology. The LFB differentiated between myelinated fibres (stained blue) and unmyelinated fibres (unstained), and the CV counterstained neuronal populations violet (Fig. 4).

DISCUSSION

TSEs have been well researched over the years but little is understood about natural transmission of these diseases within and between species. It is known that after peripheral infection, including oral challenge, the brain and spinal cord are the ultimate target sites for TSEs. However, the exact route by which infection enters the CNS remains uncertain.

The aim of this study was to create protocols, which can be used in combination with ICC and conventional histological techniques, to accurately pinpoint the entry sites of scrapie disease into the brain and spinal cord and track the spread of the infection within these tissues: this has been successfully achieved.

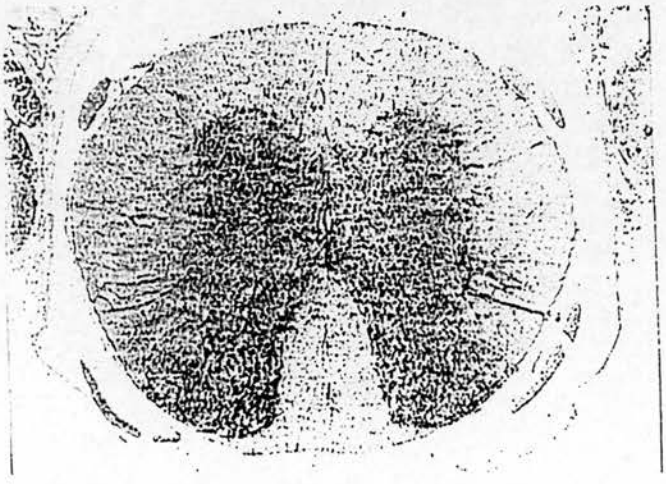

Figure 3. Strong PrP labelling throughout the grey matter of the spinal cord and tracking along fibres in the white matter.

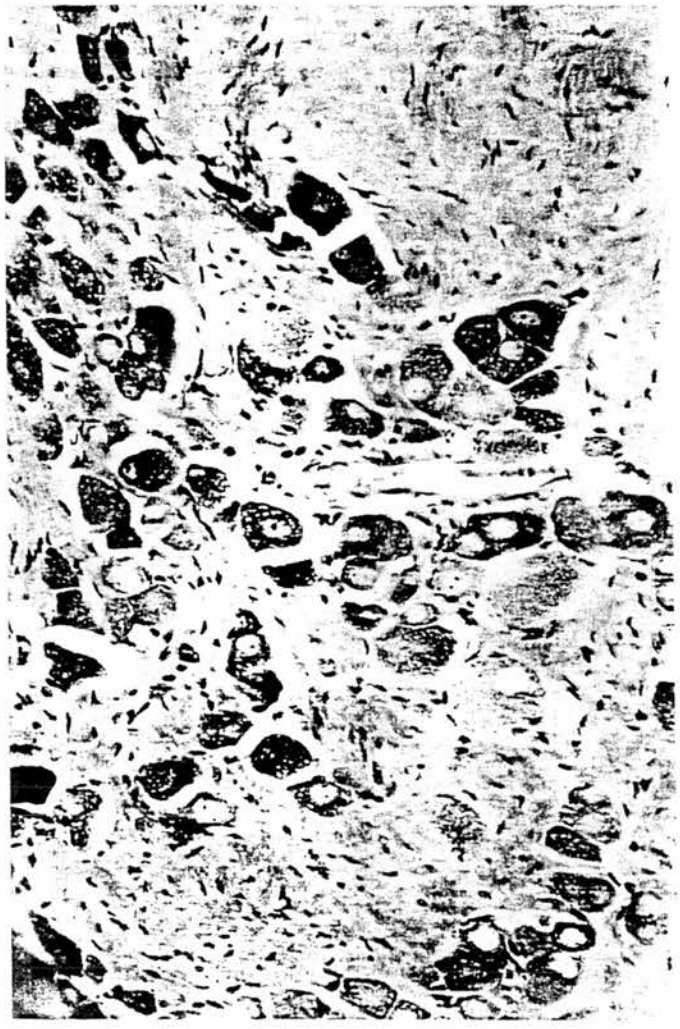

Figure 4. Dorsal root ganglion, from a hamster. LFB staining up myelinated nerve fibres, and CV staining up neuronal populations.

The importance of precise tissue fixation was highlighted by the preliminary ICC trials. These indicated that prolonged exposure of hamster tissues to PLP resulted in a detrimental effect on PrP immunolabelling. The transfer of tissues into 70% alcohol, after approximately 5 hours, allowed the sensitive detection of PrP, which was crucial to accurately pinpoint early deposits of protein.

The trimming, processing and embedding techniques developed for the brain and spinal cord accomplished high quality sections with good morphology and cellular detail. In the brain it was found that embedding thin coronal slices consecutively in a caudal to rostral direction allowed easy identification and comparison of adjacent regions. Semi-serial sectioning of the wax block also meant that all major brain areas were represented.

This study also proved that it was practicable to remove the spinal cord from hamsters and dissect between each pair of cervical and lumbar roots. Remarkably, the dorsal root ganglia remained attached via the nerve roots to the spinal cord and every segment of cord and associated ganglia could be accurately identified. These sections of cord could, with very steady hands, be embedded in paraffin wax, using a designated standard pattern for ease of subsequent recognition.

Histological demonstration of myelinated fibres and contrasting neuronal populations, within spinal cord sections, was achieved by LFB and CV. These reagents provided valuable information about the distribution of PrP in relation to the white and grey matter areas, when applied to adjacent ICC sections. H&E were chosen to show overall morphology. This familiar stain enabled the quality of the sections and the fixation to be analysed. The histology stains were useful for ascertaining the exact locations of early abnormal PrP deposits.

ICC studies confirmed that the ABC elite method was more sensitive than the indirect two step method for detecting early or subtle PrP deposits in orally infected hamster. The ABC elite method would therefore be adopted for future studies, using PrP as a marker for target sites and timing of the infection.

The technical methods defined in this study could be used to significantly improve understanding of the route taken by scrapie infection into the CNS. However, the protocols established need not be limited to hamster studies, nor to investigation of the oral route of scrapie disease. This study demonstrated that it is possible to pinpoint nerve routes and ganglia associated with every segment of spinal cord and to accurately label any infection present in these tissues. The potential application for these techniques in the field of scrapie research and other diseases of the CNS is considerable.

Acknowledgements

I would like to thank Michael Beekes from the Robert Koch Institute in Berlin, who supplied all the hamster tissues and anti-PrP antibody. Thanks also to Stephanie Collishaw, who helped with the processing and immunostaining of the tissues.

References

1. McBride PA, Wilson MI, Eikelenboom P, Tunstall A, Bruce ME. Heparan sulphate proteoglycan is associated with amyloid plaques and neuroanatomically targeted PrP pathology throughout the incubation period of scrapie-infected mice. Exp Neurol 1998; 149: 447–454.

2. Manson JC, Clarke AR, McBride PA, McConnell I, Hope J. PrP gene dosage determines the timing but not the final intensity or distribution of lesions in scrapie pathology. Neurodegeneration 1994; 3: 331–340.

3. Weissmann C, Bueler H, Fischer M, Sailer A, Aguet M. Susceptibility to scrapie in mice is dependent on PrPc. Philosophical Transactions of the Royal Society of London Biological Sciences 1994; 343: 431–433.

4. Bruce ME, Will RG, Ironside JW et al. Transmissions to mice indicate that 'new variant' CJD is caused by the BSE agent. Nature 1997; 389: 498–501.

5. Diringer H, Beekes M, Oberdieck U. The nature of the scrapie agent: the virus theory. Annals of the New York Academy of Sciences 1994; 724: 246–258.

6. Fraser H, Bruce M E, Davies D et al. The lymphoreticular system in the pathogenesis of scrapie. In Prion Diseases of Humans and Animals. pp. 308–317. Edited by SB Prusiner, J Collinge, J Powell et al. Chichester: Ellis Horwood 1992.

7. Beekes M, Baldauf E, Diringer H. Sequential appearance and accumulation of pathognomic markers in the central nervous system of hamsters orally infected with scrapie. J Gen Virol 1996; 77: 1925–1934.

8. Beekes M, McBride P A, Baldauf E. Cerebral targeting indicates vagal spread of infection in hamsters fed with scrapie. J Gen Virol 1998; 79: 601–607.

JOURNAL OF VIROLOGY, Oct. 2001, p. 9320–9327
0022-538X/01/$04.00+0 DOI: 10.1128/JVI.75.19.9320–9327.2001

Vol. 75, No. 19

Early Spread of Scrapie from the Gastrointestinal Tract to the Central Nervous System Involves Autonomic Fibers of the Splanchnic and Vagus Nerves

PATRICIA A. McBRIDE,[1]* WALTER J. SCHULZ-SCHAEFFER,[2]† MAURA DONALDSON,[1] MOIRA BRUCE,[1] H. DIRINGER,[3] HANS A. KRETZSCHMAR,[2] AND MICHAEL BEEKES[3]

Neuropathogenesis Unit, Institute for Animal Health, Edinburgh EH9 3JF, United Kingdom,[1] and Institut für Neuropathologie, 81377 Munich,[2] and Robert Koch-Institut, 13353 Berlin,[3] Germany

Received 19 March 2001/Accepted 11 June 2001

Although the ultimate target of infection is the central nervous system (CNS), there is evidence that the enteric nervous system (ENS) and the peripheral nervous system (PNS) are involved in the pathogenesis of orally communicated transmissible spongiform encephalopathies. In several peripherally challenged rodent models of scrapie, spread of infectious agent to the brain and spinal cord shows a pattern consistent with propagation along nerves supplying the viscera. We used immunocytochemistry (ICC) and paraffin-embedded tissue (PET) blotting to identify the location and temporal sequence of pathological accumulation of a host protein, PrP, in the CNS, PNS, and ENS of hamsters orally infected with the 263K scrapie strain. Enteric ganglia and components of splanchnic and vagus nerve circuitry were examined along with the brain and spinal cord. Bioassays were carried out with selected PNS constituents. Deposition of pathological PrP detected by ICC was consistent with immunostaining of a partially protease-resistant form of PrP (PrP^{Sc}) in PET blots. PrP^{Sc} could be observed from approximately one-third of the way through the incubation period in enteric ganglia and autonomic ganglia of splanchnic or vagus circuitry prior to sensory ganglia. PrP^{Sc} accumulated, in a defined temporal sequence, in sites that accurately reflected known autonomic and sensory relays. Scrapie agent infectivity was present in the PNS at low or moderate levels. The data suggest that, in this scrapie model, the infectious agent primarily uses synaptically linked autonomic ganglia and efferent fibers of the vagus and splanchnic nerves to invade initial target sites in the brain and spinal cord.

Although the clinical signs and pathological damage are indicative of central nervous system (CNS) disease, the most likely natural portal of entry of nonexperimental transmissible spongiform encephalopathy (TSE) infection is via the gastrointestinal (GI) tract. Bovine spongiform encephalopathy (BSE) and a new variant of Creutzfeldt-Jacob disease (vCJD) are linked (13, 25) and almost certainly entered their hosts via the food chain. However, little is known about how the pathogenic agent enters the GI tract and subsequently spreads to target sites in the CNS.

Evidence from natural (23, 46, 47) and experimental (2, 4, 5, 24, 30, 39) scrapie and BSE (48) implicates the peripheral nervous system (PNS) and the enteric nervous system (ENS) in the spread of the infectious agent to the CNS. In several peripherally infected rodent models of scrapie, including hamster 263K scrapie, the model of oral challenge used in this study, neural targeting of infection shows a pattern consistent with spread along visceral nerves.

A membrane-bound glycoprotein, PrP, is fundamental to the development of scrapie and related diseases (7, 11, 36). PrP mRNA and the normal cellular form of the protein (PrP^{C}) are widely expressed in the CNS (33, 35) and, less abundantly, in a number of adult and embryonic peripheral tissues (6, 15, 35, 41). A partially protease-resistant form of PrP (PrP^{Sc}) extracted from infected brains copurifies with infectivity (2, 3, 8, 16, 45). Disease-associated forms of PrP (variously termed abnormal or pathological PrP or PrP^{Sc}) accumulate in the CNS and a variety of extraneural tissues during the incubation periods of experimental and naturally occurring TSEs (5, 12, 18, 19, 37, 38, 39). When such disease-associated forms are shown to be associated with infectivity, as is the case in this study (2, 3), they may also be considered surrogate markers for an infectious agent.

Regardless of the initial mechanisms of uptake from extraneural sites, infectivity (29, 31) and pathological PrP (2, 3, 4) are first seen in the hindbrain and spinal cord of the CNS of rodents peripherally infected with scrapie. After oral challenge of hamsters with 263K scrapie, the earliest CNS target sites for pathological PrP deposition are the dorsal motor nucleus of the vagus nerve (DMNV) and the solitary tract nucleus (SN) of the brain and the gray matter of thoracic vertebrae 4 to 9 of the spinal cord (4). Subsequent spread of infection in the spinal cord occurs in both cranial and caudal directions (2, 3, 4, 29, 32), and at the end point of disease, most brain areas and all cervical and thoracic segments of the spinal cord and the corresponding dorsal root ganglion (DRG) contain substantial accumulations of pathological PrP (39). The presence of BSE agent in sensory ganglia of preclinical, orally challenged cows (48) or pathological PrP in sympathetic, sensory (39, 47) and enteric (1, 5, 46) ganglia of scrapie-fed hamsters and sheep with natural scrapie suggests that the PNS and the ENS harbor the infectious agent early in the disease process.

* Corresponding author. Mailing address: Institute for Animal Health, Neuropathogenesis Unit, Ogston Building, West Mains Rd., Edinburgh EH9 3JF, United Kingdom. Phone: 44(0)131 667 5204. Fax: 44(0)131 668 3872. E-mail: tricia.mcbride@bbsrc.ac.uk.

† Present address: Institute für Neuropathologie, 37075 Göttingen, Germany.

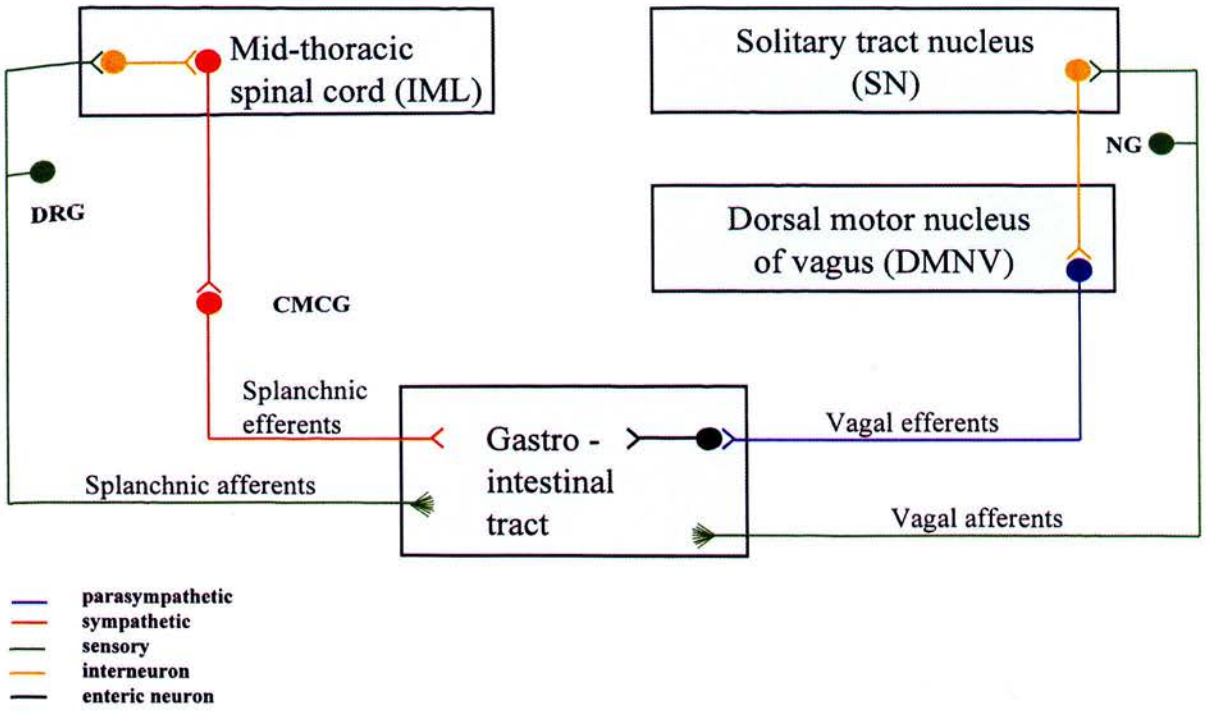

FIG. 1. Diagrammatic representation of the neural pathways that link the GI tract with the brain and spinal cord. Circuitry has been simplified to show major routes only. The infectious agent may reach the CNS by spreading along either efferent (motor) or afferent (sensory) fibers of vagus or splanchnic nerves. Efferent fibers of the vagus nerve have their nerve cell bodies in the DMNV and synapse with neurons of the ENS in ganglia of the submucosal and myenteric plexuses in the wall of the alimentary canal. The nerve cells of vagus nerve afferent fibers are located in the NG and directly innervate the alimentary canal. These fibers run to the SN, where they synapse with interneurons projecting to the DMNV. The cell bodies of splanchnic nerve efferent fibers are located in the IML and synapse with CMGC neurons that, in turn, innervate the GI tract. Afferent fibers of the splanchnic nerve originate in the DRG, run through the CMGC, and directly innervate target organs such as the alimentary canal. Adapted from reference 39, with permission from Elsevier Science.

It was previously proposed (4, 39) that the 263K scrapie agent reaches its initial target sites in the CNS by spreading, in a retrograde direction, along autonomic PNS pathways and ganglia supplying the viscera, i.e., along sympathetic and parasympathetic efferents of the splanchnic and vagus nerves (Fig. 1). To investigate this further, we carried out a time course study using our hamster model of 263K oral challenge and immunocytochemistry (ICC) and paraffin-embedded tissue (PET) blotting to identify and compare PrP deposition in the ENS, PNS, and CNS. Specific components of the vagus and splanchnic nerve circuitry were examined in addition to the brain and spinal cord, with which they form neuronal relay circuits. Jejunal and ileal ENS was included, as it forms synaptic links with both nerves. Selective bioassays were also carried out to assess the levels of infectivity in two key PNS components, the cervical vagus nerve and the celiac and mesenteric ganglion complex (CMGC).

Using these approaches, it was possible to identify the temporal sequence and location of PrP^{Sc} deposition within the CNS, PNS, and ENS and thereby to define the neuroanatomical pathways involved in early pathogenesis. The findings strongly support and expand our hypothesis that the infectious agent primarily uses autonomic ganglia and efferent fibers of the vagus and splanchnic nerves to reach and invade initial CNS target sites.

MATERIALS AND METHODS

Experimental design. Outbred Syrian hamsters were fed individual food pellets doused with 100 μl of a 10% hamster brain homogenate from 263K scrapie-infected donors or uninfected controls as previously described (2). For PrP studies, four or five hamsters were humanely sacrificed at specific time points throughout the incubation period: at 56, 62, 69, 76, 83, 90, 97, 104, 111, 118, 126, and 132 days postinfection (dpi) or at the clinical end point of disease (159 ± 4 [mean and standard error] dpi). Two mock-challenged hamsters, similarly fed with normal brain homogenate, were sacrificed at 161 dpi. For bioassay experiments, specimens were taken from five terminally ill and two mock-challenged hamsters.

Histological procedures. Hamsters were transcardially perfused with periodate-lysine-paraformaldehyde (PLP) (39). The brain and CMGC were removed from all hamsters. Spinal cord with attached DRG, jejunum, ileum (adjacent to the ileocecal sphincter), and left and right nodose ganglion (NG) with attached cervical vagus nerve were included from 69 dpi to the end point of disease. After perfusion, tissues were immersed for 5 h in PLP, transferred to and kept in 70% alcohol for a further 48 h, processed for 6 h in an enclosed tissue processor, and embedded in paraffin wax. Prior to processing and embedding, brains were trimmed coronally into 2-mm-thick slices using a brain slicing mold (SEMAT, St. Albans, United Kingdom). Spinal cords were sliced coronally between nerve roots to provide individual cervical, thoracic, and sometimes lumbar segments with corresponding left and right DRG. Pieces were marked on their cranial surface with India ink, numbered, and processed separately but embedded, in sequence, in one block (49). Sections (6 μm) of brain and spinal cord with attached DRG were taken at 100-μm intervals for PrP ICC, PET blot analysis, and cresyl violet-Luxol fast blue histochemistry. For other tissues these procedures were carried out either with serial sections or with sections taken at 50-μm intervals.

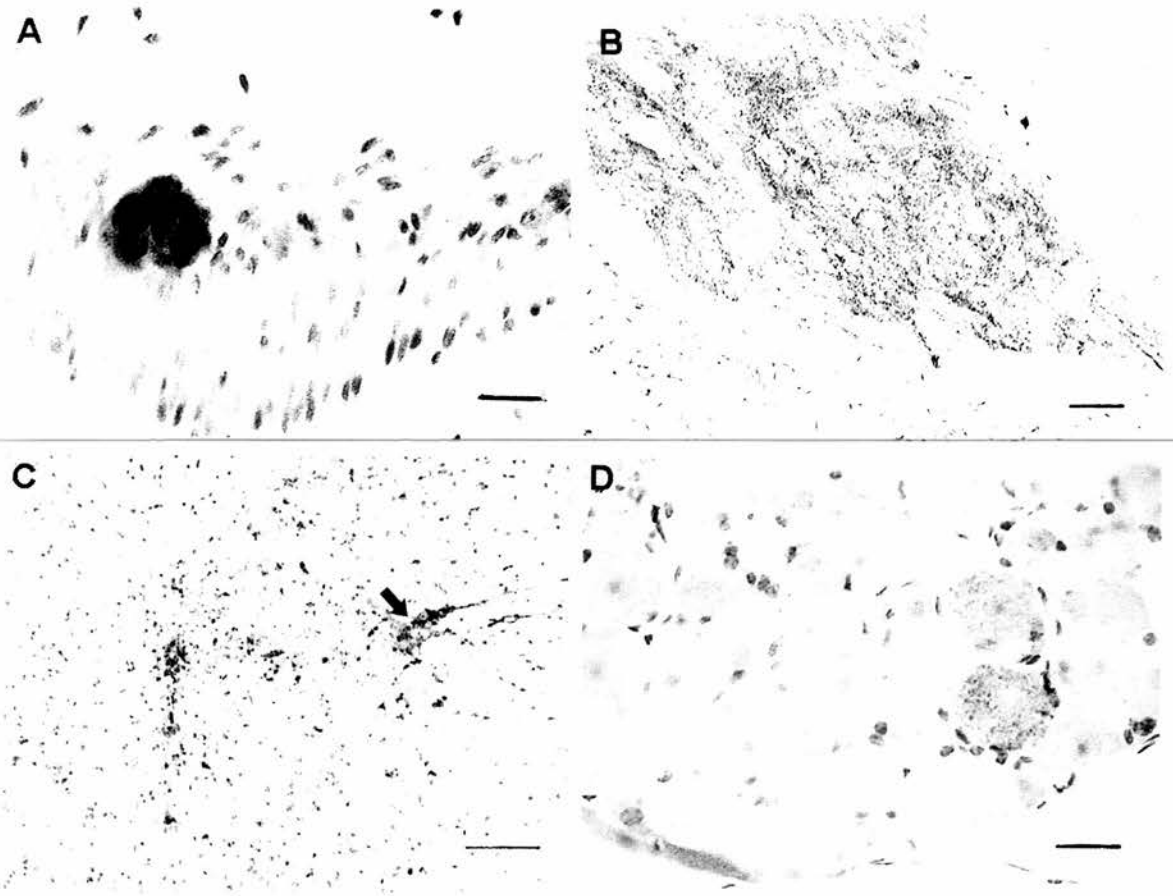

FIG. 2. PrP^{Sc} in the ENS and splanchnic nerve circuitry of the same hamster 90 days after oral challenge with 263K scrapie. (A) Myenteric ganglion. (B) CMGC. (C) Spinal cord segment T5 (arrow indicates IML). (D) DRG from segment T5. PrP^{Sc} deposition is already extensive in the ENS and CMGC but minimal in DRG. Scale bars: A and D, 20 μm; B, 50 μm; C, 100 μm.

ICC. Immunostaining was carried out according to the ABC method using mouse anti-hamster PrP monoclonal antibody 3F4 (27) or normal serum and diaminobenzidine to visualize the reaction product. Sections were pretreated with formic acid for 10 min to enhance PrP visualization. Similarly treated sections from mock-challenged hamsters served as control tissue.

PET blotting. Sections were mounted on nitrocellulose membranes (0.45 μm pore size; Bio-Rad Laboratories, Hemel Hempstead, Herts, United Kingdom), dried flat at room temperature (approximately 2 h), and incubated overnight at 37°C. PET blotting was carried out as described by Schulz-Schaeffer et al. (42). After being washed in Tris-buffered saline (TBS; 10 mM Tris-HCl, 100 mM NaCl [pH 7.8]) with 0.05% Tween 20, sections were digested with 250 μg of proteinase K/ml in a buffer containing 10 mM Tris-HCl (pH 7.8), 100 mM NaCl, and 0.1% (wt/vol) Brij 35 for 8 h at 55°C. Sections were then denatured with guanidine isothiocyanate. Immunostaining was carried out with mouse anti-hamster PrP antibody 3F4 and nitroblue tetrazolium (NBT)–5-bromo-4-chloro-3-indolylphosphate (BCIP) to visualize the reaction product. PET blots were assessed using a dissecting microscope.

Infectivity bioassays. Vagus nerve and CMGC samples were removed from two terminally ill animals (S1 and S2) and two mock-infected controls (N1 and N2). From another three terminally ill hamsters (S3 to S5) only vagus nerve samples were taken. Left and right portions (approximately 1 cm) of cervical vagus nerves were removed remote from the NG and carefully separated from surrounding tissue. The CMGC was removed attached to the abdominal aorta between the celiac, superior mesenteric, left renal, and right renal arteries. Two 0.5-cm pieces from the abdominal artery cranially and caudally adjacent to the CMGC were also taken. Samples were washed three times in TBS (10 mM Tris-HCl, 133 mM NaCl, pH 7.4), incubated at 37°C for 1.5 h in 200 μl of TBS containing 0.25% (wt/vol) collagenase (Boehringer Mannheim) and 0.025% (wt/vol) $CaCl_2$, and heated to 80°C for 10 min. The volume was adjusted to 500 μl with TBS. Aliquots (50 μl) were inoculated intracerebrally (i.c.) into groups of five recipient hamsters. Infectivity titers were estimated from the incubation periods using dose-response curves as previously described (3). The experiment was terminated at 370 dpi.

RESULTS

Early temporal and spatial deposition of PrP^{Sc} in enteric, splanchnic, and vagus nerve relays. Although the amounts of PrP^{Sc} varied between individuals culled at a given time point, the site and sequence of deposition were consistent. PrP^{Sc} was found earlier and with more frequency in autonomic (i.e., efferent) components of the circuitry than in sensory components. In the splanchnic nerve circuitry, PrP^{Sc} was seen in the CMGC and intermediolateral cell column (IML) of the spinal cord before DRG; in the vagus nerve circuitry, it was seen in the DMNV before NG. The ENS contains autonomic and sensory NS networks. Table 1 summarizes the temporal and spatial deposition of PrP^{Sc} in enteric, splanchnic, and vagus nerve relays.

(i) ENS. PrP^{Sc} was found from the earliest available time point (69 dpi) to the end point of disease in and around neurons of the myenteric and submucosal plexuses of the ileum and jejunum of all four hamsters (Fig. 2A). As the incubation period progressed, accumulations increased in individual ganglia, and the number of affected ganglia increased.

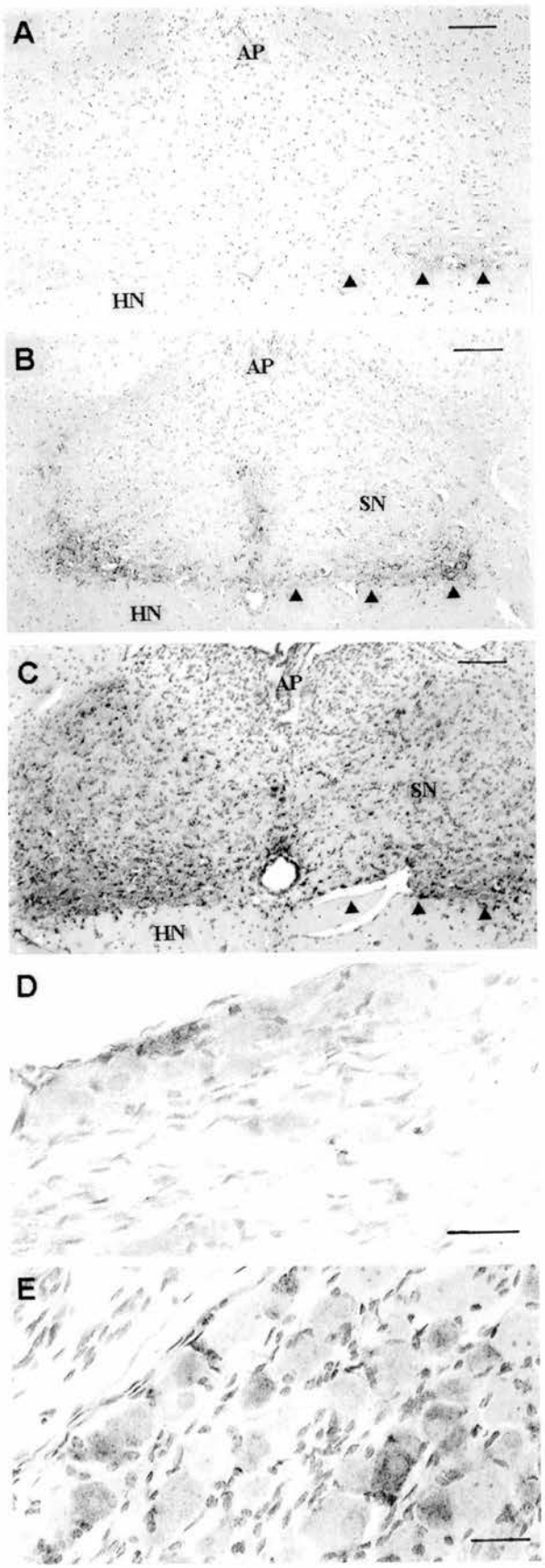

(ii) Splanchnic nerve circuitry (CMGC-IML-DRG). PrP^{Sc} was observed in the CMGC of all four hamsters at the first time point of 56 dpi (Table 1). Initial deposits were few, but PrP^{Sc} accumulated rapidly. By 76 dpi, deposition was substantial, and by 90 dpi, strongly labeled PrP^{Sc} was apparent throughout most of the complex (Fig. 2B). In the spinal cord, PrP^{Sc} was invariably seen in the IML at 69 dpi, the earliest time point at which the cord was available. Deposition was present in thoracic cord segments 3 to 8, with the largest amounts in the IML of segments 5, 6, and 7 (Fig. 2C). PrP^{Sc} was not detected in DRG until 76 dpi (two out of four hamsters). At later time points, deposition remained scant and the amount was always less than that in the corresponding IML (Fig. 2D). In all instances, PrP^{Sc} was found in DRG only after accumulations were fairly widespread within the corresponding cord segments.

(iii) Vagus nerve circuitry (DMNV-SN-NG). In the brain, the first PrP^{Sc} deposits were seen in and around neurons of the DMNV at 62 dpi (two out of four brains) and the commissural portion of the SN (one out of four brains). Deposition was minimal in both areas but was greater in the DMNV. At later time points, accumulations were typically greater in the DMNV than in the SN (Fig. 3A to C). PrP^{Sc} was either present at low levels or undetected in NG until 90 dpi (Fig. 3D), and even at this time the numbers of positively labeled cells were, at best, only moderate. As with DRG (and in contrast to the CMGC), accumulation was slow, and at the end point of disease, several neurons remained unlabeled (Fig. 3E).

Subsequent pattern of PrP^{Sc} accumulation in the PNS and the CNS. Subsequent to the IML, PrP^{Sc} was observed in the intermediate zone at 69 dpi and then extending from the IML into the adjacent white matter at 76 dpi. Accumulations became progressively greater in the initial sites and generally more widespread within ventral and dorsal gray matter. Concurrently, PrP^{Sc} appeared in the IML of thoracic segments located cranial and caudal to those first affected. This pattern of spread continued with increasing incubation, and at late stages of disease, all infected hamsters showed marked granular deposition of PrP^{Sc} throughout the brain and entire gray matter "butterfly" of each cervical, thoracic and, where present, lumbar spinal cord segment.

Once accumulation was established in the DMNV and commissural portion of the SN, PrP^{Sc} was observed in medial and intermediate regions of the SN and then in other specific brain stem nuclei, notably the medullary reticular formation (76 dpi) and vestibular complex, pons, and red nucleus (83 dpi). Labeling was then rapidly disseminated to several other sites throughout the brain.

Throughout the incubation period, the sequence and spatial

FIG. 3. PrP^{Sc} immunolabeling in the vagus nerve circuitry of hamsters orally challenged with 263K scrapie agent. Sequential accumulation in DMNV-SN (A to C) and NG (D and E) is shown. (A) 76 dpi. (B and C) 90 dpi. The amounts of PrP^{Sc} vary between individuals culled at any time point, but the sequence of deposition is consistent. Deposition is more abundant in the DMNV (arrowheads) than in the adjacent SN. The area postrema (AP) and hypoglossal nucleus (HN) are largely unlabeled. (D) Right NG at 90 dpi. (E) Right NG at end stage of disease; several sensory NG neurons remain unlabeled. Scale bars: A to C, 100 μm; D and E, 30 μm.

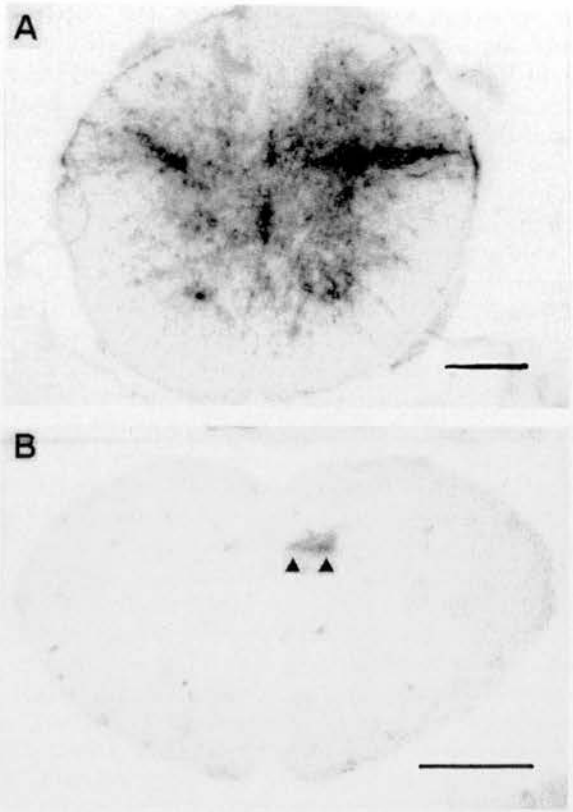

FIG. 4. Early PrP^{Sc} deposition (blue-black) in the IML and DMNV of hamsters orally challenged with 263K scrapie, as demonstrated by PET blotting. (A) IML at 90 dpi. (B) DMNV (arrowheads) at 76 dpi. Specimens represent sections adjacent or nearly adjacent to those in Fig. 2C (A) and 3A (B). Scale bars: A, 200 μm; B, 1 mm.

precision of targeting were consistent. The final PrP^{Sc} distribution pattern was reproduced in all brains, spinal cords, and ganglia and was identical to that described previously for hamsters orally infected with 263K (4, 39). PrP^{Sc} was not found in vagus, splanchnic, or spinal nerve roots, apart from a tiny amount in the vagus nerve of one terminally ill hamster. In mock-infected control hamsters, PrP^{C}, which differs in appearance from the characteristic granular forms of PrP^{Sc} (4, 5, 38, 39), was seen only in some neuronal cell bodies of the brain and the spinal cord. Staining was absent from tissues when normal serum replaced PrP antibody.

Although cellular detail cannot be resolved with PET blots, aggregations of protease-resistant PrP (PrP^{Sc}) were seen at the same sites in all tissues and at all time points that immunostaining was detected in adjacent ICC sections. However, in PET blots, deposits were stained more intensely by the blue-black chromogen and were more easily detected at low power than corresponding ICC-labeled deposits (Fig. 4).

Scrapie infectivity in the vagus and splanchnic nerve circuitry. Two PNS components, the cervical vagus nerve and the CMGC, were analyzed by bioassays for the presence of infectivity. Samples of the vagus nerve were excised from a position remote from NG to avoid the inclusion of ganglion cell bodies.

The results for the vagus nerve samples are summarized in Table 2. Mortality and incubation time for the recipients in the bioassays demonstrated a low but consistent presence of infectivity in the cervical vagus nerve trunks. The estimated amount of infectivity was approximately 10^2 50% i.c. infective doses ($ID_{50i.c.}$), corresponding to about 10^5 $ID_{50i.c.}$ per g of tissue.

Infectivity levels in the two CMGC samples (Table 3) were higher (approximately 10^3 and 10^4 $ID_{50i.c.}$), even though the CMGC represented only a minor constituent of the homogenized tissue samples. Artery samples were located cranially or caudally adjacent to the CMGC. The trace levels of infectivity detected for these control specimens probably originated from residual CMGC nervous tissue.

DISCUSSION

We used ICC, PET blotting, and selective infectivity assays in a time course study to determine the temporal sequence and location of scrapie infection in the ENS, splanchnic and vagal PNS, and CNS of hamsters after oral challenge with scrapie strain 263K. While bioassays provide the gold standard for detection of the scrapie agent per se, ICC and PET blot analyses facilitate studies on the spread of infection by using disease-associated forms of PrP (pathological PrP or PrP^{Sc}) as surrogate markers for infectivity. A close correlation between infectivity and PrP^{Sc} has been previously established in our animal model (2, 3).

Available antibodies are unable to discriminate between host- and disease-associated forms of PrP in histologically processed tissues. We can distinguish pathological PrP from PrP^{C} by differences in morphological appearance and distribution (4, 38, 39), but until now there was no formal proof that the disease-associated PrP detected by ICC corresponded to PrP^{Sc}. PET blot pretreatments destroy PrP^{C}, leaving only the proteinase K-resistant fraction (42). Here, the deposits visualized by

TABLE 1. Presence of PrP^{Sc} in enteric, splanchnic, and vagus nerve relays after ingestion of 263K scrapie

	No. of hamsters affected/no. challenged							
dpi[a]	Enteric ganglia	CMGC	Mid-T IML[b]	Mid-T DRG[b]	DMNV	SN	Right NG	Left NG
56	ND	4/4	ND	ND	0/4	0/4	ND	ND
62or63	ND	4/4	ND	ND	2/4	1/4	ND	ND
69	4/4	4/4	4/4	0/4	4/4	2/4	1/4	0/4
76	4/4	4/4	4/4	2/4	4/4	1/4	3/4	1/2[c]
83	4/4	4/4	4/4	3/4	3/3[c]	3/3[c]	3/4	2/4
90	4/4	4/4	4/4	3/4	4/4	3/4	3/4	4/4

[a] Early time points are shown (the incubation period was ~160 dpi).
[b] Mid-T IML and mid-T DRG, = IML from thoracic cord segments 3 to 8 with corresponding DRG; ND, not done.
[c] There were four animals in the group, but the region was present only in the specified number of animals.

TABLE 2. Detection of infectivity in cervical trunks of the vagus nerve by bioassays[a]

Donor	Vagus nerve sample	Incubation time (days)		Estimated titer ($ID_{50i.c.}$/sample)[b]
		Range	Mean ± SE	
S1	Left	119–292	162 ± 30	$10^{1.3}$
	Right	117–155	126 ± 7	$10^{2.7}$
S2	Left	117–239	144 ± 22	$10^{1.8}$
	Right	117–180	134 ± 11	$10^{2.3}$
S3	Left	120–260	151 ± 25	$10^{1.6}$
	Right	131–222	167 ± 18	$10^{1.3}$
S4	Left	131–183	159 ± 10	$10^{1.5}$
	Right	127–152	139 ± 4	$10^{2.0}$
S5	Left	124–242	153 ± 20	$10^{1.6}$
	Right	145–274	190 ± 21	$<10^{1.2}$

[a] Aliquots (50 μl) of homogenized left and right vagus nerves from terminally ill hamsters orally challenged with 263K were inoculated i.c. into groups of five recipients. Mortality was 100%. Recipients similarly inoculated with vagus nerves from donors previously orally mock infected with normal brain homogenate showed no clinical signs of scrapie. The experiment was terminated at 370 dpi.

[b] Total amount of infectivity in one equivalent of excised tissue, i.e., the entire donor sample, calculated by applying mean incubation time to a dose-response curve.

ICC were consistent with the PrP^{Sc} immunostaining in adjacent PET blots, even at early stages of incubation. These results provide strong evidence that pathological PrP detected by our ICC method is PrP^{Sc}.

Based on a series of studies examining the pathogenesis of 263K scrapie after oral challenge in hamsters, we proposed that the infectious agent reaches its initial CNS target sites by spreading in a retrograde direction along autonomic PNS pathways and ganglia supplying the viscera, i.e., along sympathetic and parasympathetic efferents of the splanchnic and vagus nerves (4, 39). Large parts of the alimentary canal, in particular, the esophagus, stomach, small intestine, and ascending colon, are innervated by these two nerves (17, 21), which contain fibers of autonomic (efferent) and sensory (afferent) neurons. With the neuroanatomy of the splanchnic and vagus nerve circuitry in mind (Fig. 1), the location, timing, and progression of PrP^{Sc} deposition revealed by this study strongly support and expand our hypothesis. PrP^{Sc} appeared and accumulated in a predictable temporal sequence in specific sites that accurately reflect the described autonomic and sensory relays. Deposition was always present in the CMGC and IML before the corresponding DRG. The same holds true with respect to the DMNV and NG. The results also show that, at least in this animal model, the ENS may be a key portal of entry for the infectious agent into the splanchnic and vagus nerve circuitry. As efferent and afferent fibers of both vagus and splanchnic nerves contact myenteric ganglia (17, 21), these would be the most likely sites for ENS-mediated neuroinvasion. However, infection may occur via intestinal nerve terminals not linked to ENS ganglia or other visceral tissues.

Our findings suggest that after uptake from the GI tract, the infectious agent primarily spreads by two neuroanatomical pathways: (i) along the vagus nerve to the DMNV in the brain and (ii) along the splanchnic nerve to the IML of the midthoracic spinal cord. Intramural ganglia of the gut and the CMGC are respective intervening relay points (Fig. 5). Within the CNS, the infectious agent probably travels along interneurons and sensory afferents to the SN-NG and the DRG, respectively. The reproducibility and spatial precision of PrP^{Sc} deposition indicate that spread is not random but occurs in a stepwise fashion along the synaptically linked neuronal populations. The observations indicate that initial spread occurs in a retrograde direction along efferent motor pathways, but dual efferent and sensory spread to the brain is also a possibility. The observed pattern of spread shows striking similarities to that of conventional neurotropic viruses, such as herpes simplex virus type 1 (22, 34), reovirus serotype 3 isolate T3C9 (40), and pseudorabies virus (14).

The most logical way for PrP^{Sc} to spread along peripheral nerves is by established axonal transport mechanisms. Several studies have reported that scrapie spreads within the nervous system by means of axonal pathways (20, 28), and the suggested rate of spread (0.5 to 2 mm/day) is consistent with that of slow axonal transport (10, 29, 44). It has been claimed that PrP^{C} can be transported in an anterograde direction along peripheral nerve axons (9), but it is not known whether PrP^{Sc} is so transported. Transportation per se was not formally established in this study, but the evidence presented here would be compatible with this. While an abundance of PrP^{Sc} was detected in association with cell bodies of CNS neurons or peripheral ganglia, deposition in nerves (cell processes) was minimal or undetected, even at the terminal stage of disease. The low levels of infectivity found at the end stage of disease in vagus nerves compared to those found in the brain or CMGC are a further indication that in nerve fibers, the agent is in transit rather than being actively replicated.

The study did not reveal any evidence for hematogenous spread of infection to the brain. PrP^{Sc} was not detected early in infection at sites with an impaired blood-brain barrier, such as the area postrema (Fig. 3) or the choroid plexus. In addition, routing via the blood would not be consistent with the observed selectivity of targeting.

Infection via the oral route is strongly indicated (but not formally proven) in vCJD, BSE, and natural scrapie. Disease-

TABLE 3. Detection of infectivity in the CMGC and adjacent parts of the abdominal aorta[a]

Donor	Sample	Mortality in bioassay	Incubation (days)		Estimated titer ($ID_{50i.c.}$/sample)[b]
			Range	Mean ± SE	
S1	CMGC	5/5	100–107	104 ± 1	$10^{4.1}$
	Cran. A.	1/5	318		
	Caud. A.	1/5	156		
S2	CMGC	5/5	107–128	118 ± 4	$10^{3.1}$
	Cran. A.	1/5	230		
	Caud. A.	5/5	120–240	171 ± 24	$10^{1.2}$

[a] Aliquots (50 μl) of homogenized CMGC and cranially (Cran.) or caudally (Caud.) adjacent artery (A.) from terminally ill donors orally challenged with 263K were inoculated i.c. into groups of five recipients. Mortality is given as number of hamsters that succumbed to infection/number challenged. Recipients similarly inoculated with CMGC from donors previously orally mock infected with normal brain homogenate showed no clinical signs of scrapie. The experiment was terminated at 370 dpi.

[b] Total amount of infectivity in one equivalent of excised tissue, i.e., in the entire donor sample, calculated by applying mean incubation time to a dose-response curve.

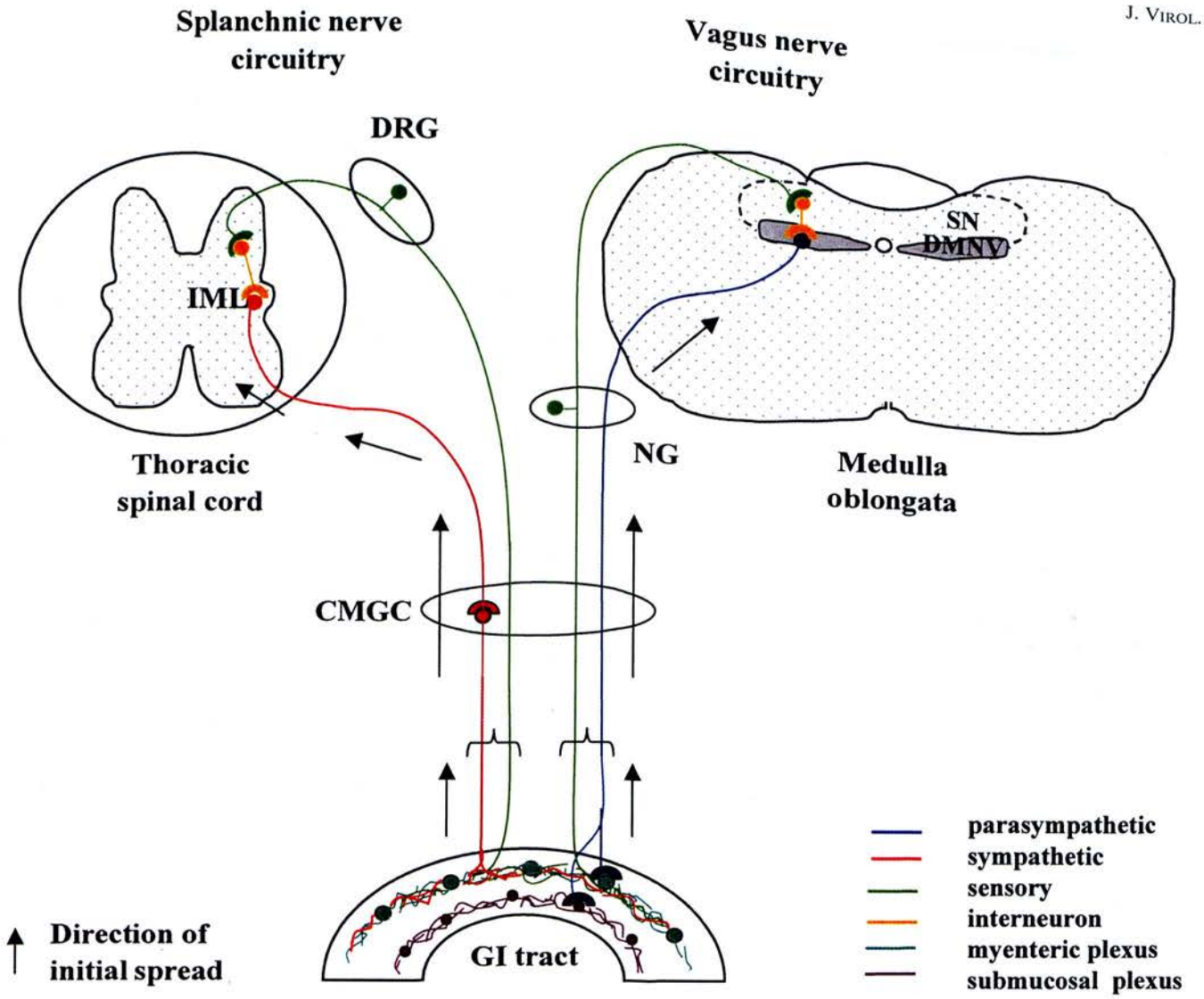

FIG. 5. Pictorial representation of the neuronal pathways used in the oral routing of 263K scrapie. Initial spread (arrows) occurs in a retrograde direction along sympathetic and parasympathetic fibers of the splanchnic and vagus nerves. Enteric and abdominal ganglia (CMCG) have an early involvement in pathogenesis.

specific PrP is found in the DMNV as a characteristic feature of both vCJD (26) and early BSE (43) infections, and spreading pathways similar to those described here have been described recently for sheep with natural scrapie (47). As the pattern of pathological PrP deposition in these nonexperimental infections closely resembles that observed in orally transmitted hamster scrapie, our findings provided new indirect evidence that vCJD in humans, BSE in cattle, and natural scrapie in sheep were caused by ingestion of TSE agent. The findings reported here for experimental 263K hamster scrapie strongly indicate that after oral challenge, infection of the CNS occurs via the splanchnic and vagus nerves. As similar pathogenic mechanisms are likely to operate in other orally acquired TSEs, this work provides baseline information about the peripheral routing of infection and a rodent model with which to study it.

ACKNOWLEDGMENTS

The skillful technical assistance of Marion Joncic and Stephanie Collishaw is gratefully acknowledged.

This work was supported by the Biotechnology and Biological Sciences Research Council (BBSRC) and in part by grants from the German Bundesministerium für Bildung und Forschung and the German Bundesministerium für Gesundheit.

REFERENCES

1. **Andréoletti, O., P. Berthon, D. Marc, P. Sarradin, J. Grosclaude, L. van Keulen, F. Schelcher, J.-M. Elsen, and F. Lantier.** 2000. Early accumulation of PrP^{Sc} in gut-associated lymphoid and nervous tissues of susceptible sheep from a Romanov flock with natural scrapie. J. Gen. Virol. **81:**3115–3126.
2. **Baldauf, E., M. Beekes, and H. Diringer.** 1997. Evidence for an alternative direct route of access for the scrapie agent to the brain bypassing the spinal cord. J. Gen. Virol. **78:**1187–1197.
3. **Beekes, M., E. Baldauf, and H. Diringer.** 1996. Sequential appearance and accumulation of pathognomonic markers in the central nervous system of hamsters orally infected with scrapie. J. Gen. Virol. **77:**1925–1934.
4. **Beekes, M., P. A. McBride, and E. Baldauf.** 1998. Cerebral targeting indi-

cates vagal spread of infection in hamsters fed with scrapie. J. Gen. Virol. **79:**601–607.
5. **Beekes, M., and P. A. McBride.** 2000. Early accumulation of pathological PrP in the enteric nervous system and gut-associated lymphoid tissue of hamsters orally infected with scrapie. Neurosci. Lett. **278:**181–184.
6. **Bendheim, P. E., H. R. Brown, R. D. Rudelli, L. J. Scala, N. L. Goller, G. Y. Wen, R. J. Kascsak, N. R. Cashman, and D. C. Bolton.** 1992. Nearly ubiquitous tissue distribution of the scrapie agent precursor protein. Neurology **42:**149–156.
7. **Beuler, H., A. Aguzzi, A. Sailer, R.-A. Greiner, P. Autenreid, M. Aguet, and C. Weissmann.** 1993. Mice devoid of PrP are resistant to scrapie. Cell **73:**1339–1347.
8. **Bolton, D. C., M. P. McKinley, and S. B. Prusiner.** 1982. Identification of a protein that purifies with the scrapie prion. Science **218:**1309–1311.
9. **Borchelt, D. R., V. E. Koliatsos, M. Guarnieri, C. A. Pardo, S. S. Sisodia, and D. L. Price.** 1994. Rapid anterograde axonal transport of the cellular prion glycoprotein in the peripheral and central nervous systems. J. Biol. Chem. **269:**14711–14714.
10. **Brady, S. T.** 1991. Molecular motors in the nervous system. Neuron **7:**521–533.
11. **Brandner, S., S. Isenmann, A. Raeber, M. Fischer, A. Sailer, Y. Kobayashi, S. Marino, C. Weissmann, and A. Aguzzi.** 1996. Normal host prion protein necessary for scrapie-induced neurotoxicity. Nature **379:**339–343.
12. **Bruce, M. E., P. A. McBride, and C. F. Farquhar.** 1989. Precise targeting of the pathology of the sialoglycoprotein, PrP, and vacuolar degeneration in mouse scrapie. Neurosci. Lett. **102:**1–6.
13. **Bruce, M. E., R. G. Will, J. W. Ironside, I. McConnell, D. Drummond, A. Suttie, L. McCardle, A. Chree, J. Hope, C. Birkett, S. Cousens, H. Fraser, and C. J. Bostock.** 1997. Transmissions to mice indicate that 'new variant' CJD is caused by the BSE agent. Nature **389:**498–501.
14. **Card, J. P., L. Rinaman, J. S. Schwaber, R. R. Miselis, M. E. Whealy, A. K. Robbin, and L. W. Enquist.** 1990. Neurotropic properties of pseudorabies virus: uptake and transneuronal passage in the rat central nervous system. J. Neurosci. **10:**1974–1994.
15. **Caughey, B., R. Race, and B. Chesebro.** 1988. Detection of prion protein mRNA in normal and scrapie-infected tissues and cell lines. J. Gen. Virol. **69:**711–716.
16. **Diringer, H., H. Gelderblom, H. Himert, M. Ozel, and C. Edelbluth.** 1983. Scrapie infectivity, fibrils and low molecular weight protein. Nature **306:**476–478.
17. **Dockray, G. J.** 1999. The brain-gut axis, p. 67–81. *In* T. Yamada (ed.), Textbook of gastroenterology, 3rd ed. Lippincott, Williams & Wilkins, Philadelphia, Pa.
18. **Farquhar, C. F., J. Dornan, R. A. Somerville, A. M. Tunstall, and J. Hope.** 1994. Effect on *Sinc* genotype, agent isolate and route of infection on the accumulation of protease-resistant PrP in non-central nervous system tissues during the development of murine scrapie. J. Gen. Virol. **75:**495–504.
19. **Foster, J. D., M. Wilson, and N. Hunter.** 1996. Immunolocalisation of the prion protein (PrP) in the brains of sheep with scrapie. Vet. Rec. **139:**512–515.
20. **Fraser, H., and A. G. Dickinson.** 1985. Targeting of scrapie lesions and spread of agent via the retino-tectal projection. Brain Res. **346:**32–41.
21. **Furness, J. B., J. C. Bornstein, W. A. A. Kunze, and N. Clerc.** 1999. The enteric nervous system and its extrinsic connections, p. 11–35. *In* T. Yamada (ed.), Textbook of gastroenterology, 3rd ed. Lippincott, Williams & Wilkins, Philadelphia, Pa.
22. **Gesser, R. M., and S. C. Koo.** 1996. Oral inoculation with herpes simplex virus type 1 infects enteric neurons and mucosal nerve fibers within the gastrointestinal tract in mice. J. Virol. **70:**4097–4102.
23. **Groschup, M. H., F. Weiland, O. C. Straub, and E. Pfaff.** 1996. Detection of scrapie agent in the peripheral nervous system of a diseased sheep. Neurobiol. Dis. **3:**191–195.
24. **Groschup, M. H., M. Beekes, P. A. McBride, M. Hardt, J. A. Hainfellner, and H. Budka.** 1999. Deposition of disease-associated prion protein involves the peripheral nervous system in experimental scrapie. Acta Neuropathol. **98:**453–457.
25. **Hill, A. F., M. Desbruslais, S. Joiner, K. C. L. Sidle, I. Gowland, J. Collinge, L. J. Doey, and P. Lantos.** 1997. The same prion strain causes vCJD. Nature **389:**448–450.
26. **Ironside, J. W.** 2000. Pathology of variant Creutzfeldt-Jacob disease. Arch. Virol. Suppl. **16:**143–151.
27. **Kascsak, R. J., R. Rubenstein, P. A. Merz, M. Tonna-Demasi, R. Fersko, R. I. Carp, H. M. Wisniewski, and H. Diringer.** 1987. Mouse polyclonal and monoclonal antibodies to scrapie-associated fibril protein. J. Virol. **61:**3688–3693.
28. **Kimberlin, R. H., and C. A. Walker.** 1980. Pathogenesis of mouse scrapie: evidence for neural spread of infection to the CNS. J. Gen. Virol. **51:**183–187.
29. **Kimberlin, R. H., and C. A. Walker.** 1982. Pathogenesis of mouse scrapie: patterns of agent replication in different parts of the CNS following intraperitoneal infection. J. Soc. Med. **75:**618–624.
30. **Kimberlin, R. H., H. Field, and C. A. Walker.** 1983. Pathogenesis of mouse scrapie: evidence for spread of infection to central from peripheral nervous system. J. Gen. Virol. **64:**713–716.
31. **Kimberlin, R. H., and C. A. Walker.** 1986. Pathogenesis of scrapie (strain 263K) in hamsters infected intracerebrally, intraperitoneally or intraocularly. J. Gen. Virol. **67:**255–263.
32. **Kimberlin, R. H., and C. A. Walker.** 1989. Pathogenesis of scrapie in mice after intragastric infection. Virus Res. **12:**213–220.
33. **Kretzschmar, H. A., S. B. Prusiner, L. E. Stowring, and S. J. DeArmond.** 1986. Scrapie prion proteins are synthesised in neurones. Am. J. Pathol. **122:**1–5.
34. **Krinke, G. J., and F. M. Dietrich.** 1990. Transneuronal spread of intraperitoneally administered herpes simplex virus type 1 from the abdomen via the vagus nerve to the brains of mice. J. Comp. Pathol. **103:**301–306.
35. **Manson, J. C., P. A. McBride, and J. Hope.** 1992. Expression of the PrP gene in the brain of *Sinc* congenic mice and its relationship to the development of scrapie. Neurodegeneration **1:**45–52.
36. **Manson, J. C., A. R. Clarke, P. A. McBride, I. McConnell, and J. Hope.** 1994. PrP gene dosage determines the timing but not the final intensity or distribution of lesions in scrapie pathology. Neurodegeneration **3:**331–340.
37. **McBride, P. A., P. Eikelenboom, G. Kraal, H. Fraser, and M. E. Bruce.** 1992. PrP protein is associated with follicular dendritic cells of spleens and lymph nodes in uninfected and scrapie-infected mice. J. Pathol. **168:**413–418.
38. **McBride, P. A., M. I. Wilson, P. Eikelenboom, A. Tunstall, and M. E. Bruce.** 1998. Heparan sulphate proteoglycan is associated with amyloid plaques and neuroanatomically targeted PrP pathology throughout the incubation period of scrapie-infected mice. Exp. Neurol. **149:**447–454.
39. **McBride, P. A., and M. Beekes.** 1999. Pathological PrP is abundant in sympathetic and sensory ganglia of hamsters fed with scrapie. Neurosci. Lett. **265:**135–138.
40. **Morrison, L. A., R. L. Sidman, and B. N. Fields.** 1991. Direct spread of reovirus from the intestinal lumen to the central nervous system through vagal autonomic nerve fibers. Proc. Natl. Acad. Sci. USA **88:**3852–3856.
41. **Oesch, B., D. Westaway, M. Walchi, M. P. McKinley, S. B. H. Kent, R. Aebersold, R. A. Barry, D. B. Teplow, D. B. Tempst, L. E., Hood, S. B. Prusiner, and C. Weissmann.** 1985. A cellular gene encodes scrapie PrP 27–30 protein. Cell **40:**735–746.
42. **Schulz-Schaeffer, W. J., S. Tschöke, N. Kranefuss, W. Dröse, D. Hause-Reitner, A. Giese, M. H. Groschup, and H. A. Kretzschmar.** 2000. The paraffin-embedded tissue blot detects PrP^{Sc} early in the incubation time in prion diseases. Am. J. Pathol. **156:**51–56.
43. **Schulz-Schaeffer, W. J., R. Fatzer, M. Vandevelde, and H. A. Kretzschmar.** 2000. Detection of PrP^{Sc} in subclinical BSE with the paraffin-embedded tissue (PET) blot. Arch. Virol. Suppl. **16:**173–180.
44. **Scott, J. R., D. Davies, and H. Fraser.** 1992. Scrapie in the central nervous system: neuroanatomical spread of infection and *Sinc* control of pathogenesis. J. Gen. Virol. **73:**1637–1644.
45. **Somerville, R. A., P. A. Merz, and R. I. Carp.** 1986. Partial copurification of scrapie-associated fibrils and scrapie infectivity. Intervirology **25:**48–55.
46. **Van Keulen, L. J. M., B. E. C. Schreuder, M. E. W. Vromans, J. P. M. Langeveld, and M. A. Smits.** 1999. Scrapie-associated prion protein in the gastro-intestinal tract of sheep with natural scrapie. J. Comp. Pathol. **121:**55–63.
47. **Van Keulen, L. J. M., B. E. C. Schreuder, M. E. W. Vromans, J. P. M. Langeveld, and M. A. Smits.** 2000. Pathogenesis of natural scrapie in sheep. Arch. Virol. Suppl. **16:**57–71.
48. **Wells, G. A. H., S. A. C. Hawkins, R. B. Green, A. R. Austin, I. Dexter, Y. I. Spencer, M. J. Chaplin, M. J. Stack, and M. Dawson.** 1998. Preliminary observations on the pathogenesis of experimental bovine spongiform encephalopathy (BSE): an update. Vet. Rec. **142:**103–106.
49. **Wilson, M. I., and P. A. McBride.** 2000. Technical aspects of tracking scrapie infection in orally dosed rodents. J. Cell Pathol. **5:**17–22.